UNITED STATES DEPARTMENT OF COMMERCE
DANIEL C. ROPER, Secretary
NATIONAL BUREAU OF STANDARDS
Lyman J. Briggs, Director

✦

Journal of Research

of the

National Bureau of Standards

✦

Volume 19, Number 6

December 1937

[Published with approval of the Director of the Budget]

UNITED STATES
GOVERNMENT PRINTING OFFICE
WASHINGTON : 1937

For sale by the Superintendent of Documents, Washington, D. C. - - - - - - Price 25 cents
$2.50 per year on subscription

The prices of the separate Research Papers appearing in this JOURNAL are given on the front cover page. If 100 or more copies of any separate are ordered, a discount of 25 percent is allowed. Those who desire copies of separate Research Papers should send their orders and remittances without delay to the Superintendent of Documents, U. S. Government Printing Office, Washington, D. C. This will aid him to determine the number of copies to be printed for sale. Research Papers are not printed from electrotypes, and usually no more reprints can be had when the first and only printing is exhausted.

U. S. Department of Commerce National Bureau of Standards

RESEARCH PAPER RP1050

Part of Journal of Research of the National Bureau of Standards, Volume 19, December 1937

METHOD AND APPARATUS FOR THE RAPID CONVERSION OF DEUTERIUM OXIDE INTO DEUTERIUM [1]

By John W. Knowlton and Frederick D. Rossini

ABSTRACT

A method and apparatus are described in detail for the rapid conversion of deuterium oxide into deuterium. A glass bulb at one end of the evacuated conversion apparatus contains a sealed ampoule holding the liquid deuterium oxide. This ampoule of deuterium oxide is broken by placing liquid air around the outer bulb, which is subsequently heated electrically to control the passage of the vapors of deuterium oxide into the reaction tube containing powdered magnesium at 480° C, where the following reaction occurs: $Mg(solid) + D_2O(gas) = MgO(solid) + D_2(gas)$. The rate of evolution of deuterium from the 1-inch reaction tube can be made as great as 1 mole in 2 hours. The evolved deuterium passes through a liquid-air filter-trap and is collected as liquid in a 50-ml brass bottle immersed in ordinary liquid hydrogen (temperature about −253° C). The connection to the conversion apparatus is closed, that to a 1-liter brass bottle is opened, and the deuterium is permitted to vaporize and fill the two brass bottles at room temperature. In this manner 95 percent of the deuterium is obtained in the 1-liter bottle as a gas under a pressure of about 23 atmospheres.

CONTENTS

		Page
I.	Introduction	605
II.	Discussion of the reaction	607
III.	Description of the apparatus	608
IV.	Method of operation	609
V.	Experimental results and conclusions	610
VI.	References	612

I. INTRODUCTION

In connection with an investigation of the heat of formation of deuterium oxide, it was necessary to devise a method and apparatus for rapidly converting 1 mole of deuterium oxide into deuterium, and obtain the latter as a gas under pressure in a metal bottle.[2]

The process selected for the conversion of the deuterium oxide into deuterium had to be one which would be relatively rapid as well as complete, because of the necessity, as will be explained later, of condensing the deuterium to liquid as fast as it would be formed, by cooling with liquid hydrogen. It was estimated that, with the re-

[1] The work described in this paper has been submitted by John W. Knowlton to the Graduate School of the University of Maryland in partial fulfillment of the requirements for the degree of Master of Science.

[2] One gram-mole of pure deuterium oxide was very generously provided for this investigation by Prof. H. L. Johnston, of the Ohio State University. Once obtained as a pure gas, the deuterium could then be made to react with oxygen in a reaction vessel in a calorimeter in the determination of the heat of formation of deuterium oxide.

frigerating facilities available, the 20 g of deuterium oxide would need to be completely decomposed in about 4 hours. This latter requirement, as well as the question of the probable presence of undesirable side reactions, eliminated the use, for the present investigation, of the classical process of electrolysis. The next obvious method which

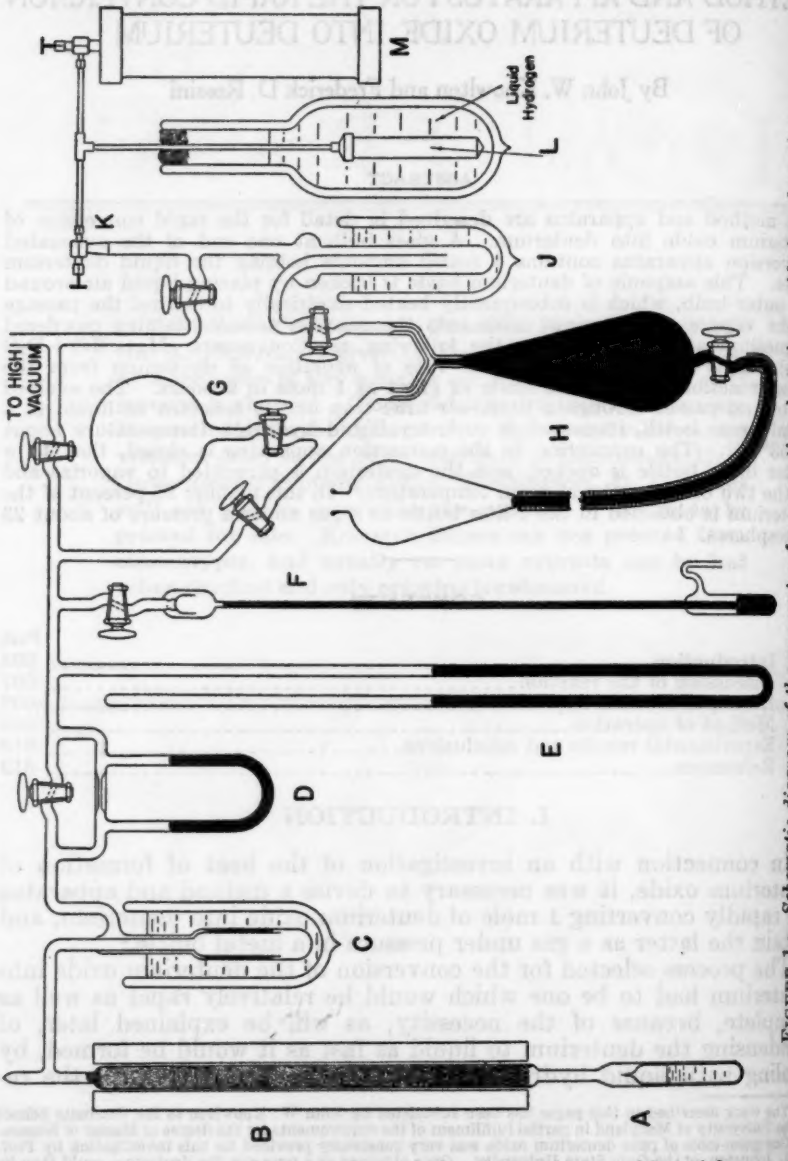

FIGURE 1.—*Schematic diagram of the apparatus for converting deuterium oxide into deuterium.*
The complete description is given in the text on pages 608-609

suggested itself was the reaction of the deuterium oxide with a metal to form the metallic oxide and deuterium. The metal would have to be one whose hydride and hydroxide are unstable at the temperature of the reaction.

Zinc dust at 400° C was used successfully by Claussen and Hildebrand [1][3] in connection with the preparation of small amounts of deuterium, but, in their work, the speed and completeness of the conversion were not important. In a preliminary experiment in this laboratory, it was found that, with a reaction tube similar to that shown at *B* in figure 1, and with water vapor passing into the reaction tube at the rate of about 1 mole in 4 hours, zinc powder at about 400° C permitted an appreciable amount of water vapor to pass undecomposed through the reaction zone. With the present apparatus, it was impractical to obtain a greater speed of reaction with zinc by elevating the temperature because of the proximity to the melting point of zinc, 419° C.

Magnesium appeared to be the most promising metal to try next, because of its higher melting point, 650° C, because its hydroxide is unstable at these elevated temperatures, and because it can be obtained in a state of high purity. In a preliminary experiment with the reaction tube shown in figure 1, it was found that with water vapor passing into the reaction zone at the rate of about 1 mole in 4 hours, magnesium powder at 475° C reacted quantitatively with all the water entering the reaction zone. No water was collected in the liquid-air trap, *C* in figure 1, during the decomposition of 1 mole of water, which indicates that no water passed undecomposed through the reaction tube.

II. DISCUSSION OF THE REACTION

The reactions which may occur in the reaction tube at 480° C under the conditions of the experiment include the desired reaction

$$Mg\ (solid)+H_2O\ (gas)=MgO\ (solid)+H_2\ (gas), \qquad (1)$$

and possible side reactions which might lead to the formation of the following substances: Magnesium hydroxide, magnesium hydride and magnesium silicide.

The free-energy data on magnesium hydroxide and magnesium oxide recently obtained by Giauque and Archibald [2] indicate definitely that the hydroxide is quite unstable at 480° C. With regard to magnesium hydride, there is no definite evidence for its existence [3], but, reasoning by analogy from the high dissociation pressures found for sodium and potassium hydrides by Keyes [4], it may safely be concluded that such a hydride would decompose completely into magnesium and hydrogen at 480° C and at a low pressure of hydrogen. Mellor [3] reports the following: molten magnesium will attack glass, forming a film of oxide on the metal; silicon dioxide is reduced by magnesium when heated, forming silicon, magnesium oxide, and some magnesium silicide; boric oxide is also reduced by magnesium, forming boron and magnesium boride. It was actually observed, in the present experiments, that some magnesium silicide was formed at the wall of the Pyrex-glass reaction tube. Compounds such as silane are known to be quite unstable at 480° C [3].

Consideration of these possible side reactions indicates that they neither consume hydrogen nor form gaseous products. From the standpoint of the conversion of water into hydrogen, then, it appears that the process occurring in the reaction tube, under the conditions of these experiments, is a substantially pure one, as represented by

[3] The numbers in brackets here and throughout the text refer to the references at the end of the paper.

reaction (1), and that, therefore, this process would be satisfactory for the analogous reaction

$$Mg\ (solid)+D_2O\ (gas)=MgO\ (solid)+D_2\ (gas). \quad (2)$$

III. DESCRIPTION OF THE APPARATUS

Figure 1 is a schematic diagram of the apparatus, all of which is made of Pyrex glass, with the exception of the metal parts *K*, *L*, and *M*. An ampoule of the deuterium oxide is contained in the bulb *A*. *B* is the reaction tube, containing a graded charge of magnesium powder. This tube is inclosed in an electrical resistance furnace, which maintains the desired reaction temperature of about 480° C. The reaction tube is connected with a liquid-air trap, *C*, packed with a filter of glass wool. A mercury flowmeter, *D*, provided with a by-passing stopcock, is inserted in the line; *E* is a mercury manometer; and *F* a safety outlet. A 1-liter storage flask, *G*, is by-connected with the gas line, and is joined to a mercury-displacement gas-transferring apparatus, *H*. Through a second liquid-air trap, *J*, the gas-transferring apparatus is connected with the metal part of the system at *K*, by means of a glass-to-metal tapered joint sealed with Pizein wax. Also at *K* there is a vacuum-tight needle valve connecting the glass-to-metal joint with the condensing bulb, *L*, which is immersed in liquid hydrogen during the reaction. The condensing bulb is connected with a 1-liter cylindrical brass bomb, *M*, fitted with a needle valve.

The sample of deuterium oxide is sealed off in a glass ampoule and placed in the bulb, *A*, in order that the whole system may be evacuated. When it is desired to begin the experiment, the ampoule is broken by rapid freezing in liquid air. Several trial experiments showed that this can be done without danger of breaking the outer bulb. The use of a slush composed of solid carbon dioxide, carbon tetrachloride, and chloroform is not completely satisfactory for breaking the water-containing bulb in this manner, because of the slower rate of freezing. In order to vaporize the deuterium oxide and cause it to pass into the reaction zone, a small tubular furnace (not shown in fig. 1) is slipped over the bulb *A*, after the ampoule is broken.

A charge of magnesium powder of graded fineness is placed in the reaction tube, *B*. A preliminary experiment showed that when the magnesium powder in the lower end of the reaction tube is too fine, the reaction is so complete at the entrance end of the tube that the magnesium oxide formed offers too much resistance to the flow of water vapor through it. The use of a charge consisting of coarse granules of magnesium at the lower (entrance) end of the reaction tube, grading to a fine powder at the upper (exit) end, was found to work satisfactorily. Two pounds each of magnesium turnings, labeled "10 mesh and finer", and "35 to 48 mesh", were sifted on nos. 12-, 20-, 30-, and 42-mesh sieves.[4] Of this material, a negligible amount was retained by the 12-mesh sieve; 19 g by the 20-mesh; 382 g by the 30-mesh; and 1,191 g by the 42-mesh sieve. This magnesium was obtained from the American Magnesium Corporation, Cleveland, Ohio, and contained as impurities 0.10 percent of magnesium oxide, 0.03 percent of aluminum plus iron, 0.002 percent of silicon, and no zinc, lead, or copper. The reaction tube, which has an internal diameter of 2.4 cm

[4] These sizes of mesh refer to the Tyler Standard Screen Scale and give the meshes per inch.

and a length of 55 cm, is filled with 10 g of "20 mesh", 30 g of "30 mesh", 50 g of "42 mesh", and 40 g of "<42 mesh" magnesium powder, or 130 g in all. This is 5.3 times the theoretical amount and completely fills the tube to its upper constriction. The charge is supported by a perforated platinum disk held in place by glass shoulders sealed on the wall of the reaction tube. A small plug of glass cotton is placed over the fine magnesium powder at the top of the charge to hold it in position while the reaction proceeds.

The filter trap, *C*, cooled with liquid air, is similar to a filtering arrangement described by Shepherd [5], and is used to retain any possible unreacted water vapor passing through the reaction zone. In the preliminary experiments with ordinary water, as well as in the conversion of the deuterium oxide, no water was condensed in this trap.

The flowmeter, *D*, is used as a measure of the speed of the reaction in order that the conditions can be adjusted so that the process will be complete within the desired time. A calibration of the flowmeter was obtained for hydrogen, and this was converted into terms of the rate of flow of deuterium by means of the factor 1/1.41, the ratio of the viscosity of hydrogen to that of deuterium [6]. A by-passing stopcock is provided on the flowmeter to facilitate the evacuation of the system. During the reaction this stopcock is normally closed.

While the reaction is in progress, the manometer, *E*, measures the pressure of the system at this point. The outlet, *F*, is provided as a safety measure.

On completion of the reaction, the residual deuterium in the system is pumped into the condensing bulb, *L*, by means of the gas-transferring apparatus, *H*. The function of the liquid-air trap, *J*, is to remove mercury vapor from the gas passing into the metal part of the system.

The metal connecting tubes, used beyond the point *K*, are made of copper-nickel alloy of low heat conductivity, composed of 80 percent of copper and 20 percent of nickel. The condensing bulb, *L*, of 50-ml capacity, is constructed of brass.

For use in the investigation of the heat of formation of deuterium oxide, it is necessary to have the deuterium produced by this method confined under pressure, so that the gas can be readily delivered to the reaction vessel in the calorimeter. The cylindrical brass bomb, *M*, of 1-liter capacity, fitted with a needle valve, is provided for this purpose.

IV. METHOD OF OPERATION

The method of operation consists in evacuating the entire system, breaking the ampoule of deuterium oxide, passing its vapor through the hot magnesium powder, and collecting the effluent deuterium gas by liquefying it in the condensing bulb. Subsequent vaporization of the deuterium fills the bomb with the pure gas, where it is stored under pressure.

After the ampoule of deuterium oxide is sealed into the bulb, *A*, and the charge of magnesium is introduced, the filling tube at the top of the reaction tube, *B*, is sealed off, and the side arm of the reaction tube is joined to the rest of the system. The whole apparatus is then evacuated, and the reaction tube is gradually heated to 500° C, while the evacuation is continued, until a pressure of about 10^{-4} mm (measured on a McLeod gage attached to the mercury diffusion pump

and backed by a liquid-air trap) is maintained overnight with the system closed off from the pump. The two connections to the vacuum line and the by-passing stopcock on the flowmeter, *D*, facilitate this pumping operation.

When the vacuum is found to hold in the system, the apparatus is ready for the reaction. The stopcocks leading to the vacuum pump and by-passing the flowmeter, *D*, are closed, and the furnace around the reaction tube, *B*, is heated to about 480° C. Liquid air is placed around the traps, *C*, and *J*. The condensing bulb, *L*, after being cooled with liquid air, is submerged in liquid hydrogen. The level of the mercury in the gas-transferring apparatus, *H*, is adjusted to a point just below the constriction on the reservoir, as shown in figure 1, and kept in this position all through the actual conversion.

When the furnace has reached a temperature of about 480° C, the ampoule of deuterium oxide in the bulb, *A*, is broken by rapid freezing with liquid air. Since the speed of the reaction is governed by the rate at which the vapor of deuterium oxide is delivered to the reaction tube, a short tubular furnace is now slipped over the water bulb, *A*, and it is heated until the reaction attains the desired rate, as measured on the flowmeter, *D*.

When the reaction is once under way, the pressure of the system rises to about ½ atmosphere, the vapor pressure of deuterium at the normal boiling point of hydrogen [7]. Readings of the pressure, as measured by the manometer, *E*, are taken at intervals throughout the experiment in order to be certain that the deuterium is being liquefied as rapidly as it is being formed. At the same time, a record is made of the rate of passage of the deuterium through the flowmeter, and of the temperatures of the reaction tube and the water bulb, to insure the maintenance of the proper conditions for the experiment.

The completion of the reaction is marked by a rapid falling off to practically zero of the rate of evolution of the deuterium. This may be checked by removing the small furnace from the water bulb, *A*, to ascertain whether all the deuterium oxide has been vaporized. The furnace is then replaced and heated to well above the boiling point of the deuterium oxide in order to drive out any last traces of the deuterium oxide.

The residual deuterium in the system is now pumped into the condensing bulb, *L*, by displacement of the mercury in the gas-transferring apparatus, *H*, and manipulation of the stopcocks leading to it. The valve, *K*, is closed, the liquid hydrogen is removed from *L*, and the deuterium is vaporized, filling the bomb, *M*, and the bulb, *L*. Then the valve on the bomb is closed, and the deuterium remaining in the condensing bulb (about 50 ml at a pressure of 23 atmospheres) is released back into the gas-transferring apparatus, and forced into the reservoir flask, *G*, where it is stored. By means of these operations, a minimum amount of deuterium is lost when the bomb is disconnected.

V. EXPERIMENTAL RESULTS AND CONCLUSIONS

In an actual experiment, in which 19.5 g of deuterium oxide was converted to the corresponding amount of deuterium, the data shown in table 1 were obtained. It had been planned to complete the entire reaction in about 4 hours, but it was found possible to decrease this

period considerably. The actual evolution of 1 mole of gaseous deuterium required slightly more than 2 hours, the gas flowing at about 600 ml per minute at a pressure of about ½ atmosphere. The rate of the conversion was controlled by the rate of input of energy into the bulb containing the liquid D_2O. From the data given in table 1, it appears that the vapor pressure of the deuterium oxide was somewhat above 1 atmosphere [8]. The pressure drop through the reaction tube (*B* in fig. 1) was, therefore, a little greater than ⅞ atmosphere. It is possible that an even greater speed of conversion could be satisfactorily used by operating with a greater pressure in the deuterium-oxide side of the reaction tube, obtained by appropriately increasing the temperature of the bulb containing the deuterium oxide.

TABLE 1.—*Experimental data from one conversion*

Time (hr. min.)	Temperature of reaction tube [a]	Temperature of D_2O bulb [b]	Rate of flow of D_2	Pressure of D_2 in system	Remarks
	°C	°C	ml/min	mm Hg	
0:00				$<10^{-4}$	Liquid air placed on D_2O bulb.
0:03					D_2O bulb cracked and ice melted.
0:45	485	76	363	67	Small furnace placed around D_2O bulb.
1:00	483	97	343	250	Pressure rising.
1:01				270	
1:03				268	Pressure appears to be constant.
1:10	488	104	655	264	
1:20	483	106	655	264	
1:26					Removed furnace from D_2O bulb and noted quiet boiling of liquid.
1:28	483	104	405	261	Effect of foregoing interruption.
1:38	480	108	634	264	
1:50	485	103	655	262	
2:00	485	105	780	264	
2:10	485	103	780	264	
2:20	488	103	780	264	
2:30	494	108	770	264	
2:40	494	110	593	263	Rate visibly dropping.
2:43			291		
2:44			198	261	
2:47			62	260	
2:54	494	141	10		
3:02					Valve on condensing bulb closed off. Barometric pressure 757 mm (corrected).

[a] These temperatures are accurate to about ±5°C.
[b] These temperatures are accurate to about ±3°C.

The remaining point of interest in connection with this method of converting deuterium oxide into deuterium concerns the possible introduction of hydrogen atoms to either the deuterium oxide or the deuterium in the course of the work. It appears that the deuterium oxide available for the present investigation had as an impurity hydrogen atoms to the extent of about 0.01 atomic percent. (See reference [9] for a detailed discussion of the composition.) Prior to the conversion, the 19.5-g sample was subjected to a threefold distillation in vacuum and was sealed in a Pyrex-glass ampoule. An analysis of the gaseous deuterium collected in the 1-liter cylindrical brass bomb (*M*, in fig. 1) was made by F. G. Brickwedde and R. B. Scott (see reference [9] for details), who measured the vapor pressure of the liquefied deuterium against that of normal or natural hydrogen in the liquid state. These data on vapor pressure indicate that the gaseous deuterium produced had as impurity hydrogen atoms to the

extent of 0.73 percent of the total number of hydrogen and deuterium atoms (corresponding to the actual presence of 1.45 percent of HD), referred to the sample of deuterium measured by Brickwedde, Scott, and Taylor [7], as being 100.00 percent.

It is apparent that this additional impurity of about 0.7 percent of hydrogen atoms was introduced in the conversion experiment either by exchange with the glass and metal walls, or from the magnesium powder. Some exchange may have also occurred during the preliminary distillation of the deuterium oxide. The hydrogen atoms introduced by exchange with the glass and metal walls would not be expected to be a large fraction of impurity, because of the large amount (1 mole) of gas converted. In any subsequent experiment with this method of conversion, the impurity of hydrogen atoms introduced in this way can be largely reduced by first "flushing" all the glass and metal surfaces and the magnesium powder with a small amount of deuterium gas, produced at the beginning of the conversion, and then discharging this impure gas from the system before beginning the formal collection of the deuterium.

The authors are greatly indebted to Prof. H. L. Johnston, Department of Chemistry, Ohio State University, for placing 19.5 g of pure deuterium oxide at their disposal; to Martin Shepherd, of this Bureau, for his advice during the course of the present investigation, and for the loan of the metal vessels used for condensing and storing the deuterium; to J. W. Cook, of this Bureau, for manipulating the liquid hydrogen during the experiment; to F. G. Brickwedde and R. B. Scott, of this Bureau, for analyzing the deuterium produced; and to Prof. M. M. Haring, Department of Chemistry, University of Maryland, for his kind interest in the problem.

VI. REFERENCES

[1]. W. H. Claussen and J. H. Hildebrand. J. Am. Chem. Soc. **56**, 1820 (1934).
[2]. W. F. Giauque and R. C. Archibald. J. Am. Chem. Soc. **59**, 561 (1937).
[3]. J. W. Mellor. A Comprehensive Treatise on Inorganic and Theoretical Chemistry **4**, 266, 271, 272; **6**, 147, 160, 216, 218, 219, 222 (Longmans, Green, and Co., London, 1922).
[4]. F. G. Keyes. J. Am. Chem. Soc. **34**, 779 (1912).
[5]. Martin Shepherd. BS J. Research **2**, 1145 (1929) RP75.
[6]. H. C. Torrey. Phys. Rev. **47**, 644 (1935).
[7]. F. G. Brickwedde. R. B. Scott, and H. S. Taylor. J. Research NBS **15** 463 (1935) RP841.
[8]. F. T. Miles and A. W. C. Menzies. J. Am. Chem. Soc. **58**, 1067 (1936).
[9]. F. D. Rossini and J. W. Knowlton. Forthcoming publication in J. Resear NBS.

WASHINGTON, October 5, 1937.

U. S. Department of Commerce National Bureau of Standards

RESEARCH PAPER RP1051

Part of Journal of Research of the National Bureau of Standards, Volume 19, December 1937

DIMENSIONAL CHANGES IN AERIAL PHOTOGRAPHIC FILMS AND PAPERS

By Raymond Davis and Emory J. Stovall, Jr.

ABSTRACT

Results of a study of dimensional changes in aeromapping photographic film and papers under controlled conditions are presented. Both films and papers are subject to a shrinkage from processing. These materials are hygroscopic, consequently their dimensions change with the varying moisture content of the air. Dimensional changes from both processing and moisture content are least in the machine direction, that is, along the roll. Films continue to shrink with time, because of a loss of solvents and plasticizer. This shrinkage is illustrated by accelerated-aging tests at 120° F covering a period of 32 days. Two new instruments developed for measuring film shrinkage are described. A reduction of differential shrinkage in the final print or duplicate negative can be had by crossing the machine directions of the negative and printing material during exposure.

CONTENTS

		Page
I.	Introduction	613
II.	Materials	614
III.	Apparatus and methods for measuring shrinkage	614
IV.	Reproducibility of the measurements	617
V.	Film shrinkage as a function of conditioning time	619
VI.	Film shrinkage as a function of accelerated-aging time	620
VII.	Shrinkage of aerofilms as a function of relative humidity	621
VIII.	Film shrinkage due to processing and accelerated aging	629
IX.	Shrinkage of photographic papers caused by processing	631
X.	Summary and recommendations	636

I. INTRODUCTION

Photographic films and papers are not stable with respect to their dimensional characteristics. It is well known that these materials not only change their dimensions with a change in moisture content, which tends to follow similar changes in the atmosphere, but are subject to shrinkage caused by the process of developing, fixing, and washing. For aeromapping the dimensional change is not serious if uniform in all directions and its magnitude known, as a change of scale is all that would be needed for correction. The actual case is complicated by the fact that both papers and films shrink more in one direction than in the other. Both paper and celluloid are manufactured by a continuous process, the product being in the form of a long ribbon. The greatest shrinkage is always in the crosswise direction.

While these facts have been known for a long time, only meager and incomplete data on the magnitude of the effects of moisture and processing under controlled conditions have been available. During the last few years, aerial surveying has been undertaken on a large

scale, and the need for information on the dimensional changes in films and papers has become acute. For work in which high accuracy is desired, considerable difficulty has been encountered in obtaining film and paper with satisfactory shrinkage characteristics. The better aerial cameras are fitted with lenses selected for minimum distortion. The magnitude of the distortion for these lenses is of the order of 0.04 mm at the edge of a 22.9- by 22.9-cm (9 in. by 9 in.) plate. This value amounts to 0.035 percent. In films distortion is measured by the difference in shrinkage, expressed as a percentage, in the two directions and is called "differential shrinkage." The differential shrinkage in films should not exceed the distortion of the lenses, that is, 0.035 percent.

II. MATERIALS

The American Society of Photogrammetry, through its President, Col. H. H. Blee, secured the film and paper samples from photographic manufacturers, governmental agencies, and privately operated aerosurveying services. The film and paper samples tested are representative of those in current use for aeromapping with the exception of two samples of cut film, one of which was experimental. From two to eight samples of each brand of film were tested, each sample being from a different lot of the same trade name. The different samples of the same brand are grouped together in the tables. From these groups an idea of the uniformity of the product can be had. In all, 24 separate lots of film were tested and, with the exception of two samples, all were on nitrate base.

Most of the papers submitted were regular photographic papers—in all, there were 57 items of which only 8 were marked "special low shrink" or " aeromapping papers."

III. APPARATUS AND METHODS FOR MEASURING SHRINKAGE

Apparatus suitable for measuring film shrinkage may be of two general types—optical or mechanical. The optical devices generally used consist of either a micrometer microscope actuated by a calibrated screw, such as used for measuring line-spectrum negatives, or the comparator type of instrument with which a length standard is compared by two micrometer microscopes with reference marks on the film.

The use of devices employing microscopes is both slow and laborious, each an important factor in a large number of measurements. Rapid and convenient means of measuring film shrinkage not being available, two different instruments were designed and constructed for this work, one a rapid and accurate mechanical gage or extensometer for measuring films, and the other an optical extensometer suitable for both paper and films.

The use of this mechanical extensometer, referred to throughout this report as "pin gage", does not necessitate the use of a darkroom as no developed image is used in the measurements.

The procedure with the pin gage is as follows: Strips 2 inches wide and 10 inches long are cut from the film for lengthwise samples. Crosswise samples are cut to the same width but to a length 9½ inches,

which is the full width of the 24-cm aerofilm. The difference in length serves to distinguish the lengthwise samples from the crosswise samples. However, each individual test strip is also given an identifying number. After the samples are cut, which may be done in a lighted room, they are numbered and hung up by wooden photoclips in the conditioning room for the prescribed time. Two pairs of holes ¼ inch in diameter and 8 inches apart are then punched in the film (see fig. 1). The holes may be 5 inches apart for use with a 5-inch gage in the case of narrow film.

The punched film is measured on the pin gage and the readings recorded. The samples are then developed, fixed, washed and dried, and returned to the conditioning room. After reconditioning for the prescribed time, they are again measured with the pin gage. The difference between the pin-gage readings before and after developing the film gives the dimensional change due to processing.

The 8-inch pin gage, removed from its case, is illustrated in figure 2. *A* and *B* are steel pins ¼ inch in diameter and have rounded ends. Pin *A* is fixed to the heavy-steel face plate *C* at a distance of 7¾ inches from pin *B*, the outside measure being 8 inches. Pin *B* passes through a slot in the face plate and is fastened to a suspension bridge *D* immediately below. The bridge supporting this movable pin *B* is suspended from the underside of the face plate by two spring-steel flexure plates *E*, 0.005 inch thick, one at each end, which permit the bridge supporting the movable pin to move toward and away from the fixed pin a total distance of approximately 0.1 inch. A dial gage *F* fastened to the underside of the face plate is connected to the suspension bridge at the point *G* by a metal rod *H*. The face plate and bridge are made of steel, and the rod *H* is of duralumin of such a length that it compensates for any changes of temperature. For the work reported here, temperature compensation was unnecessary; but the correction was so simple to make that this feature was incorporated in the design. A coil spring (not shown in fig. 2) fastened to the face plate and suspension bridge maintains tension of about 75 grams on the sample placed over the pins. The holes in the film were made with a punch (fig. 3) designed for the purpose. The lever bar and punch pins were from a commercial paper punch. The punch was machined to specified dimensions, and hardened-steel dies made to fit were imbedded in the steel base plate. This punch makes clean holes for either the 5-inch or 8-inch gage lengths. A metal plate (not shown) may be used to keep the film flat during the punching operation. Since the film is measured after punching and before processing, high accuracy in the spacing of the holes is unnecessary. However, if care is taken excellent reproducibility can be obtained.

Ordinarily, 30 test strips were cut from each roll of aerofilm tested, 15 cut crosswise and 15 lengthwise. One group of strips, five in each direction, was left unprocessed in the conditioning room as a control. The processed samples were first conditioned as mentioned, developed for 3 minutes in trays of metol-hydroquinone developer, rinsed in a dilute acetic acid short-stop bath, fixed 12 to 15 minutes in an acid fixing bath, washed 30 to 60 minutes in running water, and hung up to dry in the uncontrolled atmosphere of the laboratory. The dried samples were returned to the conditioning room, conditioned for the prescribed time, and remeasured along with the control strips to deter-

mine the shrinkage due to processing. A third group of film strips, cut, punched, processed, and measured, as explained above, were put in a paper envelope (to prevent excessive curling) and placed in an oven maintained at 120° F (49° C), usually for 7 days, then taken back into the conditioning room to be reconditioned and measured.

Excellent results on film were obtained with the pin gage, but with photographic papers this procedure was not satisfactory. Paper is not sufficiently flexible nor does it have the mechanical strength or wear resistance to give good reproducibility. Using the mechanical principles of the pin gage, an optical extensometer was designed for measuring paper shrinkage. This instrument is shown in figure 4. The box contains a mechanism similar to the pin gage, but the two pins are replaced by two 32-mm Micro-Tessar objectives, one movable and the other fixed. These lenses are in fixed focus on the upper surface of the plate-glass top of the instrument. The glass is painted black on the underside except for two rectangular patches immediately above the objectives. By means of prisms the beams from the lenses

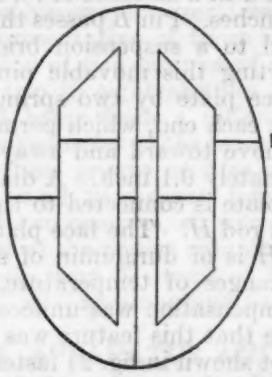

FIGURE 5.—*Pattern observed in the eyepiece of the optical gage.*

A is imaged by the fixed objective, *B* by the movable objective.

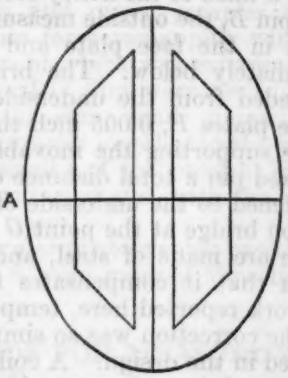

FIGURE 6.—*Pattern observed in the eyepiece of the optical gage.*

A is imaged by the fixed objective, *B* by the movable objective.

are brought to a focus on a Lummer-Brodhun photometric cube, which brings the separate images into juxtaposition. A brass tube fitted with a lens and hard-rubber cap with a small hole constitutes the eyepiece of the instrument; this is focused on the photometric cube. On the end of the box to the right a micrometer is fitted to move the lens and measure its displacement. On the other end of the box is a dial gage, which also indicates the position of the lens. Either micrometer or dial gage may be read; however, while slightly less accurate than the micrometer, the dial gage is preferable because of ease of reading. The gage length (distance between lenses) of this instrument is 6 inches. The following illustrates the operation of the instrument: if a print on paper or film having a pair of parallel lines spaced 6 inches apart is placed face down on the glass top of the instrument so that the lines are in the field of view of the lenses one would see in the eyepiece a pattern as shown in figure 5. In figure 5 line *A* is produced by the fixed lens and line *B* is from the movable lens. If the micrometer screw is turned in the proper direction line *B*

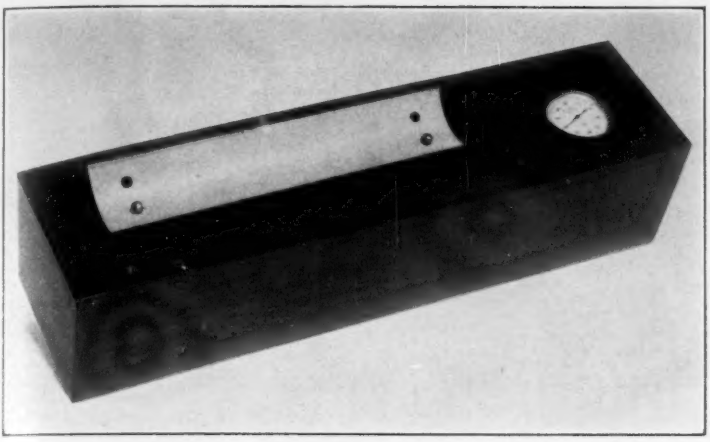

FIGURE 1.—*Pin gage, with strip of film in place for measurement.*

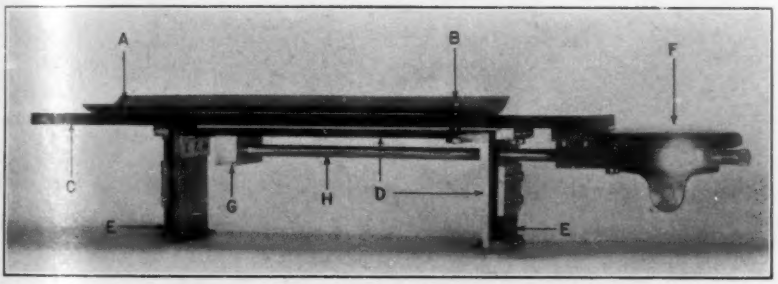

FIGURE 2.—*Pin gage removed from its case.*

A—Fixed pin.
B—Movable pin.
C—Face plate.
D—Suspension bridge.
E—Flexure plate.
F—Dial gage.
G—Anchor block for *H*.
H—Duralumin rod for temperature compensation.

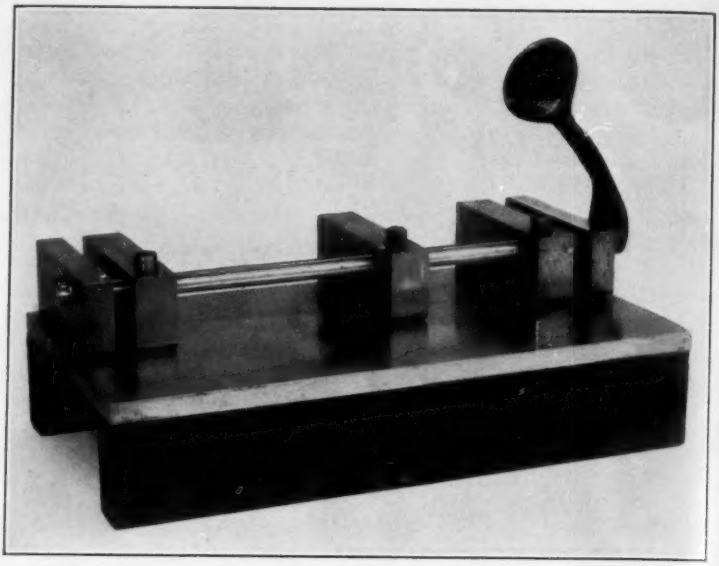

FIGURE 3.—*Punch used for making reference holes in films, either 5 or 8 inches apart.*

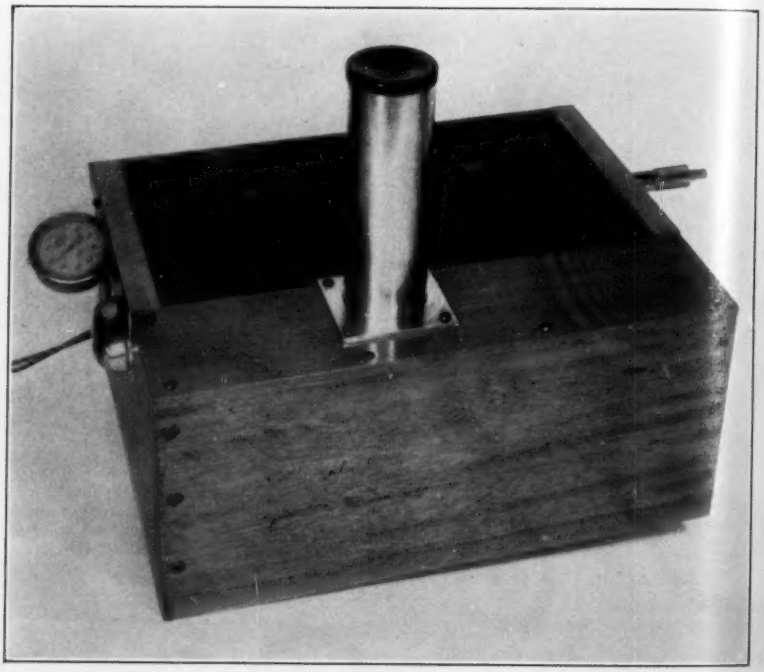

FIGURE 4.—*Optical gage.*

will be moved into coincidence with line *A*, as shown in figure 6. The magnification is 10 diameters. The obvious advantage of this instrument, in which both fields are seen in a single eyepiece, over the usual comparators is that a single setting is sufficient. Comparators ordinarily require separate settings on two reference lines. Matching ends of lines, as in the present instrument, is more accurate than centering a line between two parallel hairs or centering on cross hairs in two observing microscopes for a single measurement.

To determine the shrinkage of photographic paper or film with this optical gage, the sample, after conditioning in the dark, is exposed in the conditioning room under a negative of a Max Levy ruled-glass grid consisting of fine lines spaced ½ inch, as shown in figure 7. After developing, fixing, and washing and drying, the sample is reconditioned for a prescribed interval of time and then measured. In the measuring operation, the first step is to measure a similar reference print of this grid made on a photographic plate, in six different positions, three lengthwise and three crosswise. With the fixed dimensions of the

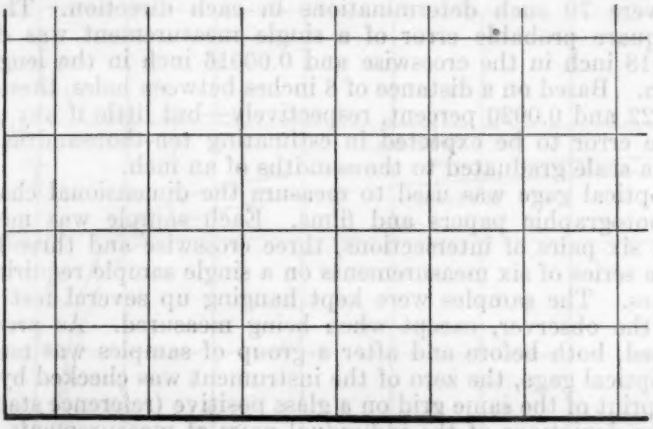

FIGURE 7.—*Section of a photograph of the ruled-glass grid, full size, to show character of ruling.*

plate as standard the separations of six pairs of points on the sample are compared with those of the same pairs of points on the grid. After measurement of the paper or the film has been completed the standard plate is again measured to check the zero of the instrument.

IV. REPRODUCIBILITY OF THE MEASUREMENTS

Careful handling of the film is necessary to obtain accurate readings with the pin gage and to avoid damage to the film. The manner of placing the film on the pins and removing it is important. The strip with the emulsion side up should be grasped at the ends between fingers and thumbs, held under tension, and slipped over both pins simultaneously. The strip is then pushed into contact with the top plate of the gage, the thumbnails pressing lightly on the outside of the pins. The instrument is then tapped lightly with the finger or a pencil so as to eliminate friction or sticking in the dial gage. The dial gage, graduated to thousandths of an inch, is read to ten thousandths of an inch. The strip is removed from the instrument by

grasping the ends as before and holding it under tension while lifting it off the two pins simultaneously. These operations consume only about 10 seconds.

The strips are kept hanging up several feet away from the observer except during the actual operations of measurement, so that the effect of moisture from the observer's breath and body on their dimensions will be small. The zero of the pin gage should be checked each time a series of measurements is made by noting the readings on the dial gage when the movable pin is displaced to its imposed limits. In the present study, these readings never vary by more than 0.0002 inch, so no zero-correction was ever found necessary.

To test the reproducibility of measurements made on the pin gage, 10 strips of film, 5 cut crosswise and 5 lengthwise, were conditioned, two pairs of holes punched in each, and measured. They were then kept in the conditioning room (unprocessed) and remeasured seven times during a period of 8 days. The deviation of the change in spacing from the initial measurement from the average change between 10 pairs of holes measured at the same time was recorded. There were 70 such determinations in each direction. The root mean square probable error of a single measurement was derived as 0.00018 inch in the crosswise and 0.00016 inch in the lengthwise direction. Based on a distance of 8 inches between holes, these errors are 0.0022 and 0.0020 percent, respectively—but little if any greater than the error to be expected in estimating ten-thousandths of an inch on a scale graduated to thousandths of an inch.

The optical gage was used to measure the dimensional change of both photographic papers and films. Each sample was measured between six pairs of intersections, three crosswise and three lengthwise, the series of six measurements on a single sample requiring 2 or 3 minutes. The samples were kept hanging up several feet to one side of the observer, except when being measured. As previously mentioned, both before and after a group of samples was measured on the optical gage, the zero of the instrument was checked by measuring a print of the same grid on a glass positive (reference standard). From the deviations of the individual pairs of measurements on the reference standard, the probable error of a single measurement on the instrument was computed. Based on 20 sets of measurements of the plate, 240 individual measurements, the probable error here was 0.00009 inch, or 0.0015 percent of the 6-inch gage length. As with the pin gage, this error is not greater than the error to be expected in estimating ten-thousandths on a scale graduated to thousandths of an inch.

The probable errors of both instruments are about 0.002 percent. The dimensions of the films are not nearly so reproducible when the surrounding conditions are changed. A group of 10 strips of film were hung on a line for 24 hours in the conditioning room, measured, and rehung. A 40-watt lamp was placed at a distance varying from 1 to 3 feet from the film samples and kept burning for several hours. The lamp was removed, and after a period of 24 hours the films were again measured. The probable fluctuations of the measurements were then 0.004 percent crosswise and 0.008 percent lengthwise in 8 inches, from 2 to 4 times the probable error of the gages. The prob-

able fluctuation of the measured dimensional change of a strip of film, due to accelerated aging (120° F for 7 days), was computed for several groups of strips of film and was found to be about 0.02 to 0.04 percent. This is about 10 to 20 times the error of the instruments.

The measurements used in computing the probable errors of the gages were made by an experienced observer, who has made several thousand measurements on each of the two instruments, and hence has acquired a technique for handling the strips rapidly and precisely. Precautions were taken to eliminate as much as possible the effect of heat from the lamp and of moisture from the observer's body and breath on the samples of film. If these precautions are not taken the fluctuations will, of course, be larger.

V. FILM SHRINKAGE AS A FUNCTION OF CONDITIONING TIME.

It is well known that photographic film changes in dimension with change in moisture content, and that the amount of moisture in the

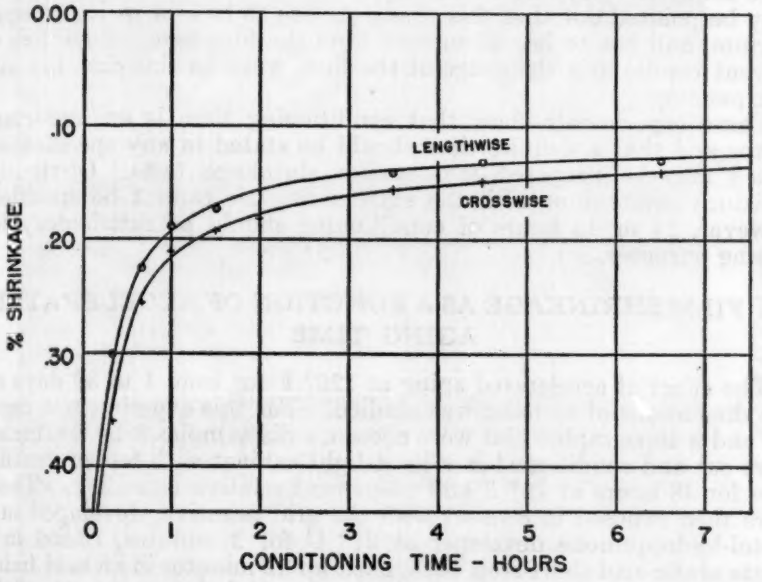

FIGURE 8.—*Graph showing percentage of shrinkage as a function of conditioning time for special aerofilm.*

film tends to follow a change in the atmosphere. However, no information on the time required for film to reach equilibrium was available.

The rate of approach to dimensional equilibrium with humidity was investigated for three different films: A regular, a topographic, and a special low-skrinkage film. These films were in rolls 9½ inches wide and 25 feet long. Test strips of these were conditioned at 65 percent relative humidity and processed. When each strip was thoroughly dry it was put in a paper envelope and kept in an oven at 120° F for 24 hours, and then put in an open can and returned to the

oven for an additional 24 hours. At the end of this period the can was covered, sealed with tape, and transferred to the conditioning room, where the can was opened and the film strips measured immediately and the time noted. While the moisture in the film was coming to equilibrium with the air in the conditioning room, a series of measurements were made, extending over a period of 16 days. From these measurements was computed the dimensional change of the films, based on their original measurement before processing.

The results for the topographic film, shown in figure 8, were plotted on a linear scale as a percentage dimensional change against time up to about 7 hours. These curves, rising steeply for 1 or 2 hours and then leveling off, seem to indicate that equilibrium is approximately reached within a few hours. However, this is not strictly true. The results from all three films, shown in figures 9, 10, and 11, were plotted as percentage dimensional change against the logarithm of the conditioning time, up to 16 days. These curves show that dimensional equilibrium was not reached even after 2 weeks of conditioning, and that about 100 days would be required to establish equilibrium. It may be pointed out that this change is due to lack of moisture equilibrium, and not to loss of solvent from the film base. Such loss of solvent results in a shrinkage of the film, while in this case the film is expanding.

These experiments show that conditioning time is an important factor and that a definite time should be stated in any specification which may be prepared for aerofilm shrinkage tests. Obviously, moisture equilibrium with the surrounding air cannot be specified; however, 24 or 48 hours of conditioning should be satisfactory for testing purposes.

VI. FILM SHRINKAGE AS A FUNCTION OF ACCELERATED-AGING TIME

The effect of accelerated aging at 120° F for from 1 to 32 days on the dimensions of aerofilm was studied. For this experiment a regular and a topographic film were chosen. Six samples 8 by 9½ inches were cut and conditioned in a light-tight cabinet with forced ventilation for 48 hours at 72° F and 65-percent relative humidity. These were then exposed in contact with the grid negative, developed in a metol-hydroquinone developer at 21° C for 2 minutes, rinsed in a dilute acetic acid short-stop bath, fixed for 12 minutes in an acid fixing bath, washed 30 minutes in running water, and then dried overnight in the laboratory. After reconditioning for 48 hours at 72° F and 65-percent relative humidity, the samples were measured on the optical gage. After measuring each film it was put in a paper envelope and placed in an oven maintained at 120° F (49° C). One sample from each roll was removed after 1, 2, 4, 9, 16, and 32 days, respectively. The samples were then reconditioned at 72° F and 65-percent relative humidity for 48 hours and again measured on the optical gage.

The shrinkage of the films due to accelerated aging was computed from the difference in the dimensions of the film after processing and after oven treatment. The results in figure 12 were plotted with percentage shrinkage as ordinates and the logarithm of the time in the oven in days as abscissas. It will be noted that the points lie approxi-

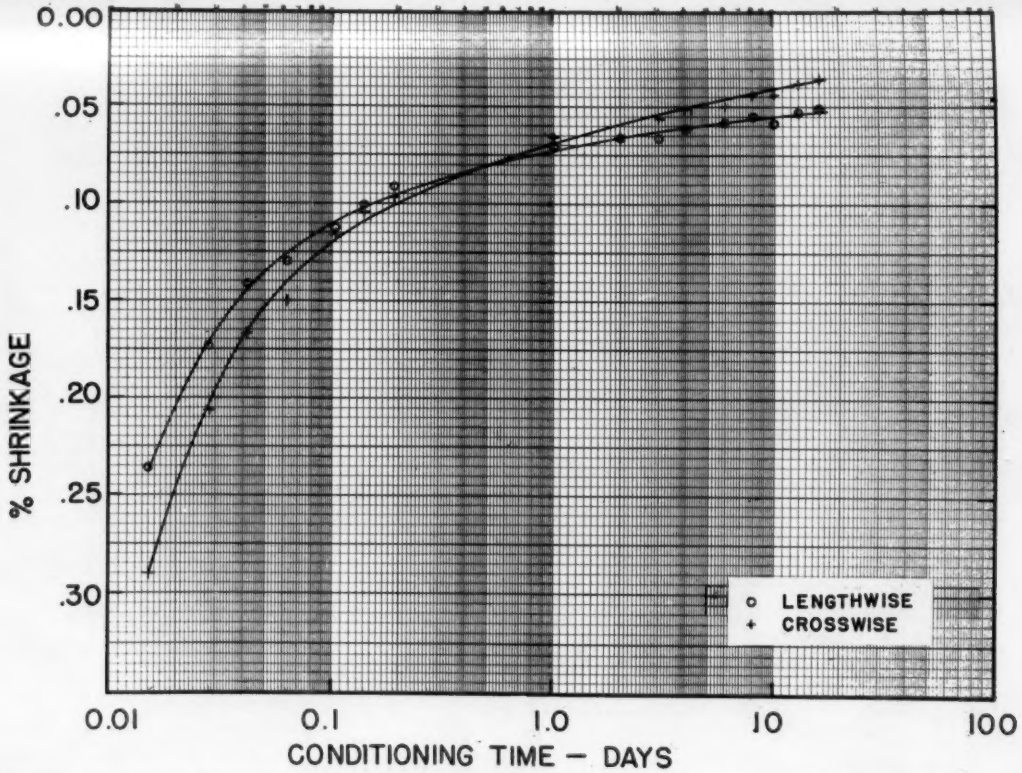

FIGURE 9.—*Graph showing percentage of shrinkage as a function of the logarithm of conditioning time for topographic film.*

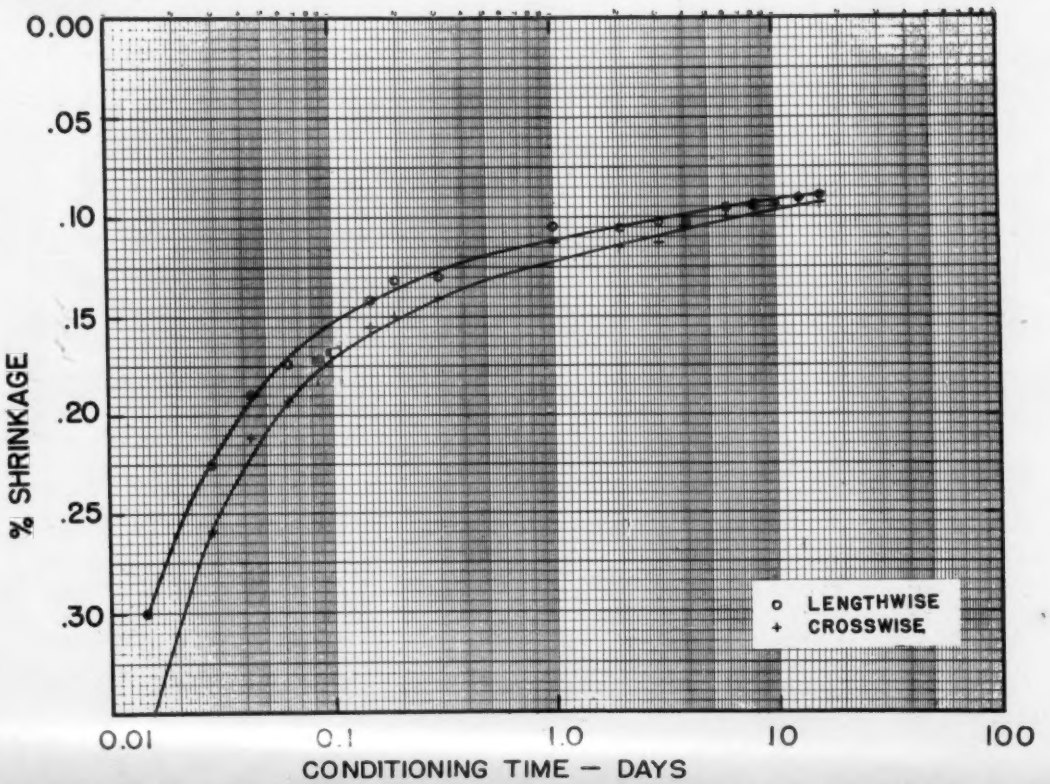

FIGURE 10.—*Graph showing percentage of shrinkage as a function of the logarithm of conditioning time for special aerofilm.*

FIGURE 10.—*Graph showing percentage of shrinkage as a function of the logarithm of conditioning time for special aerofilm.*

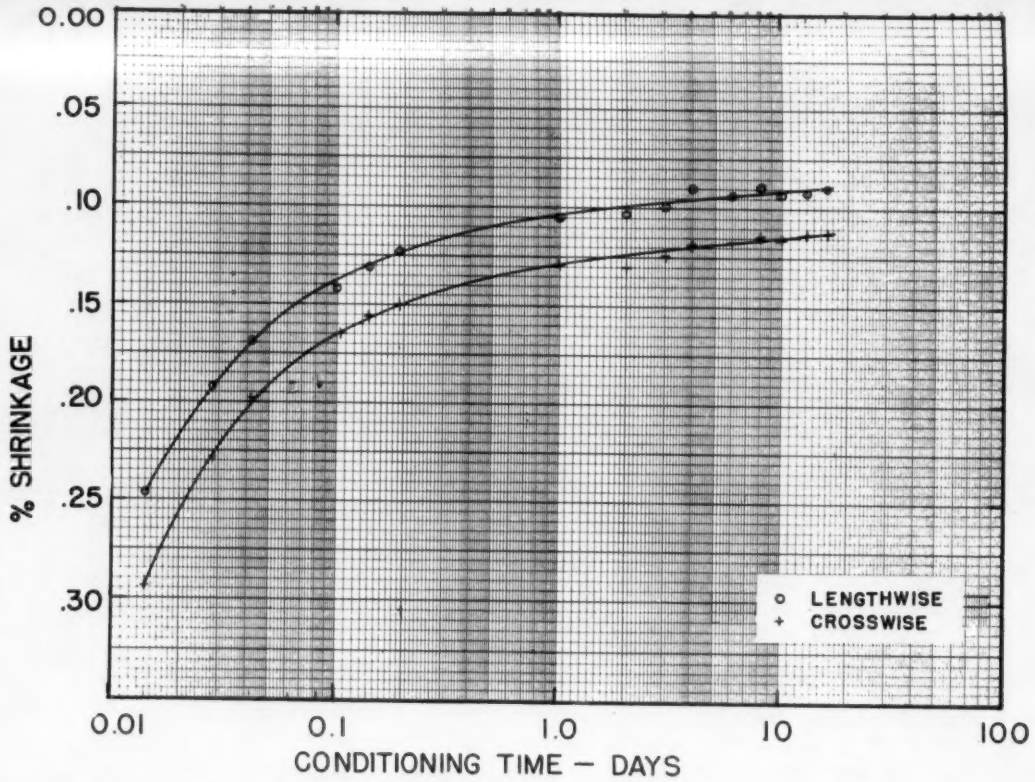

FIGURE 11.—*Graph showing percentage of shrinkage as a function of the logarithm of conditioning time for regular aerofilm.*

UNIV. OF MICH.

mately on a straight line. The shrinkage is seen to be greater in the crosswise direction, and the rate of shrinkage is greater in the crosswise direction, for both films. The shrinkage of the regular film is much greater than that of the topographic film and also its rate of shrinkage is slightly greater.

The position of the lines through the points in figure 12 was obtained by least squares. The same data, plotted on a linear time scale, are shown in figure 13. The solid lines in this figure are trans-

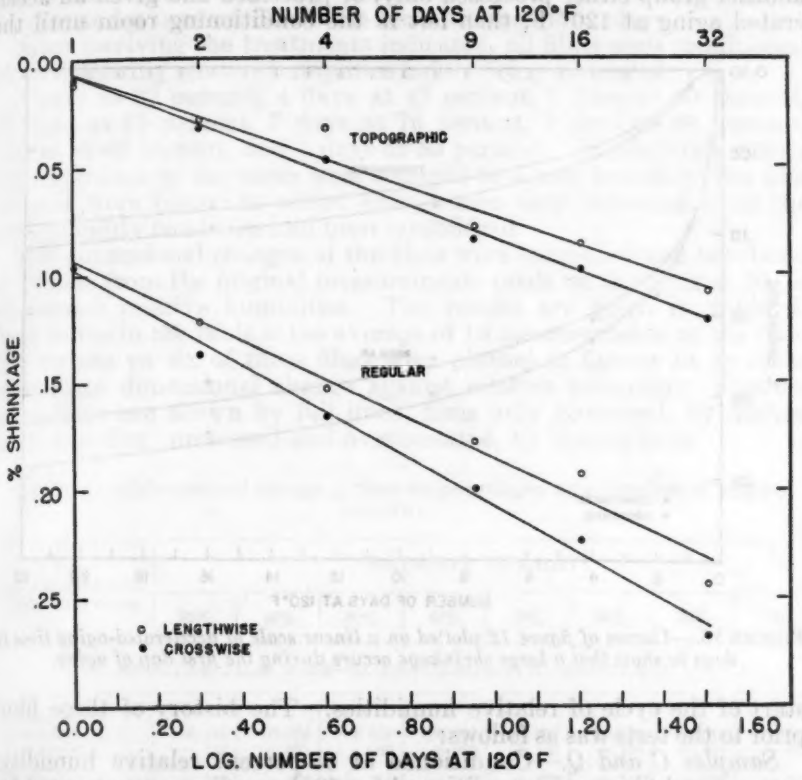

FIGURE 12.—*Linear relationship between percentage of shrinkage and the logarithm of the time in days of accelerated aging for regular- and topographic-base films.*

formed from the straight lines in figure 12. The dashed portions of the curves are estimates of the behavior of the films in the oven for less than 1 day, and, of course, this may not be exact.

VII. SHRINKAGE OF AEROFILMS AS A FUNCTION OF RELATIVE HUMIDITY

In connection with a separate project, the conditioning room ordinarily maintained at 50-percent relative humidity was to be operated at a series of relative humidities. The program called for periods of approximately a week's duration at 32, 43, 65, 76, 86, 65,

and 50-percent relative humidity, the temperature to be kept constant at 72° C.

Advantage was taken of this schedule to determine the film shrinkage under these conditions. Seventeen samples of aerofilms representing six different brands of films were studied. Some of these samples had already been used for other purposes and consequently had been cut, conditioned, and measured some time previously. In each case, one group of test strips was left in the conditioning room unprocessed and another group either processed only, or processed and given an accelerated aging at 120° F, then left in the conditioning room until the

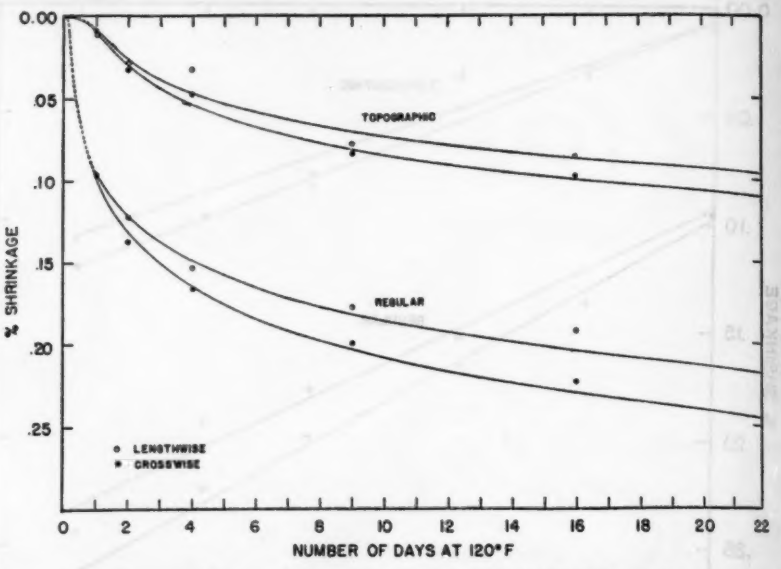

FIGURE 13.—*Curves of figure 12 plotted on a linear scale of accelerated-aging time in days to show that a large shrinkage occurs during the first day of aging.*

start of the cycle of relative humidities. The history of these films prior to the tests was as follows:

Samples C and Q.—Conditioned at 65-percent relative humidity; unprocessed films were conditioned for 53 days; films oven-treated for 7 days were reconditioned for 42 days; films oven-treated for 14 days were reconditioned for 35 days.

Sample F.—Conditioned at 50-percent relative humidity; unprocessed films were conditioned for 22 days; and films oven-treated for 7 days were reconditioned for 11 days.

Sample G.—Conditioned at 50-percent relative humidity; unprocessed films were conditioned for 19 days; and films oven-treated for 7 days were reconditioned for 9 days.

Sample I.—Conditioned at 50-percent relative humidity; unprocessed films were conditioned for 11 days; and films oven-treated for 7 days were reconditioned for 2 days.

Sample J.—Unprocessed films were conditioned for 8 days at 50-percent relative humidity; and films oven-treated for 7 days were started in the cycle of humidities at 32 percent immediately after removing from oven.

Sample O.—Conditioned at 50-percent relative humidity; unprocessed films were conditioned for 24 days; films oven-treated for 7 days were reconditioned for 15 days.

Samples A, B, C, H, K, N, P, Q, R, S, T, and U.—Conditioned at 50-percent relative humidity; unprocessed films were conditioned for 3 days; and processed films were reconditioned for 2 days.

After receiving the treatments indicated, all films were conditioned at the following relative humidities before being measured:

3 days at 32 percent, 4 days at 43 percent, 7 days at 50 percent, 10 days at 65 percent, 7 days at 76 percent, 5 days at 86 percent, 7 days at 65 percent, and 7 days at 50 percent. Immediately before the conditions in the room were changed to a new humidity, the film samples were placed in sealed cans, where they remained until the new humidity condition had been established.

The dimensional changes of the films were computed and tabulated as change from the original measurements made on the films at 50- or 65-percent relative humidities. The results are given in table 1. Each value in the table is the average of 10 measurements on the film. The results on six of these films were plotted in figures 14 to 19 as percentage dimensional change against relative humidity. Unprocessed films are shown by full lines; films only processed, by dashed lines; and film processed and oven-treated, by dotted lines.

TABLE 1.—*Dimensional change of films in percentages as a function of relative humidity*

Treatment and direction of measurement	RELATIVE HUMIDITY							
	32%	43%	50%	65%	76%	86%	65%	50%
REGULAR FILM BASE—Ss. PANCHROMATIC—SAMPLE *A*								
Unprocessed:								
Crosswise	−0.144	−0.089	−0.049	+0.059	+0.091	+0.155	+0.015	−0.110
Lengthwise	−.132	−.081	−.040	+.085	+.127	+.180	+.050	−.071
Processed:								
Crosswise	−.212	−.159	−.116	+.015	+.070	+.141	−.029	−.163
Lengthwise	−.186	−.133	−.085	+.045	+.104	+.167	+.014	−.103
REGULAR FILM BASE—Ss. PANCHROMATIC—SAMPLE *B*								
Unprocessed:								
Crosswise	−0.166	−0.111	−0.063	+0.053	+0.082	+0.146	−0.001	−0.133
Lengthwise	−.149	−.099	−.046	+.069	+.107	+.160	+.023	−.104
Processed:								
Crosswise	−.245	−.198	−.144	−.009	+.049	+.114	−.062	−.204
Lengthwise	−.199	−.152	−.106	+.023	+.070	+.131	−.032	−.168

TABLE 1.—*Dimensional change of films in percentages as a function of relative humidity*—Continued

Treatment and direction of measurement	RELATIVE HUMIDITY							
	32%	43%	50%	65%	76%	86%	65%	50%
REGULAR FILM BASE—Ss. PANCHROMATIC—SAMPLE *C*								
Unprocessed:								
Crosswise	−0.139	−0.090	−0.062	+0.048	+0.077	+0.119	−0.007	−0.121
Lengthwise	−.137	−.086	−.055	+.077	+.114	+.158	+.038	−.080
Processed:								
Crosswise	−.214	−.165	−.125	+.013	+.063	+.112	−.036	−.162
Lengthwise	−.206	−.152	−.111	+.041	+.094	+.138	−.010	−.126
Unprocessed:								
Crosswise	−.285	−.238	−.184	−.058	−.018	+.040	−.088	−.219
Lengthwise	−.276	−.224	−.168	−.056	−.016	+.041	−.078	−.217
Oven-treated 7 days:								
Crosswise	−.409	−.372	−.321	−.193	−.119	−.073	−.213	−.320
Lengthwise	−.382	−.344	−.301	−.181	−.115	−.070	−.202	−.318
Oven-treated 14 days:								
Crosswise	−.426	−.383	−.335	−.208	−.133	−.088	−.236	−.348
Lengthwise	−.382	−.346	−.297	−.176	−.117	−.073	−.212	−.321
REGULAR FILM BASE—Ss. PANCHROMATIC—SAMPLE *F*								
Unprocessed:								
Crosswise	−0.168	−0.114	−0.074	+0.031	+0.061	+0.109	−0.015	−0.131
Lengthwise	−.144	−.092	−.058	+.056	+.095	+.144	+.023	−.110
Oven-treated 7 days:								
Crosswise	−.260	−.216	−.184	−.071	−.025	+.035	−.098	−.226
Lengthwise	−.217	−.174	−.137	−.041	−.002	+.062	−.062	−.187
REGULAR FILM BASE—Ss. PANCHROMATIC—SAMPLE *G*								
Unprocessed:								
Crosswise	−0.224	−0.195	−0.130	+0.024	+0.052	+0.135	−0.046	−0.237
Lengthwise	−.216	−.189	−.122	+.011	+.056	+.146	−.027	−.211
Oven-treated 7 days:								
Crosswise	−.377	−.342	−.285	−.151	−.078	+.023	−.156	−.328
Lengthwise	−.336	−.305	−.251	−.130	−.066	+.039	−.136	−.297
REGULAR FILM BASE—Ss. PANCHROMATIC—SAMPLE *H*								
Unprocessed:								
Crosswise	−0.154	−0.115	−0.055	+0.044	+0.082	+0.136	+0.005	−0.130
Lengthwise	−.143	−.103	−.040	+.087	+.140	+.190	+.070	−.067
Processed:								
Crosswise	−.216	−.174	−.112	+.007	+.065	+.132	−.030	−.183
Lengthwise	−.199	−.160	−.083	+.048	+.114	+.174	+.011	−.130
REGULAR FILM BASE—Ss. PANCHROMATIC—SAMPLE *I*								
Unprocessed:								
Crosswise	−0.141	−0.103	−0.038	+0.063	+0.121	+0.211	+0.077	−0.054
Lengthwise	−.121	−.086	−.023	+.085	+.139	+.221	+.091	−.028
Oven-treated 7 days:								
Crosswise	−.192	−.155	−.089	+.012	+.078	+.183	+.025	−.106
Lengthwise	−.154	−.118	−.068	+.031	+.080	+.176	+.028	−.090
REGULAR FILM BASE—Ss. PANCHROMATIC—SAMPLE *J*								
Unprocessed:								
Crosswise	−0.145	−0.106	−0.053	+0.058	+0.115	+0.178	+0.068	−0.068
Lengthwise	−.124	−.080	−.030	+.092	+.143	+.201	+.094	−.026
Oven-treated 7 days:								
Crosswise	−.202	−.158	−.100	+.012	+.076	+.153	+.020	−.113
Lengthwise	−.154	−.108	−.060	+.035	+.082	+.150	+.030	−.089

TABLE 1.—*Dimensional change of films in percentages as a function of relative humidity*—Continued

Treatment and direction of measurement	RELATIVE HUMIDITY							
	32%	43%	50%	65%	76%	86%	65%	50%
REGULAR FILM BASE—Ss. PANCHROMATIC—SAMPLE								
Unprocessed:								
Crosswise	−0.190	−0.137	−0.087	+0.038	+0.090	+0.193	−0.003	−0.064
Lengthwise	−.144	−.108	−.059	+.043	+.082	+.148	+.004	−.123
Processed:								
Crosswise	−.261	−.207	−.151	+.006	+.081	+.180	−.055	−.241
Lengthwise	−.191	−.156	−.101	+.019	+.061	+.127	−.039	−.174
REGULAR FILM BASE—INFRARED SENSITIVE—SAMPLE *N*								
Unprocessed:								
Crosswise	−0.154	−0.115	−0.060	+0.040	+0.098	+0.136	−0.004	−0.149
Lengthwise	−.143	−.102	−.059	+.038	+.100	+.136	−.003	−.137
Processed:								
Crosswise	−.206	−.168	−.110	−.004	+.072	+.119	−.038	−.182
Lengthwise	−.191	−.147	−.094	+.017	+.076	+.119	−.033	−.166
TOPOGRAPHIC FILM BASE—Ss. PANCHROMATIC—SAMPLE *O*								
Unprocessed:								
Crosswise	−0.179	−0.120	−0.080	+0.040	+0.091	+0.134	+0.025	−0.103
Lengthwise	−.160	−.113	−.073	+.043	+.093	+.138	+.028	−.098
Oven-treated 7 days:								
Crosswise	−.231	−.187	−.147	−.027	+.034	+.099	−.030	−.164
Lengthwise	−.221	−.180	−.142	−.042	+.016	+.073	−.045	−.173
TOPOGRAPHIC FILM BASE—Ss. PANCHROMATIC—SAMPLE *P*								
Unprocessed:								
Crosswise	−0.155	−0.094	−0.051	+0.060	+0.095	+0.176	+0.054	−0.067
Lengthwise	−.151	−.095	−.048	+.086	+.130	+.201	+.085	−.048
Processed:								
Crosswise	−.215	−.151	−.102	+.025	+.085	+.170	+.011	−.121
Lengthwise	−.207	−.152	−.088	+.050	+.109	+.183	+.032	−.098
TOPOGRAPHIC FILM BASE—Ss. PANCHROMATIC—SAMPLE *Q*								
Unprocessed:								
Crosswise	−0.136	−0.096	−0.057	+0.063	+0.106	+0.191	+0.055	−0.053
Lengthwise	−.134	−.083	−.053	+.077	+.119	+.192	+.064	−.040
Processed:								
Crosswise	−.194	−.146	−.100	+.045	+.108	+.178	+.023	−.095
Lengthwise	−.205	−.149	−.097	+.046	+.103	+.164	+.017	−.101
Unprocessed:								
Crosswise	−.225	−.182	−.124	−.004	+.049	+.144	+.007	−.111
Lengthwise	−.221	−.174	−.118	−.011	+.033	+.122	−.007	−.126
Oven-treated 7 days:								
Crosswise	−.290	−.252	−.194	−.047	+.004	+.065	−.045	−.188
Lengthwise	−.295	−.260	−.205	−.079	−.030	+.022	−.081	−.216
Oven-treated 14 days:								
Crosswise	−.293	−.261	−.197	−.055	+.005	+.070	−.053	−.190
Lengthwise	−.296	−.261	−.211	−.082	−.031	+.017	−.091	−.211
TOPOGRAPHIC FILM BASE—Ss. PANCHROMATIC—SAMPLE *R*								
Unprocessed:								
Crosswise	−0.151	−0.108	−0.044	+0.080	+0.135	+0.210	+0.089	−0.048
Lengthwise	−.140	−.086	−.045	+.071	+.122	+.190	+.062	−.054
Processed:								
Crosswise	−.213	−.167	−.093	+.040	+.120	+.194	+.032	−.107
Lengthwise	−.200	−.146	−.088	+.045	+.104	+.169	+.020	−.100

TABLE 1.—*Dimensional change of films in percentages as a function of relative humidity*—Continued

Treatment and direction of measurement	RELATIVE HUMIDITY							
	32%	43%	50%	65%	76%	86%	65%	50%
TOPOGRAPHIC FILM BASE—FINE-GRAIN PANCHROMATIC—SAMPLE *S*								
Unprocessed:								
Crosswise	−0.138	−0.094	−0.048	+0.068	+0.115	+0.214	+0.087	−0.045
Lengthwise	−.135	−.090	−.049	+.058	+.108	+.189	+.062	−.054
Processed:								
Crosswise	−.193	−.142	−.082	+.040	+.106	+.202	+.044	−.096
Lengthwise	−.190	−.140	−.089	+.035	+.088	+.174	+.018	−.103
LOW-SHRINKAGE FILM—Ss. PANCHROMATIC—SAMPLE *T*								
Unprocessed:								
Crosswise	−0.148	−0.098	−0.075	+0.042	+0.095	+0.159	+0.004	−0.132
Lengthwise	−.144	−.094	−.071	+.051	+.108	+.151	+.013	−.115
Processed:								
Crosswise	−.219	−.170	−.134	+.012	+.084	+.130	−.036	−.187
Lengthwise	−.228	−.177	−.140	+.018	+.084	+.123	−.036	−.177
LOW-SHRINKAGE FILM—Ss. PANCHROMATIC—SAMPLE *U*								
Unprocessed:								
Crosswise	−0.150	−0.097	−0.065	+0.055	+0.093	+0.145	+0.005	−0.124
Lengthwise	−.166	−.109	−.077	+.068	+.106	+.158	+.027	−.099
Processed:								
Crosswise	−.226	−.174	−.135	+.011	+.074	+.116	−.046	−.188
Lengthwise	−.238	−.182	−.134	+.024	+.081	+.127	−.026	−.163

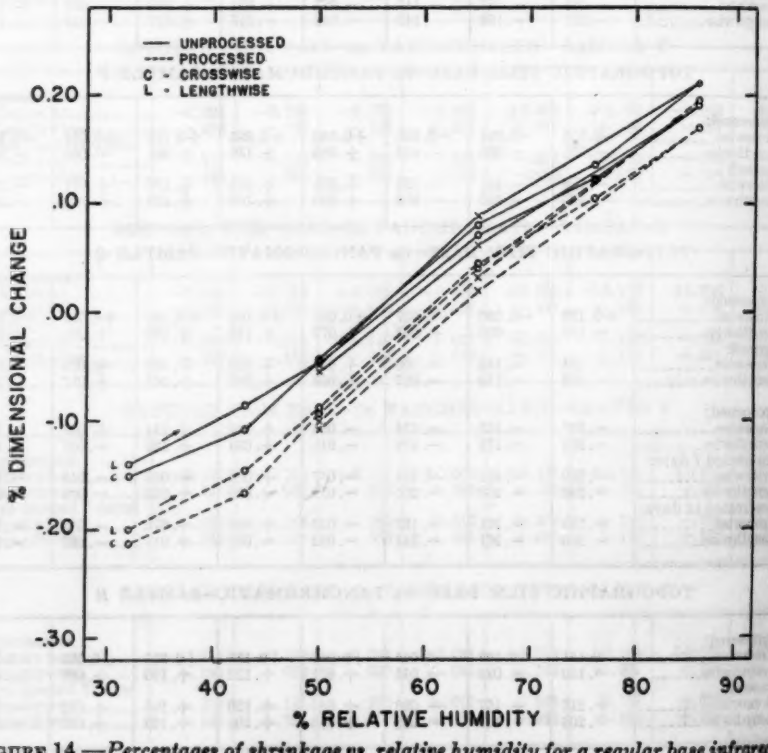

FIGURE 14.—*Percentages of shrinkage vs. relative humidity for a regular base infrared-sensitive film (sample N, table 1).*

It was expected that the film should show a hysteresis effect when the humidity was varied—that is, the dimensional changes of the film should lag behind the changes in relative humidity. Ordinarily, a curve showing the relation between cause and effect in a material which exhibits hysteresis is an S curve or a lenticular-shaped curve. The curves of figures 14 to 19, as a whole, do not properly fit this description. It should be remembered that this series of measurements at different relative humidities was made over a long period of time (about 9 weeks), and that the films were losing some solvent,

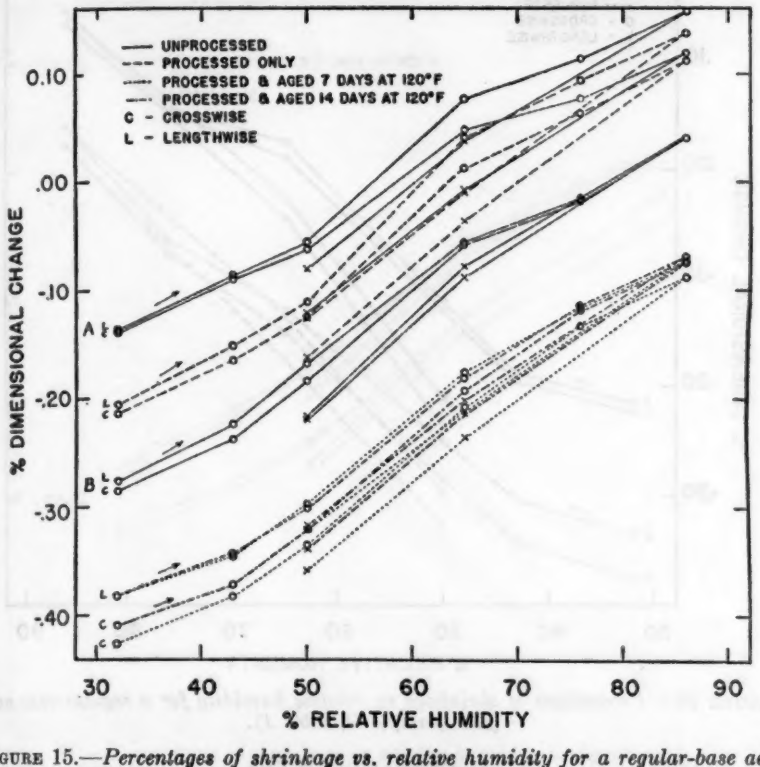

FIGURE 15.—*Percentages of shrinkage vs. relative humidity for a regular-base aero-film (sample C, table 1).*

consequently shrinking somewhat all the time. The rate of shrinkage due to this cause is probably not the same at different humidities, and therefore, it would be difficult to make a correction for it. This shrinkage is suggested in that the descending portions of most of the curves shown lie below the ascending portions, instead of above them as in the case of hysteresis curves of paper. With this in mind, it can be seen that certain of the curves, sample *N*, figure 14, the oven-treated test strips of sample *C*, figure 15, and sample *O*, figure 17, are S-shaped.

At 76-percent relative humidity and above, most of the curves seem erratic. In these cases, the observed expansion is too high, probably owing to the gelatin which takes on water more readily than the celluloid and being in contact with the celluloid may have the effect of accelerating the hydration. Hydration and dehydration of the gelatin coating are accompanied by larger expansion and contraction than the celluloid base. This effect is illustrated in figure 20, which shows

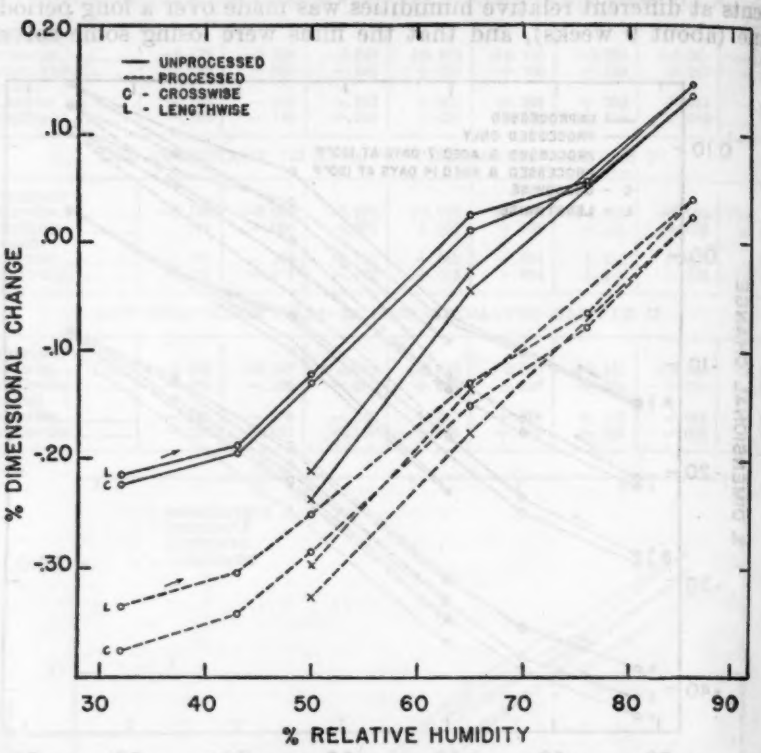

FIGURE 16.—*Percentages of shrinkage vs. relative humidity for a regular-base aero-film (sample G, table 1).*

four bottles, each containing two strips of film, one cut lengthwise and the other cut crosswise from the roll. The bottles are closed and each contains a solution to maintain a fixed relative humidity. The relative humidities are, from left to right, 11, 37, 77, and 88 percent. The emulsion sides of the films are to the right. It will be noticed that the film cut lengthwise tends to uncurl as the humidity increases. The sample cut crosswise actually bends backward in the 88-percent relative humidity bottle (fig. 20). At about 65- to 70-percent relative humidity films do not curl.

VIII. FILM SHRINKAGE DUE TO PROCESSING AND ACCELERATED AGING

The effect of processing and of accelerated aging on the dimensions of aerofilm was investigated. Accelerated aging consists in keeping the film in an oven at 120° F (49° C) for 7 days. Two sets of conditions were imposed: One in which the films were conditioned at 50-percent relative humidity and 72° F, and the other in which they were conditioned at 65-percent relative humidity and 72° F.

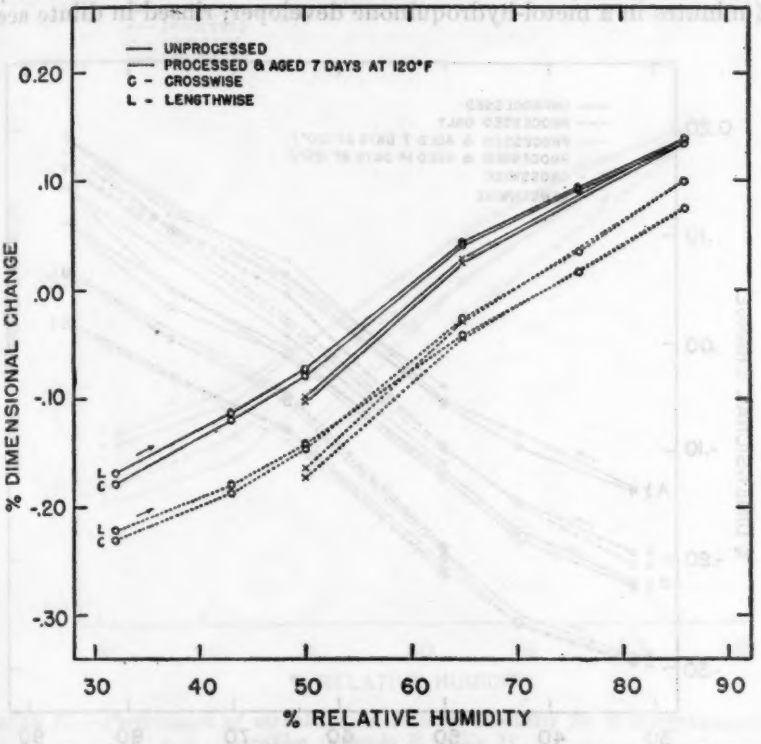

FIGURE 17.—*Percentages of shrinkage vs. relative humidity for topographic-base aerofilm (sample O, table 1).*

For the determinations at 50-percent relative humidity samples were taken from 21 different rolls of film, each having a different emulsion number, and representing six different types. Test strips were conditioned at 50-percent relative humidity and 72° F for 1 or 2 days, measured, processed, reconditioned for 2 days, and remeasured. Then one group of film strips was kept in an oven at 120° F (49° C) for 7 days, reconditioned at 50-percent relative humidity and 72° F (49° C) for 1 to 2 days, and remeasured to determine the shrinkage due to oven treatment (accelerated aging).

For the shrinkage determinations at 65-percent relative humidity, 8 by 9½-inch samples were taken from the same 21 rolls of films, and also 1 sample each from three 8- by 10-inch cut films. Sample *X* is chloride emulsion on a cellulose acetate base loaded with some material to make it white and fairly opaque. Its shrinkage is about the same as that of low-shrink base. Two separate determinations were made. The samples were conditioned at 65-percent relative humidity and 72° F in a light-tight cabinet with forced ventilation for 64 and 48 hours, respectively, then exposed in contact with a negative of a Max Levy ruled-glass grid with lines ½ inch apart. They were developed 2¼ minutes in a metol-hydroquinone developer, rinsed in dilute acetic

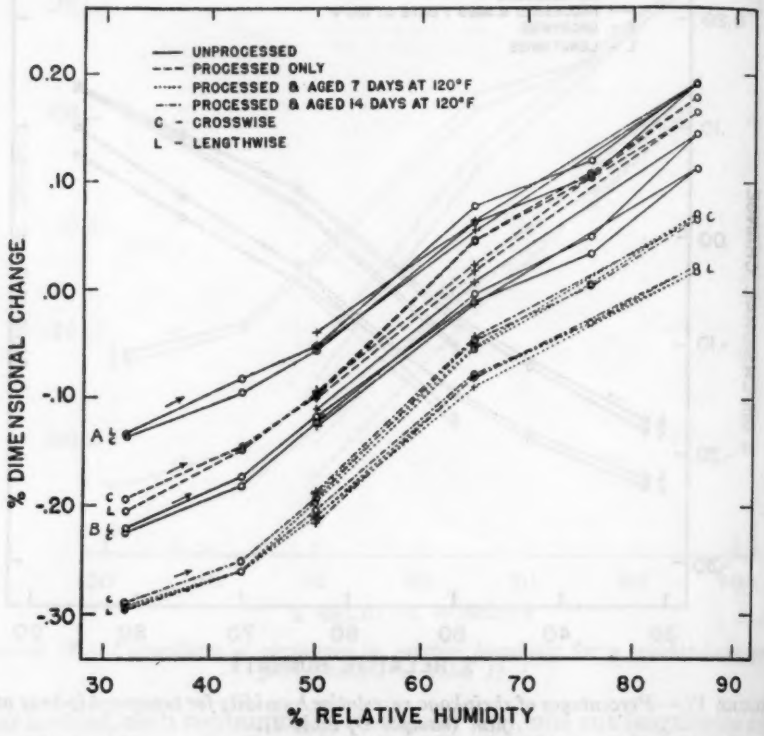

FIGURE 18.—*Percentages of shrinkage vs. relative humidity for a topographic-base aerofilm (sample Q, table 1).*

acid short-stop bath, fixed 12 minutes, washed ½ to 1 hour in running water, and dried in the laboratory. Then they were hung up and conditioned for 21 and 44 hours, respectively, at 65-percent relative humidity and 72° F, and measured on the optical gage to obtain the dimensional change caused by processing. After being measured they were placed in the oven for 7 days at 120° F (49° C) followed by 2 days reconditioning at 65-percent relative humidity and 72° C, and again measured to obtain the dimensional change due to accelerated aging.

The shrinkage of films based upon measurements at 50-percent relative humidity (table 2) is much greater than the shrinkage based on measurements at 65 percent (table 3). For instance, at 65-percent relative humidity, all the samples of aerofilm would pass Air Corps

Specification 31004B with respect to shrinkage, whereas at 50 percent, eight samples would not have passed this specification. This shows the need of specifying the conditions under which shrinkage is to be measured, if the specifications are to have a definite meaning.

The shrinkage of the aerofilm on special low-shrink base is just as large as that of the topographic aerofilm, both in amount of shrinkage and differential shrinkage. The amount of shrinkage is perhaps a little greater for the special low-shrink base.

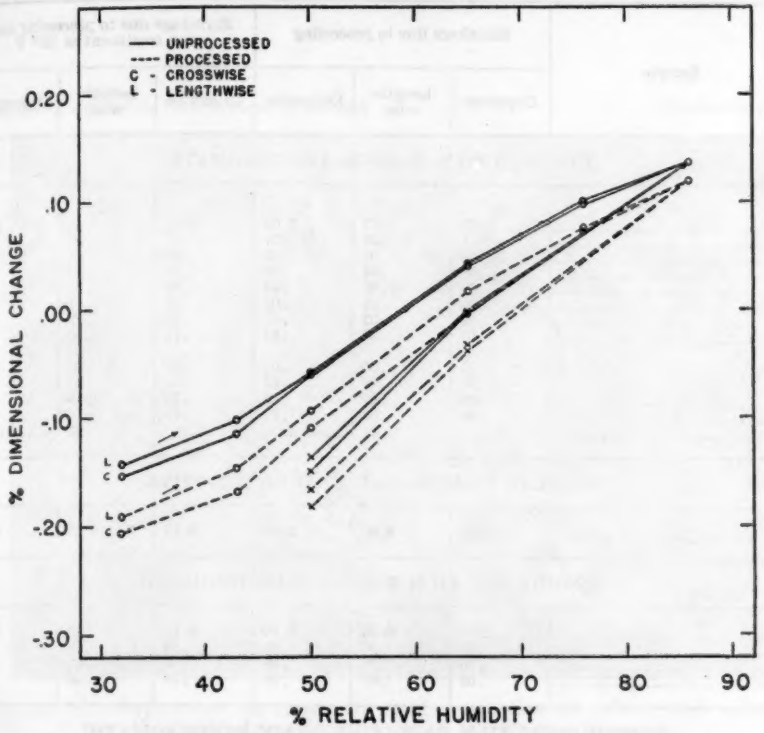

FIGURE 19.—*Percentages of shrinkage vs. relative humidity for a topographic-base aerofilm (sample R, table 1).*

IX. SHRINKAGE OF PHOTOGRAPHIC PAPERS CAUSED BY PROCESSING

The effect of processing on the dimensions of photographic printing papers was investigated for 32 different samples of contact printing papers and 25 different samples of projection papers. These were in sheets measuring 8 by 10 inches. The paper samples were conditioned in a light-tight conditioning cabinet with forced ventilation, for 24 hours at 65-percent relative humidity and 72° F. They were then exposed in contact with the grid. They were processed as follows: Contact papers developed 45 sec, projection papers 1.5 minutes, rinsed in acetic acid short-stop bath, fixed about 12 minutes, washed in running water for an hour, surface water blotted off, dried on cheesecloth covered drying racks in uncontrolled atmosphere and returned

to the conditioning room. After reconditioning for several days at 65-percent relative humidity and 72° F the papers were measured on the optical gage. The distance between lines 6 inches apart was measured at the center, and also about 1 inch from each edge, in both directions, crosswise and lengthwise.

TABLE 2.—*Percentage of shrinkage of aeromapping film*

[Conditioned at 50-percent relative humidity. Temperature 72° F.]

Sample	Shrinkage due to processing			Shrinkage due to processing and oven treatment at 120° F		
	Crosswise	Lengthwise	Difference	Crosswise	Lengthwise	Difference
	%	%	%	%	%	%
REGULAR FILM BASE—Ss. PANCHROMATIC						
A	0.07	0.05	0.02	0.14	0.09	0.05
B	.11	.07	.04	.17	.15	.02
C	.08	.06	.02	.20	.14	.06
D	.08	.03	.05	.34	.27	.07
E	.01	+.03	.04	.42	.27	.15
F	.05	.03	.02	.16	.11	.05
G	.04	.02	.02	.24	.22	.02
H	.09	.07	.02	.16	.10	.06
I	.01	.00	.01	.07	.05	.02
J	.03	.00	.03	.10	.06	.04
K	.10	.07	.03	.22	.18	.04
L	.00	.01	.01	.18	.16	.02
M	----------	.01	----------	----------	.23	----------
REGULAR FILM BASE—INFRARED SENSITIVE						
N	0.07	0.06	0.01	0.15	0.13	0.02
TOPOGRAPHIC FILM BASE—Ss. PANCHROMATIC						
O	0.03	0.03	0.00	0.13	0.13	0.00
P	.08	.07	.01	.14	.09	.05
Q	.06	.06	.00	.11	.09	.02
R	.08	.07	.01	.10	.10	.00
TOPOGRAPHIC FILM BASE—FINE GRAIN PANCHROMATIC						
S	0.06	0.07	0.01	0.10	0.10	0.00
LOW-SHRINKAGE BASE—Ss. PANCHROMATIC						
T	0.07	0.08	0.01	0.18	0.14	0.04
U	.07	.08	.01	.18	.15	.03

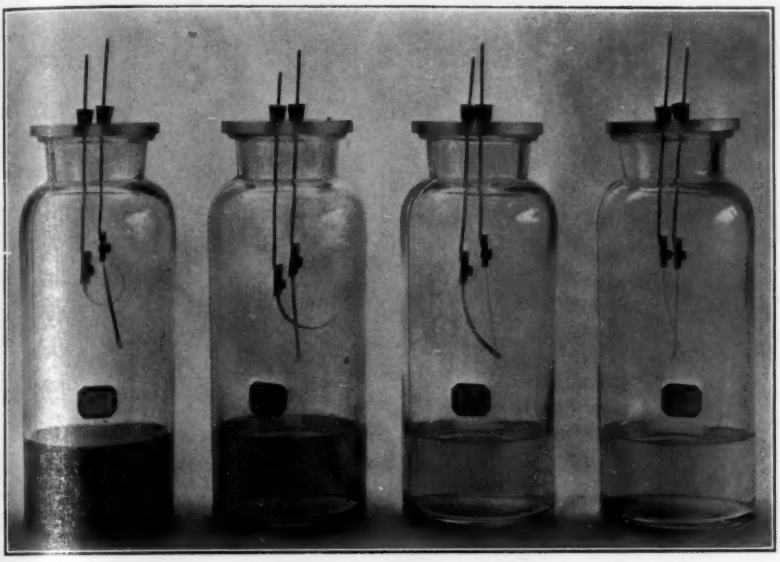

FIGURE 20.—*Differences in expansion and contraction of gelatin and celluloid, respectively, with differences in relative humidity.*

Gelatin side of films is to the right. Each bottle contains two samples of film, one cut lengthwise and one cut crosswise. From left to right the relative-humidity condition in the bottles is 11, 37, 77, and 88 percent, respectively. The sample cut lengthwise uncurls with increasing moisture.

UNIV. OF MICH.

TABLE 3.—*Percentage of shrinkage of aeromapping film*

[Conditioned at 65-percent relative humidity. Temperature 72° F.]

Sample	Shrinkage due to processing			Shrinkage due to processing and oven treatment at 120° F.		
	Crosswise	Lengthwise	Difference	Crosswise	Lengthwise	Difference
REGULAR FILM BASE—Ss. PANCHROMATIC						
	%	%	%	%	%	%
A	0.03	0.04	0.02	0.14	0.14	0.00
B	.03	.02	.01	.13	.11	.02
C	.02	.02	.00	.14	.13	.01
D	.05	.03	.02	.20	.18	.02
E	.05	.02	.03	.18	.17	.01
F	.02	.03	.01	.10	.12	.02
G	.02	.01	.01	.19	.18	.01
H	.03	.00	.03	.12	.08	.04
I	.02	.00	.02	.06	.08	.02
J	.00	.01	.01	.06	.07	.01
K	+.01	.01	.02	.14	.12	.02
L	.—	.02	.—	.—	.10	.—
M	.—	.02	.—	.—	.19	.—
REGULAR FILM BASE—INFRARED SENSITIVE						
N	0.02	0.02	0.00	0.11	0.11	0.00
TOPOGRAPHIC FILM BASE—Ss. PANCHROMATIC						
O	0.00	0.02	0.02	0.08	0.09	0.01
P	.01	.01	.00	.08	.09	.01
Q	.00	.01	.01	.05	.08	.03
R	.01	.01	.00	.06	.08	.02
TOPOGRAPHIC FILM BASE—FINE GRAIN PANCHROMATIC						
S	+0.01	0.01	0.02	0.05	0.07	0.02
LOW-SHRINKAGE BASE—Ss. PANCHROMATIC						
T	0.00	0.02	0.02	0.10	0.11	0.01
U	.01	.02	.01	.10	.11	.01
NITRATE CUT FILM—ORTHOCHROMATIC PRESS						
V	0.13	0.11	0.02	0.51	0.45	0.06
SAFETY CUT FILM—ORTHOCHROMATIC PRESS						
W	0.01	0.00	0.01	0.11	0.11	0.00
EXPERIMENTAL SAFETY CUT FILM						
X	0.01	0.01	0.00	0.11	0.10	0.01

The results of the measurements given in tables 4 and 5 were computed and tabulated as percentage dimensional changes of the papers caused by processing, along the machine direction, across the machine direction, and the difference between the changes in the two directions.

TABLE 4.—*Percentage of shrinkage of contact papers*

[Conditioned at 65 percent relative humidity. Temperature 70° F.]

Brand	Type of paper	Shrinkage		
		Crosswise	Lengthwise	Difference
SINGLE-WEIGHT REGULAR PAPERS—GLOSSY SURFACE				
A	Extra soft	0.23	0.15	0.08
	Normal	.32	.21	.11
	Medium	.22	.16	.06
B	Soft	.42	.02	.40
	Normal	.53	.01	.52
	Hard	.53	.04	.49
C	Extra soft	.23	.09	.14
	Soft	.19	.17	.02
	Normal	.24	.15	.09
	Medium	.27	.25	.02
	Hard	.23	.11	.12
	Extra hard	.26	.20	.06
D	Soft	.39	.23	.16
	Normal	.38	.26	.12
	Medium	.41	.29	.12
	Hard	.38	.25	.13
(*)	(*)	.22	.21	.01
SINGLE-WEIGHT REGULAR PAPERS—MATTE SURFACE				
A	Extra soft	0.29	0.27	0.02
	Hard	.21	.16	.05
DOUBLE-WEIGHT REGULAR PAPERS—GLOSSY SURFACE				
A	Normal	0.28	0.12	0.16
	Hard	.27	.10	.17
DOUBLE-WEIGHT REGULAR PAPERS—MATTE SURFACE				
A	Soft	0.34	0.14	0.20
	Normal	.30	.10	.20
	Medium	.32	.09	.23
	Hard	.28	.12	.16
	Extra hard	.35	.07	.28
B	Normal	.40	.34	.06
(*)	(*)	.39	.13	.26
(*)	(*)	.22	.12	.10
SPECIAL AEROMAPPING PAPERS				
X	Double weight	0.02	0.01	0.01
Y	Single weight	.44	.29	.15
	Double weight	.13	.12	.01

* Unknown.

TABLE 5.—*Percentage of shrinkage of enlarging papers*

[Conditioned at 65-percent relative humidity. Temperature 70° F.]

Brand	Type of paper, contrast and surface	Shrinkage		
		Crosswise	Lengthwise	Difference
SINGLE-WEIGHT REGULAR PAPERS				
E	Medium	0.27	0.17	0.10
F	Medium semimatte	.41	.27	.14
G	Medium semimatte	.36	.24	.12
	Medium glossy	.29	.15	.14
	Medium extra hard	.54	.31	.23
(a)	Glossy (a)	.30	.28	.02
DOUBLE-WEIGHT REGULAR PAPERS				
H	Medium matte	0.41	0.21	0.20
	Hard matte	.27	.24	.03
I	Hard	.23	.09	.14
J	Soft matte	.45	.17	.28
	Normal matte	.39	.17	.22
	Medium matte	.39	.11	.28
	Hard matte	.43	.16	.27
	Extra hard matte	.41	.15	.26
K	Medium semigloss	.48	.13	.35
	Hard semigloss	.43	.12	.31
L	Hard matte	.35	.08	.27
(a)	Medium matte	.34	.33	.01
	White rough matte	.44	.13	.31
	White rough matte	.60	.14	.46
SPECIAL AEROMAPPING PAPERS				
W	Hard matte	0.43	0.29	0.14
X	Double weight	.03	.02	.01
Y	Single weight	.44	.25	.19
	Double weight	.18	.16	.02
METAL LAMINATED PAPER				
Z	Semimatte	0.004	+0.001	0.005

(a) Unknown.

The following papers were found to have very small shrinkage: Brand *Z*, a bromide paper, is a laminated material composed of a sheet of hard aluminum foil cemented between paper. Its shrinkage from processing was less than 0.01 percent. One sample was dried in the oven at 120° F for 24 hours and remeasured. It shrank only 0.03 and 0.01 percent, respectively, in two directions at right angles. Brand *X* is a waterproof paper, made with both contact and enlarging emulsions. The shrinkage of the contact and enlarging papers from processing was 0.02 and 0.03 percent along and 0.01 and 0.02 percent across the sheet, respectively. Their shrinkage caused by 24 hours in the oven at 120° F was 0.02 and 0.03 percent along and 0.07 and 0.06 percent across the sheet, respectively.

The rest of the papers were found to have a maximum shrinkage ranging from about 0.20 to 0.50 percent, four papers having more than 0.50 percent. The differential shrinkage of the papers (i. e., the difference in shrinkage in two directions) ranged from 0.01 to 0.35 percent. Four samples had a differential shrinkage of 0.45 to 0.50 percent. Nine samples had a differential shrinkage of 0.03 percent or less (exclusive of the three papers mentioned above with low maximum shrinkage).

X. SUMMARY AND RECOMMENDATIONS

This investigation shows that, under controlled conditions, film shrinkage caused by processing is quite small. Even with 7 days of accelerated aging, the differential shrinkage is, with one exception, under 0.10 percent. A comparison of the data in tables 2 and 3 shows that the shrinkage is noticeably smaller at 65-percent relative humidity conditioning; in fact, the films which had the highest differential shrinkage at 50 percent show small shrinkage at 65 percent. This indicates that the best results from an accuracy standpoint could be had if all of the work with films is done in a room conditioned at 65-percent relative humidity and 72° F. A humidity much above 65 percent could not be recommended, because at higher humidities the dimensional behavior of films is erratic.

With photographic papers the results are not so satisfactory. The differential shrinkage is generally above 0.10 percent, but occasionally very low values were obtained without apparent reason, while in other papers of the same brand having different contrast numbers, the shrinkage was much higher. Another inconsistency is that double-weight papers, as a class, have larger differential shrinkage than single-weight papers. Two of the special aeromapping papers gave very low shrinkage and low differential shrinkage. One of these consists of two pieces of waterproofed paper laminated with a sheet of hard aluminum-alloy foil; the other is a cellulose lacquered paper.

The hygroscopic nature of film and paper makes it necessary to adopt, as standard, a fixed condition of temperature and moisture content of the air to which such materials may be subjected at the time of testing. In use, these materials are generally handled under uncontrolled conditions. The shrinkage values given in this paper therefore will not be realized in practice.

Undoubtedly, differential shrinkage in paper can be greatly reduced. Since handmade paper does not have this effect it would seem that paper manufacturers might, after some study, find methods for laying the pulp on the wire so as to prevent lining up the fibers with the machine direction and for reducing the tension to a minimum on the machine. This is an old problem, the cause is known, and the cure should not be too difficult for modern engineers.

We recommend that the machine direction of cut-to-size film and paper be identified by the manufacturer, either on the package or by printing on the back in the case of paper. If this is done, the total differential shrinkage of the combined negative and print or enlargement can be kept at a minimum by having the machine direction of negative and positive material at right angles to each other.

For example:

	Machine direction parallel shrinkage (%)			Machine direction at right angles shrinkage (%)		
	Cross-wise	Length-wise	Diff.	Cross-wise	Length-wise	Diff.
Negative	0. 42	0. 27	0. 15	0. 42	0. 27	0. 15
Positive	. 23	. 09	. 14	. 09	. 23	. 14
	0. 65	0. 36	0. 29	0. 51	0. 50	0. 01

Under the recommended conditions the combined differential shrinkage of the positive and negative material would always be less than the value for the material having the greatest differential shrinkage.

It would appear that only nitrate film is used in aerosurveying. Nitrate film is known to be unstable chemically, decomposing spontaneously with time, so that negatives made on this type of base cannot be classed as permanent. In addition, a large quantity of nitrate film concentrated in one place constitutes a serious fire hazard with the consequent danger to such official records and personnel as may be in the immediate vicinity. The better grades of cellulose acetate base are much more stable chemically than the nitrate base, being in a class with high grade paper with respect to fire hazard and permanence. Acetate film is not used in surveying because it is believed to have inferior shrinkage characteristics. We are unable to find any reliable data on this point and would recommend that a study, similar to that given in this report, be made on acetate film. Considering the lack of permanence and the hazard in storing nitrate film, together with the good behavior of two samples of acetate cut film given in table 3 (last two films), it seems that further attention to this kind of film is warranted.

WASHINGTON, October 19, 1937.

U. S. Department of Commerce National Bureau of Standards

RESEARCH PAPER RP1052

Part of Journal of Research of the National Bureau of Standards, Volume 19, December 1937

GULOHEPTONIC ACIDS AND α-*d*-α-GULOHEPTOSE [1]

By Horace S. Isbell

ABSTRACT

The barium and lead salts of the guloheptonic acids have been made and used for the preparation of the corresponding free acids. The gamma lactone of *d*-α-guloheptonic acid was prepared and reduced with sodium amalgam to give *d*-α-guloheptose, which crystallized in the alpha modification. This new sugar is structurally related to α-*l*-talose and exhibits similar properties. Its mutarotation is complex, consisting in a fast change followed or accompanied by a smaller slow change. The proportions of the constituents involved in the rapid reaction vary with temperature so that a change in temperature results in a rapid mutarotation. The temperature coefficient for the rapid mutarotation corresponds with those for the rapid reactions which cause the deviations in the mutarotations of galactose, arabinose, talose, ribose, and *d*-β-glucoheptose, while the temperature coefficient for the slow change agrees with those for the mutarotations of glucose, mannose, gulose, and other reactions which consist in the interconversion of the alpha and beta pyranoses. The parallelism between the properties of talose and *d*-α-guloheptose is evidence that the configurations of the first five carbon atoms determine in large measure the composition of equilibrium solutions of these sugars.

CONTENTS

	Page
I. Mutarotation and properties of α-*d*-α-guloheptose	639
II. The guloheptonic acids and their salts	644
III. Experimental details	646
1. Separation of the acids obtained from the cyanhydrin synthesis	646
2. *d*-β-Guloheptonic acid	646
3. *d*-α-Guloheptonic acid	647
4. Preparation of α-*d*-α-guloheptose	648
IV. Summary	649
V. References	650

I. MUTAROTATION AND PROPERTIES OF α-*d*-α-GULOHEPTOSE

In the course of an investigation [1, 2, 3] [2] of the alpha and beta sugars, a large number of the heptoses have been examined [4] in order to bring out the similarity of structurally related sugars. It has been emphasized that each pentose, ketose, heptose, or other sugar can be considered as structurally related to one of the fundamental types represented by the eight hexoses, glucose, mannose, galactose, talose, gulose, idose, allose, and altrose. Glucose, mannose, and galactose have been investigated extensively, but very

[1] Read at the meeting of the American Chemical Society, Rochester, N. Y., September 1937.

[2] The numbers in brackets here and elsewhere in the text correspond to the numbered literature references at the end of this paper.

little is known about substances containing the talose, gulose, idose, allose, and altrose structures.

Recently [5] the reactions and properties of α-*d*-talose (I) and β-*d*-talose (II) have been studied in the Bureau's laboratory and found to correspond in large measure with those of *l*-ribose (III). It is of further interest to extend the study to the structurally related heptoses. The heptoses structurally related to α-*d*-talose are α-*d*-β-mannoheptose (IV) and α-*l*-α-guloheptose (V). These substances are obtained by means of the cyanhydrin synthesis from *d*-mannose and *l*-gulose, respectively. Crystalline *d*-β-mannoheptose was prepared by Ettel [6], while crystalline *l*-α-guloheptose is not known at present. The author has prepared crystalline α-*d*-α-guloheptose (VI), which is enantiomorphic with α-*l*-α-guloheptose and hence has like properties, except as to the sign of the rotation and as to reactions involving asymmetric substances.

The new sugar crystallizes in slender needle-like prisms which melt at 127° C and give $[\alpha]_D^{20}=-45.7$. When dissolved in water the sugar exhibits the complex mutarotation given in table 1. This mutarotation can be represented by the following equations:

$$[\alpha]_D^{20.1}=-5.2\times10^{-.0179t}-23.6\times10^{-.0897t}-16.9 \quad (1)$$

$$[\alpha]_D^{0.3}=-5.9\times10^{-.00307t}-16.3\times10^{-.0187t}-20.2 \quad (2)$$

in which t is the time measured in minutes after the sugar is dissolved in water. The complex mutarotation shows that the equilibrium is established between certain modifications more rapidly than between the others, and that the solution contains at least three modifications of the sugar in dynamic equilibrium. Inspection of the data and equations representing the mutarotation at 20° C reveals that the rapid reaction, m_2, is responsible for a change of 23.6°, whereas the slow reaction, m_1, is responsible for a change of 5.2°. In other words, the rapid reaction predominates. This is in marked contrast to the mutarotation of glucose, which consists almost exclusively in the slow reaction. On the other hand, the mutarotation of levulose appears to consist almost exclusively in the rapid reaction,[3] and that of talose like that of α-*d*-α-guloheptose consists in the two reactions, with the fast reaction predominating.

[3] The temperature coefficients, effect of catalysts, and other evidence indicate that the normal mutarotation of levulose is like the *rapid* initial mutarotation reaction found for many aldoses and differs from the normal α-β pyranose mutarotation. The mutarotations of levulose and related substances are being studied in the Bureau's laboratory from this viewpoint.

TABLE 1.—*Mutarotation of α-d-α-guloheptose in water* [1]

0.9957 g in 25 ml at 20.1°C in a 4-dm tube

$°S = -2.38\times10^{-.0179t} - 10.87\times10^{-.0887t} - 7.77$

$[\alpha]_D^{20.1} = -5.2\times10^{-.0179t} - 23.6\times10^{-.0887t} - 16.9$

Initial rotation, $[\alpha]_D^{20.1} = -45.7$

Equilibrium rotation, $[\alpha]_D^{20.1} = -16.9$

Time	Observed reading	$m_1\times10^3$	Deviation	$m_2\times10^3$
Minutes	°S			
2.01	−17.15		7.18	
2.83	−15.90		6.61	94.1
3.68	−14.88		5.06	91.0
5.02	−13.67		3.96	85.8
6.91	−12.27		2.71	86.3
8.89	−11.17		1.75	89.1
11.36	−10.37		1.11	86.7
14.28	−9.59		.50	94.3
17.50	−9.20		.27	92.0
20.22	−8.99		.18	87.9
25.42	−8.62		(.01)	
30.44	−8.45			
35.82	−8.31	18.6		
45.30	−8.14	17.8		
61.13	−7.97	17.3		
∞	−7.77			
Average		17.9		89.7

1.0022 g in 25 ml at 0.3° C in a 4-dm tube

$°S = -2.71\times10^{-.0830t} - 7.56\times10^{-.0187t} - 9.36$

$[\alpha]_D^{0.3} = -5.9\times10^{-.0830t} - 16.3\times10^{-.0187t} - 20.2$

Initial rotation, $[\alpha]_D^{0.3} = -42.4$

Equilibrium rotation, $[\alpha]_D^{0.3} = -20.2$

3.27	−18.58		6.57	
4.76	−18.14		6.16	18.8
6.99	−17.56		5.65	17.6
9.91	−16.90		5.01	17.7
12.57	−16.33		4.49	17.8
15.55	−15.73		3.94	18.1
21.82	−14.68		2.99	18.4
25.05	−14.25		2.62	18.3
29.81	−13.72		2.16	18.2
35.08	−13.12		1.64	18.9
40.07	−12.73		1.34	18.8
49.93	−12.07		.80	19.6
60.48	−11.61		.48	19.9
70.05	−11.29		.28	20.5
90.37	−10.85		(.06)	
133.02	−10.42			
158.24	−10.24	3.20		
181.04	−10.10	3.25		
241.48	−9.84	3.17		
294.61	−9.73	2.83		
341.70	−9.62	2.92		
∞	−9.36			
Average		3.07		18.7

[1] The equations and values for the mutarotation constants, m_1 and m_2, were determined by the method described by Isbell and Pigman (J. Research NBS 18, 156 (1937) RP969). The values given in the column headed "deviation" represent the differences between the observed rotations and those calculated for like times by extrapolation of the mutarotation data for the latter part of the reaction, using the constant, m_1 and beginning the extrapolation after the rapid reaction is complete.

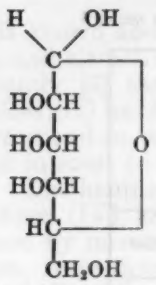

(I) *α-d*-Talose

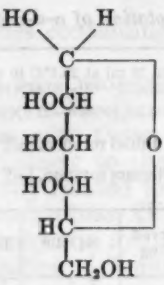

(II) *β-d*-Talose

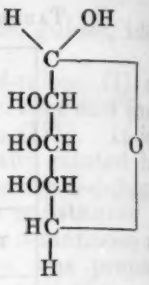

(III) *α-l*-Ribose

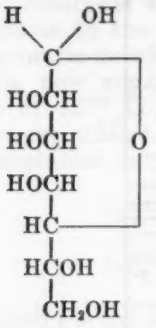

(IV) *α-d-β*-Mannoheptose

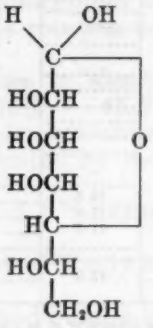

(V) *α-l-α*-Guloheptose

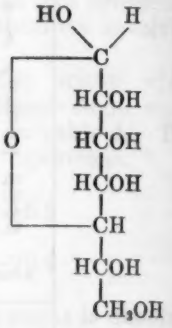

(VI) *α-d-α*-Guloheptose

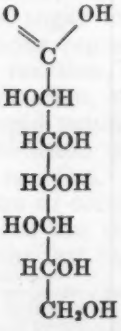

(VII) *d-β*-Guloheptonic acid

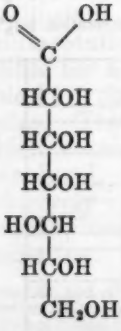

(VIII) *d-α*-Guloheptonic acid

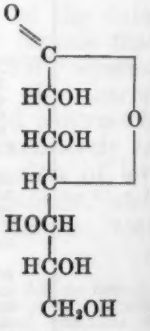

(IX) *d-α*-Guloheptonic-γ-lactone

The rapid mutarotation reaction for *α-d-α*-guloheptose is similar to the rapid mutarotation reactions of galactose [7, 8], arabinose [9], ribose [10], *β*-glucoheptose [11], talose [12], and levulose. As previously pointed out, whenever the temperature of a solution of galactose, arabinose, or talose is changed a mutarotation occurs. The changes in optical rotation suggest that the equilibrium proportions of the constituents responsible for the rapid reactions vary with temperature, whereas the equilibrium proportions of the constituents responsible for the slow reactions do not vary with temperature. The results given in table 2 show a similar thermal-mutarotation for

d-α-guloheptose. After the solution of d-α-guloheptose is cooled the optical rotation increases in the levo direction at a rate comparable to that of the rapid reaction (m_2). This change comprises the larger part of the mutarotation and shows that the change in temperature causes a disturbance in the equilibrium proportions of the labile constituents. This initial change appears to be followed by a readjustment of the proportions of the normal alpha and beta isomers. This causes a very small decrease in the optical rotation which occurs at a rate comparable to that of m_1. The large alteration in the equilibrium proportions of the constituents concerned in the rapid reaction shows that this reaction involves a large energy change, whereas the small alteration in the equilibrium proportions of the constituents involved in the slow reaction shows that in this case the heat of reaction is small.

TABLE 2.—*Mutarotation of a 5.5-percent aqueous solution of d-α-guloheptose after cooling from 30° to 0.4° C*

$°S = -0.4\times10^{-.00321t} + 3.6\times10^{-.0134t} - 12.8$

Time	Saccharimeter reading	$m_1\times10^3$	Deviation	$m_2\times10^3$
Minutes	°S		°S	
5.88	−10.20	----------	3.01	----------
8.45	−10.41	----------	2.79	12.8
11.03	−10.62	----------	2.57	13.3
14.05	−10.88	----------	2.31	14.1
17.28	−11.07	----------	2.11	13.5
20.73	−11.27	----------	1.90	13.5
24.81	−11.50	----------	1.66	13.7
30.20	−11.73	----------	1.42	13.4
37.21	−11.98	----------	1.15	13.3
45.41	−12.22	----------	0.90	13.3
60.92	−12.52	----------	.59	12.9
75.26	−12.70	----------	.36	13.3
156.41	−12.90	----------	(.06)	----------
240.00	−12.90	----------	----------	----------
310.00	−12.87	2.92	----------	----------
----------	−12.82	----------	----------	----------
Average...	----------	2.92	----------	13.4

The effects of temperature on the rates of reaction (m_1 and m_2) clearly demonstrate that the fast and slow reactions are fundamentally different. Previous measurements [4] have revealed that the temperature coefficients for the slow reactions are in every case less than those for the corresponding fast reactions. Thus, application of the Arrhenius equation to the measurements on mannose, galactose, talose, arabinose, and ribose gave for Q an average value of 16,900 from m_1, and 13,200 from m_2. Application of the same equation to the data for α-d-α-guloheptose gives corresponding values of 14,180 and 12,610. These are equal to temperature coefficients of 2.2 and 2.0 for m_1 and m_2, respectively.

Since nearly all of the free crystalline sugars contain the pyranose ring, it is probable that the new sugar is also a pyranose. If this be true, the oxygen of the ring lies to the left, and since the sugar is the more levorotatory number of the α-β pair, according to the author's nomenclature this should be designated α-d-α-guloheptose. The

[4] Page 165 of reference [3].

changes in optical rotation which have been found for *d*-α-guloheptose resemble in all respects the changes previously reported for α-*d*-talose. The marked parallelism illustrates in striking manner the advantages gained by basing the classification of the alpha and beta sugars on configurations of the pyranose ring, rather than on the configuration of the terminal asymmetric carbon.

II. THE GULOHEPTONIC ACIDS AND THEIR SALTS

In order to prepare the new sugar, it was necessary to study the separation of the epimeric acids obtained from *d*-gulose by the cyanhydrin synthesis. Previously, La Forge [14] applied the cyanhydrin synthesis to *d*-gulose and prepared the barium salts of the two guloheptonic acids. One of these acids he separated in the pure crystalline state; the other he obtained merely in an impure amorphous condition. The acid derived from the crystaline barium salt gave a levorotatory phenylhydrazide. This levorotation indicates that the hydroxyl on the second carbon lies to the left [15], and since the configurations of the remaining carbons are the same as those of *d*-gulose, the acid has the structure indicated by formula VII. As this was the first guloheptonic acid to be isolated, in accordance with the nomenclature of Fischer it was designated α-guloheptonic acid; and the second acid, which was not obtained pure, was called β-guloheptonic acid. Subsequently, in order to systematize the nomenclature,[5] the author suggested that the names be changed, so that the acids and their derivatives would be called alpha or beta according to whether the second carbon is of the same or different configuration from that of the terminal asymmetric carbon. In this paper the revised nomenclature is used, as illustrated by the names and formulas given on page 642.

The author has succeeded in preparing both of the guloheptonic acids in the crystalline state, as well as the crystalline lead and barium salts. Lead *d*-α-guloheptonate is more levorotatory than barium *d*-α-guloheptonate. The direction of these rotations is evidence [16] that the hydroxyl of the alpha carbon lies to the right, as illustrated in formula VIII. This acid also forms a crystalline phenylhydrazide which is dextrorotatory. The dextrorotation of this derivative substantiates the allocation of the hydroxyl of the alpha carbon to the right. When the crystalline acid is dissolved in water it undergoes lactone formation which gives rise to the mutarotation given in table 3.

TABLE 3.—*d-α-Guloheptonic acid*

4.100 g per 100 ml at 20° C in a 2-dm tube

$[\alpha]_D^{20} = {}^\circ S \times 4.222$

Time	Observed rotation	$[\alpha]_D^{20}$	Time	Observed rotation	$[\alpha]_D^{20}$
Hours	°S		*Hours*	°S	
0.04	−2.99	−12.6	7.2	−2.62	−11.1
.25	−2.99	−12.6	25.2	−1.85	−7.8
.50	−2.96	−12.5	50.7	−0.73	−3.1
1.0	−2.95	−12.5	96.5	+.35	+1.5
2.0	−2.92	−12.3	120.0	+.89	+3.8
2.9	−2.92	−12.3	144.5	+1.08	+4.6
4.2	−2.81	−11.9	168.5	+1.34	+5.7

[5] Page 529 of reference [4].

By dehydrating an aqueous solution of *d*-α-guloheptonic acid at 100° C the gamma lactone is formed. This substance is useful for the final purification of the acid and for the preparation of α-*d*-α guloheptose. The lactone is slowly hydrolyzed by water with regeneration of the free acid in small quantity and establishing an equilibrium state. This gives rise to the mutarotation given in table 4.

TABLE 4.—*d-α-Guloheptonic γ-lactone*

4.042 g per 100 ml at 20° C in a 4-dm tube		
Time	Observed rotation	$[\alpha]^{20}_D$
Hours	°S	
0.05	+11.91	25.5
5.6	+11.71	25.1
24	+11.55	24.8
72	+10.90	23.3
744	+8.30	17.8
105 days	+7.80	16.7

The salts of *d*-β-guloheptonic acid resemble those of *d*-α-guloheptonic acid and can be separated only by laborious fractional crystallization. Barium *d*-β-guloheptonate gives $[\alpha]^{20}_D = +1.5$, and lead *d*-β-guloheptonate gives $[\alpha]^{20}_D = +16.7$. The high dextrorotation of the lead salt in comparison with the rotation of the barium salt and the *l*-configuration of the alpha carbon are in harmony with the rule [16] correlating the optical rotations of the lead and alkaline earth salts with their configurations. The lead salt on treatment with sulphuric acid gives the free acid, which crystallizes readily. In aqueous solution the acid undergoes lactone formation, giving rise to the complex mutarotation reported in table 5. The character of the mutarotation shows that the delta lactone is formed more rapidly than the gamma lactone. Judging from the changes in optical rotation, the delta lactone is levorotatory in accordance with Hudson's lactone rule.

TABLE 5.—*d-β-Guloheptonic acid*

3.976 g per 100 ml at 20° C in a 4-dm tube $[\alpha]^{20}_D = °S \times 2.1768$					
Time	Observed rotation	$[\alpha]^{20}_D$	Time	Observed rotation	$[\alpha]^{20}_D$
Hours	°S		*Hours*	°S	
0.07	+5.88	+12.8	3.2	+4.81	+10.5
.2	+5.75	+12.5	5.0	+4.95	+10.8
.3	+5.61	+12.2	6.7	+5.16	+11.2
.5	+5.43	+11.8	23.5	+7.44	+16.2
1.0	+5.12	+11.1	47.9	+9.83	+21.4
2.0	+4.77	+10.4	72	+11.72	+25.5
2.5	+4.76	+10.4	222	+19.44	+42.3

III. EXPERIMENTAL DETAILS

1. SEPARATION OF THE ACIDS OBTAINED FROM THE CYANHYDRIN SYNTHESIS

The nitriles of *d*-α- and *d*-β-guloheptonic acids were formed by treating 500 g of gulose-calcium chloride [17] in a 10-percent aqueous solution with an equivalent quantity of sodium cyanide [18]. Hydrolysis of the product with an excess of lime gave a precipitate of basic calcium salts which was collected on a filter and washed. The basic salts were decomposed by carbonation to give a solution containing the normal calcium salts. This solution was mixed with sufficient sulphuric acid to combine with the calcium, and after the addition of one-half volume of isopropyl alcohol, the solution was filtered and the insoluble calcium sulphate was discarded. Rapid evaporation of the aqueous alcoholic solution under diminished pressure yielded 100 g of crystalline acid, which was separated by filtration. The crystalline product contained *d*-α-guloheptonic acid mixed with a small quantity of *d*-β-guloheptonic acid. In the absence of nuclei of crystalline *d*-β-guloheptonic acid, nearly pure *d*-α-guloheptonic acid is obtained at this point.

The crystalline acid thus obtained was used for the preparation of *d*-α-guloheptonic γ-lactone, as described in a separate paragraph. The amount of soluble acids and lactones in the mother liquor was ascertained by titration of a small sample with standard alkali, and then the equivalent quantity of lead oxide was added to convert the acids to normal lead salts. After the lead oxide had dissolved, the mixture was seeded with lead *d*-β-guloheptonate. After standing for several hours an abundant crystallization occurred. The crystalline salts were separated and found to be a mixture of lead *d*-β-guloheptonate and lead *d*-α-guloheptonate. By fractional recrystallization from hot water about 110 g of pure lead *d*-β-guloheptonate and 50 g of lead *d*-α-guloheptonate were obtained. The separation of the two salts, which may be followed by the optical rotations, requires numerous crystallizations. Both salts are relatively difficultly soluble in water and crystallize readily. Lead *d*-α-guloheptonate gives an optical rotation of -6.6, while lead *d*-β-guloheptonate gives $+16.7$.

2. *d*-β-GULOHEPTONIC ACID

Equivalent quantities of lead *d*-β-guloheptonate and 1 *N* sulphuric acid were mixed and then diluted with an equal volume of isopropyl alcohol. After separating the lead sulphate by filtration, the solution of *d*-β-guloheptonic acid was evaporated rapidly under diminished pressure to a thin sirup from which the crystalline acid separated in good yield. The acid crystallizes in diamond-shaped plates which frequently form in laminated clusters. The crystals melt at 135° C, and in a 4-percent aqueous solution give $[\alpha]_D^{20}=+12.8$. The new acid is soluble in water and much less soluble in alcohol and in acetic acid. After drying at 40° C in vacuo over calcium chloride the new acid corresponds to the following analysis: Calculated for $C_7H_{14}O_8$: C, 37.17; H, 6.24. Found: C, 37.23; H, 6.02. It tastes sour, reacts definitely acid, and requires one equivalent of alkali for neutralization.

Lead d-β-guloheptonate was first obtained from the crude acid resulting from the cyanhydrin synthesis. But for analysis the pure

salt was prepared from *d*-β-guloheptonic acid and an equivalent quantity of lead oxide. The salt crystallizes in concentric clusters of rhombic-shaped plates which are difficultly soluble in cold water, fairly soluble in hot water; at 20° C about 1 g dissolves in 100 ml. In a 2-percent aqueous solution, the new substance gives $[\alpha]_D^{20} = +16.7$. After drying in vacuo at 40° C over calcium chloride it corresponds to the following analysis: Calculated for Pb $(C_7H_{13}O_8)_2$: C, 25.57; H, 3.98; Pb, 31.51. Found: C, 25.67; H, 3.96; Pb, 31.6.

Barium d-β-guloheptonate, first prepared by La Forge [15], was obtained by neutralization of the acid with barium carbonate. The salt crystallizes in rhombic-shaped plates frequently truncated, thereby forming elongated hexagons. In a 3-percent aqueous solution the product gives $[\alpha]_D^{20} = +1.5$. After drying at 40° C in vacuo over calcium chloride it corresponds to the following analysis: Calculated for $Ba(C_7H_{13}O_8)_2$: C, 28.61; H, 4.46; Ba, 23.37. Found: C, 28.29; H, 4.34; Ba, 23.25.

3. *d*-α-GULOHEPTONIC ACID

The crude crystalline acid, obtained from the cyanhydrin synthesis, was purified by converting it into the crystalline γ-lactone, which was recrystallized and then converted into lead *d*-α-guloheptonate. This salt was mixed with an equivalent quantity of dilute aqueous sulphuric acid and after the addition of one-half volume of isopropyl alcohol the solution was filtered. The filtrate was concentrated under reduced pressure to a thin sirup which was then mixed with an equal volume of isopropyl alcohol. Crystalline *d*-α-guloheptonic acid separated in long slender triangular prisms which melt at 128° C. The crude product was recrystallized by dissolving 10 g in 15 ml of water, adding 25 ml of acetic acid, and cooling to 0° C. After standing for several hours about 5 g of *d*-α-guloheptonic acid was separated. In a 4-percent aqueous solution the new acid gives $[\alpha]_D^{20} = -12.6$. After drying at 40° C in vacuo it corresponds to the following analysis: Calculated for $C_7H_{14}O_8$: C, 37.17; H, 6.24. Found: C, 36.35; H, 6.07. The product is sour, reacts acid, and requires one equivalent of alkali for neutralization. The analysis indicates that the product was slightly impure, but as only a small quantity of the material was at hand it was not purified further.

d-α-Guloheptonic γ-lactone was prepared by evaporating and heating an aqueous solution of *d*-α-guloheptonic acid in the presence of a few drops of hydrochloric acid The resulting thick sirup was dissolved in ethyl alcohol and allowed to stand. In the course of 2 days a new substance crystallized in irregular clusters of triangular-shaped plates (possibly truncated rectangular prisms). This substance was separated, recrystallized from ethyl alcohol, and dried at 40° C in vacuo, The product thus obtained is slightly sweet, reacts neutral, but is readily saponified by dilute alkali. It melts at 145° C and in a 4-percent aqueous solution it gives $[\alpha]_D^{20} = +25.5$ and the mutarotation given in table 4. The new substance which is *d*-α-guloheptonic γ-lactone corresponds to the folowing analysis: Calculated for $C_7H_{12}O_7$: C, 40.39; H, 5.81. Found: C, 40.56; H, 5.81.

d-α-Guloheptonic phenylhydrazide was prepared by mixing 1 g of α-guloheptonic acid with 1 ml of phenylhydrazine dissolved in 10 ml of 80-percent (by volume) aqueous ethyl alcohol. After standing for

several hours, crystalline *d*-α-guloheptonic phenylhydrazide separated in slender needle-like prisms which grew into elongated plates. The crystals, which melt with decomposition at 156° C, are difficultly soluble in 95-percent ethyl alcohol but readily soluble in 80-percent aqueous alcohol. After recrystallization from alcohol and drying at 40° C in vacuo the substance in water solution gives $[\alpha]_D^{20}=+29.3$ (0.4962 g in 25 ml read +6.72° S in a 4-dm tube) and corresponds to the following analysis: Calculated for $C_{13}H_{20}O_7N_2$: C, 49.36; H, 6.37. Found: C, 49.37; H, 6.32.

Barium d-α-guloheptonate was prepared in aqueous solution from equivalent quantities of *d*-α-guloheptonic acid and barium hydroxide. The salt crystallizes in rhombic-shaped plates which resemble those of barium *d*-β-guloheptonate. The product obtained after recrystallization from hot water and drying at 40° C in vacuo over calcium chloride gives $[\alpha]_D^{20}=-1.4$ in a 4-percent aqueous solution and corresponds to the following analysis: Calculated for $Ba(C_7H_{13}O_8)_2$: C, 28.61; H, 4.46; Ba, 23.37. Found: C, 28.78; H, 4.50; Ba, 23.37.

Lead d-α-Guloheptonate, $Pb(C_7H_{13}O_8)_2$, was prepared by mixing in an aqueous solution equivalent quantities of *d*-α-guloheptonic acid and lead oxide. The salt crystallizes from hot water in rhombic-shaped plates, which are relatively difficultly soluble in cold water; at 20° C, 0.824 g dissolved in 100 ml of water. The salt also crystallizes in needles which contain 1 molecule of water of crystallization. The anhydrous salt after drying at 40° C in vacuo gives $[\alpha]_D^{20}=-6.6$ in a 1-percent aqueous solution and corresponds to the following analysis: Calculated for $Pb(C_7H_{13}O_8)_2$: C, 25.57; H, 3.98; Pb, 31.51. Found: C, 25.55 H, 4.09; Pb, 31.3.

4. PREPARATION OF α-*d*-α-GULOHEPTOSE

Forty-five grams of *d*-α-guloheptonic γ-lactone, dissolved in 450 ml of water and 150 ml of ethyl alcohol, was reduced with 1,200 g of 3.25-percent sodium amalgam. The reduction was conducted at 0° C, while the solution was stirred and maintained at about pH 3.0 by adding 10-percent aqueous sulphuric acid. After the reaction was complete the resulting crystalline sodium sulphate and mercury were separated. The solution was then evaporated to a thin sirup, which was diluted with three volumes of methyl alcohol. This caused the crystallization of considerable sodium sulphate which was discarded. The solution was then evaporated to a sirup (50 ml) which was extracted with five volumes of ethyl alcohol. After standing several days, about 26 g of crystalline α-*d*-α-guloheptose separated. The crude sugar (25 g) was dissolved in water and the solution was clarified with decolorizing carbon and then concentrated under diminished pressure to a heavy sirup of about 85 Brix. This sirup was mixed with 50 ml of acetic acid and seeded with crystalline α-*d*-α-guloheptose. A satisfactory crystallization occurred during the course of several hours. The crystalline sugar was collected upon a filter and washed, first with acetic acid and finally with ethyl alcohol. This product was then recrystallized in like manner, with the exception that ethyl alcohol was substituted for the acetic acid. The resulting sugar was dried at 40° C in vacuo and used for the analysis and the mutarotation measurements reported in table 1. The sugar crystallizes in

long slender prisms which melt at 127° C. In a 4-percent aqueous solution the new sugar gives an initial specific rotation of −45.7; at equilibrium, $[\alpha]_D^{20}=-16.9$. The sugar is anhydrous, as shown by the following analysis: Calculated for $C_7H_{14}O_7$: C, 40.00; H, 6.71. Found: C, 39.93; H, 6.70.

IV. SUMMARY

By treating *d*-gulose $CaCl_2.H_2O$ with sodium cyanide followed by lime, basic calcium salts of the epimeric guloheptonic acids were precipitated. Decomposition of the mixture with aqueous sulphuric acid and concentration of the resulting solution gave *d*-α-guloheptonic acid ($C_7H_{14}O_8$), which melts at 128° C and gives $[\alpha]_D^{20}=-12.6$; *d-α-guloheptonic γ-lactone* ($C_7H_{12}O_7$) melts at 145° C and gives $[\alpha]_D^{20}=+25.5$; *d-α-guloheptonic phenylhydrazide* ($C_7H_{13}O_7N_2H_2C_6H_5$) melts at 156° C and gives $[\alpha]_D^{20}=+29.3$; *lead d-α-guloheptonate*, $Pb(C_7H_{13}O_8)_2$ gives $[\alpha]_D^{20}=-6.6$; and *barium d-α-guloheptonate*, $Ba(C_7H_{13}O_8)_2$, gives $[\alpha]_D^{20}=-1.4$. The mother liquor from *d*-α-guloheptonic acid yielded *d-β-guloheptonic acid*, $C_7H_{14}O_8$, which melts at 135° C and gives $[\alpha]_D^{20}=+12.8$; *lead d-β-guloheptonate*, $Pb(C_7H_{13}O_8)_2$, gives $[\alpha]_D^{20}=+16.7$; and *barium d-β-guloheptonate*, $Ba(C_7H_{13}O_8)_2$ gives $[\alpha]_D^{20}=+1.5$. The lead and barium salts are useful for the purification and separation of the two acids. Reduction of *d*-α-guloheptonic γ-lactone with sodium amalgam gives *d*-α-guloheptose, which was separated in the crystalline alpha form.

α-*d*-α-Guloheptose ($C_7H_{14}O_7$) melts at 127° C and in water solution gives $[\alpha]_D^{20}=-45.7$ initially, and exhibits mutarotation until at equilibrium $[\alpha]_D^{20}=-16.9$. Mutarotation measurements were conducted at two temperatures: at 20.1° C $[\alpha]_D=-5.2\times10^{-.0179t}-23.6\times10^{-.0897t}-16.9$; at 0.3° C $[\alpha]_D=-5.9\times10^{-.00307t}-16.3\times10^{-.0187t}-20.2$. The mutarotations show a fast change accompanied by a smaller slow change. Hence the equilibrium solution contains at least three modifications of the sugar in dynamic equilibrium. The proportions of the constituents involved in the rapid reaction vary with temperature so that a change in temperature results in a rapid mutarotation. The temperature coefficient for the rapid mutarotation reaction corresponds with those for the rapid reactions which cause the deviations in the mutarotations of galactose, arabinose, talose, ribose, and *d*-β-glucoheptose. On the other hand, the temperature coefficient for the slow change agrees with those for the slow reactions which cause the normal mutarotations of glucose, mannose, galactose, gulose, and talose. The structure, reactions, and properties of the new sugar resemble those of α-*d*-talose and provide additional evidence that the properties of the sugars are determined in large measure by the configuration of five carbon atoms comprising the pyranose ring.

The author expresses his appreciation to Clement J. Rodden of this Bureau who made the microanalyses, and to William F. Sager, Leonard Smith, and Alexander Sadle, student assistants, who prepared the gulose-calcium chloride and assisted in the preparation of the guloheptonic acids and the reduction of *d*-α-guloheptonic γ-lactone.

V. REFERENCES

[1] H. S. Isbell, J. Am. Chem. Soc. **54,** 1692 (1932).
[2] H. S. Isbell and W. W. Pigman, BS J. Research **10,** 337 (1933) RP534.
[3] H. S. Isbell and W. W. Pigman, J. Research NBS **18,** 141 (1937) RP969.
[4] H. S. Isbell, J. Research NBS **18,** 505 (1937) RP990.
[5] W. W. Pigman and H. S. Isbell, J. Research NBS. **19,** 189 (1937) RP1021.
[6] V. Ettel, Collection Czechoslov. Chem. Communications **4,** 504 (1932).
[7] C. N. Riiber and J. Minsaas, Ber. deut. chem. Ges. **59,** 2266 (1926).
[8] G. F. Smith and T. M. Lowry, J. Chem. Soc. **1928,** 666.
[9] C. N. Riiber, Kgl. Norske Videnskab Selskabs Forh. **3,** 66 (1930).
[10] F. P. Phelps, H. S. Isbell, and W. W. Pigman, J. Am. Chem. Soc. **56,** 747 (1934).
[11] H. S. Isbell, J. Am. Chem. Soc. **56,** 2789 (1934).
[12] H. S. Isbell and W. W. Pigman, J. Research NBS **16,** 553 (1936) RP892.
[13] H. S. Isbell, J. Chem. Education **12,** 96 (1935).
[14] F. B. La Forge, J. Biol. Chem. **41,** 251 (1920).
[15] P. A. Levene, J. Biol. Chem. **23,** 145 (1915).
[16] H. S. Isbell, J. Research NBS **14,** 306 (1935) RP770.
[17] H. S. Isbell, BS J. Research **5,** 741 (1930) RP226.
[18] C. S. Hudson, O. Hartley, and C. B. Purves, J. Am. Chem. Soc. **56,** 1248 (1934).

WASHINGTON, September 22, 1937.

U. S. DEPARTMENT OF COMMERCE NATIONAL BUREAU OF STANDARDS

RESEARCH PAPER RP1053

Part of Journal of Research of the National Bureau of Standards, Volume 19, December 1937

ARC AND SPARK SPECTRA OF YTTERBIUM

By William F. Meggers and Bourdon F. Scribner

ABSTRACT

A new description of conventional arc and spark spectra of ytterbium (neoytterbium, aldeberanium) has been completed in the wave-length range 2000 to 11 000 A. Wave-length measurements and intensity estimates are presented for 1,668 lines, 400 of which characterize neutral Yb atoms (Yb I spectrum), about 1,250 are due to singly ionized atoms (Yb II spectrum), and possibly a dozen belong to doubly ionized atoms (Yb III spectrum). Some spectral regularities are given for neutral and for singly ionized atoms. The ground states of Yb, Yb^+, and Yb^{++} atoms appear to be associated with the electron configurations, $4f^{14}6s^2$, $4f^{14}6s$, and $4f^{14}$, respectively.

CONTENTS

	Page
I. Introduction	651
II. Experiments	652
III. Results	653
IV. References	664

I. INTRODUCTION

In 1878, Marignac [1][1] discovered in gadolonite a new earth which he named ytterbium (Yb). Nearly 30 years later Urbain [2] succeeded in splitting ytterbium into two components, which he named neoytterbium (Ny) and lutecium (Lu). The same separation was made independently (and probably somewhat earlier) by Auer [3], who proposed the names aldeberanium (Ad) and cassiopeium (Cp). The common usage now is to represent the elements having atomic numbers 70 and 71 by the symbols Yb and Lu, respectively, except in Austria and Germany where Ad and Cp are more generally used.

Owing to the difficulty of separating rare earths from one another, and to the complex nature of their spectra, descriptions of the latter have long been in a most unsatisfactory state. In our recent paper [4] on the arc and spark spectra of lutecium, we remarked that all available samples of lutecium were contaminated by ytterbium and thulium so that the spectra of the former could not be unambiguously determined without simultaneous comparison with ytterbium and thulium spectra. Thus our attempt to produce a complete and trustworthy description of lutecium spectra naturally led to the production of similar data for thulium and ytterbium. Improved descriptions of these spectra are essential not only for purposes of spectroscopic identification and analysis, but also for the term analyses and interpretation or spectral structures characteristic of different

[1] Numbers in brackets refer to literature citations at the end of this paper.

atoms and ions. In the present paper we make public our latest description of the conventional arc and spark spectra of ytterbium, including some preliminary details about spectral structures.

The only spectroscopic tables published for ytterbium since the discovery of lutecium are the following [5]. Auer [3] first gave a list of 200 spark spectrum lines (2621.24 to 5897.56 A), but most of the wave lengths were borrowed from a table which Exner and Haschek had given for old ytterbium containing unrecognized lutecium. In 1910, Eder and Valenta [6] published 58 lines (5474.24 to 5788.87 A) observed in the arc spectrum and in 1911, reproduced spectrograms and gave tables of wave lengths [7] for the arc spectrum (169 lines 2615.48 to 6799.87 A) and for the spark spectrum (195 lines 2615.48 to 6799.87 A). The most complete tables were published, in 1911, by Exner and Haschek, who list 905 lines (2320.95 to 6799.91 A) observed in the arc spectrum [8] and 795 lines (2224.58 to 6489.31 A) in the spark spectrum [9]. These tables contain a considerable number of lutecium and thulium lines, and many ytterbium lines are common to both, without positive indication as to whether they belong to neutral or to ionized atoms. In 1914, Blumenfeld and Urbain [10] measured the wave lengths of 499 lines (2309.6 to 3499.4 A) most of which were believed to represent ytterbium, although many were recognized as possible impurities. The latest extensive description of Yb spectra consists of 422 lines (2271.51 to 7699.49 A) observed in the arc spectrum by Eder [11], neglecting more than 200 lines ascribed to impurities, principally Tm. The salts available for these early investigations of rare-earth spectra were so impure that great difficulty was experienced in sorting the lines and frequently the same lines were ascribed to two different elements. For example, [12] 2615.41 Yb, Lu; 2693.33 Yb, Lu; 3283.40 Yb, Tm; 3362.61 Yb, Tm; 3425.10 Yb, Tm; 3441.51 Yb, Tm; 3472.48 Yb, Lu; 3887.34 Yb, Er; 5074.32, De, Tm, Yb; 5307.11 Yb, Tm. Except for the temperature classification of 399 lines (2935.09 to 6799.58 A) by King [13], no further investigations of Yb spectra have been reported in the past 22 years.

II. EXPERIMENTS

Our first measurements of Yb spectra were made in 1929 when the investigation of Lu spectra was begun [4]. Samples of Lu and Yb oxides prepared by Auer, and obtained from Eder in 1919 when he discontinued his work in spectroscopy, were available. Although the chemical separation was far from complete, it was possible to make a fairly satisfactory assignment of lines to Lu and Yb by simultaneous comparison of arc and spark spectra. However, both salts contained some Tm as impurity which could not be completely identified without comparable data for Tm spectra. The first sample of Tm salt available for this purpose was generously supplied in 1933, by Professor B. S. Hopkins, University of Illinois, who also supplied a sample of Lu oxide and three samples of Yb oxide, one of which contained more Lu than Tm, another more Tm than Lu, and the third was entirely free from both Lu and Tm, but contained considerable lanthanum. This ytterbium material was purified by the electrolytic reduction method devised by L. F. Yntema [14]. Alkali (Li, Na, K) and alkaline-earth (Mg, Ca, Sr, Ba) impurities are usually present in rare-earth salts, but these have extremely simple spectra, which are

easily identified. Miscellaneous impurities were detected by comparing our final wave-length list with Kayser's Hauptlinien [12] and with a description of lanthanum spectra [15].

The procedures employed to insure the correct assignment of spectral lines to their emitter, both as regards chemical element and stage of ionization, were the same as for the study of Lu spectra [4], and the details regarding light sources, spectrographs, photographic plates, etc., given there need not be repeated here.

III. RESULTS

The measured wave lengths and estimated relative intensities of 1,668 Yb lines observed in arc and spark spectra are presented in table 1. Each line in this table was observed on two or more spectrograms except a few with questioned intensities which were seen only on the strongest exposures. The brightest Yb lines were measured on eight or nine spectrograms, and many of them were measured a number of times on Lu and Tm spectrograms, where they appeared as impurities. The concordance of values from different spectrograms and the coincidence of wave lengths with impurity lines indicates that the final results for most lines are correct within 0.01 A, but errors of 0.02 A or more may exist among faint lines. Hazy lines which occur so frequently in spark spectra are not only subject to larger accidental errors but may show some systematic error, since they are usually unsymmetrical. Otherwise, Yb lines appear to be sharp and free from hyperfine structure. No information on the isotopic constitution of Yb is available, but since hyperfine structures have been detected only for lines of rare earths with odd atomic number, Yb (Z=70) may be assumed to be immune.

In 1915 Eder [11] published 177 lines, which he suspected belonged to a new element, denebium (De). It now appears that at least 110 of these lines are due to ytterbium, and many of the remainder are due to thulium.

TABLE 1.—*Arc and spark spectra of ytterbium* (Z=70)

d=Double.
e=Enhanced at electrode.
h=Hazy.
H=Very hazy.

1=Shaded to longer waves.
I=Spectrum of neutral atoms.
II=Spectrum of singly ionized atoms.

III=Spectrum of doubly ionized atoms.

λ air A	Intensity and character		Spectrum	λ air A	Intensity and character		Spectrum	λ air A	Intensity and character		Spectrum
	Arc	Spark			Arc	Spark			Arc	Spark	
2073.70	.....	8h	II	2102.72	20	200	II	2127.54	.....	2h	II
2078.12	.....	10h	II	2106.46	.....	2	II	2128.82	.....	2	II
2083.65	.....	2	II	2108.20	.....	5	II	2129.64	.....	4h	II
2087.37	.....	3h	II	2109.60	.....	100h	II	2130.45	.....	2h	II
2088.05	.....	15h	II	2110.26	.....	5h	II	2131.37	10	20	II
2091.28	.....	20h	II	2110.60	.....	3	II	2131.71	.....	2h	II
2092.31	.....	30h	II	2115.46	.....	4h	II	2133.17	.....	3	II
2093.18	.....	6h	II	2115.84	.....	2	II	2133.34	.....	3	II
2094.82	.....	10h	II	2116.65	50	250	II	2133.66	.....	4h	II
2095.28	.....	200h	III?	2117.83	.....	4h	II	2134.98	.....	3h	II
2096.84	.....	30h	II	2119.25	.....	30h	II	2135.22	.....	20h	II
2097.41	.....	2	II	2121.54	.....	15	II	2136.33	.....	2	II
2098.16	.....	3	II	2122.81	.....	3	II	2137.52	.....	9	II
2098.40	.....	50h	II	2123.30	.....	15	II	2137.71	.....	15 Lu?	II
2102.10	.....	3h	II	2126.72	40	200	II	2138.32	.....	10	II

TABLE 1.—*Arc and spark spectra of ytterbium* (Z=70)—Continued

λ air A	Intensity and character		Spectrum
	Arc	Spark	
2139.25		2	II
2139.96		25	II
2140.41		2	II
2141.00		10	II
2141.67		5	II
2142.18		4	II
2143.42		5?	II
2143.86		4?	II
2144.74		30 Ag?	II
2146.46		3?	II
2147.15		1	II
2147.50		3h	II
2148.07		8	II
2148.49		4	II
2148.92		10 Cu?	II
2149.43		3	II
2150.45		3	II
2150.93		2	II
2151.20		2h	II
2152.32	3?	10h	II
2153.44		1	II
2153.67		1	II
2154.16		80h	II, III?
2155.18		7	II
2155.51		40	II
2156.51		3	II
2156.79		2	II
2157.87		3h	II
2158.79		4	II
2159.29		1	II
2159.88		3h	II
2160.27		10h	II
2161.60	100	250	II
2163.49		1	II
2163.87		10	II
2165.19		8h	II
2165.53		3	II
2168.09		3	II
2169.10		7	II
2169.77		5	II
2172.13		3	II
2172.58		2	II
2173.34	2	5	II
2174.28	4	10	II
2175.38		3h Lu?	II
2175.88		1	II
2177.04		1	II
2177.50		5	II
2178.80		8h	II
2180.24		7h	II
2181.51		2	II
2181.85		2	II
2182.55		3h	II
2183.29		7	II
2183.61		3h	II
2184.78		2 Lu?	II
2185.69	60	100	II
2188.25		5	II
2189.42		8	II
2193.08		2	II
2193.40		4*d*	II
2195.16		2	II
2198.14		20h	II
2201.19		3?	II
2203.07		2?	II
2211.87		2	II
2214.64	1	8	II
2221.47		2h?	II
2224.45	20	40	II
2224.83		2	II
2227.70		3	II
2231.55		2	II
2237.48		3	II
2240.09	5	25	II
2244.25		8h	II
2255.46		1?	II
2257.01	4	40	II
2261.12		3	II
2262.25	2	30	II
2263.16		3h	II
2263.85		2	II
2265.65	3	50	II
2267.15		1	II
2268.28	1	4	II
2268.64		3h	II
2271.12	8?		I
2276.07	2?		I
2282.99	5	50	II
2283.38	8	10	II
2283.98		8h	II
2285.80	3?		I
2285.85		8h	II
2288.93	1	6	II
2291.63		3h	II
2292.27		3h	II
2292.81	1	3	II
2297.88	2	4	II
2298.65	1	4	II
2303.30		2*d* Lu?	II
2305.33	8	100	II
2307.41	1	6h	II
2308.49		2h	II
2309.26		20	II
2310.67	2?Lu?		I
2312.56	1	2	II
2314.48	4	50	II
2315.20	5	10	II
2320.80	20	5	I
2323.17	1	2	II
2326.91	2	6h	II
2333.39		2	II
2335.42	3?		I
2335.47		15h	II
2337.95	2	40	II
2340.39	2?		I
2340.46		8h	II
2340.75		3h	II
2344.65	5	20	II
2349.39	1	8	II
2350.03		1	II
2361.09		6	II
2362.87	10	20	II
2363.48		4h	II
2365.45		15	II
2366.78	3	12	II
2367.58		10h	II
2369.44		10	II
2369.87		1?	II
2370.10		3h	II
2373.06	1	5	II
2373.89	2	8	II
2377.32		2h	II
2380.37	2	9	II
2382.56		2	II
2385.00	1	5	II
2388.40	1	3	II
2390.72	10	30	II
2397.32		1?	II
2397.83		3	II
2398.00	10	5	I, III?
2403.39		3	II
2404.07		4h	II
2406.07	1	5	II
2418.39		2h	II
2421.36	8	25	II
2422.81	2	4	II
2424.56		2h	II
2425.65		2h	II
2426.16		1	II
2433.62		6h	II
2439.30		4	II
2439.67		3	II
2440.57		5h	II
2447.23		4	II
2454.7		20*H*	II
2456.00		5h	II
2457.65		2	II
2458.23		1h	II
2460.24	6	30 Ag?	II
2461.38		5h	II
2464.48	20	5	I
2465.11		3?	II
2466.62	2	10	II
2471.04		2?	II
2481.40	1	4	II
2484.28		2	II
2484.88	3	8	II
2487.03		2	II
2488.96		3	II
2490.45	2	40	II
2491.69		3	II
2493.63	2	5	II
2495.03		1	II
2495.69		10h	II
2498.35	1	4	II
2500.57		2	II
2500.89		1	II
2501.17		2	II
2501.99	10	30	II
2505.46	5	10	II
2508.04	2?	2	II
2509.85		2	II
2510.27		1	II
2510.50	1	5	II
2512.04	20	100	II
2512.58		10h	II
2515.60		5	II
2516.36	4	10	II
2516.83	3	30	II
2517.99		7	II
2520.32		3	II
2521.02	1	6	II
2522.41	8	15	II
2524.98		4	II
2526.28		5h	II

TABLE 1.—*Arc and spark spectra of ytterbium* (Z=70)—Continued

λ air A	Intensity and character		Spectrum	λ air A	Intensity and character		Spectrum	λ air A	Intensity and character		Spectrum
	Arc	Spark			Arc	Spark			Arc	Spark	
2527.85	2	10	II	2619.90	2	5	II	2717.66	----------	3	II
2528.32	----------	7	II	2621.13	2e	100	III	2718.35	7	40	II
2529.54	----------	4h	II	2621.66	1	4	II	2719.00	----------	27	II
2532.58	----------	3h	II	2623.20	1	5	II	2722.19	----------	6	II
2536.01	1	10	II	2627.04	----------	20	II	2729.06	----------	1	II
2537.64	8	25	II	2628.04	1	4	II	2729.49	----------	2	II
2538.18	2	6	II	2628.78	----------	2	II	2731.53	----------	1	II
2538.68	30	40	II	2631.70	1	4	II	2732.74	8	40	II
2539.63	----------	2	II	2632.66	----------	4	II	2734.08	1	6	II
2540.61	----------	2	II	2634.32	5	20	II	2736.56	----------	3	II
2541.1	----------	3H	II	2635.39	----------	5h	II	2737.61	----------	3	II
2542.82	----------	8H	II	2636.49	----------	5h	II	2738.81	----------	2	II
2545.85	----------	2	II	2638.09	1e	60	III	2740.38	----------	1	II
2547.30	----------	1	II	2639.44	5	15	II	2740.78	----------	1	
2547.47	----------	4	II	2640.52	----------	15h	II	2741.15	----------	1	II
2548.06	----------	1h	II	2641.90	4	10	II	2741.72	2	20	II
2548.73	----------	8	II	2642.55	5e	150	III	2742.64	----------	1	II
2550.04	2	4	II	2643.65	----------	5	II	2745.11	----------	2	II
2550.42	----------	3	II	2644.31	5	40	II	2745.70	----------	4	II
2550.79	----------	4h	II	2646.45	2	10	II	2747.59	2	20	II
2552.13	10	40	II	2647.25	----------	4	II	2748.03	----------	3	II
2552.69	8	30	II	2647.46	2	7	II	2748.65	10	40	II
2555.31	----------	50h	II	2648.80	2	8	II	2749.64	----------	2	II
2556.26	----------	3	II	2649.78	4	10	II	2749.96	----------	10	II
2557.24	2	8	II	2650.73	2	4	II	2750.47	50	200	II
2557.70	----------	4	II	2651.72	2e	60	III	2751.44	3	20	II
2559.03	----------	1	II	2652.23	2e	60	III	2753.67	----------	3h	II
2559.94	----------	2	II	2653.74	50	200	II	2754.93	----------	4	II
2560.57	----------	5	II	2656.11	2	7	II	2756.02	----------	4	II
2561.64	----------	1	II	2659.27	2	5	II	2756.79	----------	3?	II
2565.56	5	15	II	2660.01	----------	6	II	2758.99	1	10	II
2566.80	----------	3	II	2661.86	----------	1	II	2759.54	----------	4	II
2567.63	10e	300	III	2665.02	10	60	II	2760.78	3	25	II
2568.17	----------	2h	II	2666.11	5e	150	III	2761.38	3	25	II
2571.34	6	20	II	2666.98	5e	150	III	2764.42	1	10	II
2572.11	----------	3	II	2668.75	2	20	II	2765.04	----------	1	II
2573.13	3	10	II	2671.98	10	2	I	2765.54	----------	7	II
2574.78	1	3	II	2672.65	20	80	II	2768.27	----------	2	II
2577.68	2	30	II	2673.37	----------	2	II	2771.34	3	30	II
2579.58	5e	200	III	2674.87	----------	4	II	2774.32	----------	4	II
2583.72	----------	2	II	2676.13	----------	2	II	2775.45	----------	2	II
2586.26	1	4	II	2677.37	----------	40	II	2776.28	10	50	II
2588.65	----------	8h	II	2678.60	----------	1?	II	2780.03	----------	3	II
2591.02	1	5	II	2680.40	----------	3	II	2782.21	----------	1	II
2592.71	----------	3	II	2683.42	----------	10	II	2782.57	----------	1	II
2594.18	1	5	II	2684.75	3	25	II	2784.66	3	30	II
2594.48	2	5	II	2685.99	----------	3	II	2785.80	----------	2	II
2596.15	2	6	II	2687.95	----------	5	II	2787.00	----------	1	II
2596.29	2	7	II	2690.99	----------	40	II	2787.98	----------	4	II
2596.73	2	3	II	2691.99	----------	6	II	2788.31	----------	10	II
2597.26	1	20	II	2692.40	----------	2	II	2789.44	----------	3	II
2599.16	2	50	II	2692.69	----------	2	II	2791.58	----------	1	II
2600.19	1	3	II	2694.61	----------	1?	II	2793.28	2	10	II
2600.84	1	3	II	2695.43	1	9	II	2794.44	1	7	II
2602.41	----------	1	II	2696.63	----------	6	II	2794.78	----------	4	II
2604.04	4	10	II	2700.80	----------	10	II	2795.10	----------	4	II
2607.86	3	7	II	2704.52	----------	3	II	2795.62	----------	10	II
2608.45	----------	2	II	2708.08	----------	1	II	2797.79	----------	8	II
2609.12	----------	4	II	2708.84	1	5	II	2798.21	----------	10	II
2610.86	3	20	II	2709.72	----------	2	II	2799.39	2	3	II
2612.03	1	4	II	2710.56	3	15d	II	2800.04	3	15	II
2612.60	1	4	II	2712.66	3	7	II	2803.44	----------	80	II, III
2615.25	5	20	II	2714.42	----------	5	II	2804.27	----------	4	II
2617.00	6	25	II	2715.94	----------	2	II	2806.05	----------	1	I?
2619.06	2	6	II	2717.19	----------	2h	II	2807.22	----------	3d	II

TABLE 1.—*Arc and spark spectra of ytterbium* (Z=70)—Continued

λ air A	Intensity and character		Spectrum	λ air A	Intensity and character		Spectrum	λ air A	Intensity and character		Spectrum
	Arc	Spark			Arc	Spark			Arc	Spark	
2807.82	----------	1	II	2881.92	----------	5	II	2970.84	2	20	II
2808.30	----------	5	II	2882.14	----------	4	II	2972.50	----------	3	II
2808.56	----------	2	II	2883.87	----------	2h	II	2975.58	----------	2	II
2809.33	----------	1	II	2884.42	1?	----------	I	2977.54	----------	4	II
2810.11	----------	3	II	2885.07	----------	1	II	2978.91	----------	3	II
2810.72	----------	4	II	2885.98	2	7	II	2979.69	----------	2	II
2811.17	----------	1?	II	2886.26	3	10	II	2979.86	----------	4	II
2812.66	----------	1?	II	2888.03	8	40	II	2981.52	----------	2	II
2814.25	----------	3	II	2891.38	100	200	II	2982.09	----------	2	II
2814.53	2	10	II	2893.63	2	15	II	2982.50	3	15	II
2814.87	----------	1	II	2894.99	----------	10d	II	2982.65	1	4	II
2816.34	1	4	II	2896.91	1	10	II	2983.70	2	8	II
2816.96	----------	40	II	2898.34	----------	20	II	2983.98	10	70	II
2818.75	1	150	{ II III?	2899.24	----------	2	II	2984.81	----------	5?	II
2819.47	----------	2	II	2899.72	4	20	II	2985.08	5	30	II
				2902.39	----------	2	II	2985.87	2	9	II
2821.15	10	50	II	2902.92	----------	6	II	2987.93	----------	2	II
2823.57	----------	6	II	2906.34	----------	40	II	2989.21	----------	2	II
2824.20	----------	2	II	2906.88	----------	4	II	2989.79	----------	1	II
2824.97	3	20	II	2908.10	----------	4	II	2990.36	3	15	II
2827.90	----------	4	II								
				2908.33	1	5	II	2991.86	4	20	II
2828.49	----------	2	II	2909.19	2	7	II	2993.93	1	7	II
2830.98	8	80	II	2909.47	2	8	II	2994.81	10	80	II
2832.20	----------	4	II	2911.51	5	40	II	2995.86	2	10	II
2834.98	1	15	II	2912.86	----------	3	II	2998.04	----------	9	II
2838.65	----------	3	II								
				2914.21	10	60	II	2998.38	----------	3	II
2841.34	----------	4	II	2914.49	----------	4?	II	3000.46	5	40	II
2842.19	----------	1	II	2915.27	10	40	II	3001.29	----------	3	II
2842.30	----------	2	II	2916.43	1	10	II	3002.04	----------	3	II
2842.58	----------	4	II	2916.84	----------	1	II	3002.61	3	20	II
2843.01	----------	10	II								
				2919.34	15	90	II	3005.76	30	200	II
2843.80	----------	3h	II	2921.12	4	20	II	3006.86	1	4	II
2844.77	----------	3h	II	2924.23	3	15	II	3009.39	6	40	II
2846.29	----------	1h	II	2927.12	----------	1	II	3010.61	5	30	II
2847.18	10	?	II?	2927.86	2	10	II	3014.45	4	30	II
2847.25	?	60h	II								
				2934.34	3	? Ag	I, II?	3017.56	10	80	II
2848.44	4	30	II	2935.10	3	15	II	3019.06	----------	3	II
2849.33	1	8	II	2937.18	2	10	II	3019.47	----------	2	II
2851.12	20	100	II	2938.19	----------	3	II	3020.70	----------	10	II
2851.86	----------	4	II	2939.52	2	6	II	3022.45	1	7	II
2853.40	1	8	II								
				2940.51	3	25	II	3023.62	----------	4	II
2853.68	----------	2	II	2942.04	1	6	II	3024.93	----------	1	II
2854.12	3	20	II	2942.82	----------	5	II	3026.67	10	80	II
2854.49	2	15	II	2944.47	----------	3	II	3028.39	----------	2	II
2855.86	----------	2	II	2945.91	10	60	II	3029.53	----------	70h	{ II III?
2856.95	----------	2?	II								
				2946.30	3	15	II	3031.11	50	60	II
2858.35	2	10	II	2946.77	1	8	II	3031.62	----------	2?	II
2858.45	1	8	II	2947.11	----------	2	II	3033.85	----------	4	II
2859.39	4	40	II	2950.32	2	10	II	3034.64	3	10	II
2859.80	20	60	II	2951.02	----------	4	II	3036.83	----------	4	II
2860.40	2	15	II								
				2951.41	----------	2	II	3038.00	2	6	II
2861.21	6	60	II	2953.03	----------	5	II	3038.55	----------	2	II
2861.31	5	50	II	2955.31	3	9	II	3039.67	4	25	II
2862.87	----------	1	II	2957.64	----------	3	II	3040.49	1	5	II
2863.19	----------	2h	II	2960.85	1	5	II	3042.65	4	30	II
2864.78	----------	3d	II								
				2961.81	----------	3	II	3044.02	1	5	II
2865.34	----------	2	II	2962.53	4	20	II	3044.83	1	5	II
2866.18	----------	5	II	2963.21	----------	10	II	3046.48	3	15	II
2867.05	10	80	II	2963.46	2	20	II	3047.06	2	9	II
2868.55	----------	1	II	2964.41	----------	5h	II	3053.98	----------	2	II
2870.06	2	20	II								
				2964.75	8	30	II	3054.67	----------	1	II
2871.71	----------	1	II	2965.16	----------	4	II	3055.16	1	5	II
2872.15	----------	2	II	2966.76	----------	15	II	3063.14	2	7	II
2873.50	1?	----------	I	2969.60	----------	1?	II	3063.69	----------	8	II
2875.90	----------	15	II	2970.56	100	150	II	3064.92	----------	2	II
2879.16	1	10	II								

TABLE 1.—*Arc and spark spectra of ytterbium* (Z=70)—Continued

λ air A	Intensity and character		Spectrum	λ air A	Intensity and character		Spectrum	λ air A	Intensity and character		Spectrum
	Arc	Spark			Arc	Spark			Arc	Spark	
3065.04	10	50	II	3175.75	1	7	II	3315.38		5	II
3067.38		4	II	3180.91	4	40	II	3316.83		3	II
3068.29		4	II	3186.59		4	II	3319.18	2	15	II
3071.61		4	II	3190.81		1	II	3319.43	4		I
3073.70	1	5	II	3191.41		10h	II	3320.31		4	II
3074.52		1	II	3192.88	20	120	II	3322.97		5	II
3076.04	1	4	II	3194.24	1	4	II	3324.16	1	5	II
3080.15		1?	II	3194.76		5	II	3324.46		1	II
3080.55		1	II	3195.57	2	9	II	3325.57		4	II
3084.36		6	II	3196.06		2	II	3327.77		2	II
3085.82		6	II	3196.35		2	II	3331.21		1	II
3086.99	1	6	II	3198.66	4	30	II	3333.07	3	15	II
3087.99		2?	II	3199.81		2	II	3337.18	6	2	I
3089.11	5	20	II	3201.16	8	60	II	3342.94	8	2	I
3089.61		2?	II	3204.69	1	4	II	3343.06	2?	10	II
3090.79		2	II	3206.16	1	4	II	3346.50	3		I
3092.54		40	II	3207.70		2	II	3347.53	3	15	II
3093.44		3	II	3210.11	1	10	II	3349.94		1	II
3093.87	5	25	II	3214.33		1	II	3351.08	2	1	I
3094.92		3	II	3215.49		2	II	3352.49	4		I
3095.24		2	II	3215.94		2	II	3353.74		2	II
3097.34		1?	II	3217.19	4	20	II	3355.88		4	II
3101.36	2	20	II	3218.33	3	15	II	3356.98		4	II
3102.07	1	10	II	3221.26		4	II	3361.61		1	II
3107.79		30?	II	3221.51		3	II	3362.43	3		I
3107.91	15	100	II	3223.17		1?	II	3363.61	2		I
3109.79		2	II	3225.86	4	20	II	3365.97		7	II
3112.98		2	II	3226.75		3	II	3369.90		1?	II
3115.33	4	30	II	3228.63		15	II	3375.48	5	25	II
3116.07	1	4	II	3229.84		3	II	3378.43		1	II
3116.50		5	II	3231.99	2	9	II	3379.78		5	II
3116.71	3	9	II	3236.16	3	15	II	3382.58	2?		I
3117.81	15	50	II	3237.82	1?		I	3384.04		5	II
3122.22		2	II	3239.20	2	10	II	3387.49	5	1	I
3123.52		3	II	3239.60	2		I	3390.32	3		I
3125.45	1	2	II	3242.07		2	II	3391.10	1	9	II
3126.06		40h	II	3244.97		2h?	II	3392.40		1	II
3127.14		2	II	3246.07	2		I	3394.44	1	5	II
3127.86	1	6	II	3252.14		1?	II	3396.32		4	II
3129.14		3	II	3254.22	1	3	II	3400.58	1		I
3132.61	2	8	II	3256.05		1	II	3401.02	2	7	II
3135.14		2	II	3259.10	2	10	II	3402.28		1	II
3136.76	3	20	II	3261.51	4	25	II	3404.11	2	7	II
3138.63		6	II	3261.70		7	II	3408.50		2	II
3140.92	10	40	II	3264.92		2	II	3409.88		1?	II
3141.72	3	15	II	3265.08		2	II	3410.54		1	II
3145.06	4	20	II	3265.95		1?	II	3411.24	1		I
3145.55	3	2	I	3271.18		4	II	3412.45	2	1	I
3146.13		2	II	3271.53		3	II	3414.86		2	II
3148.99	1	5	II	3275.81	1	6	II	3415.04		1?	II
3150.44		1?	II	3286.97		5	II	3415.98		2	II
3151.45		2	II	3289.36	400	800	II	3416.88		3	II
3152.45		2	II	3294.33		4	II	3418.40	3	1	I
3153.17	2	7	II	3297.85		4	II	3419.62		3	II
3153.86	4	40	II	3298.82		1	II	3420.35	1		I
3155.18	3	20	II	3302.42		1	II	3426.06	10	3	I
3155.79		2	II	3304.57	2	10	II	3428.48	4	20	II
3158.29	2	25	II	3304.76	2	10	II	3431.14	8	3	I
3162.31	2		I	3305.27	3		I	3434.62	2	5	II
3163.79	3	25	II	3305.73	5	30	II	3436.46	2	7	II
3165.20	2	20	II	3306.79	1	7	II	3438.73	3	20	II
3168.41		2	II	3309.38	2	8	II	3438.83	4	30	II
3169.05	3	30	II	3310.95		1	II	3443.59	1		I
3171.19	1	5	II	3313.80		1?	II	3446.89	2	6	II
3173.77	1	8	II	3315.11	2		I	3448.00		1	II

TABLE 1.—*Arc and spark spectra of ytterbium* (Z=70)—Continued

λ air A	Intensity and character		Spectrum	λ air A	Intensity and character		Spectrum	λ air A	Intensity and character		Spectrum
	Arc	Spark			Arc	Spark			Arc	Spark	
3452.41	3	----------	I	3634.54	3	—	I	3887.31	—	8	II
3454.08	10	60	II	3637.76	7	15	II	3890.86	—	1?	II
3456.30	----------	1?	II	3644.23	1	3	II	3900.86	20	2	I
3458.27	4	20	II	3648.13	2	—	I	3904.82	3	20	II
3458.36	4	----------	I	3648.46	—	2	II	3905.88	—	2	II
3460.27	7	2	I	3649.74	—	2	II	3908.02	2?	—	I
3461.71	1	6	II	3652.96	—	1?	II	3911.28	6	—	I
3462.36	1?	----------	I	3655.73	3	—	I	3934.30	—	4	II
3464.36	100	20	I	3664.56	—	2	II	3938.26	1	5	II
3467.05	----------	3	II	3664.76	—	2	II	3938.53	1	4	II
3469.92	----------	2	II	3669.71	6	10	II	3946.94	—	3	II
3470.78	----------	2	II	3670.68	1	8	II	3948.23	—	1?	II
3474.81	2	5	II	3675.08	5	20	II	3949.59	1	1	I II
3476.31	30	8	I	3687.15	—	2	II	3949.88	—	1?	II
3478.84	15	80	II	3687.60	—	3	II	3968.03	—	3	II
3485.76	3	10	II	3690.54	—	10?	II				
3488.42	3	----------	I	3691.48	—	4	II	3975.28	3	—	I
3488.80	1	3	II	3691.71	2	—	I	3980.37	1?	—	I
3491.63	----------	1?	II	3694.19	500	1000	II	3987.98	2000	100	I
3495.92	5h	----------	I	3698.59	3	15	II	3990.89	40	4	I
								3993.75	2	—	I
3502.18	----------	3	II	3699.50	2	—	I				
3506.14	----------	3	II	3699.81	—	4	II	3994.86	1	----------	I
3507.83	3	15	II	3700.57	3	—	I	3999.81	----------	2	II
3515.86	1	4	II	3701.03	2?	—	I	4000.89	----------	6h	II
3517.02	1?	----------	I	3703.42	—	4	II	4007.36	5	----------	I
								4009.24	----------	1?	II
3518.16	1	5	II	3708.66	1	3	II				
3520.28	5	30	II	3710.32	2	7	II	4019.35	----------	7	II
3531.24	----------	2	II	3716.15	2?	—	I	4024.01	----------	2	II
3534.07	----------	1?	II	3720.98	—	2	II	4028.27	----------	8h	II
3539.33	----------	2	II	3722.29	2	10	II	4032.92	----------	1	II
								4040.09	1	8	II
3541.40	----------	1	II	3724.22	3	15	II				
3542.40	----------	2?	II	3729.80	—	2	II	4043.06	----------	8h	II
3543.15	----------	2	II	3730.39	1	3	II	4047.39	----------	4	II
3545.71	2	----------	I	3734.70	6	1	I	4050.10	----------	3	II
3549.82	4	15	II	3741.61	—	3	II	4052.28	8	2	I
								4056.18	----------	10	II
3552.33	1	3	II	3743.15	2?	—	I				
3559.00	1	----------	I	3749.68	2	7	II	4074.70	----------	2	II
3560.33	6	15	II	3753.05	—	2?	II	4077.27	4	30	II
3560.71	4	30	II	3753.89	—	3	II	4082.98	2	----------	I
3562.70	----------	1	II	3761.00	—	4	II	4086.62	----------	1	II
								4089.69	40	7	I
3563.93	1	5	II	3762.54	1	6	II				
3567.12	1	7	II	3766.10	1	4	II	4091.49	1	4	II
3570.56	3	10	II	3770.10	15	3	I	4093.73	1?	----------	I
3572.49	----------	2	II	3773.43	2	3	II	4097.87	2	8	II
3574.54	2h	----------	I	3774.32	2	—	I	4109.60	5h	----------	I
								4113.04	2	7	II
3575.58	----------	1?	II	3779.28	—	2	II				
3577.02	1	5	II	3782.54	2	15	II	4119.26	4	----------	I
3582.83	----------	1?	II	3784.40	—	3	II	4119.46	5	10?	II
3585.47	15	25	II	3786.37	2?	—	I	4122.86	1	6	II
3586.84	----------	2?	II	3791.74	8h	2	I	4127.34	2	----------	I
								4131.00	----------	3h?	II
3600.38	----------	1	II	3798.18	2	—	I				
3600.74	----------	4	II	3798.44	2?	—	I	4132.14	3h	----------	I
3603.85	----------	3	II	3807.54	3	15	II	4135.10	10	60	II
3606.47	5	25	II	3814.22	—	8	II	4139.05	2	----------	I
3608.48	----------	3	II	3816.21	2	7	II	4141.49	----------	2	II
								4147.80	----------	2	II
3610.23	1	4	II	3816.34	—	2?	II				
3611.30	2	8	II	3839.46	1	3	II	4149.07	40	6	I
3614.05	----------	2	II	3839.92	5	—	I	4164.64	----------	2	II
3618.08	----------	2	II	3840.33	—	3	II	4169.12	1?	----------	I
3619.81	8	30	II	3847.48	—	3	II	4170.11	3	20	II
								4172.24	----------	2	II
3621.00	1	5	II	3847.86	3	—	I	4172.36	1?	----------	I
3624.65	—	2	II	3857.61	3	—	I	4174.57	10	1	I
3629.91	1	3	II	3858.55	—	2	II	4180.82	40	100	II
3631.08	—	2	II	3863.46	1	5	II	4186.90	----------	10h	II
3632.56	—	3d	II	3872.85	20	2	I	4190.30	4	30	II

TABLE 1.—*Arc and spark spectra of ytterbium* (Z=70)—Continued

λ air A	Intensity and character		Spectrum
	Arc	Spark	
4210.30	4		I
4216.72		5	II
4218.55	4	50	II
4218.64	15	?	I
4224.19		1	II
4227.94		10	II
4229.66	2		I
4230.24		4	II
4231.99	10	2	I
4233.45	2?		I
4234.55	2	15	II
4244.21		2h	II
4247.88	2	7	II
4251.52	4	1	I
4252.53	5	20	II
4254.78	2	4	II
4255.78	3	8	II
4256.77	3h		I
4257.66	3	15	II
4266.99	2	8h	II
4270.55		3h	II
4272.12	2		I
4273.32		3	II
4277.73	9h	2	I
4283.01	7 Ca?		I
4300.99	6	1	I
4305.49	2		I
4305.96	20h	3	I
4306.49		3	II
4309.82	8		I
4312.36	2		I
4316.96	10	40	II
4322.23	3	20	II
4325.28		3	II
4326.40	5h		I
4329.72	1		I
4336.48		3h?	II
4339.10	2	10	II
4344.21	2		I
4344.29		2?	II
4352.94	6h		I
4356.65	3		I
4363.30		6	II
4370.81	5	40	II
4371.42	1?		I
4372.60		1	II
4376.48	4		I
4376.92		1h	II
4386.10		2h?	II
4389.76	1	10	II
4392.83	2	15	II
4393.75	30h		II
4396.49	1	2	I
4398.95	5	1	I
4402.30	4	20	II
4409.35	6	10	II
4410.23	1?		I
4411.10	5		I
4427.44	10h		I
4430.22	6	1	I
4439.21	100	10	I
4448.94	1?		I
4463.48		2	II
4467.14		2	II
4472.19		3	II
4472.43	20h		I
4480.27		2	II
4482.44	10	2	I
4484.43		3h	II
4487.27	2	10	II
4488.28	4		I
4493.96	2	10	II
4503.51		2h?	II
4503.62	5		I
4513.40	6	1	I
4514.04		2?	II
4515.16	30	100	II
4520.66		1?	II
4529.90	20	2	I
4533.50	4	1	I
4536.80		2?	II
4539.30		2	II
4539.70	1?		I
4541.35		6	II
4543.90		4	II
4547.01		1	II
4548.35	2	2	I, II?
4553.58	10	40	II
4557.94	2	6	II
4564.00	50	2	I
4565.99		2h?	II
4567.38	5	1	I
4568.80	2h		I
4576.21	200	10	I
4580.75	2		I
4582.36	50	5	I
4585.82		2h	II
4587.14		2h	II
4589.22	20	1	I
4590.84	30	?	I
4593.36	2		I
4597.25		2	II
4598.37	10	50	II
4610.22	2h		I
4610.66		4?	II
4618.53		3?	II
4624.46	4h		I
4633.18	2		I
4634.04	2	15h	II
4641.62	2		I
4644.54	10	1	I
4650.06	10		I
4651.67	3		I
4657.04	9h		I
4658.47	1?		I
4661.81	2h		I
4667.08	2		I
4670.59	3	7	II
4683.83	8	40	II
4684.27	7	1	I
4688.51	1	4h	II
4690.80	1	5	II
4702.36	3		I
4704.90	3		I
4712.82		30h	II
4718.66	20h		I
4720.79	6	1	I
4726.08	60	250	II
4732.02	1	7	II
4732.96		3	II
4743.38	1?		I
4745.52		2	II
4746.70		15h	II
4750.01		4h	II
4751.77	4		I
4752.93	3	20h	II
4758.32	2	1	I
4761.16		5h	II
4765.37	3h		I
4770.17	2		I
4774.61	3h		I
4774.84	3h		I
4779.00	3		I
4781.89	200	5	I
4784.52	3		I
4785.34	2		I
4786.62	100	500	II
4797.85	1		I
4808.51		4h	II
4809.47		2	II
4812.91	3h		I
4816.40	40h	1	I
4818.38	3	30	II
4820.25	20	80	II
4830.70	2		I
4831.31	2		I
4831.55		2h	II
4831.96	3h		I
4834.72		10h	II
4836.96	20	120	II
4837.47	20	1	I
4841.18	2	2	I, II
4848.45	3	20h	II
4851.17	8	10	II
4853.84	3		I
4871.16		8h	II
4871.64		3h	II
4893.48	2		I
4894.63	50		I
4894.98	3	10	II
4897.94		2	II
4903.72		8h	II
4912.38	20		I
4917.04		4h	II
4918.14	2?		I
4918.46		3h?	II
4929.31		3h	II
4931.95	10		I
4935.51	500	20	I
4936.96	8h		I
4937.22	5	100	II
4942.23	1?		I
4942.78	1	5h	II
4944.09	5	20	II
4944.96		7h	II
4954.67		4h	II
4956.17	2h		I
4956.49	2		I
4966.91	100	4	I
4972.30		3h?	II
4973.90		2h?	II
4974.16	10		I
4988.30	4	1	I
5009.53	20	50	II
5014.50		10	II

TABLE 1.—*Arc and spark spectra of ytterbium* (Z=70)—Continued

λ air A	Intensity and character		Spectrum
	Arc	Spark	
5019.66	4		I
5021.14	2	10	II
5027.66	10		I
5032.61		2h?	II
5033.33		2h?	II
5038.28		3h?	II
5047.12		2h?	II
5049.87	2	30h	II
5058.60	2		I
5058.76		2h?	II
5062.95		15	II
5067.33	5	5	I II
5067.68		3h?	II
5067.80	10		I
5069.15	30	2	I
5074.33	200	5	I
5074.68		3?	II
5076.75	50	1	I
5081.00	3		I
5082.60	4		I
5085.74		4h	II
5087.64	1	10	II
5088.97		3h	II
5090.67		2h	II
5101.60		4h	II
5104.43	1	50	II
5105.06		5	II
5111.51		6h	II
5113.34	3		I
5116.23		1h?	II
5117.75		3h	II
5121.61	1	15	II
5126.80	4		I
5128.54		5h	II
5129.60		3h	II
5129.65	2		I
5130.52	1		I
5132.41		5h	II
5136.00	6	50	II
5139.53	3		I
5142.31		5h	II
5147.02	3	50	II
5152.34		5h	II
5173.13	1	15h	II
5178.73	3		I
5180.36	2	10	II
5184.18	8	30	II
5187.38	2		I
5193.87	4h		I
5194.76	3h?		I
5196.09	20	3	I
5200.57		10	II
5211.59	40	2	I
5215.45		5h	II
5217.98		7h	II
5226.19		4	II
5227.09		3?	II
5227.25	10		I
5228.18	5		I
5229.99		2?	II
5236.68		7h	II
5240.51	10	40	II
5244.11	50	5	I
5244.65		10	II
5246.41		1?	II
5249.84		8	II
5254.21		1	II
5255.68		8	II
5257.50	15	100	II
5258.19	5		I
5262.07		1	II
5263.61		10	II
5275.58	3		I
5277.08	200	6	I
5279.56	15	100	II
5280.53		1	II
5286.14		4	II
5287.30		5	II
5299.86	2		I
5300.95	6	60	II
5306.53		1h	II
5309.33	2	5	II
5321.14		6	II
5328.51		1h?	II
5334.04	2h		I
5335.15	150	400	II
5338.77		3	II
5345.68	20	100	II
5345.82	10	50	II
5347.21	40	200	II
5351.33	50	3	I
5352.96	100	250	II
5357.12		1	II
5358.65	15	100	II
5359.98		10	II
5362.46		2	II
5363.66	25	2	I
5364.12		2	II
5364.84		1?	II
5365.44		3	II
5367.36		2	II
5367.79	2	3	II
5368.29	2	20	II
5376.99		10	II
5380.26	2		I
5380.57	3		I
5383.96		2	II
5386.73		2	II
5388.01	5		I
5389.87	8	30	II
5390.68	30		I
5390.85	30		I
5393.40		6	II
5393.85	6h		I
5395.78		7	II
5399.71	2		I
5399.76		15	II
5403.14	20	1	I
5409.43		2	II
5414.29	1	20	II
5424.68		10h	II
5426.91	2	60	II
5429.86		1h?	II
5431.20		2	II
5432.73	5	100	II
5440.58		5	II
5445.52		1	II
5449.30	20	100	II
5454.01	5		II
5455.08	1	6	II
5457.45		2	II
5458.22		2h?	II
5471.21	2?		II
5474.05	10		I
5478.52	10	50	II
5481.94	60	2	I
5486.59		4	II
5493.10	1?		I
5498.86		20h?	II
5504.04	1?		I
5505.50	40	2	I
5508.30		2h	II
5511.46		2h	II
5518.39	1?		I
5520.24		4h	II
5524.55	10		I
5527.81	1?		I
5529.09	1	9	II
5529.95		8h	II
5539.09	200	5	I
5545.85	2?		I
5547.19	2	15	II
5548.97		2h	II
5556.48	1500	50	I
5562.07	50	2?	I
5568.11	20	1	I
5572.55	1	6	II
5573.14	1		I
5575.73	1	2	II
5578.23	5		I
5580.82	3	30	II
5585.43	2		I
5586.35	20		I
5587.29	1?		I
5588.46	30	100	II
5597.19	4		I
5598.48	15		I
5600.03	2h?		I
5607.38		2h	II
5608.92		2h	II
5620.17	2		I
5620.24	1	10	II
5620.90		1?	II
5627.89		5	II
5631.52		3h	II
5632.00	2		I
5637.80	2		I
5637.86		5	II
5639.35	1?		I
5652.00	50	80	II
5653.29		5	II
5654.33		2	II
5663.19	1		I
5669.98	1?		I
5683.60	2	6	II
5686.53	5		I
5686.57	?	10h	II
5689.71		1h	II
5689.92	10		I
5693.71	1	10	II
5705.00		2	II
5706.79		1?	II
5713.75	1	10	II
5717.30		15h	II
5720.01	300	8	I

TABLE 1.—*Arc and spark spectra of ytterbium* (Z=70)—Continued

λ air A	Intensity and character		Spectrum	λ air A	Intensity and character		Spectrum	λ air A	Intensity and character		Spectrum
	Arc	Spark			Arc	Spark			Arc	Spark	
5723.72	3		I	6001.05		1?	II	6312.99		1h?	II
5728.86	5		I	6002.52		2?	II	6324.42		1?	II
5730.02	4	60	II	6003.65	5		I	6324.73		2	II
5735.80	2	15	II	6004.53	2?		I	6324.78	3		I
5736.95	3?		I	6007.42	4	80h	II	6333.36		1?	II
5745.80	6		I	6014.95	3		I	6335.72	8		I
5749.92	8	10	II	6020.56	2	5	II	6345.02	15h		I
5754.79		1h?	II	6021.97		15h	II	6345.74	2	7	II
5755.90	15		I	6024.08	2	5	II	6355.40	2	50h	II
5764.65		1h?	II	6031.80	10		I	6356.68		2h?	II
5767.23	2	10h	II	6035.72	2		I	6372.71	6		I
5771.67	30	50	II	6040.80	3	10	II	6377.04		6h	II
5773.86	2		I	6042.26		2?	II	6382.93	1	2	II
5774.35	2		I	6048.43	15		I	6387 72	3		I
5775.68		1?	II	6052.88	8	30	II	6393.79	2?		I
5778.00		3	II	6054.56	10		I	6400.40	200h	4h	I
5786.60		6	II	6056.48	1	20h	II	6402.64		1h?	II
5789.94	5		I	6059.25	10		I	6404.62	2h		I
5799.59		2h?	II	6075.25		3	II	6417.97	120	3	I
5803.45	15		I	6082.40		10h	II	6421.02	1?		I
5808.69		2	II	6083.29		2	II	6421.54	3		I
5810.68	2?		I	6083.85		1?	II	6432.73	30	40	II
5811.95		1?	II	6088.72		3	II	6438.01		1h?	II
5819.43	7	100	II	6098.51		1	II	6440.81		5	II
5824.35		2?	II	6106.22		4	II	6456.92		4	II
5831.82	1		I	6110.19		4	II	6463.15	10	100	II
5834.00	60h	1	I	6111.28	7		I	6474.74	5	50	II
5834.58	1?		I	6118.40	10h?		I	6488.50		1	II
5835.54		1?	II	6120.38		20h	II	6489.10	800	40	I
5836.22		2?	II	6122.99	4		I	6489.27	?	30	II?
5837.15	50	150	II	6123.03		4	II	6492.74	3	50	II
5838.67		2	II	6126.37		2?	II	6503.02	2	4	II
5842.45	1?		I	6128.21		6	II	6509.11	2?		I
5844.46	2?		I	6131.61		2h?	II	6523.24		4?	II
5847.24		2h	II	6134.31		5	II	6541.37	1?		I
5854.52	30	1	I	6142.85		1?	II	6550.19	10	?	I
5865.65		2	II	6146.94		15h	II	6553.34	2	?	I
5868.40		6	II	6150.64	30h		I	6555.15	3	?	I
5874.70	1	30h	II	6152.58	60	80	II	6568.35	2	?	I
5875.96	2?		I	6171.65		2	II	6585.42	7	20	II
5882.81	2	10	II	6175.59		1	II	6592.75		3?	II
5896.61	5		I	6189.07		1?	II	6605.93		4h	II
5897.22	7	100h	II	6190.81	3	15	II	6607.07	20		I
5898.80	3	50h	II	6194.85	3		I	6617.06	10	6	I
5903.37		2	II	6208.11	2	20h	II	6643.54	50		I
5908.36	20	30	II	6208.68		1?	II	6644.07	2	5h	II
5920.39	1	10	II	6215.57		6	II	6661.90		4h?	II
5927.70	2		I	6223.65		15	II	6667.85	1000	20	I
5935.06	3	40	II	6233.38		5	II	6678.17	20		I
5938.47	2		I	6234.86		5	II	6679.32		4?	II
5943.55	1	2	II	6235.27	2		I	6692.42	2?		I
5946.02	4	100	II	6236.15		2?	II	6699.38	10	8	I, II?
5947.28	1	5	II	6236.56	2		I	6715.79	5		I
5950.65	3		I	6246.97	40	60	II	6727.62	30	60	II
5950.98		8	II	6247.99	3		I	6745.22	2	7	II
5955.35	2		I	6260.80	4	50h	II	6749.40	7		I
5958.70	10		I	6265.46		1?	II	6755.42		4?	II
5959.31	3		I	6270.33		1?	II	6768.70	80	2	I
5961.85		2h?	II	6271.16	1?	3	II	6777.22	2		I
5972.71	1?		I	6274.79	100	150	II	6782.17	4h		I
5985.35	1	5	II	6277.13		5	II	6785.16	1	5	II
5986.80		2h?	II	6286.26	8		I	6790.82	1?		I
5987.91	2	20h	II	6297.38		15h	II	6799.61	1000	50	I
5989.32	15		I	6303.28	3	4	II	6802.47	2	20	II
5991.51	50	150	II	6308.16	20	30	II	6813.66	1?		I

TABLE 1.—*Arc and spark spectra of ytterbium* (Z=70)—Continued

λ air A	Intensity and character		Spectrum	λ air A	Intensity and character		Spectrum	λ air A	Intensity and character		Spectrum
	Arc	Spark			Arc	Spark			Arc	Spark	
6820.04	3h		I	7175.14	10			8053.41	10		
6826.06		2?	II	7187.06	5			8607.51	8		
6828.90	1	6	II	7222.72	3			8922.61	20		I
6833.57	2h?		I					9094.44	3		
6864.26		10h?	II	7244.47	20			9104.06	3		I
				7251.5	2?						
6871.54	10		I	7305.25	15			9304.44	15		
6877.94		8h?	II	7313.10	20			9349.27	20		
6878.12	3?		I	7342.3	2?			9392.8	5		
6881.43		4h?	II					9524.43	4		
6889.60		4?	II	7350.09	40			9677.8	2?		
				7361.8	1?						
6913.55	2?		I	7377.55	4			9688.6	3?		
6934.04	15	10	I, II?	7405.92	3			9760.37	100		
				7422.1	4?			9799.88	10		
6951.51	2		I					9870.07	6		
6963.11	2	5	II	7448.33	30			9976.40	4		
6977.68	2		I	7527.56	80		I				
				7699.49	1500		I	10267.36	7		
6982.00	3	2	I, II?	7722.58	2			10321.64	5		
6999.87	15	3	I	7734.5	1?			10770.1	2Lu?		
7020.16	5										
7027.78	2?			7758.03	10						
7032.04	3			7781.5	1?						
				7877.30	15						
7032.91	2			7895.12	20						
7043.79	8			7922.40	7						

The data of table 1 represent at least three different spectra, each characteristic of Yb in some form or another. About 400 lines belong to neutral Yb atoms (Yb I spectrum), approximately 1,250 characterize singly ionized atoms (Yb II spectrum), and possibly a dozen belong to doubly ionized atoms (Yb III spectrum). We found no evidence of band heads which could be assigned to a molecular spectrum of ytterbium compounds.

The successive atomic spectra are differentiated mainly on the basis of intensity comparisons of arc and spark spectra, but since the latter were not recorded beyond 7,000 A the lines of longer wave length from ionized atoms remain unobserved, or unrecognized if recorded in arc spectra. The Yb I spectrum is surprisingly simple, but may not be fully developed in the arc. It may possess more lines in the infrared but the available Yb material was too scarce and precious to permit long exposures required to photograph beyond 10,500 A. The Yb II spectrum is probably even more complex than is apparent because in addition to being undetermined beyond 7,000 A some lines are probably overlooked on account of being masked by silver lines or by the air spectrum.

Our assignment of lines to successive spectra agrees almost perfectly with King's [13] separation of ionization stages based upon a study of the electric-furnace spectra of Yb. This grouping of lines is further confirmed by the spectral-term analyses, insofar as they have been carried out.

Since no details concerning regularities in the spectra of ytterbium have heretofore been published, we present a preliminary report, as follows: Soon after making our first measurements and identifications of lines from neutral Yb atoms, in 1930, we found from repeated differences among wave numbers three energy levels with separations of 703.5 and 1718.4 cm^{-1}. These were interpreted as $(f^{14}sp)^3P_{0,1,2}$ by

Prof. H. N. Russell, who promptly identified two singlet levels $(f^{14}sp)^1P_1$ and $(f^{14}s^2)^1S_0$, which account for the two lines of outstanding intensity and easy excitation in the Yb I spectrum. These terms and their combinations are displayed in table 2 where the term symbols and relative values appear on the margin and the wave lengths (intensities) and wave numbers of the observed combinations at intersections of lines and columns. Only the terms which can be interpreted with considerable certainty are given now, the remainder being reserved until the analysis is completed and confirmed by observations of Zeeman effects, which, up to the present time, have not been produced for Yb spectra. It appears certain that the normal state of neutral Yb atoms is described by $(4f^{14}6s^2)^1S_0$ and that the most intense line of the Yb I spectrum is $(4f^{14}6s^2)^1S_0-(4f^{14}6s6p)^1P_1$ with wave length 3,987.99 A. This spectrum closely resembles that of an alkaline earth. Indeed, the fact that Yb may be bivalent accounts for its separation by electrolytic reduction from other trivalent rare earths [14].

Proceeding in a similar manner with Yb II lines the authors found several score of levels combining to produce some hundreds of lines, but it was impossible to group the levels into terms and identify them. Two lines of extraordinary intensity featuring the Yb II spectrum were not included among our level combinations and Professor Russell suggested that they represent the transition $(f^{14}s)^2S_0-(f^{14}p)^2P_{1,2}$. When the f shell is completely filled (f^{14}) it contributes nothing to the spectrum and a single-valence electron will produce an alkali-like spectrum with $(s)^2S_0$ describing the normal state. However, the relatively great complexity of the Yb II spectrum indicates that most of the excited states must arise from electron configurations of types $f^{13}s^2$, $f^{13}sd$, $f^{13}d^2$, $f^{13}sp$, $f^{13}sd$, which produce large families of spectral terms. This is probably the explanation of the numerous levels first discovered, but further attempts to interpret them and connect them with terms arising from configurations with f^{14} electrons will be postponed until Zeeman effects are available.

TABLE 2.—*Terms and combinations in the* Yb I *spectrum*

Term symbol	Value	$(4f^{14}6s6p)^3P_2^o$ 17288.5	$(4f^{14}6s6p)^3P_1^o$ 17992.0	$(4f^{14}6s6p)^3P_0^o$ 19710.4	$(4f^{14}6s6p)^1P_1^o$ 25068.2
$(4f^{14}6s^2)^1S_0$	0.0		5556.48(1500) 17992.0		3987.98(2000) 25068.2
$(4f^{14}6s7s)^3S_1$	32094.7	6489.10(800) 15406.2	6799.61(1000) 14702.7	7699.49(1500) 12984.3	
$(4f^{14}6s5d)^3D_1$	39808.7	4439.21(100) 22520.2	4582.36(50) 21816.7	4974.16(10) 20098.3	6782.17(4) 4740.5
$(4f^{14}6s5d)^3D_2$	39838.0		4576.21(200) 21846.0	4966.91(100) 20127.6	6768.70(80) 4769.8
$(4f^{14}6s5d)^3D_3$	39966.1			4935.51(500) 20255.7	
$(4f^{14}6s5d)^1D_2$	40061.5		4529.90(20) 22069.4	4912.38(20) 20351.1	6667.85(1000) 4993.2
$(4f^{14}6s8s)^3S_1$	41614.9	4109.60(5) 24326.4	4231.99(10) 23622.9	4564.00(50) 21904.5	
$(4f^{14}6s6d)^1D_2$	44760.3		3734.70(6) 26768.3	3990.89(40) 25050.0	5076.75(50) 19692.2

The resonance lines of Yb II are interpreted with considerable certainty, as shown in table 3. The most intense line emitted by singly ionized Yb atoms is expected to be $(f^{14}6s)^2S_{1/2}-(f^{14}6p)^2P_{1/2}$ with wave length 3289.36 A, but the estimated intensities appear to be somewhat anomalous. Apparently 3694.19A is the strongest Yb II line.

No attempt has been made to analyze the Yb III spectrum, but it may be expected that the ground state of doubly ionized Yb atoms is described by $(4f^{14})^1S_0$. The full shell of *f*-type electrons is likely to have high stability on account of which the fundamental lines emitted by Yb^{++} ions will probably lie in the extreme ultraviolet.

TABLE 3.—*Terms and combinations in the* Yb II *spectrum*

Term symbol		$(4f^{14}6p)^2P^o_{3/2}$	$(4f^{14}6p)^2P^o_{1/2}$
Value		27061.9	30392.3
Term symbol	Value		
$(4f^{14}6s)^2S_{1/2}$	0.0	3694.19(1000) 27061.9	3289.36(800) 30392.3
$(4f^{14}7s)^2S_{1/2}$	54304.3	3669.71(10) 27242.4	4180.82(100) 23912.0

IV. REFERENCES

[1] C. Marignac, Compt. rend. **87**, 578 (1878).
[2] G. Urbain, Compt. rend. **145**, 759 (1907).
[3] C. Auer v. Welsbach, Sitzber Akad. Wiss. Wien **116** IIb, 1425 (1907).
[4] W. F. Meggers and B. F. Scribner, BS J. Research **19**, 31 (1937). RP 1008.
[5] For earlier history see: H. Kayser, Handbuch der Spectroscopie **6**, 192 (S. Hirzel, Leipzig, 1912).
[6] J. M. Eder and E. Valenta, Sitzber. Akad. Wiss. Wien **119**, IIa, 6 (1910).
[7] J. M. Eder and E. Valenta, Atlas typischer Spektren, Wien Akad. (1911).
[8] F. Exner and E. Haschek, Spektren der Elemente bei normalem Druck **2**, 2 (Franz Deuticke, Wien, 1911).
[9] F. Exner and E. Haschek, Spektren der Elemente bei normalem Druck **3**, 4 (Franz Deuticke, Wien, 1911).
[10] J. Blumenfeld and G. Urbain, Compt. rend. **159**, 401 (1914).
[11] J. M. Eder, Sitzber. Akad. Wiss. Wien **124**, IIa, 707 (1915).
[12] H. Kayser, Tabelle der Hauptlinien der Linienspektra aller Elemente (J. Springer, Berlin, 1925).
[13] A. S. King, Astrophys. J. **74**, 328 (1931).
[14] R. W. Ball with L. F. Yntema, J. Am. Chem. Soc. **52**, 4264 (1930).
D. W. Pierce, C. R. Naeser, with B. S. Hopkins, Trans. Electrochem. Soc. **69**, 557 (1936).
[15] W. F. Meggers, BS J. Research **9**, 239 (1932.) RP 468.

WASHINGTON, Sept. 29, 1937.

U. S. DEPARTMENT OF COMMERCE NATIONAL BUREAU OF STANDARDS

RESEARCH PAPER RP1054

Part of Journal of Research of the National Bureau of Standards, Volume 19, December 1937

NEW TEST FOR DIMENSIONAL CHANGES IN OFFSET PAPERS

By Charles G. Weber and Martin N. V. Geib

ABSTRACT

Change of dimension of paper is a serious factor in many of its uses, particularly in multicolor offset printing where changes of dimensions cause the greatest difficulty—misregister of prints. The changes are caused by variations in the relative humidity of the surrounding air. To predict the relative constancy of dimensions of papers in use, a method was devised for determining the expansivity of paper with variations in relative humidity. Specimens of paper approximately 24 inches in length are mounted under constant tension in a cabinet in which humidity is controlled by salt solutions. Changes of length of the paper are measured by means of an optical lever, with a sensitivity of 0.00025 inch and the humidity and temperature inside the cabinet are determined with a wet- and dry-bulb hygrometer. The data thus obtained checked closely with those obtained by measuring specimens on a flat surface with a micrometer rule and were much more conveniently obtained and more reproducible.

CONTENTS

	Page
I. Introduction	665
II. Description of the apparatus	666
III. Effects of some conditions of testing	668
1. Stress on specimen	668
2. Effects of expansion and contraction of the cabinet	669
3. Precision of measurements	669
IV. Measurements on typical papers	671
V. Suggested method of test for expansivity of offset papers	673
1. Apparatus	673
2. Specimen	673
3. Procedure	673

I. INTRODUCTION

The changes of dimensions of paper with changes of moisture content are serious in offset papers used for multicolor printing and for other purposes where nearly constant dimensions are desired. The expansivity of such papers has been determined at the National Bureau of Standards by measuring with a micrometer rule specimens 24 or more inches in length, under different atmospheric conditions.[1] While satisfactory results can be obtained in this manner, the method requires the operation of a testing chamber at two or more widely different humidities, and is practicable only for research purposes. Numerous methods of determining the expansivity of paper have been proposed but not considered satisfactory because tests were generally

[1] BS J. Research 9, 431 (Sept. 1932) RP480.

made on small specimens and with devices in which the exact conditions surrounding the specimens were not conveniently controlled and measured.

The new method permits the testing of specimens of length sufficient to give a reliable reading, and wide enough to permit a load sufficient to minimize the effects of friction without excessive stretch. The apparatus is self-contained to the extent that it can be used under ordinary room conditions, hence it is adapted to use in the laboratory, print shop, or mill.

This study is one of a series made with the cooperation and financial support of the Lithographic Technical Foundation, paper manufacturers, printing-equipment manufacturers, and air-conditioning engineers. The studies are planned with the counsel of an advisory committee composed of technical representatives of the cooperating firms under the chairmanship of Prof. R. F. Reed, Director of Lithographic Research, University of Cincinnati.

II. DESCRIPTION OF THE APPARATUS

The apparatus consists essentially of a wooden cabinet approximately 40 in. high, 16 in. wide, and 12 in. deep, inside dimensions. Relative humidity inside the cabinet is controlled by circulating the air with a motor-driven fan over a suitable salt solution within a tray in the base.

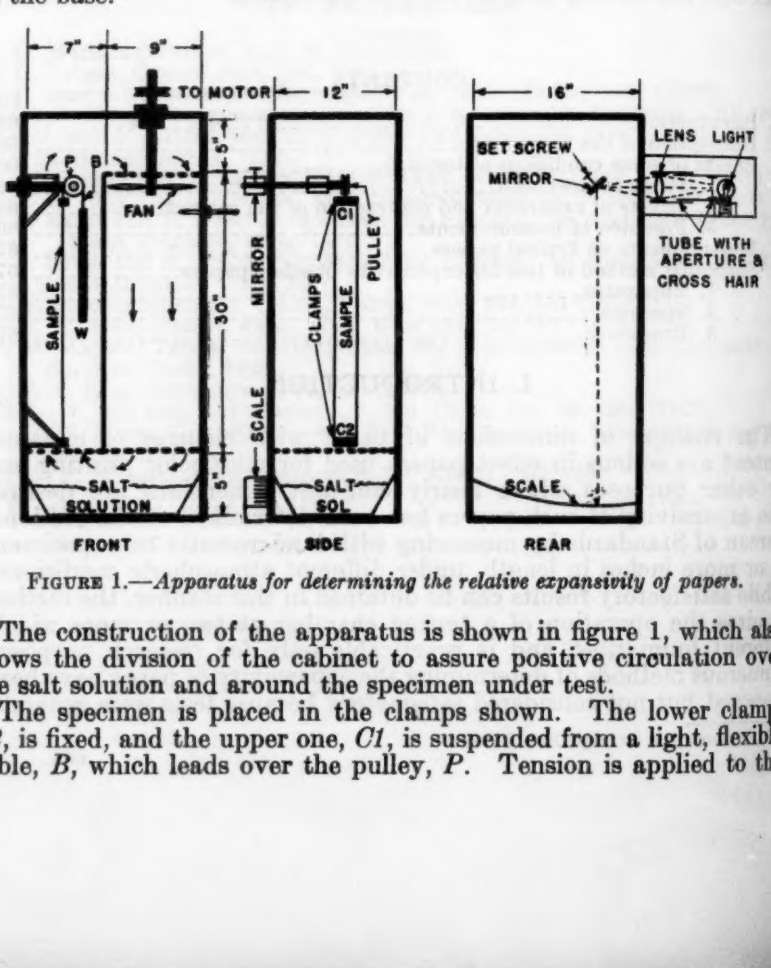

FIGURE 1.—*Apparatus for determining the relative expansivity of papers.*

The construction of the apparatus is shown in figure 1, which also shows the division of the cabinet to assure positive circulation over the salt solution and around the specimen under test.

The specimen is placed in the clamps shown. The lower clamp, *C2*, is fixed, and the upper one, *C1*, is suspended from a light, flexible cable, *B*, which leads over the pulley, *P*. Tension is applied to the

specimen by a dead-weight load on the other end of the cable at *W*, the tension being equal to the difference between the total load and the load required to move the upper jaw. The pulley shaft extends through the back of the cabinet and a mirror is mounted on the end outside the cabinet. Movement of the mirror, through rotation of the shaft, changes the position of a spot of light reflected by the mirror to a graduated scale near the base of the cabinet. The beam originates from the tube shown. Light from the source, a 40-watt bulb, admitted through a ⅛-in. circular aperture with a horizontal cross hair through its center, is focused onto the mirror by a 2-in. double convex lens near the other end of the tube. The mirror is mounted at an angle to reflect the beam of light onto the scale where the image of the cross hair makes a very satisfactory reading line. The tube is made in two sections, telescoped one within the other, to permit moving the section containing the lens so as to adjust the focus on the mirror to obtain a sharp image on the scale. The sections are 4 in. in length, telescoped to form a tube approximately 6 in. long. This tube is so placed that the lens is approximately 7½ in. from the mirror. The cross hair is a copper wire 0.005 in. in diameter (no. 36 AWG), and the lens is from an ordinary hand reading glass, having a focal length of 4.9 in. (8.00 diopters).

Expansion or contraction of the specimen turns the shaft through travel of the cable over the pulley. Using the ratio of the radius of the pulley to the distance of the mirror from the scale, which is the radius of curvature of the scale, the change in length of the specimen can be calculated from the travel of the light beam on the scale. The scale on the apparatus was calibrated for direct reading by raising and lowering clamp *C2*, measuring its movement with a micrometer caliper, and correlating this movement with the scale readings. The readings were found to be 2 cm per 0.01-in. movement of the clamp, hence the smallest scale division, 0.1 cm, corresponds to 0.0005-in. expansion. It was read to the nearest half of a scale division in the tests reported.

The cabinet is constructed of wood, 1 in. thick, covered on the inside with a heavy coating of wax and painted inside and outside with asphalt paint to minimize infiltration of air and moisture. The entire front is a hinged door which closes against a small rubber tube as a seal. The door is divided at the top of the bottom compartment so that the salt-solution trays can be interchanged without opening the remainder of the cabinet. The atmospheric conditions inside the cabinet are ascertained from wet and dry bulb readings taken in the air stream 3 in. below the fan by inserting the thermometers through holes provided in the door. The circulating fan is 8 in. in diameter and operates at 1,450 rpm. The air speed, as determined with a tube type of velocimeter, is 500 feet per minute around the specimen and 800 feet around the thermometer bulbs. This rapid circulation quickly brings the vapor pressure of the air to a steady state, conditions the test specimen rapidly, and ensures reliable wet-bulb readings.[2]

A wide range of humidities is obtainable by the use of different salt solutions or other materials suitable for controlling vapor pressure. Data for a selected list of solutions suitable for most requirements are given in an article by Carson.[3]

[1] F. T. Carson. Paper Trade J. **94**, no. 2 (January 14, 1932).
[2] F. T. Carson, Paper Trade J. **93**, no. 18 (October 29, 1931).

III. EFFECTS OF SOME CONDITIONS OF TESTING

1. STRESS ON SPECIMEN

In order to obtain data on the importance of stress, the same paper was tested under dead-weight tensions ranging from 50 to 1,000 g for the specimens 2 in. in width. The results are shown graphically in figure 2. The data were obtained for a range of relative humidities of

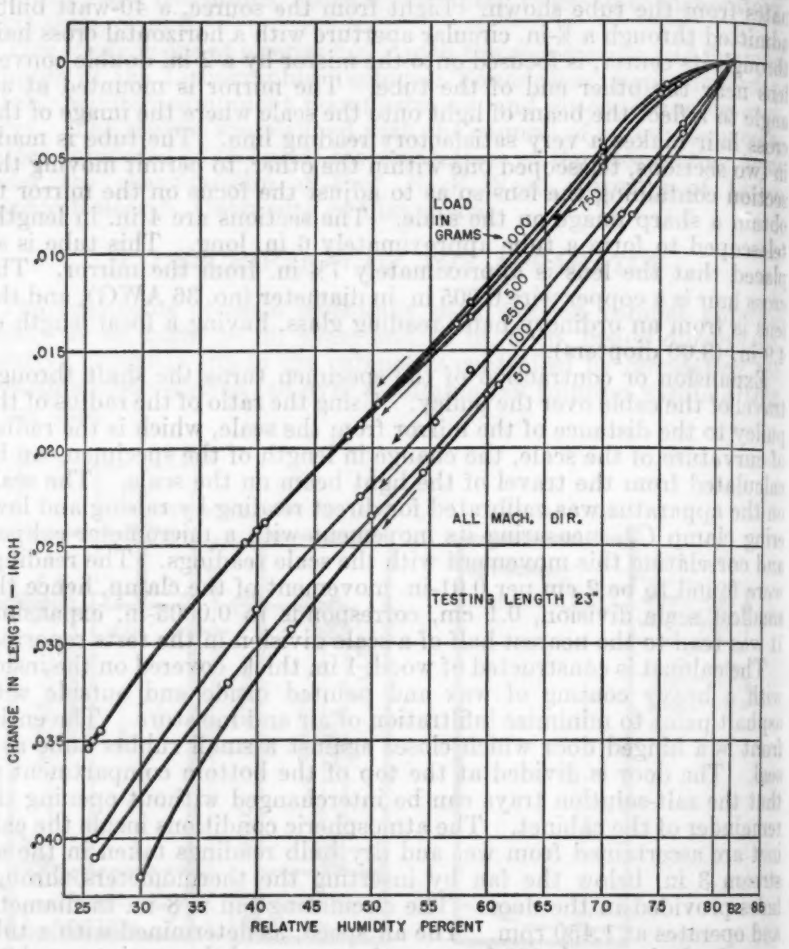

FIGURE 2.—*Effect of tension on the hygrometric expansivity of offset paper; desorption curves for the same paper with different tensions.*

82 to 26 percent. In order to avoid variations due to hysteresis effects, the same procedure was followed for each determination. The specimen was mounted and conditioned first at 50-percent relative humidity, then to the starting point at 82 percent. From this point, the specimen was conditioned at the other humidities indicated, in order of decreasing values. Scale readings for length of specimen and wet- and dry-bulb readings for relative humidity were taken for each condition after the specimen had reached constant length.

Although increased tension resulted in stretch of the specimen as indicated by separation of the curves, for the range of tensions used, nearly all the stretch occurred at humidities above 70 percent. Varying the tension from 25 to 500 g per inch of width did not change appreciably the slope of the curve in the region below 70-percent humidity. Hence, if the expansivity is taken from this part of the curve, precise control of tension is not important. For further experiments reported herein, a tension of 50 g per inch of width was used.

2. EFFECTS OF EXPANSION AND CONTRACTION OF THE CABINET

The magnitude of the possible errors introduced by thermal and hygrometric expansivity of the cabinet itself was investigated by using as the test specimen a steel tape having a known coefficient of expansion. The results of expansivity tests of the steel tape are shown in table 1.

The wood in the cabinet appears to be quite effectively sealed against moisture as shown by the slight errors caused by large humidity changes. However, the thermal effects are apparent and large variations in temperature during a test should be avoided.

TABLE 1.—*Results of expansivity tests of steel tape showing errors due to thermal and hygrometric expansivity of the cabinet*

Relative-humidity change	Temperature change	Scale-reading change	Thermal change of length of tape [1] (computed)	Apparent error of reading caused by change of cabinet
Percent	°C	*Inch*	*Inch*	*Inch*
+27	+3.0	+0.0005	+0.0008	0.00030
−50	+0.6	0	+.00016	.00016
0	+3.0	+.00075	+.00080	.00005
+1	+2.2	+.00025	+.00058	.00033
−3	−2.4	−.00025	−.00064	.00039
+1	+2.4	+.00075	+.00064	.00011

[1] Coefficient of expansion of tape 0.0000116 per degree centigrade.

3. PRECISION OF MEASUREMENTS

Comparative tests were made to learn how well the data obtained with the method compared with those obtained by measuring the papers on a flat surface with the micrometer rule. Satisfactory agreement was obtained, as illustrated by the data given in table 2.

TABLE 2.—*Comparison of expansion data obtained by two methods*

	Measurements made with micrometer rule		Direct readings with expansivity tester (100-g tension)	
Paper	Expansion between 50- and 65-percent rh	Average deviation of five readings	Expansion between 50- and 65-percent rh	Average deviation of five readings
	Percent	*Inch*	*Percent*	*Inch*
A	0.062	0.0022	0.065	0.0002
B	.067	.0007	.070	.0003
C	.049	.0009	.054	.0003

The slightly higher values obtained in the cabinet can be attributed to the tension on the specimens. When no tension is applied, expan-

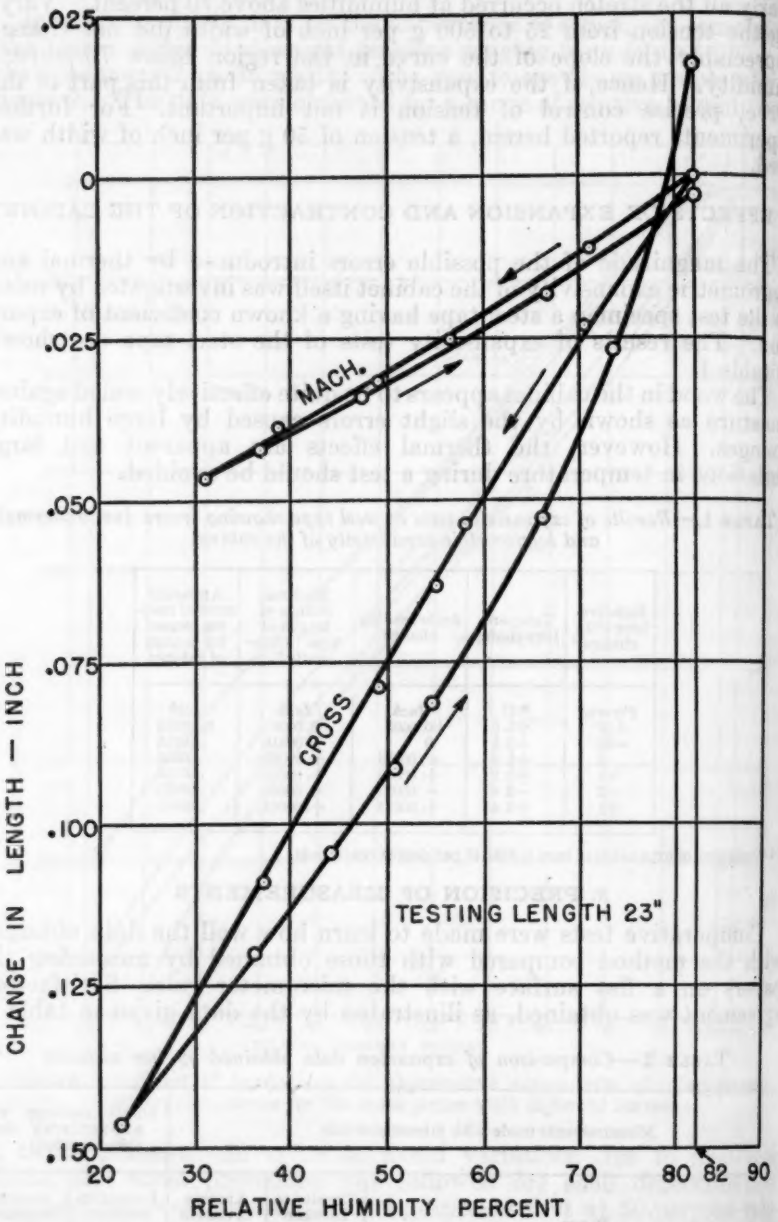

FIGURE 3.—*Curves showing changes of dimensions of offset paper for a complete cycle of humidity changes, from 82 percent to 23 percent by desorption and back to the starting point by adsorption.*

sion and contraction of paper are accompanied by distortion in the form of waving and curling, and this distortion probably is never

completely "ironed out" when measuring on a flat surface. Better reproducibility in individual readings was obtained with the expansivity tester as shown by the average deviation of readings.

The sensitivity of the method was found satisfactory. The scale divisions are comparatively large, and are easily read to the nearest half, which is 0.00025 in. The expansion measured is of the order of 0.065 percent which is 0.015 in. for a 23-in. sample. Hence when the readings are made to 0.00025 in. the precision is approximately 1 part in 60.

One potential source of error in the expansivity determination is in the measurement of relative humidity. This is determined only to the nearest 0.5 percent; hence, if measurements are made at only two points, differing by 15 percent in relative humidity, an uncertainty of 1 part in 30 is thereby introduced. If, however, measurements are made at several points, and a smooth curve is drawn and used as a basis for finding the hygrometric expansivity, the probable error from this source is greatly reduced.

IV. MEASUREMENTS ON TYPICAL PAPERS

Measurements were made on a series of lithographic papers, and curves plotted from the data on a typical paper are shown in figure 3. These curves show changes in length for cross and machine directions for the complete cycle of humidity changes from the starting point at 82 percent. They have the same general form as typical moisture regain curves for similar humidity cycles.[4]

Curves for the data on four lithographic papers of different fiber composition are shown in figure 4. The hygrometric expansivity of these papers can be computed from their curve by dividing the change in length for a given humidity range by the testing length, 23 in. The curves are approximately straight in the region of 40- to 65-percent relative humidity, and it appears satisfactory to base the expansivity per unit of relative humidity change on that region of the curve. For example, in figure 4, curve *A* shows a linear change of 0.0134 in., or 0.0134/23=0.058 percent, and *C* 0.0094 in. or 0.0094/23 =0.041 percent between 65-percent and 50-percent relative humidity.

For the various conditions of relative humidity at which the data given were obtained, the solutions and solid substances listed in table 3 were used.

TABLE 3.—*Solutions used to control relative humidity*

Solution or solid substance	Relative humidity corresponding to vapor pressure of solution	Relative humidity obtained in the cabinet
	Percent	*Percent*
Potassium sulphate (saturated sol.)	95	82 to 83
Barium chloride (saturated sol.)	88	76 to 78
Sodium chloride (saturated sol.)	75.8	66 to 71
Sodium bromide (saturated sol.)	58	56 to 59
Sodium dichromate (saturated sol.)	52	50 to 57
Potassium carbonate (saturated sol.)	43	44 to 49
Magnesium chloride (crystals)	33	36 to 38
Calcium chloride (solid)	----------	24 to 27

[4] BS J. Research 12, 53 (Jan. 1934) RP633.

It will be noted that the relative humidities obtained were not, in most instances, the conditions ascribed to the solution or chemical. This apparent inconsistency between the observed and the expected humidities is doubtless explained largely by temperature differences between that of the air in the cabinet and the temperature of the conditioning substance. Evaporation to obtain a high humidity cools the solution and condensation to dehumidify warms the solution.

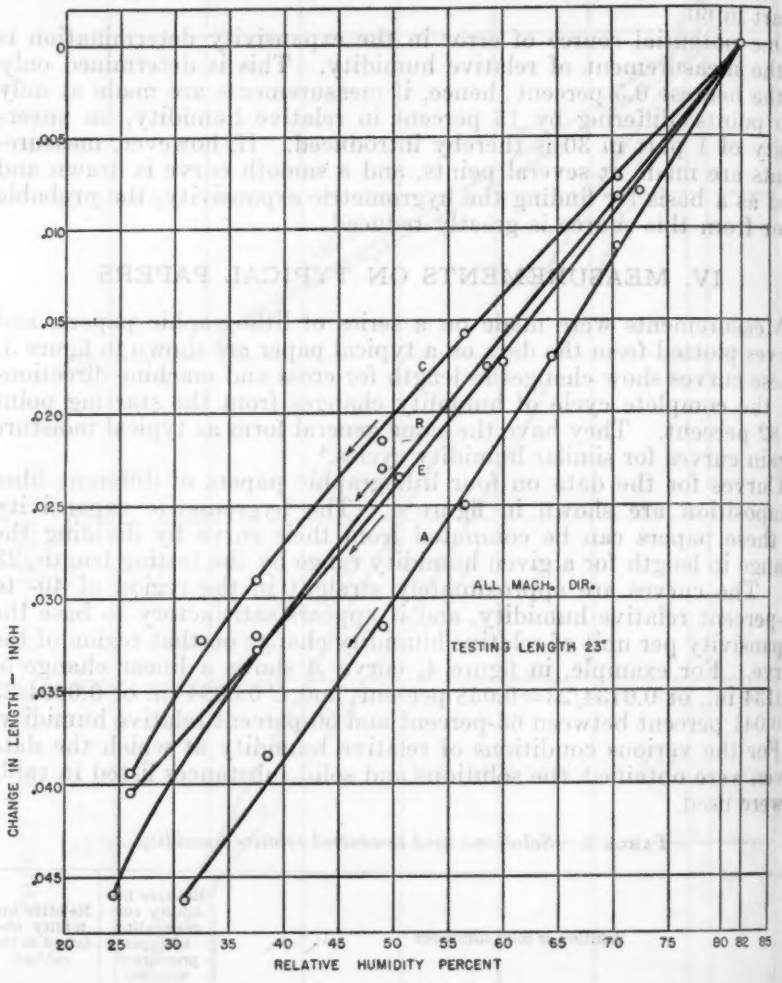

FIGURE 4.—*Expansivity curves for four typical offset papers; desorption curves.*

Differences as great as 3° C were noted in the operation. No attempt was made to exactly obtain any predetermined humidity, but simply to obtain a suitable range of humidities for plotting a curve and to exactly measure each condition.

Although the data shown are for lithographic papers, a wide variety of types have been tested with equally good results, and the method is considered suitable for papers in general.

V. SUGGESTED METHOD OF TEST FOR EXPANSIVITY OF OFFSET PAPERS

1. APPARATUS

The apparatus should consist of a cabinet of the design and approximate size shown in figure 1. The pulley shaft should be free to turn in ball or other low-friction bearings, and the fan should provide an air flow around the specimen of not less than 500 feet per minute. The mirror should be so clamped to the shaft as to permit simple adjustment to obtain a zero setting when the specimen is mounted. The cable connecting the upper clamp and the weight should be very flexible to prevent slippage. If constructed of wood, the cabinet should be coated on the inside and outside with a moisture-resistant coating, metal-lined, or otherwise treated to minimize swelling.[5] If constructed of metal, it should be insulated.

2. SPECIMEN

The specimen should be cut 2 in. wide and approximately 25 in. long, with the long dimension parallel to the major direction for which data are desired.

3. PROCEDURE

The specimen is mounted in the cabinet under a tension of 50 g per inch of width, and conditioned first at a relative humidity of 50 percent or lower, then at 80 percent or above. When the length becomes constant at the high humidity, the zero setting is made by adjusting the position of the mirror. Data for an expansion curve as illustrated in figure 4 are then obtained by conditioning at two or more lower humidities in order of decreasing values, ranging down to 50 percent or below. Humidity determinations and scale readings are made for each condition and the changes of length are plotted against humidity as shown in figure 4. The expansivity value is taken from this curve. It is obtained by dividing the change in length between two convenient points on the regular part of the curve by the testing length of the specimen. Relative humidities of 50- and 65-percent are usually convenient points to use when expressing the hygrometric expansivity as a percentage change of length per 15 percent relative humidity change. Data on one specimen are sufficient for an ordinary test; however, in instances where smooth curves are not obtained, check tests should be made.

The thermometers used for determining wet- and dry-bulb temperatures should conform to the following specifications: range, 0 to 50° C (32 to 122° F); graduation, 0.2° C (0.5° F). They should be matched to within 0.1° C (¼° F) throughout the range used. Temperatures should be taken with the bulbs in the air stream where the velocity of air is not less than 10 feet per second.

The temperature of the air surrounding the cabinet should not vary more than ±5° F while a test is in progress.

WASHINGTON, October 1, 1937.

[5] A. J. Stamm. Arch. Record (Feb. 1937).

U. S. Department of Commerce National Bureau of Standards

RESEARCH PAPER RP1055

Part of Journal of Research of the National Bureau of Standards, Volume 19, December 1937

AN IMPROVED APPARATUS FOR MEASURING THE THERMAL TRANSMISSION OF TEXTILES

By Richard S. Cleveland

ABSTRACT

An apparatus is described for measuring the thermal transmission of textiles. A horizontal plate is heated electrically and maintained at a constant temperature by means of a thermostat. The plate is surrounded by a guard plate which is also maintained at the same temperature to prevent lateral flow of heat into or out of the central plate. A second guard heater is placed below the central plate to prevent the downward flow of heat. The specimen to be tested is laid flat without tension on the apparatus and enclosed in a copper hood placed several inches above it to eliminate the disturbing influence of air currents of the room. Since the thermostatic control results in an intermittent supply of heat to the central heater, an electric clock is added to the circuit, thus automatically adding the periods during which heat is being supplied. The difference in temperature from the central plate to the top of the hood is measured by means of a thermocouple and microammeter. The amount of heat supplied to the central heater per unit of time divided by the difference in temperature from the central plate to the hood and by the area of the hot plate is taken as a measure of the thermal transmission of the specimen.

The reproducibility of results, the influence of differences in temperature between the central plate and the guard plates, and the influence of the height of the hood are discussed, and values of thermal transmission for typical fabrics are given. The regulation of temperatures is essentially automatic and little attention is required from an operator except during the 15 minutes a test is actually in progress. The hot plates can be operated at any temperature desired. About seven tests can be made in an 8-hour day, allowing proper time for the attainment of a steady state. The results are usually reproducible to about 1 percent.

CONTENTS

	Page
I. Introduction	676
II. Description of the apparatus	677
III. Quantities to be measured	681
IV. Performance tests	681
1. Effect of time before testing	681
2. Effect of a difference in temperature between the central and guard-ring plates	682
3. Effect of a difference in temperature between the central plate and the lower heater	682
4. Effect of changing the difference in temperature between the central plate and the hood	683
5. Effect of distance from central plate to hood	684
6. Reproducibility in the measurement of thermal transmission	684

I. INTRODUCTION

The apparatus used since 1924 in the Textile Section of the National Bureau of Standards for measuring thermal transmission of textiles is an extension by Sale [1] of a hot-plate method used by the National Bureau of Standards for measuring the thermal conductivity of insulating materials, employing the well-known guard-ring principle. With this type of apparatus, the rate of flow of heat is measured between two flat metal plates which differ in temperature by a known amount and between which the specimen is held. Because this method does not simulate sufficiently well the conditions under which textile fabrics are used as thermal insulation, it was altered by Sale by laying the fabric over the hot plate and maintaining a constant temperature difference between this plate and the air above the fabric in an air-conditioned room. Heated guard plates were used, as in the previous apparatus, to prevent loss of heat from the central plate in directions other than through the sample.

Such an arrangement better simulates the conditions of use in which the heat is supplied by the human body on one side of the fabric and transferred to the air on the other side. It is not intended to imply, either for this apparatus or the new one about to be described, that the simulation is complete. The transfer of heat from the human body through one or more layers of material to the air and surroundings without, is a very complex process and cannot be approximately duplicated by such a hot-plate apparatus except in the more simple cases. The methods described in this paper are concerned with one phase of the problem.

The chief disadvantages of Sale's apparatus are the great length of time required to adjust the electric circuits in the guard plates to attain temperature equilibrium, and the fact that no provision was made to prevent disturbances resulting from air movements in the room. The testing of a single sample with this apparatus frequently takes a whole day.

More recently Schiefer [2] developed an apparatus to make measurements similar to those of Sale. The hot plate is automatically maintained at a constant temperature by a thermostat, and heat is supplied intermittently. After the apparatus has once attained a steady state, a number of samples can be tested in a comparatively short period, because the effect of the thermal lag of the apparatus itself is eliminated by keeping it at constant temperature. The time required for a sensibly steady state to be reached in the sample itself is relatively short. When this condition is reached, the rate at which heat must be supplied to maintain a given difference in temperature from the hot plate to the air of the room is then measured over a period of half an hour. Guard heaters were not used, but the hot plate and heating element were placed in the mouth of a vacuum (Thermos) jar to prevent lateral and downward flow of heat.

While the method is both rapid and convenient, it is not altogether satisfactory for materials having high insulating value, because of a correction which must be applied for heat loss through the vacuum jar. This correction may be as much as 80 percent of the total heat input.

---

[1] P. D. Sale. *Specification for constructing and operating a heat transmission apparatus for testing the heat insulating value of blankets.* Tech. Pap. BS **18**, 595–607 (1924) T269.

[2] *Apparatus for measuring the thermal transmission of textiles.* Tech. News Bul. NBS (February 1931); J. Research NBS **13**, 322 (1934) RP711. A modified apparatus has been described by H. S. Schenker, Melliand Textile Mo. **5**, 115–117 (1933).

As has already been indicated, thermal conductivity alone is not a sufficient measure of the thermal transmission of fabrics. Although the flow of heat through a thick fabric may be largely by conduction,[3] the rate at which heat is transferred from its surface depends also on the convection to the air overlying the fabric and on radiation to the solid surroundings. The new instrument to be described takes account of this by enclosing the fabric with a hood that absorbs the heat transferred through the fabric and dissipates it to the outer air. The hood encloses a definite layer of air that overlies the fabric and at the same time shuts out the disturbing air currents of the room. A measure is obtained of the thermal transmission from the hot plate to the hood, which is but a few degrees warmer than the room.

The new instrument combines the automatic features and the short-test-period characteristic of Schiefer's apparatus with the guard-ring principle used in other equipment.

II. DESCRIPTION OF THE APPARATUS

A cross sectional drawing of the apparatus is shown in figure 1. The central plate P_c, which is a hollow copper plate 6 in. square, is heated electrically by the resistance ribbon H_c. The cavity C_a is filled with methyl alcohol and connected by a tube, T, and sleeve, R_c, to a glass U-tube containing mercury and alcohol. A rubber sleeve extracted with methyl alcohol has been found satisfactory for making the connection. As the plate becomes heated, the methyl alcohol expands into the U-tube, causing the mercury to rise in the capillary, C, and make contact with the wire, W. This closes the coil circuit of a relay which then cuts off the heating current. Conversely, when the plate cools, the current is automatically turned on again. In this manner, the plate is regulated to a surface temperature constant within about 0.02° C. This fluctuation was made small by using a relatively large amount of a highly expansible medium, methyl alcohol, a small capillary, and numerous heat-conducting bridges across the cavity in the copper plate to facilitate the passage of heat from its under to its upper surface and thus speed transfer of heat to the expansible medium.

The central plate is surrounded by a hollow copper guard plate, P_g, 2 in. wide, equipped with a similar thermostat which also holds the temperature constant within about 0.02° C.

Both hot plates were painted with a flat black lacquer to give them a high emissivity comparable to that of the human body.

The bulb, a, of the U-tube is a reservoir for both alcohol and mercury of such size that the mercury will not enter the copper plate when at its lowest temperature and the alcohol will not be driven into the capillary when it is at its highest temperature. The bulb, b, is of such size that the lowest temperature to which the plate is subjected will not cause the mercury in the bulb to be lowered sufficiently to permit air to be drawn into the plate.

These U-tubes were designed for a wide range of operating temperatures. The desired temperature is attained in two steps. The stopcock, S_c, is opened, permitting the mercury to pass into reservoir R until the plate has reached the approximate temperature desired. The stopcock is then closed so that further expansion of the methyl alcohol causes the mercury to rise rapidly in the capillary and make

[3] J. L. Finck. *Mechanism of heat flow in fibrous materials.* BS J. Research 5, 973-984 (1930) RP 243.

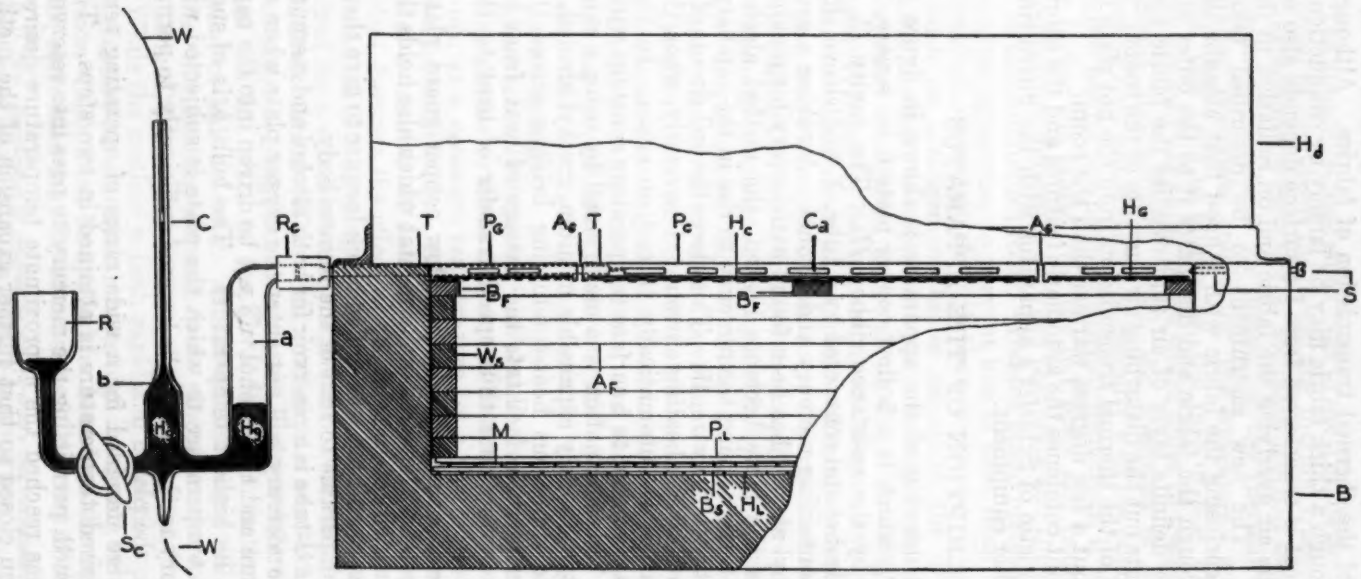

FIGURE 1.—*Cross-sectional drawing of the apparatus.*

a, bulb for mercury and methyl alcohol.
a_F, aluminum foil.
a_g, air gap.
b, bulb for mercury.
B, wooden box.
B_F, Bakelite supporting frame.
B_S, Bakelite sheet on which heating coil is wound.
C, capillary tube.
C_a, cavity filled with methyl alcohol.
H_c, central heating coil.
H_d, hood.
H_o, guard-ring heating coil.
H_L, lower heating coil.
M, mica insulation.
P_c, central copper hot plate.
P_g, guard-ring copper hot plate.
P_L, lower copper plate.
R, reservoir for mercury.
R_c, rubber sleeve.
S, screws holding plates in position.
S_c, stopcock.
T, bronze tube connecting center plate to glass U-tube.
W, wire in coil circuit of relay.
W_s, wood spacers.

contact with the wire, *W*. Very fine adjustments of temperature can then be made by raising or lowering the wire in the capillary. By this means the temperature of the two plates can be regulated to within $\frac{1}{40}$° C of each other.[4]

The two hot plates are supported by the Bakelite frame, B_F. Below the frame are six layers of aluminum foil, A_F, spaced about ¼ in. apart by small wood spacers, W_S, and a $\frac{1}{16}$-in. copper plate, P_L. Aluminum-foil insulation was used because its very low heat capacity would aid in the rapid establishment of a steady state. A lower heater, H_L, just beneath the copper plate, is wound on a $\frac{1}{16}$-in. sheet of Bakelite, B_S, and electrically insulated from the copper plate by a thin sheet of mica, *M*. The whole unit is then mounted in a wooden box and secured by the set screws, *S*, at each side.

The lower heater is regulated manually to within 0.1° C of the temperature of the central hot plate.

The apparatus was designed to operate in a horizontal position to facilitate mounting the sample. The specimen to be tested is cut 13 in. square and placed over the entire surface of the hot plates and the edges of the box in a flat, unstretched condition. Its thermal properties are thus not changed by stretching or compressing.

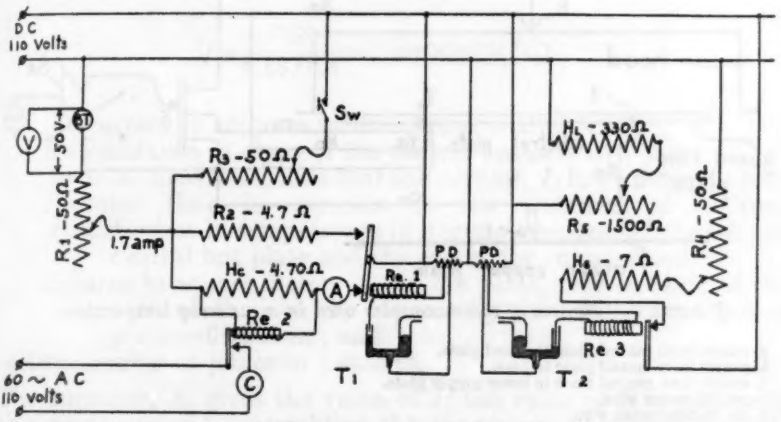

FIGURE 2.—*Heating, regulating, and timing circuits.*

A copper hood is placed over the fabric to prevent air currents of the room from affecting the results. It is painted inside and out with a flat black lacquer to aid in the absorption of heat and its subsequent reradiation to the external surroundings.

With a guard plate to prevent lateral flow of heat and the lower heater to prevent its downward flow, heat energy supplied to the central plate must pass vertically upward through the specimen placed upon it.

Figure 2 is a wiring diagram of the heating and regulating circuits. Current from a 110-volt d-c. source passes through a ballast tube, *BT*,[5] across which the drop in voltage is regulated by the resistance, *R1*, to 50 volts and which, therefore, delivers a virtually constant current. The circuit then divides into three paths, the first through the central heater, H_c; the second through the resistance, *R2*, which is equal to

[4] These plates were made as thin as practicable ($\frac{1}{32}$ in.) in order to reduce the area of their edges. The heat conducted and radiated across the $\frac{1}{16}$ in. air gap between them is proportional to the area of their edges. To reduce this area permits more latitude in the allowable difference in temperature between the two plates.

[5] This tube delivers a nearly constant current through a range in voltage of 40 to 60 volts.

H_c; and the third, through the resistance, *R3*. Relay 1 (*Re*1) is a double-pole relay which simultaneously closes the heater circuit, H_c, and opens the circuit, *R2*, thus aiding the operation of the ballast tube by keeping the equivalent resistance of the parallel circuit unchanged. *R3* is set to divide the current so that the desired portion flows through the heater and the remainder by-passes through *R3*. Initial heating can be greatly accelerated by opening the switch, *Sw*, so that a much larger current passes through the heater.

The coil of a telegraphic relay (*Re*2) is connected across the heater so that when current flows in the heater, the relay closes the circuit of a self-starting electric clock, *C*. Thus the time intervals during which the current flows through the heater are automatically added by the clock.

H_G is the guard-plate heater and *R4* is a variable resistance. This circuit is opened and closed by the relay, *Re*3. H_L is the lower heater and *R5* is a variable resistance to control the current through the heater.

T1 and *T2* are mercurial thermostats of the type illustrated in figure 1 in the coil circuits of the relays and the two *PD*'s are potential dividers providing emf's for the coil circuit.

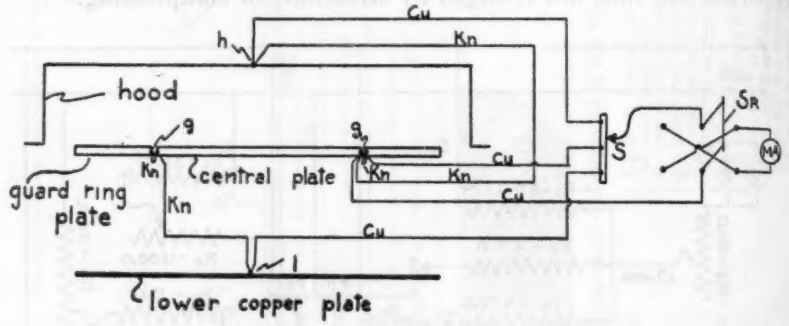

FIGURE 3.—*System of thermocouples used in measuring temperature.*

g, couple from central plate to guard plate.
h, couple from central plate to hood.
l, couple from central plate to lower copper plate.
Cu, no. 30 copper wire.
Kn, no. 28 constantan wire.
S, selecting switch.
S_R, reversing switch.

The system of copper-constantan thermocouples used to measure temperature differences is shown schematically in figure 3. Number 30 copper and no. 28 constantan (B. & S. gage) wire were used. The switch, *S*, puts the desired couple in series with the microammeter, *MA*, and the reversing switch, S_R, gives the current the proper direction. The temperature-emf relation was known for the particular wires used and the microampere-emf relation was found experimentally with a potentiometer and the microammeter, *MA*. The two relationships were then combined in a chart to give directly the temperature difference corresponding to any given microammeter reading for each couple.

The chart giving the temperature-microampere relations was computed for a cold-junction temperature of 25° C. The temperature of the cold junction is indicated by a thermometer placed in a shallow thermometer well in the top of the hood. For a temperature difference

of 15 to 25° C, the cold junction may depart from 25° C by ±4° C without introducing over 1 percent error in the indicated temperature difference. This is as great a range in the cold-junction temperature as would normally be experienced with this equipment. If greater precision is desired, a table of corrections may be computed and applied to the indicated temperature difference.

Four couples, *g*, (only two are shown in fig. 3) are in parallel, each with one junction on the inner vertical edge of the guard plate and the other on the edge of the central plate so that the combination gives the average difference in temperature between the two plates at their four edges. The couples, *h* and *l*, give the difference in temperature between the central plate and the hood, and that between the central plate and the copper plate beneath the foil insulation.

III. QUANTITIES TO BE MEASURED

The average quantity of heat supplied to the central plate per second, divided by the temperature difference between the plate and the hood and by the area of the plate, is the quantity that is determined. This quantity is that hereafter called the "thermal transmission" of the fabric and it is expressed as follows:

$$Q=\frac{I^2Rt}{4.18T\theta A}\text{cal/(sec}\times m^2\times\text{°C)}$$

where

I=current in amperes in the central heater,
R=resistance in ohms of the central heater=4.70 ohms,
t=total time in seconds that the current, I, flows during a test,
T=total time in seconds of the duration of a test,
θ=difference in temperature in degrees centigrade between the central hot plate and the top of the copper hood,
A=area in square meters of the hot plate, plus one-half of the area of the air gap separating the central and guard plates=0.0232 m^2, and
4.18=number of joules in 1 calorie.

The ammeter, *A*, gives the value of *I;* the value of *R* is measured with a bridge prior to assembling the apparatus; *t* is found by subtracting the initial reading of the electric clock from the final reading; *T* is measured with a stop watch from a moment when the current turns on to another moment about 15 minutes later when the current again turns on; and θ is measured with the thermocouple, *h*. The readings of the microammeter for couples *g* and *l* are observed occasionally to ascertain the departure from zero during test.

IV. PERFORMANCE TESTS

1. EFFECT OF TIME BEFORE TESTING

After about 10 minutes of initial heating the relays start operating. The value of *Q* does not become constant at once, but in 3 hours it comes to within 0.5 to 2 percent of its final value. Furthermore, when one sample is removed and another of widely different insulating value is mounted in its place, *Q* becomes virtually constant in half

an hour. Therefore, before making a test, 3 hours was allowed to pass after starting the apparatus and ½ hour to pass after mounting a new specimen. This permits the making of about seven tests in an 8-hour day.

2. EFFECT OF A DIFFERENCE IN TEMPERATURE BETWEEN THE CENTRAL AND GUARD-RING PLATES

Tests were made with the central and guard plates at different temperatures in order to determine what error might arise in Q from this source. The solid lines of figure 4 show the amount of uncertainty introduced into the value of Q by operating the two plates at slightly

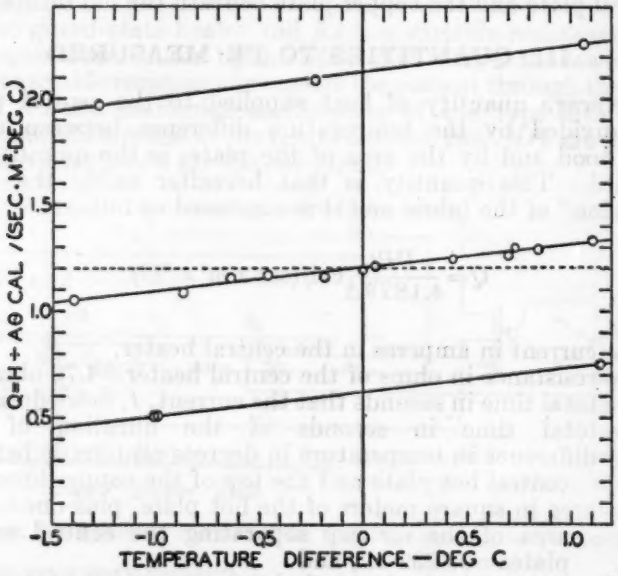

FIGURE 4.—*Relationship between Q and the temperature difference between the central and guard plates and between the central and lower copper plate.*

The solid lines show the effect of maintaining the central hot plate and the guard plate at unequal temperatures.
The dotted line shows the effect of maintaining the central hot plate and the lower copper plate at unequal temperatures.
The abscissa is the number of degrees centigrade that the central hot plate is above the guard ring or the lower copper plate.

different temperatures. The curves show the behavior for three fabrics of different insulating value. These curves indicate that the change in Q is not more than 0.13 cal/(sec$\times$m$^2\times$°C) for a 1° difference in temperature between the plates and is also virtually independent of the magnitude of Q. The difference in temperature is controlled to about 0.025° C. The error due to a lack of balance of 0.025° C is seldom greater than 0.5 percent.

3. EFFECT OF A DIFFERENCE IN TEMPERATURE BETWEEN THE CENTRAL PLATE AND THE LOWER HEATER

Tests were made with the central plate and the copper plate of the lower heater at different temperatures to determine what error might arise in the value of Q from this source. The dotted line in figure 4

shows Q as a function of the difference in temperature between these two plates. The value of Q was found to change by 0.003 cal/-(sec×m²×°C) for a 1° difference in temperature over the range ±5° C difference in temperature. No points fell within the range shown in figure 4. The difference in temperature is controlled to within 0.1° C and the error arising from a lack of balance of 0.1° C is negligible.

4. EFFECT OF CHANGING THE DIFFERENCE IN TEMPERATURE BETWEEN THE CENTRAL PLATE AND THE HOOD

The relationship between Q and the difference in temperature between the central plate and the hood is shown in figure 5 for several specimens that differ in insulating value. It is important to emphasize at this point that Q has been defined as the ratio of $I^2 R\ t/4.18\ T$, which we will call H, to θ A. The area, A, is a constant of the apparatus, so that Q is proportional to the ratio H/θ. It is seen in figure 5 that H/θ increases as the difference in temperature increases, and also at a rate that increases with the thermal transmission. This behavior is attributed primarily to the effect of radiation.

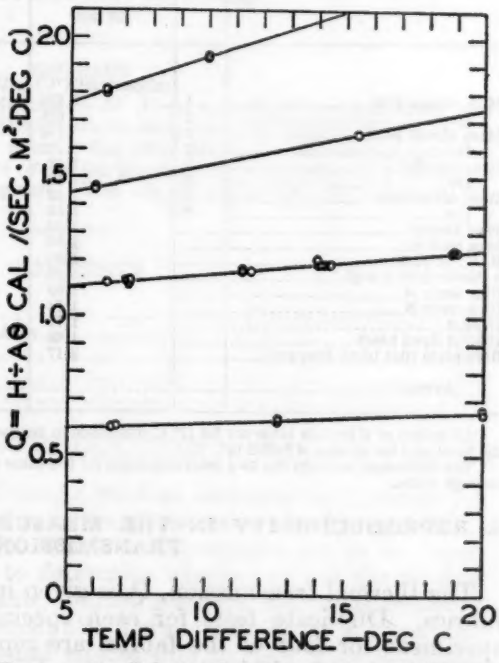

FIGURE 5.—*Relationship between Q and difference in temperature from the central hot plate to the hood for (1) no specimen on the hot plate; (2) a fabric of low insulating value; (3) a fabric of medium insulating value; and (4) a fabric of high insulating value.*

Convection in the air space between the fabric and the hood is also a factor, although probably less important than radiation, in making the relation between heat loss and temperature difference nonlinear.

It is probable that if hot plates of different areas were used, the relation between heat loss and area would also be nonlinear owing to the varying degree to which convection would be involved. However, this could not be tested with a single apparatus.

Since Q for any specimen is not constant for various differences in temperature between the hot plate and the hood, it might appear improper to divide by θ and A in expressing thermal transmission. This procedure is justified, however, by the fact that it reduces to an approximately common basis the results obtained with different areas and temperature differences.

The temperature difference and area used should be stated when giving results.

5. EFFECT OF DISTANCE FROM CENTRAL PLATE TO HOOD

Table 1 gives Q for several fabrics determined with hoods 4 in. and 8 in. in height. There is no consistent difference between the two sets of results and they differ only by a few percent. The 4-in. hood was used in all other tests.

TABLE 1.—*Values of Q for several typical fabrics.*

Fabric	Fabric no.	Q[a]			Reproducibility with 4-in. hood
		4-in. hood		8-in. hood	
		1st test	2d test		
		cal/(sec×m²×°C)	cal/(sec×m²×°C)	cal/(sec×m²×°C)	[b] *Percent*
5/16-in. alpaca pile	1	0.628	0.628	0.620	0.0
Do	2	.628	.616	.620	1.9
3/8-in. alpaca pile	1	.753	.740		1.7
Do	2	.732	.740		1.1
Gray blanket	1	1.12	1.12	1.14	0.8
Do	2	1.12	1.09	1.12	2.7
Wool underwear		1.52	1.52	1.53	0.0
Do	2	1.54	1.54		0
30-oz kersey		1.52	1.51	1.57	.7
16-oz melton		1.63	1.62		.6
B. V. D. cloth		1.66	1.69	1.72	1.8
Athletic shirt jersey		1.22	1.21	1.22	0.8
Blue serge *A*		1.69	1.68		.6
Blue serge *B*		1.74	1.73	1.78	.6
Drill *A*		1.71	1.71	1.74	.0
Drill *A* dyed black		1.68	1.70	1.68	1.2
Bare plate (flat black lacquer)		2.17	2.17		0.0
Average					0.9

[a] All values of Q in this table are for 17° C difference in temperature between the central hot plate and the hood and for an area of 0.0232 m².

[b] The difference between the two determinations for the same sample is expressed as a percentage of the average value.

6. REPRODUCIBILITY IN THE MEASUREMENT OF THERMAL TRANSMISSION

The thermal transmission, Q, is given in table 1 for several typical fabrics. Duplicate tests for each specimen and tests of duplicate specimens for four of the fabrics are reported. On the average, Q was reproduced within 1 percent and in the worst example within 2.7 percent. The maximum difference in Q for two specimens of the same material is 3 percent.

The thermal transmission ranges approximately from 2.17 cal/(sec×m²×°C) for the bare plate to 0.62 cal/(sec×m²×°C) for the 5/16-in. alpaca pile fabric and is reproduced within ±0.015 cal/(sec×m²×°C) of the mean value for any sample. The apparatus is therefore sufficiently sensitive to measure relatively small differences in the thermal transmission of materials. It is particularly well adapted for routine testing and for research work involving systematic studies of thermal transmission as affected by such factors as construction, laundering, finishing treatments, and combinations of different materials.

WASHINGTON, October 1, 1937.

U. S. Department of Commerce National Bureau of Standards

RESEARCH PAPER RP1056

Part of Journal of Research of the National Bureau of Standards, Volume 19, December 1937

EFFECT OF YAW ON VANE ANEMOMETERS

By Roy H. Heald and Paul S. Ballif

ABSTRACT

The effect of yaw on the performance of three vane-type anemometers was determined in the wind tunnel. Observations were made for angles of yaw within a range of 35 degrees on either side of the zero position. Maximum positive errors of 1, 4, and 5.5 percent were found for the three instruments when the angle of yaw was approximately 15 degrees. The magnitude of the error depends on the design.

CONTENTS

		Page
I.	Introduction	685
II.	Description of the anemometers	686
III.	Method of test	687
IV.	Results	688
V.	Conclusions	690

I. INTRODUCTION

The customary practice in using a vane anemometer is to mount the instrument so that the axis of rotation of the vane wheel is parallel to the axis of the fan or duct for which measurements are to be made. Usually no attempt is made to determine whether or not the air flow is parallel to the duct or fan axis, it being assumed that no appreciable error is introduced on this account. Ower [1] states, for a particular instrument, that the directional effects due to yaw may introduce errors of the order of 1 percent for angles of inclination less than about 20 degrees, but points out the uncertainties involved in drawing conclusions from the performance of a single instrument. Differences in design of anemometers constructed by different manufacturers are often encountered in practice. Hence differences in response to directional effects are to be expected, especially when the direction of air flow makes a large angle with the reference axis.

Recently, in determining the air deliveries of electric fans, the direction of air flow was found to be inclined 20 degrees or more to any plane containing the fan axis. In such cases, accurate results can be obtained with an anemometer mounted with its axis parallel to the fan axis only if the correction factor for airstream inclination is known and applied. For this reason an investigation was undertaken

[1] E. Ower. Measurement of Air Flow, 2d ed., p. 119. (Chapman and Hall, London, 1933.)

to determine the effect of airstream inclination, in yaw,[2] on the performance of the three vane anemometers used in the fan tests. The information may be of interest to other investigators who have occasion to use vane anemometers under unfavorable conditions of air flow.

II. DESCRIPTION OF THE ANEMOMETERS

The anemometers used in these experiments are shown in the halftone figure 1, and in the detail drawings, figure 2. The length/diameter ratios of the cylindrical housings are 0.43 for anemometer *A*; 0.32 for anemometer *B*; and 0.59 for anemometer *C*. Anemometers

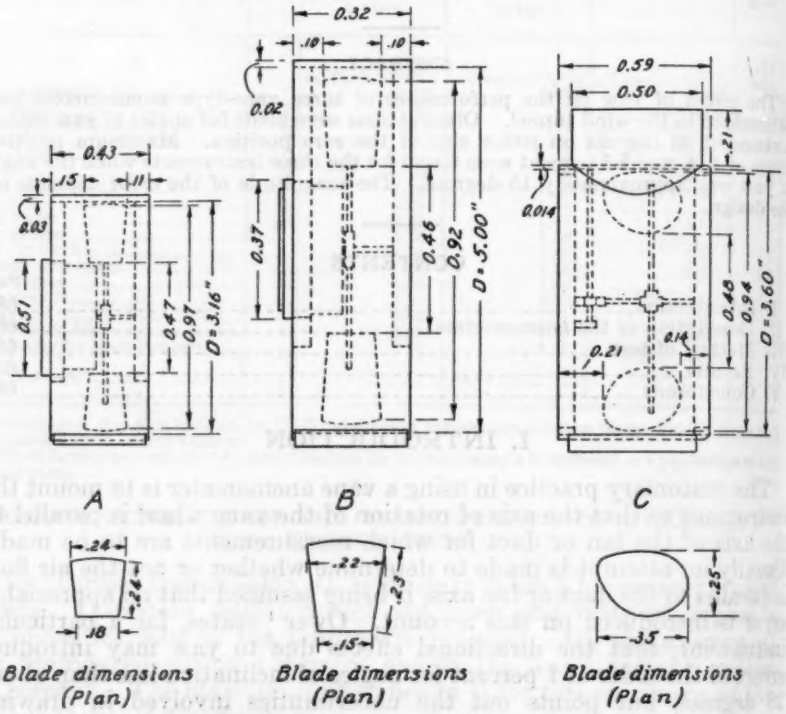

FIGURE 2.—*Line drawings of the anemometers.*

The dimensions are given as decimals of the inside diameter of the housing.

A and *B* are dial indicating. Anemometer *C* transmits signals electrically.

The plane of rotation of the upstream tips of the rotor vanes is 0.11 diameter within the housing for anemometer *A*; 0.10 diameter for anemometer *B*; and 0.14 diameter for anemometer *C*, the inside diameter of each housing being used as a reference. The rotor vanes have plane surfaces.

[2] The yaw angle is defined as the angle in a horizontal plane between the axis of the instrument and the direction of air flow. Since the anemometer is nearly a symmetrical instrument the effects of pitch, i. e., of inclination in a plane normal to the yaw plane, are not expected to differ greatly from the effects of yaw.

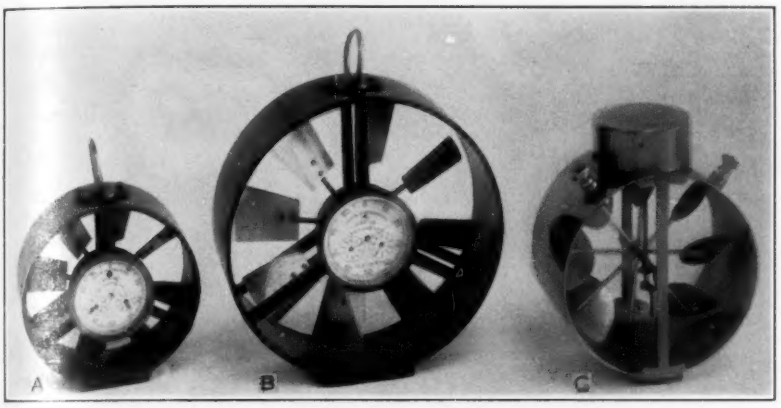

FIGURE 1.—*Three vane-type anemometers (A, B, and C) used in the experiments.*

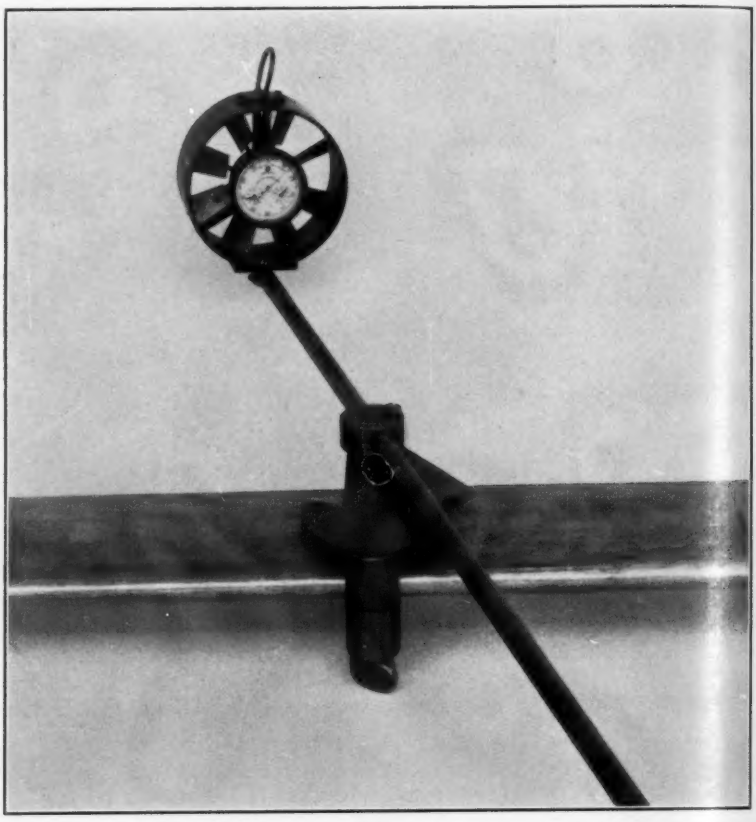

FIGURE 3.—*Anemometer support.*

III. METHOD OF TEST

The anemometers were tested in the 54-inch wind tunnel of the National Bureau of Standards. The instrument under test was attached to a cylindrical mounting rod ⅜ inch in diameter and 3 feet long. The mounting rod was clamped to a faired strut (fig. 3) fixed to the tunnel walls. The effect of the presence of the strut and clamping device was determined for each anemometer by observing the indicated velocity when the instrument was mounted various distances ahead of the strut. As may be seen in figure 4, the effect of the strut and clamp was found to be small for positions more than 6 inches ahead of the strut.

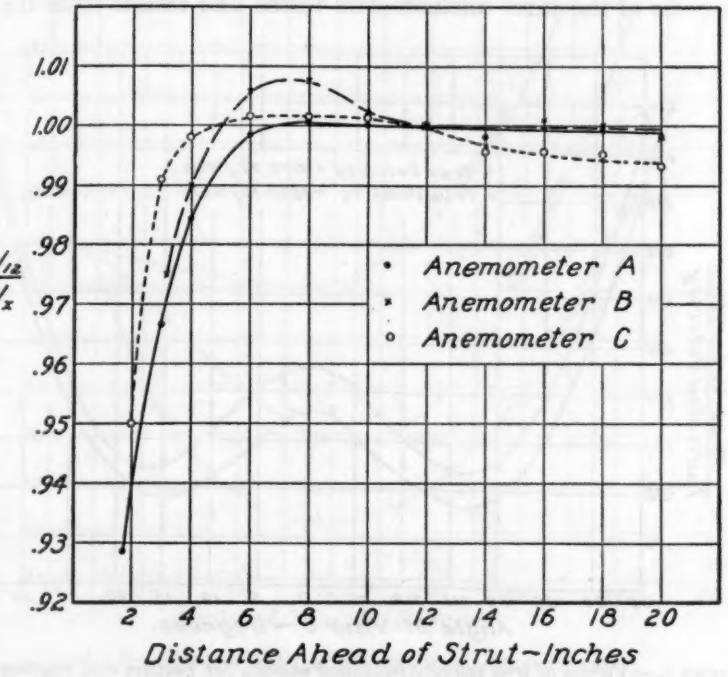

FIGURE 4.—*Effect of support interference on the velocity indications for zero yaw.*

V_{12} = indicated velocity at point 12 inches ahead of the strut.
V_x = indicated velocity at point x inches ahead of the strut.

The method of mounting the anemometers, illustrated in figure 3, permitted yawing of the mounting rod through an angle of about 45 degrees on either side of the center position. Yaw settings were read on a graduated scale mounted on the clamp. The mounting screw in the base of the anemometer was maintained at a point 12 inches ahead of the strut and midway between opposite walls of the wind tunnel for all angle settings by adjusting the clamp and mounting rod. Thus the effect of the small velocity gradient in the wind tunnel was eliminated.

The velocity indicated by each anemometer was observed for angles of yaw in intervals of 5 degrees through a range of −35 to +35 degrees. At least two observations of indicated velocity were made

for each yaw setting and for each of two air velocities, approximately 800 feet per minute and approximately 1,500 feet per minute. The constancy of the air velocity through the tunnel during the tests was of the order of 1 percent. The time interval for each observation was about 2 minutes.

IV. RESULTS

The ratio of the true air velocity in the wind tunnel to the velocity indicated by the anemometer was computed for each observation. The results for anemometer *B* are plotted in figure 5. The curves are similar to those obtained for instruments *A* and *C*. The difference in the value of the ratio, true velocity/indicated velocity, for air velocities of 800 feet per minute and 1,500 feet per minute is characteristic of the three anemometers tested and results from the non-

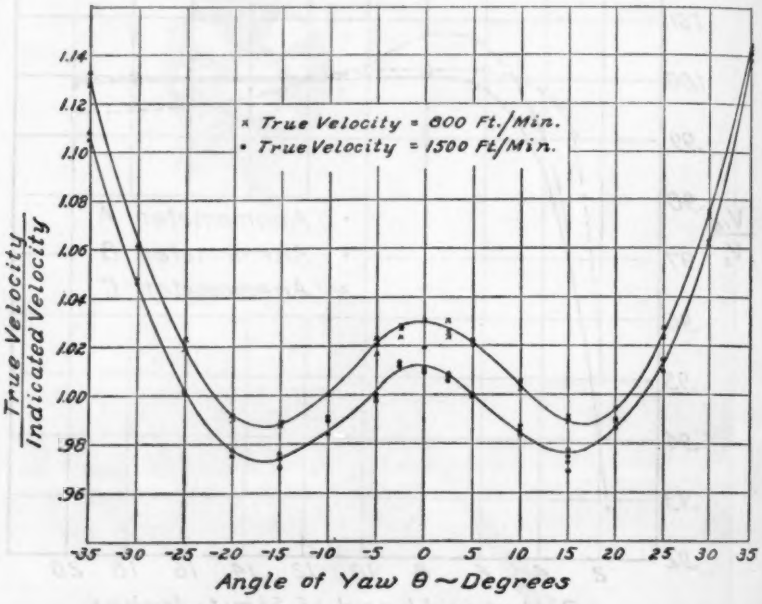

FIGURE 5.—*Values of true velocity/indicated velocity for positive and negative angles of yaw, anemometer B.*

linear relationship between the friction of the bearings and indicating-mechanism load and the torque applied to the vanes by the air stream. Ordinarily, corrections for this difference are made by using the calibration curve for the instrument.

The ratio of the indicated velocity V_0 for zero yaw, to the indicated velocity V_θ for angle of yaw Θ, was computed for each observation. The curves in figure 6 show the mean values of V_0/V_θ, all of the observations obtained for a given angle of yaw for each instrument being used. In general, the indicated velocity increased as the angle of yaw was increased, reaching a maximum when the angle of yaw was about 15 degrees. Further increase in the angle of yaw resulted in a decrease in indicated velocity. The indicated velocity for 15 degrees of yaw, for anemometers *A*, *B*, and *C*, was about 5.5, 4, and

1 percent, respectively, greater than the indicated velocity at zero yaw; for approximately 30, 27, and 18 degrees of yaw, respectively, the indicated velocity was the same as for zero yaw and for greater angles of yaw the indicated velocity was less than for zero yaw.

It will be noted from figures 1 and 2 that anemometer *A* which showed a maximum positive error of 5.5 percent, is substantially different in design from anemometer *C*, which showed a maximum positive error of about 1 percent. For example, there is a decided difference in the shape of the vanes. Also, the dial of anemometer *A* exerts a blocking effect over about 25 percent of the area of the housing, while the housing of anemometer *C* is comparatively free from obstruction. Further, the length/diameter ratios of the housings are

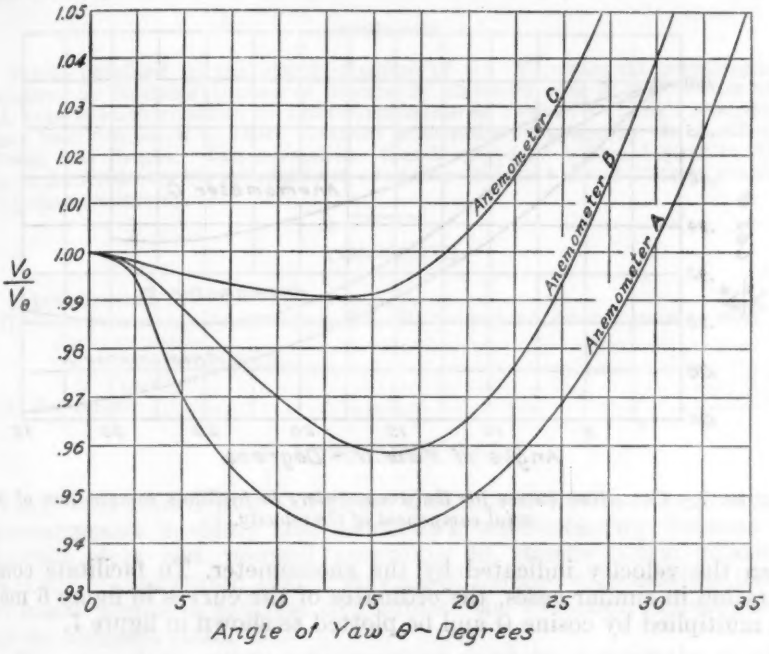

FIGURE 6.—*Effect of angle of yaw on the velocity indications.*
The curves give mean values of V_θ/V_0.

different. Other dissimilarities are to be found, such as differences in wall thickness and external fittings.

A few experiments were made wherein the length/diameter ratio of anemometer *A* was increased about one-third by adding a cylindrical extension to the housing. The results showed a decrease of a small amount in the directional error. Hence it appears that the magnitude of the error due to inclination of the airstream depends on the design of the anemometer, and it is not possible to ascribe the differences in directional sensitivity of the instruments used to any one design characteristic.

The use of the curves in figure 6 is shown by the following example. Suppose the reading of anemometer *A*, corrected for the calibration error at zero yaw, to be 1,240 feet per minute. Also suppose the

direction of air flow with respect to the anemometer axis to be 20 degrees. This angle corresponds to the angle Θ and usually may be determined with sufficient accuracy by means of a light thread and a protractor. Referring to figure 6, the correction factor for anemometer *A* when Θ is 20 degrees is 0.949. Hence the true velocity, in a direction making an angle of 20 degrees with the anemometer axis, is 1,240 × 0.949=1,176 feet per minute.

In most cases it is desired to know the component of the airstream velocity parallel to the axis of the fan or duct. This component is determined by resolving the true velocity, obtained as above, in the direction of the anemometer axis. In the example the value is 1,176× cos 20°=1,105 feet per minute. It will be noted that the component of airstream velocity parallel to the axis of the fan is 10.8 percent less

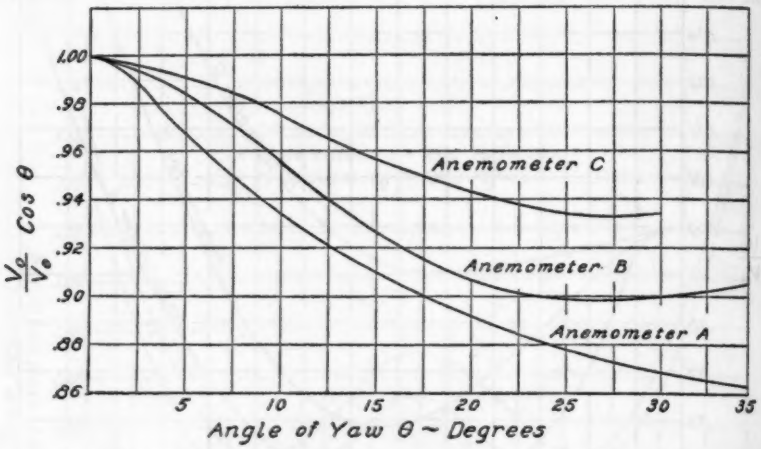

FIGURE 7.—*Correction curves for the anemometers to facilitate computation of the axial component of the velocity.*

than the velocity indicated by the anemometer. To facilitate computation in similar cases, the ordinates of the curves in figure 6 may be multiplied by cosine Θ and be plotted as shown in figure 7.

V. CONCLUSIONS

The effect of airstream inclination on the performance of three vane anemometers was determined in the wind tunnel. The results show the presence of substantial directional errors within the 0- to 35-degree range of yaw angles. A maximum directional error of about 5.5 percent occurred when one of the instruments was displaced about 15 degrees from alignment with the air stream of the wind tunnel. An error of about 1 percent was observed when an anemometer of substantially the same diameter but of different design was displaced the same amount. The experiments indicate that the magnitude of the error due to inclination of the air stream depends on the design of the anemometer.

WASHINGTON, September 25, 1937.

U. S. DEPARTMENT OF COMMERCE NATIONAL BUREAU OF STANDARDS

RESEARCH PAPER RP1057

Part of Journal of Research of the National Bureau of Standards, Volume 19, December 1937

USE OF ARSENIOUS OXIDE IN THE STANDARDIZATION OF SOLUTIONS OF POTASSIUM PERMANGANATE

By Harry A. Bright

ABSTRACT

Values obtained in the standardization of 0.1 *N* potassium permanganate solutions by National Bureau of Standards' standard sample of arsenious oxide 83, using potassium iodide or potassium iodate as a catalyst (Lang's procedure), have been compared to those obtained with sodium oxalate by the method of Fowler and Bright. The normalities found agreed to within 1 part in 3,000 which demonstrates the suitability of arsenious oxide as a direct primary standard in permanganimetry.

CONTENTS

	Page
I. Introduction	691
II. Procedure for standardizing 0.1 *N* potassium permanganate with arsenious oxide	692
1. Potentiometrically	692
2. Visually	692
III. References	693

I. INTRODUCTION

It is well known that the direct titration of trivalent arsenic with permanganate in dilute acid solutions is unsatisfactory, because the reaction does not proceed according to stoichiometric relations. R. Lang [3] has stated that a very small amount of potassium iodate or iodide acts as a catalyst to complete the reduction of manganese to the divalent state.

His data show satisfactory precision, and he apparently checked the accuracy of the procedure by means of iodine (through permanganate-iodide and thiosulphate), though this is not stated clearly, Kolthoff, Laitinen, and Lingane [2] compared the normality of 0.5 *N* potassium permanganate determined by Lang's procedure with that found by direct potentiometric titration of potassium iodide with permanganate in very dilute acid solution. The factors obtained by the two methods agreed within 0.03 percent. Recently the author has made a careful comparison of Lang's procedure with the sodium oxalate procedure of Fowler and Bright [1][1] to determine whether the former is sufficiently accurate to permit the use of the National Bureau of Standards' standard sample 83 of arsenious oxide (now issued as an iodimetric standard) as a fundamental standard in permanganimetry.

[1] Numbers in brackets refer to the literature references at the end of this paper.

The experimental details, in brief, were as follows: Weight burettes were used, and all weights were corrected to the vacuum standard. National Bureau of Standards' sodium oxalate sample 40c (purity taken as 99.95 percent) and arsenious oxide sample 83 (purity taken as 99.98 percent) were used. Both of these materials were dried for 1 hour at 105° C immediately before use. In the potentiometric titration the usual bright platinum-calomel electrode arrangement was used. Standardization with sodium oxalate was done as described by Fowler and Bright. With arsenious oxide Lang's procedure, as described in the next section, was used except that 0.3- to 0.6-g samples were taken.

II. PROCEDURE FOR STANDARDIZING 0.1 *N* POTASSIUM PERMANGANATE WITH ARSENIOUS OXIDE

Accurately weigh approximately 0.25 g of the dried oxide and transfer to a 400-ml beaker. Add 10 ml of a cool 20-percent solution of sodium hydroxide, free from oxidizing or reducing substances. Let stand for 8 to 10 minutes, stirring occasionally. When solution is complete, add 100 ml of water, 10 ml of hydrochloric acid (sp gr 1.18) and 1 drop of 0.0025 *M* potassium iodate or potassium iodide. The titration can be followed potentiometrically or visually.

1. POTENTIOMETRICALLY

Titrate with the permanganate solution to the maximum value of the ratio ($\Delta E/\Delta V$), change in potential per unit volume of solution added. Add the last 1 to 1.5 ml dropwise, allowing equilibrium to be reached before the ΔE reading is taken. In the potentiometric titration the blank is negligible provided the reagents are free from interfering substances.

2. VISUALLY

Titrate with the permanganate solution until a faint-pink color persists for 30 seconds. Add the last 1 to 1.5 ml dropwise, allowing each drop to become decolorized before the next is introduced. Determine the volume of permanganate required to duplicate the pink color of the end point. This is done by adding permanganate to a solution containing the same amounts of alkali, acid, and catalyst as were used in the test. The corrections should not amount to much more than 0.03 ml. The end point can also be taken with ferrous phenanthroline indicator. In this case, 1 drop of a 0.025 *M* solution of the indicator is added as the end point is approached. Permanganate is then slowly added until the pink color of the indicator changes to a very faint blue. The blank correction should average about 0.02 ml.

The normalities indicated for two approximately 0.1 *N* solutions of potassium permanganate are shown in table 1. The data show that the recommended procedures yield results of a very satisfactory order of precision and that standardizations of permanganate solutions by the use of the National Bureau of Standards' standard samples of sodium oxalate 40c and arsenious oxide 83 should agree within 1 part in 3,000.

TABLE 1.—*Comparison of the normality of approximately 0.1 N* $KMnO_4$, *as indicated by titration of* As_2O_3 *and* $Na_2C_2O_4$

Normality by As_2O_3	Number of determinations	Average deviation from mean	Difference from $Na_2C_2O_4$ value	Catalyst
Series 1. Normality by $Na_2C_2O_4$=0.10015 [a]				
		Percent	*Percent*	
0.10016	3	0.022	0.01	KIO_3
[b].10018	3	.029	.03	KIO_3
.10019	2	.002	.04	[c] KIO_3
.10019	3	.028	.04	KI
Series 2. Normality by $Na_2C_2O_4$=0.10391 [a]				
0.10387	1	----------	0.04	[d] KIO_3
.10388	1	----------	.03	[d] KI
.10390	4	.015	.01	KIO_3
.10389	2	.015	.02	KI

[a] Normality as indicated by Fowler and Bright's method. In the first series the value is the average of 8 determinations (average deviation=0.014 percent), and in the second, the average of 7 determinations (average deviation=0.010 percent).
[b] 0.6000 g of arsenious oxide used, all others 0.3000 g.
[c] $KMnO_4$ added slowly, about 7 ml per minute.
[d] End point with orthophenanthroline.

III. REFERENCES

[1] Fowler and Bright, J. Research NBS **15,** 493 (1935) RP843.
[2] Kolthoff, Laitinen, and Lingane, J. Am. Chem. Soc. **59,** 429 (1937).
[3] Lang, Z. anal. Chem. **152,** 197 (1926).

WASHINGTON, September 15, 1937.

U. S. DEPARTMENT OF COMMERCE NATIONAL BUREAU OF STANDARDS

RESEARCH PAPER RP1058

Part of Journal of Research of the National Bureau of Standards, Volume 19, December 1937

SOIL-CORROSION STUDIES, 1934. BITUMINOUS COATINGS FOR UNDERGROUND SERVICE

By Kirk H. Logan

ABSTRACT

This paper summarizes the results of the studies of bituminous coatings for pipe lines, which were conducted under the auspices of the National Bureau of Standards between 1922 and 1935. Most of the fundamental data in the paper have been published. The paper attempts to interpret those data. Nine types of protective coatings, most of which have been represented by several varieties of coatings, are considered, and the characteristics of each type are discussed. The data indicate that the same degree of protection for a pipe line can be secured in a number of ways. The data show only two outstanding coatings. Neither of these was perfect and neither is in general use. Most coatings, though imperfect, afford sufficient protection to justify their application to pipe lines exposed to corrosive soil. Other important conclusions reached by the author are given in the summary at the close of the paper.

CONTENTS

	Page
I. Origin and scope of the investigation	695
II. Coatings tested	697
III. Conditions under which coatings were tested	698
1. Physical properties of the soils at the test sites	698
2. Basis for selection of test sites	701
IV. Effect of soil properties on the behavior of protective coatings	701
V. Effectiveness of protective coatings	709
1. Criterion for effectiveness	709
2. Cutbacks	710
3. Shielded cutbacks	711
4. Emulsions	712
5. Dip coatings	714
(a) For wrought pipe	714
(b) For cast-iron pipe	716
6. Thick unfilled coatings	717
7. Bituminous enamels	722
8. Reinforced bituminous coatings	733
9. Grease coatings	736
10. Mastic coatings	736
VI. Application of data to pipe lines	737
VII. Summary	738

I. ORIGIN AND SCOPE OF THE INVESTIGATION

As a part of its soil-corrosion investigation, the National Bureau of Standards buried four widely different types of bituminous coatings in 30 soils in 1922. These coatings, together with other types buried in 1924 and 1926, are described in detail in the first report on the

soil-corrosion investigation.[1] That paper also describes the soils to which the coatings were exposed and gives some of the early results of the tests. These results are still of some interest because several of the coatings failed within the short period of exposure covered by the report.

The results of the earlier investigations and the corrosion experience of pipe-line operators led to the appointment in 1928, by the American Petroleum Institute, of G. N. Scott as a Research Associate to study the problem of pipe-line protection for oil lines. The American Gas Association in 1929 appointed S. P. Ewing to cooperate in the study of pipe coatings and corrosion.

Although the work of these men was an integral part of the Bureau's soil-corrosion investigation, the results of their investigations have appeared in the publications [2] [3] of the associations named above.

These reports contain practically all of the primary data resulting from the examinations of coatings in the field. Since they were prepared as progress reports, the discussions of the data were brief and, as a result, many pipe-line operators have not derived the benefit from these reports that might be obtained through an intensive study of the data presented. The field work on protective coatings has been supplemented by the determination of some of the physical properties of the coating materials and by other laboratory tests. The results of most of this work have not been published.

Since all experimental work on bituminous pipe coatings has now been suspended, it seems desirable that the net results of all of the investigations should be assembled. This necessitates the reproduction of some data already published, but this duplication will be limited as much as is consistent with the production of an understandable summary.

The purpose of protecting a pipe line is to reduce the total annual charges on the line. Since a discussion of economics is beyond the scope of this paper no attempt will be made to show whether or not a protective coating for any line is desirable. Before this economic problem can be solved the effectiveness of the protective coating must be known. This is the subject of this paper. It will be shown that the effectiveness of a coating depends to a large extent on the soil conditions to which it is subjected. The paper must therefore discuss soil characteristics and correlate them insofar as is possible with the behavior of pipe coatings.

In all of the tests conducted by the National Bureau of Standards the coatings have been applied by or under the direction of the manufacturer of the coating. Although several manufacturers cooperated both in the tests sponsored by the AGA and those of the API, no coatings in the two tests are identical in all particulars. Nor are any of the soils in the two tests identical. In the AGA and the API tests of coatings applied to short lengths of pipe, only one sample of each material was removed from each site at a given inspection.

---

[1] K. H. Logan, S. P. Ewing, and C. D. Yeomans, *Bureau of Standards soil-corrosion studies; I. Soils, materials, and results of early observations.* Tech. Pap. BS **22**, 447 (1928) T368, 50c.

[2] G. N. Scott. *API pipe-coating tests.* Proc. Am. Petroleum Inst., pt. IV of volumes 11 to 15, incl. (1930 to 1934).

[3] S. P. Ewing. *AGA studies of coatings for pipe lines.* Proc. Am. Gas Assn., p. 774 (1931); p. 741 (1933); p. 627 (1936).

II. COATINGS TESTED

The most commonly used pipe coatings are made from bituminous materials. These materials have two general sources—coal-tar pitch and petroleum asphalt. In the second group have been included for convenience greases having petroleum as a base. As to structure, the bituminous coatings may be classified as dips and cutbacks, the latter class covering all of the very thin coatings except greases, unreinforced coatings, enamels, and fabric reinforced or shielded materials. In each class are several materials which differ rather widely in physical properties and behavior.

The coatings in the National Bureau of Standards' tests were described in Technologic Paper 368,[4] and those in the AGA tests in the 1931 proceedings of the AGA.[5] Scott [6] has described the structure of the coatings in the API test but has given no results of laboratory tests similar to those in the other sets of coatings. On this account, tests of the physical characteristics of many of the materials in the API tests were made by H. S. Christopher. His results are summarized in table 1. The laboratory tests which were applied to the coating materials were not designed to determine the effectiveness of protective coatings, and they are not altogether satisfactory for identifying the materials.

TABLE 1.—*Characteristics of bituminous coating materials in the API tests*

[Determinations by H. S. Christopher]

Designation of material	Specific gravity	Ring and ball softening point	Penetration (Dow) at 115° F in 5 seconds				Ductility (Dow) at 115° F	Consistometer hardness (Abraham) at 115° F.	Insoluble in CS_2	Ash
			50 g	100 g	150 g	200 g				
		°F.					cm		%	%
E	1.028	186	20				14.0	14.7	2.12	0.98
G, N	1.420	202	3				0.7	67.1	42.9	26.5
H, L	1.628	205	2	6	9	12	3.9	54.8	55.4	37.8
K, U	1.266	192	16	24	32	36	16.0	23.5	29.1	18.9
M	1.418	145	83	* 11			60.0	* 44.5	37.4	22.9
S	0.996	194		* 23			* 3.2	10.9	1.0	0.4
T	1.350	191					4.1	63.5	34.1	14.4
X, Z	0.997	238	16				2.5	17.1	0.7	0.13
a	1.300	241				7	2.7	34.5	42.8	10.9
d, dd	1.360	190					3.6	56.5	32.7	13.2
g, zz, zzz	1.610	205	2	6	11	15	3.8	61.3	55.6	35.3
h	1.685	189	21				10.3	13.0	61.6	61.3
k, kk	1.259	192	27				62.0	9.1	21.9	5.6
n	1.032	190	14				12.6	16.9	4.6	2.4
q, qq	1.006	232	33	* 21			2.5	16.0	0.8	0.4
t, tt	1.421	195	2				2.8	63.0	40.6	26.9
v	1.420	158	25	* 5			58.2	10.0	39.3	21.4
vv	1.050	320+				5	0.0	36.7	17.0	13.4
w, ww	1.470	163	30				7.2	8.8	42.2	39.9
y, yy, yyy	1.011	189		* 24			* 3.2	10.9	1.1	0.5
z	1.638	222	0	1	2	5	1.7	65.4	57.6	40.2

* Temperature of test 77° F instead of 115° F.

[4] K. H. Logan, S. P. Ewing, and C. D. Yeomans, Tech. Pap. BS 22, 447 (1928); T368.
[5] See footnote 3.
[6] See footnote 2.

Since this paper deals with the results of tests by three investigators, some confusion may arise as to the coatings under discussion, especially as both Scott and Ewing designated some coatings by capital letters. To avoid confusion the coatings which Scott designated by capital letters are printed in boldfaced type in this paper to indicate that they were applied to working pipe lines.

Because of uncontrolled variables, the behavior of a single specimen at a given site may be accidental and not reproducible, and since for the short lengths of pipe no two specimens are even nominally similar as to structure and exposure, there is no way to determine the accuracy of the observations. In order to obtain an idea of the behavior of the different types of materials it seems advisable to combine the data for similar materials, even though some manufacturer may feel that his product is superior to another which has been placed in the same group.

III. CONDITIONS UNDER WHICH COATINGS WERE TESTED

The general characteristics of the National Bureau of Standards' test sites are described in Technologic Paper 368.[7] Data on the chemical properties of the soils at these test sites are given in Research Paper 945.[8] Some of the physical and chemical characteristics of the soils in the AGA tests have been given by Ewing,[9] in his 1931 report. Scott [10] has described his test sites very briefly, but he has given none of the characteristics of the soils except their resistivities.

1. PHYSICAL PROPERTIES OF THE SOILS AT THE TEST SITES[11]

The physical properties of soils which might be expected to influence the performance of protective coatings are shown in table 2 for the soils at all the test sites. The aeration of the soils was estimated from careful inspection of the test sites, employing such criteria as the texture of the soil, degree of mottling, average depth of water table, the depth at which mottling appears, and the depth at which the specimens were placed. The terms characterizing the degree of aeration are likewise indicative of drainage conditions except for those soils which, although naturally poorly drained, receive little or no rainfall.

The aeration or drainage of the soils is indicated by the value of the "air pore space," which is the percentage of the total volume of the soil occupied by air under specified conditions. This value is determined in the laboratory from the total volume of previously saturated soil which has been compacted centrifugally by a force of 1,000 times gravity, the volume of the water retained under this force, and the volume of the soil particles. These values naturally are not indicative of the drainage of those soils in which the natural drainage is restricted by the presence of an impermeable layer below the depth at which the specimens were buried.

The moisture equivalent, defined as the percentage of moisture retained by a previously saturated soil under a centrifugal force of

[7] See footnote 4.
[8] K. H. Logan. *Soil-corrosion studies 1934. Rates of loss of weight and penetration of nonferrous materials.* NBS J. Research 17, 781 (1936) RP945, 10c.
[9] S. P. Ewing, *AGA studies of coatings for pipe lines.* Proc. Am. Gas Assn. p. 774 (1931); p. 741 (1933); p. 627 (1936).
[10] G. N. Scott. *API coating tests.* Proc. Am. Petroleum Inst. 12, pt. IV, 53 (1931).
[11] Section 1 was prepared by I. A. Denison.

1,000 times gravity, is a measure of the retentiveness of water by the soil and of the texture of the soil. Because of the use of a larger volume of soil, the values shown in table 2 are usually somewhat lower than those obtained by the conventional method.

The specific gravity of the soils in their natural state was determined by measurements made on undisturbed lumps of soil from the test sites. The lumps were immersed in a dish filled with mercury, and the volume of the lump determined by measuring the volume of the mercury displaced. The weight per unit volume was then calculated by dividing the weight of the soil by its volume.

Shrinkage was determined by measuring the volume of the soil at the moisture equivalent and again in the oven-dried condition, the change in volume being expressed as percentage of the volume at the moisture equivalent.

Resistivity was determined by alternating current (60-cycle), the soil samples being saturated with water.

Consideration of all of the data in table 2 for any one soil gives a clear idea of the properties of the soil. From the data given for soil 27, it is seen that the high moisture equivalent, 44.6 percent, the high specific gravity, 2.01, the high shrinkage, 32.5 percent, and the low air pore space, 1.9 percent, are indicative of a heavy, dense, impermeable, and poorly aerated clay. This conclusion is confirmed by the aeration based on field observations. On the other hand, the corresponding values for soil 36 are indicative of a porous, coarse-textured, well-drained, and well-aerated soil.

TABLE 2.—*Properties of soils* [a] *at test sites*

[Aeration of soils: *G*=Good; *F*=Fair; *P*=Poor; *VP*=Very poor]

Soil	Soil type	Location	Moisture equivalent	Aeration	Air pore space	Apparent specific gravity	Volume shrinkage	Resistivity at 60° F (15.6° C)
	NATIONAL BUREAU OF STANDARDS SITES							
			%		%	%	%	Ohm-cm
1	Allis silt loam	Cleveland, Ohio	20.2	*P*	1.1		6.6	1,215
2	Bell clay	Dallas, Tex	35.2	*P*	2.0	1.95	23.0	684
3	Cecil clay loam	Atlanta, Ga	29.9	*G*	18.2	1.60	7.0	30,000
4	Chester loam	Jenkintown, Pa	22.9	*P*	7.0	1.78	2.2	6,670
5	Dublin clay adobe	Oakland, Calif	27.5	*P*	4.9	2.00	22.6	1,346
6	Everett gravelly sandy loam.	Seattle, Wash	9.5	*G*	40.6	1.50	0.1	45,100
7	Silt loam	Cincinnati, Ohio	36.4	*P*	3.7	2.02	34.5	2,120
8	Fargo clay loam	Fargo, N. D	34.8	*P*	8.7	1.56	21.0	350
9	Genesee silt loam	Sidney, Ohio	15.6	*F*	15.8	1.74	5.6	2,820
10	Gloucester sandy loam	Middleboro, Mass	9.0	*F*	27.8	1.58	0.2	7,460
11	Hagerstown loam	Baltimore, Md	31.3	*G*	15.5	1.49	8.6	11,000
12	Hanford fine sandy loam.	Los Angeles, Calif	7.5	*G*	33.5	(b)	0	3,190
13	Hanford very fine sandy loam.	Bakersfield, Calif	14.2	*G*	34.5	(b)	0	290
14	Hempstead silt loam	St. Paul, Minn	12.2	*F*	14.4	1.76	1.0	3,520
15	Houston black clay	San Antonio, Tex	50.5	*P*	5.7	2.08	39.8	489
16	Kalmia fine sandy loam	Mobile, Ala	16.5	*F*	12.0	1.65	.6	8,290
17	Keyport loam	Alexandria, Va	27.7	*P*	4.4	1.72	5.4	5,980
18	Knox silt loam	Omaha, Neb	22.0	*G*	16.6	1.26	1.3	1,410
19	Lindley silt loam	Des Moines, Iowa	26.3	*F*	3.9	1.76	11.8	1,970
20	Mahoning silt loam	Cleveland, Ohio	18.6	*P*	3.8	1.90	3.9	2,870
21	Marshall silt loam	Kansas City, Mo	24.8	*P*	10.8	1.66	6.5	2,370
22	Memphis silt loam	Memphis, Tenn	28.4	*G*	9.6	1.67	3.0	5,150

[a] Determinations by I. A. Denison, R. B. Hobbs, and I. C. Frost.
[b] Not determined.

TABLE 2.—*Properties of soils at test sites*—Continued

Soil	Soil type	Location	Moisture equivalent	Aeration	Air pore space	Apparent specific gravity	Volume shrinkage	Resistivity at 60° F (15.6° C)
		NATIONAL BUREAU OF STANDARDS SITES—Continued						
23	Merced silt loam	Buttonwillow, Calif.	18.4	*F*	6.1	1.69	0.2	279
24	Merrimac gravelly sandy loam.	Norwood, Mass.	9.7	*G*	34.7	1.4	0	11,400
25	Miami clay loam	Milwaukee, Wis.	18.6	*F*	9.5	1.95	7.6	1,780
26	Miami silt loam	Springfield, Ohio	13.3	*F*	20.9	1.95	1.0	2,980
27	Miller clay	Bunkie, La.	44.6	*P*	1.9	2.01	32.5	570
28	Montezuma clay adobe	San Diego, Calif.	19.6	*VP*	2.5	(b)	5.9	408
29	Muck	New Orleans, La.	40.9	*VP*	26.6	(b)	5.8	1,270
30	Muscatine silt loam	Davenport, Ia.	24.0	*P*	7.2	1.81	7.5	1,500
31	Norfolk sand	Jacksonville, Fla.	2.3	*G*	38.1	1.55	0	20,500
32	Ontario loam	Rochester, N. Y.	11.8	*G*	11.7	1.85	0.1	5,700
33	Peat	Milwaukee, Wis.	75.5	*VP*	34.0	(b)	16.9	800
34	Penn silt loam	Norristown, Pa.	22.9	*P*	11.7	1.82	8.4	4,900
35	Ramona loam	Los Angeles, Calif.	15.8	*G*	10.9	1.89	3.1	2,000
36	Ruston sandy loam	Meridian, Miss.	14.9	*G*	16.0	1.62	0	11,200
37	St. Johns fine sand	Jacksonville, Fla.	7.0	*F*	(b)	(b)	0	11,200
38	Sassafras gravelly sandy loam.	Camden, N. J.	5.3	*G*	32.1	1.59	0	38,000
39	Sassafras silt loam	Wilmington, Del.	18.3	*P*	7.5	1.72	3.8	7,440
40	Sharkey clay	New Orleans, La.	31.0	*P*	2.3	1.78	16.4	970
41	Summit silt loam	Kansas City, Mo.	28.1	*F*	6.9	1.61	14.6	1,320
42	Susquehanna clay	Meridian, Miss.	24.8	*F*	14.9	1.79	4.7	13,700
43	Tidal marsh	Elizabeth, N. J.	(b)	*VP*	(b)	(b)	(b)	60
44	Wabash silt loam	Omaha, Neb.	25.3	*G*	7.2	1.55	6.0	1,000
45	Unidentified alkali soil	Casper, Wyo.	10.5	*P*	18.7	(b)	0	203
46	Unidentified sandy loam	Denver, Colo.	7.2	*G*	23.2	(b)	0	1,500
47	Unidentified silt loam	Salt Lake City, Utah	21.1	*P*	2.6	1.72	3.7	1,700
51	Acadia clay	Spindletop, Tex.	39.9	*P*	1.4	2.07	37.9	190
52	Alkali knoll	League City, Tex.	36.6	*P*	3.7	[c] 1.97	33.9	264
53	Cecil clay loam	Atlanta, Ga.	29.9	*G*	18.2	1.60	7.0	30,000
67	Cinders	Milwaukee, Wis.	(b)	*VP*	(b)	(b)	(b)	435
54	Fairmount silt loam	Cincinnati, Ohio	19.8	*P*	4.7	1.96	6.1	890
55	Hagerstown silt loam	Baltimore, Md.	31.3	*G*	15.5	1.49	8.6	11,000
56	Lake Charles clay	El Vista, Tex.	32.2	*P*	5.0	2.03	30.1	406
57	Merced clay adobe	Tranquillity, Calif.	32.3	*P*	5.1	1.89	29.5	128
66	Mohave sandy loam	Phoenix, Ariz.	15.8	*G*	20.1	1.79	2.7	222
58	Muck	New Orleans, La.	56.3	*VP*	22.4	1.43	36.9	712
59	Peat	Kalamazoo, Mich.	(b)	*VP*	(b)	(b)	(b)	(b)
60	do	Plymouth, Ohio	40.2	*VP*	33.2	1.28	9.1	218
61	Sharkey clay	New Orleans, La.	31.0	*P*	2.3	1.78	16.4	970
62	Susquehanna clay	Meridian, Miss.	24.8	*F*	14.9	1.79	4.7	13,700
63	Tidal marsh	Charleston, S. C.	46.4	*VP*	19.5	1.47	18.8	84
64	Docas clay	Chalome Flats, Calif.	32.0	*VP*	4.7	1.88	27.7	62
65		Wilmington, Calif.	27.2	*F*	15.8	1.41	5.7	148
		AMERICAN GAS ASSOCIATION SITES						
1	Cinders	Pittsburgh, Pa.	18.1	*G*	(b)	(b)	(b)	730
2	do	Milwaukee, Wis.	9.5	*VP*	(b)	(b)	(b)	880
3	Tidal marsh	Brockton, Mass.	80.3	*VP*	(b)	(b)	(b)	44
4	do	Atlantic City, N. J.	93.7	*VP*	(b)	(b)	(b)	32
5	Muck	West Palm Beach, Fla.	74.2	*VP*	(b)	(b)	(b)	1,180
6	do	Miami, Fla.	29.1	*VP*	(b)	(b)	(b)	1,630
7	Cecil clay loam	Atlanta, Ga.	29.5	*G*	18.2	1.53	5.7	43,800
8	do	Raleigh, N. C.	32.7	*G*	6.6	1.51	8.0	16,000
9	Susquehanna clay	Shreveport, La.	31.2	*P*	5.3	2.01	18.9	6,843
10	Miller clay	do	28.9	*P*	2.0	2.00	16.5	6,843
11	do	Bryan, Tex.	43.0	*P*	1.5	1.98	36.4	1,000
12	White alkali soil	Los Angeles, Calif.	41.0	*P*	2.2	1.72	30.3	93
13	Black alkali soil	do	14.5	*G*	30.6	1.45	0	1,668
14	Marshall silt loam	Kansas City, Mo.	24.7	*G*	11.5	1.73	12.1	3,150

[a] Determinations by I. A. Denison, R. B. Hobbs, and I. C. Frost.
[b] Not determined.
[c] Measurement made on 20-mesh soil after centrifuging.

TABLE 2.—*Properties of soils at test sites*—Continued

Soil	Soil type	Location	Moisture equivalent	Aeration	Air pore space	Apparent specific gravity	Volume shrinkage	Resistivity at 60° F (15.6° C)
		AMERICAN PETROLEUM INSTITUTE SITES						
1	Bell clay	Temple, Tex	31.6	(b)	5.1	2.00	28.0	947
2	(b)	Arkansas City, Kans	20.7	(b)	19.2	1.76	5.1	1,295
3	Lake Charles clay	Beaumont, Tex	40.7	(b)	2.6	2.00	35.8	495
4	(b)	League City, Tex	21.1	(b)	5.1	1.93	6.7	1,485
5	Miami silt loam	Preble, Ind	21.5	(b)	6.9	1.87	6.4	2,201
6	(b)	Council Hill, Okla	25.4	(b)	5.5	1.78	11.6	5,180
7	(b)	Caney, Kans	20.6	(b)	13.8	2.04	7.2	3,510
8	(b)	Spindle Top Gulley, Tex.	7.6	(b)	2.9	2.04	42.7	259
9	(b)	Long Beach, Calif	9.8	(b)	29.9	1.47	0	353
10	Muscatine silt loam	Mt. Auburn, Ill	(b)	(b)	(b)	(b)	(b)	(b)
11	(b)	Skeatook, Okla	15.7	(b)	16.6	1.65	0	440
12	Merced clay loam	Mendota, Calif	36.8	(b)	7.2	1.84	31.2	61
13	Miller clay	Bunkie, La	38.0	(b)	2.5	2.01	30.2	674
14	Hagerstown silt loam	Chambersburg, Pa	21.3	(b)	8.3	1.46	1.4	5,088
15	(b)	Cholame, Calif	36.8	(b)	3.8	1.88	29.1	155

[b] Not determined.

2. BASIS FOR SELECTION OF TEST SITES

In all the tests of protective coatings the object has been to secure typical rather than destructive soils. It will be shown later that some soils to which certain of the coatings were exposed were neither destructive with respect to coatings nor corrosive with respect to unprotected steel. It is evident that the effectiveness of the coating is indicated by the condition of the protected metal only when the characteristics of the soil involved are known, and it obvious that two coatings cannot be compared unless they were exposed to similar soil conditions. For these reasons it is in many cases impossible to compare the coatings in the three tests.

Since this paper is not a report on the results of tests but is a compilation of information derived from various sources, only such soils and coatings are discussed as are of importance to users of protective coatings. Details of the behavior of coatings in the less-corrosive soils will be found in the reports referred to above.

IV. EFFECT OF SOIL PROPERTIES ON THE BEHAVIOR OF PROTECTIVE COATINGS [12]

It has been generally recognized that coatings applied to pipe lines are not equally effective under all soil conditions. From a number of field inspections Scott [13] and Ewing [14] concluded that the pressure exerted on the coating by the soil, the penetration of stones, clods, etc., and the expansion and contraction of the soil with changes in moisture content, tend to puncture and disrupt protective coatings. This is illustrated by figure 1. Taking the clay or colloidal content of soils as a rough measure of the tendency of soils to form hard clods, Ewing showed that the distortion of coatings is related to the softening

[12] Section IV was prepared by I. A. Denison.

[13] G. N. Scott. *The use and behavior of protective coatings on underground pipes.* Bul. Am. Petroleum Inst. **10**, 78 (1929); Proc. Ninth annual meeting.

[14] S. P. Ewing. *AGA-BS studies of a long gas line.* Am. Gas Assn. Monthly **13**, 70 (Feb. 1931).

point of the coating material and to the clay content of soils. Since the physical properties of soils are determined by the quality or physical behavior of the colloidal material as well as by its amount, it is not to be expected that this relation would apply generally.

In order to relate the distortive power of soils to a definite property of the soil, which is determined by the quality as well as by the quantity of colloidal material, Ewing [15] compared the distortion observed on the first set of coated specimens in the AGA test with the volume shrinkage of soils. Except for two soils, for which the shrinkage was relatively great, although little distortion occurred, the shrinkage values were indicative of degree of distortion. The method used by Ewing for determining shrinkage, although producing precise results, was open to the objection that it required thorough working of the moist soil. The consequent breaking down of the natural structure of the soil might be expected to produce degrees of shrinkage which would not be necessarily comparable to the shrinkage of soil which had not been subjected to mechanical pretreatment, as in nature.

Accordingly, in order to avoid this objection the method described in a previous section was adopted for determining the shrinkage of soil samples from the AGA and API test sites. As will be recalled, the moist soil is compressed by centrifugal force in order to throw out excess water and to produce, so far as possible, a weight per unit volume of soil equal to that of the natural, undisturbed soil.

The measure of distortion adopted was the electrical conductance per square foot of coal-tar enamel coatings, supplemented by visual examination of the coatings. Since conductance due to absorption of water by coal-tar enamels is negligible, at least for the period represented by the tests, the measured conductance of these coatings probably resulted from rupture or puncture of the coating by the soil. Coatings which failed for any other reason, such as cracking or the rupture of air bubbles, were either excluded from this study or the cause of failure was noted.

The conductances of the coal-tar enamel coatings in the AGA test after approximately 5½ years of exposure are shown in table 3 for comparison with the shrinkages of the soils. Values of shrinkage are given only for those soils in which this property may be expected to be a factor in distortion. The values for specific gravity of the soils in the field condition may be regarded as supplementing the shrinkage data. Since the specific gravity is a measure of the denseness of a soil clod, values for this property might be taken to indicate in a general way the relative hardness of clods.

It is apparent from table 3 that the maximum values for conductance occur in the soils having the highest capacity for shrinkage. For a coating of a given hardness and thickness it is generally true that the greater the shrinkage the more severe is the distortion as measured by conductance. High values for specific gravity also are seen to be associated usually with soils in which distortion is severe. In such soils, in addition to the distortion attributable to shrinkage, a distorting effect may result from contact with dense clods under pressure from the weight of the overlying soil.

[15] S. P. Ewing. *AGA studies of coatings for pipe lines, 1931.* Proc. Am. Gas. Assn. p. 774 (1931).

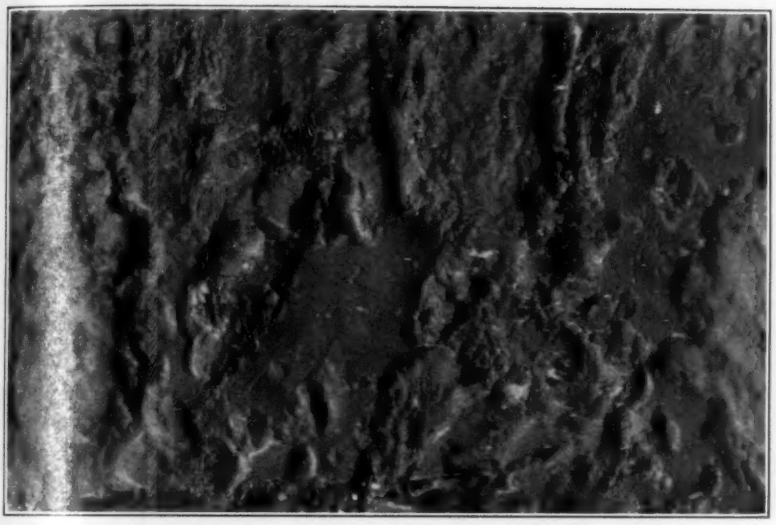

FIGURE 1.—*Distortion of a bituminous coating by clods.*

UNIV. OF MICH.

TABLE 3.—*Conductance of coal-tar enamels in AGA tests (third inspection)*

Coating	Ring and ball softening point	Average thickness	Conductance (in micromhos/ft²) at sites—							
			13	7	8	14	10	9	12	11
	°F	in.								
S	162	0.034	200	145	805	2,090	13,700	1,930	32,200	40,300
B	167	.038	564	-------	2,420	1,770	15,300	2,900	9,660	37,000
WR	184	.051	185	1,770	1,610	515	2,090	2,190	22,500	18,500
WL	184	.052	56	80	370	1.53	805	8,050	4,830	4,830
W	208	.058	600	0	12.2	0	805	250	0.056	137
A	232	.070	0	0	-------	25.8	15,300	338	2,900	29,000
Volume shrinkage			0	5.7	8.0	12.1	16.5	18.9	30.3	36.4
Apparent specific gravity			1.45	1.53	1.51	1.73	2.00	2.01	1.72	1.98

The high values for conductance observed in soils 9, 10, 11, 12 indicate that the attempt to protect a pipe line in such soils by most unreinforced coal-tar enamels would result in certain failure. However, the resistance to distortion shown by the thicker enamels of higher softening point in the lighter soils (nos. 7, 8, 13, and 14) raises the question whether such coatings would not provide adequate protection in such soils, provided of course that they could be applied perfectly to a pipe line.

It is not to be inferred from the emphasis which has been placed on shrinkage as a factor in distortion that other factors producing distortion have been overlooked. In fact, severe distortion has been produced in the AGA test in soils in which shrinkage was nonexistent. These soils, which are cinders at Milwaukee (site 2) and the muck soil at Miami (site 6), are continuously wet and therefore not subject to shrinkage. Although distortion is usually severe at these sites, it is sufficient that such conditions can be recognized and appropriate measures of protection taken to prevent distortion.

In order to study further the influence of soil shrinkage on the distortion of protective coatings, the condition of the enamel coatings which were applied to short pipe sections in the API test was compared with the shrinkage values of soils from the corresponding test sites. The periods of exposure for which data are available are approximately 2 and 4 years. Because of the fact that relatively few of the harder enamel coatings showed appreciable conductance, a more sensitive indication of distortion was provided by visual examination of the coatings. In table 4 the results of this examination which pertain to distortion are shown for comparison with the values for shrinkage. The table shows the average condition of the eight coal-tar enamels. In expressing the results of the inspection, three separate classifications of distortion were made, namely, (1) surface distortion to a depth of 10 mils; (2) distortion greater than 10 mils; and (3) number of punctures. To express the extent of surface represented by the first two classes, numbers from 1 to 3 were assigned which have the following meaning: (1) distorted area less than 10 in.² on total area of 1 ft²; (2) distorted area between 10 and 50 in.²; and (3) distorted area greater than 50 in². The number of punctures from one to three are indicated. The number 3, however, may indicate any number of punctures greater than three.

With the exception of the data for sites IV and VI, it is evident that distortion tends to increase with increasing shrinkage. Excepting these two sites, very few punctures of the coating have occurred in any soils having a shrinkage below 10 percent. Much superficial roughening of the surface, as shown for example by the coatings from site IX, may represent merely the roughening attributable to imbedded sand particles and as such may have little significance. It is surprising that such severe distortion should occur at sites IV and VI, and it appears that a factor other than shrinkage is the probable cause of distortion in these soils.

By comparing the condition of the coatings at the end of the 2- and 4-year periods (table 4), it is seen that in those soils in which distortion is marked, the condition of the coatings is generally worse at the later inspection. This evidence of progressive distortion suggests that temporary measures to resist soil stress can be only partly successful.

TABLE 4.—*Average conditions of coal-tar enamels on short pipe sections (1934 inspections API tests)*

Site	Volume shrinkage	Exposure	Distortion [a]		
			Surface	>10 mils	Puncture
	%	yr			
IX	0	2	3.0	0.4	0
		4	2.6	.3	0
XI	0	2	2.9	1.4	.3
		4	1.9	1.3	.4
XIV	1.4	2	3.0	0.5	.4
		4	2.6	.3	.3
II	5.1	2	2.6	.3	.1
		4	2.1	.3	0
V	6.4	2	2.9	0	0
		4	2.9	0	.1
IV	7.2	2	2.3	1.8	.8
		4	3.0	2.8	1.6
VII	7.2	2	2.9	1.4	0
		4	2.9	1.4	.1
X	[b] 7.5	2	3.0	1.3	0
		4	2.6	0.8	0
VI	11.6	2	3.0	2.3	1.1
		4	3.0	2.6	2.1
I	28.0	2	2.1	1.8	1.9
		4	3.0	2.9	1.8
XVI	29.1	2	2.8	1.8	.1
		4	2.1	1.9	1.1
XIII	30.2	2	2.3	1.5	0.5
		4	2.6	1.8	.9
III	35.8	2	1.5	1.6	.5
		4	3.0	2.1	1.3

[a] The values used to indicate surface and subsurface distortion are averages of numerals which have the following meaning:
1. Distorted area less than 10 in.^{2}/ft.^{2}
2. Distorted area between 10 and 50 in.^{2}/ft.^{2}
3. Distorted area greater than 50 in.^{2}/ft.^{2}

As applied to punctures, the numerals give the number of punctures, except that the numeral 3 is also applied to any number greater than 3.

[b] Data from same soil type at National Bureau of Standards test site 30.

Thus far, study of the effect of soil properties on the distortion of protective coatings has been confined to observations made on short lengths of coated pipe. The study was extended to include the effects of soil stress on coatings under actual service conditions by comparing the conductances of the harder coal-tar enamels applied to the operating lines in the API test with the properties of the soils at the test sites.

Comparison between the effects of distortion, as measured by the conductance of the coating and the shrinkage of the soils, is complicated somewhat by the fact that coatings conduct current not only because of ruptures caused by soil stress but also because of a variety of other causes, such as mechanical abrasion, cracking, etc. However, since the coatings were carefully examined at each inspection period, it is possible in the case of each value of conductance to state whether or not the conductance was due chiefly to soil stress. In table 5 the conductances of the three harder coal-tar enamels in the API test are given for each test site for each of the three periods of inspection insofar as data were available. The values for shrinkage and apparent specific gravity of the soil samples are shown for the purpose of comparison.

TABLE 5.—*Comparison of certain soil properties with conductance of coal-tar enamels on operating lines in API tests*

Site	Volume shrinkage	Apparent specific gravity	Exposure	Conductance of coatings [a] (micromhos/ft.²)		
				K	*L*	*N*
	%		yr			
IX	0	1.47	1	----------	145	165
			2	----------	[b] 90	[c] 225
			4	----------	19	32
XI	0	1.65	1	300	95	[d] 1,440
			2	[d] 2,900	720	[d] 5,155
			4	[e] 220	280	[e] 1,225
XIV	1.4	1.46	1	[d] 20,000	----------	----------
			2	1,800	----------	----------
			4	780	----------	----------
II	5.1	1.76	1	----------	0.01	0.22
			2	[e] 2,100	190	[b] 60
			4	[e] 23,250	95	2,100
V	6.4	1.87	1	[d] 1,110	----------	----------
			2	[b] 2,750	----------	----------
			4	[b e] 2,850	----------	----------
VII	7.2	2.04	1	[d] 430	0.07	196
			2	120	0.0	729
			4	205	.05	[b] 55
X	7.5	1.81	1	0	0.1	0
			2	.02	490	[f] 620
			4	36	225	[b] 272
VI	11.6	1.78	1	1.0	14,300	925
			2	450	10,300	700
			4	220	2,400	625
XVI	29.1	1.88	1	----------	44,000	44,000
			2	----------	44,000	44,000
			4	----------	30,000	37,500
XIII	30.2	2.01	1	2,150	----------	----------
			2	[b c] 1,020	----------	----------
			4	2,000	----------	----------
XII	31.2	1.84	1	----------	21,100	29,500
			2	----------	15,500	34,500
			4	----------	17,500	23,500
III	35.8	2.00	1	22,000	9,295	10,220
			2	5,900	25,900	2,450
			4	1,185	8,300	1,518
VIII	42.7	2.04	1	----------	44,000	9,900
			2	----------	33,500	1,090
			4	----------	16,000	6,400

[a] For characteristics of these coatings see table 1, and for their thickness see table 16.
[b] Ruptured air holes.
[c] Abrasion.
[d] Mechanical injury.
[e] Cracked.
[f] Holidays.

It is evident from table 5 that severe distortion, as indicated by high values of conductance, is confined chiefly to the soils having high shrinkage values. It will be noted that in all of the soils in which the shrinkage is less than 10 percent the conductances are not only usually small but, in most cases, are due to causes other than distortion. The rather marked distortion observed at site VI cannot be accounted for by the rather small shrinkage of 11.6 percent, shown by this soil.

Although the coated sections were inspected carefully at the time the conductance measurements were made in order to determine the cause of the conductance, it was impossible to detect minor defects in the condition of the coating, such as pinholes due to faulty application. Consequently, it cannot be concluded that even the small conductances shown by the specimens in certain soils were actually due to soil stress. In fact, Ewing [16] has concluded that the application of the coatings applied to the line by hand was usually imperfect. It would appear therefore that soil stress is a negligible factor in the behavior of the coal-tar enamels in sites II, V, VII, IX, X, XI, and XIV. The soils at these sites show shrinkages under 10 percent.

In addition to the mechanical action of soils on protective coatings, the drainage or aeration of the soil has an important influence on the performance of coatings. Ewing [17] concluded that the number of coated specimens in the AGA test which were pitted at the end of 5½ years of exposure was lower in the well-drained soils than in the poorly drained soils. Because of the good areation associated with well-drained soils, ferrous ions formed in the process of corrosion are readily oxidized and precipitated in the pinholes in the coating as the difficultly soluble ferric hydroxide. The sealing of these holes by the dense, tightly adherent precipitate results in the cessation of corrosion. On the other hand, because of the deficiency of oxygen in poorly drained soils, ferrous ions remain in the deoxidized condition and diffuse through the ruptures in the coating without being precipitated. Under these conditions the process of corrosion proceeds without interruption.

In a further study of the relation between the areation of the soils at the AGA test sites and the performance of certain classes of coatings, the soils were classified according to degree of aeration. For each of the two classes of coatings studied, the cutbacks and the asphalt emulsions, the deepest pits on the coated specimens at each test site were averaged and the ratios of these pits to the depth of deepest pits on the corresponding bare specimens were calculated. The data were then arranged as shown in table 6.

[16] S. P. Ewing. *AGA field tests of pipe coatings, 1936.* Proc. Am. Gas Assn. p. 627 (1936).
[17] See footnote 16.

TABLE 6.—*Ratio of depth of deepest pit on coated pipe to pit depth on bare pipe, for soils differing in degree of aeration (AGA tests)*

[Approximate exposure 5.5 years]

Aeration very poor				Aeration poor				Aeration good			
Soil	Soil type	Pit depth on coated pipe / Pit depth on bare pipe		Soil	Soil type	Pit depth on coated pipe / Pit depth on bare pipe		Soil	Soil type	Pit depth on coated pipe / Pit depth on bare pipe	
		Average of 4 cutbacks	Average of 5 asphalt emulsions			Average of 4 cutbacks	Average of 5 asphalt emulsions			Average of 4 cutbacks	Average of 5 asphalt emulsions
4	Tidal marsh	2.40	0.96	12	White alkali	0.30	0.48	14	Marshall silt loam	0.21	0.24
6	Muck	0.51	.21	11	Miller clay	.52	.39	13	Black alkali	.37	.13
3	Tidal marsh	2.60	1.16	10	Miller clay	.29	.60	8	Cecil clay loam	.12	.37
5	Muck	0.42	0.47	9	Susquehanna clay	.54	.61	7	Cecil clay loam	.18	.18
2	Cinders	.79	.69					1	Cinders	.48	.33
	Average	1.34	0.70		Average	0.41	0.52		Average	0.27	0.25

It is evident from table 6 that the effectiveness of cutbacks and asphalt emulsions depends largely on the aeration of the soil. Under conditions of good aeration, they are effective in reducing the rate of

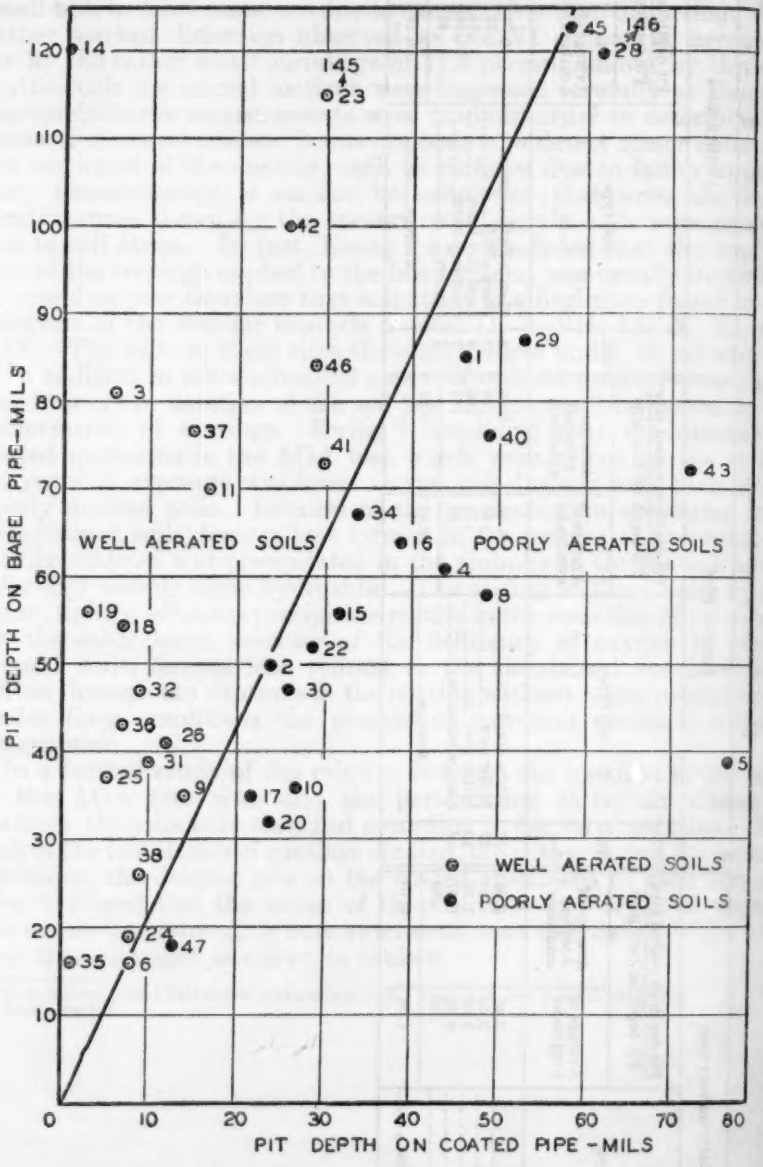

Fig. 2.—Comparison between depths of pits on coated and bare pipe.

pitting, but under conditions of very poor aeration they are usually worthless.

The measurements of depths of pits on sections of coated pipe after burial for 10 years in the Bureau test provide a further opportunity for

studying the effect of soil properties on the behavior of thin, porous coatings. The coatings examined are referred to as nos. 4 and 7, in the publication in which they were described.[18] Both coatings were applied by dipping. No. 4 is a Mexican asphalt with an average thickness of 0.011 in. No. 7 is a soft coal-tar pitch with a thickness of about 0.007 in. In addition to these coatings there were buried in six soils an additional group of thin coatings consisting of various types of asphalts and coal tars (nos. 1, 2, 3, 5, 6, 8, 9). All of these coatings were applied to steel pipe 1½ inches in diameter and 17 inches long.

The effect of the soils on the behavior of these coatings was studied by comparing the average depths of the five deepest pits on the specimens with the average depth of the five deepest pits on an equal area of bare steel pipe exposed for the same length of time. The data are expressed as the averages of the five deepest pits on each specimen rather than the maximum pit, in order to represent the average or over-all condition of the coating in the particular soil.

For each of the soils, except nos. 23, 24, 28, 29, 43, and 45, the value for the depth of pit on the coated pipe is obtained by averaging the mean depth of the five deepest pits on specimens 4 and 7. The values for the soils enumerated above are averages of the mean depth of the five deepest pits on specimens 1 to 9, inclusive. This comparison is shown graphically in figure 2.

It is seen from the figure that the soils fall naturally into two groups with respect to their effect on the behavior of thin coatings. For any specified depth of pit on the bare pipe the pit depth on coated pipe is greater in poorly aerated soils than in well aerated soils. In fact, it is only in the latter that these coatings have had any important protective value.

The benefit of thin coatings in the reduction of pitting in well-drained soils is more apparent than real, since in few of the well-drained soils in either the AGA or the Bureau test would a coating of any kind likely be specified. Although the depths of pits in many of these soils would be considered large for the period of exposure, it has been concluded from a study of pit depth-time curves typical of these soils that these pits are not likely to increase to a considerable extent with time.

V. EFFECTIVENESS OF PROTECTIVE COATINGS

1. CRITERION FOR EFFECTIVENESS

The proper criterion from which the effectiveness of a protective coating should be determined has not been established. At one time a number of manufacturers of protective coatings promulgated an elaborate form for the recording of observations when a coating was to be inspected. The form was intended to show how and why the coating changed as well as the extent of its deterioration. Ewing and Scott used three criteria for studying the behavior of coatings: (1) the pattern test which indicates the presence or absence of pinholes and other flaws in the coating; (2) the electrical conductance test which indicates the extent to which moisture has reached the pipe through flaws, pinholes, or absorption; and (3) the condition of the pipe be-

[18] K. H. Logan, S. P. Ewing, and C. D. Yeomans. *Bureau of Standards soil-corrosion studies. I. Soils, materials, and results of early observations.* Tech. Pap. BS 22, 447 (1928) T368, 50¢.

neath the coating. Both Ewing and Scott modified their methods of making pattern and conductance tests in the course of their investigations, and it is for this reason the results of these tests from year to year cannot be compared directly.

If the condition of the pipe is expressed in terms of the depth of the deepest pit, the result depends partly on the corrosiveness of the soil to which the pipe was exposed and the time required for the soil solution to reach the metal beneath the coating. A soil might be destructive to a coating and not be corrosive, or it might be corrosive and not destructive with respect to coatings. Nevertheless, the pipe-line operator is interested chiefly in the extent to which protective coatings will reduce corrosion. From this viewpoint the greatest amount of information can be obtained by an examination of data on the condition of the surface of pipes from which coatings have been removed. This procedure is subject to the serious objection that since the condition of the pipe is determined by the corrosiveness of the soil a comparison of coatings is possible only when they have been exposed to the same soil conditions. Unfortunately, few of the many coatings to be discussed in this paper were so exposed. For this reason the data presented herewith must be used with care if comparisons are made. Because of this peculiarity of the data an attempt has been made in certain parts of the paper to express the effectiveness of the coatings in terms of the leaks to be expected when the coatings are used under certain conditions. Obviously, if the soil were less corrosive or the pipe wall thicker the number of leaks would be reduced.

In weighing the data on protective coatings the question arises as to the relative merits of tests of coatings on working lines and on short lengths of small-diameter pipe. Scott [19] reached the conclusion that tests of coatings which differ greatly in structure on short lengths of pipe do not in general agree closely with line tests when the coatings are arranged in order of their behavior. He regards the tests on short lengths of pipe as useful in eliminating very poor coatings and in the study of the relative merits of coatings belonging to the same class. He also concluded that the tests of coatings on working lines are more severe than on small-pipe sections. Ewing [20] concludes that the two tests give similar results when conditions of application of the coating are the same and that it is impracticable to apply a coating satisfactorily by hand in the field.

It is probable that the apparently poorer performance with respect to corrosion of some coatings when applied to working lines is the result of the inspection of larger pipe areas. These conclusions are of great importance to anyone who is interested in the effectiveness of protective coatings. In this paper data from both types of tests have been used, but greater weight has been given to the line tests because it was felt that these more nearly simulated practical pipe-line conditions.

2. CUTBACKS

Bituminous materials reduced to a paint-like consistency by the addition of a volatile solvent are called cutbacks. They are applied to the pipe by spraying, brushing, or dipping. After exposure to the air for a few hours they form a thin paint-like coating. Their chief

[19] G. N. Scott. *API coating tests.* Proc. Am. Petroleum Inst. **15**, pt. IV, 18 p. (1934).
[20] S. P. Ewing. *AGA field tests of pipe coatings.* Proc. Am. Gas Assn., p. 627 (1936).

virtues are low cost and ease of application. Cutbacks are made from two classes of materials—coal-tar pitches and asphalts. Some also contain finely divided mineral matter. All of the cutback-coated pipes reported on in table 7 were either primed with a bituminous primer or coated with two applications of the cutback. Nevertheless, nearly all of the coatings contained numerous pinholes, as indicated by the electrical tests. Table 7 reveals the fact that on the average the asphalt-base cutbacks were thicker than the coal-tar base materials. It will also be seen that the former type showed slightly less corrosion. Generally speaking, the thicker coatings were superior to the thinner ones.

TABLE 7.—*Performance of cutback coatings*

Asphalt base								Coal-tar-pitch base				
Average exposure	Sponsor	Number of soils	Identification	Thickness	Pipes corroded	Pipes with pits deeper than 9 mils	Pipes with pits deeper than on bare pipes	Identification	Thickness	Pipes corroded	Pipes with pits deeper than 9 mils	Pipes with pits deeper than on bare pipes
yr				in.	%	%	%		in.	%	%	%
0.78	AGA	11	*M*	0.010	100	18	9	*SS*	0.007	100	18	9
.78	AGA	11	*L*	.024	100	18	9	*K*	.009	100	18	9
.96	API	8						*C*	.020	100	56	44
1.82	API	14	*cc*	.045	79	14	0	*zz*	.012	100	29	7
1.82	API	14	*u*	.047	100	36	7	*b*	.020	86	14	0
1.84	API	8						*C*	.020	100	100	44
2.44	AGA	14	*M*	.010	86	43	14	*SS*	.007	100	71	14
2.44	AGA	14	*L*	.024	71	36	0	*K*	.009	100	71	7
3.78	API	14	*cc*	.045	100	36	7	*zz*	.012	100	50	0
3.78	API	14	*u*	.047	100	43	7	*b*	.020	100	57	14
3.83	API	8						*C*	.020	100	75	36
5.47	AGA	14	*M*	.010	100	71	14	*SS*	.007	100	100	14
5.47	AGA	14	*L*	.024	100	64	14	*K*	.009	100	93	21

A very large percentage of each variety of cutback coating failed to protect completely the pipe to which it was applied for as much as 2 years. After the initial periods of exposure, from 14 to 56 percent of the specimens were definitely pitted. In several instances the maximum pits on the coated specimens were deeper than on the corresponding bare specimens. The performance of the best of these materials is not good enough to justify its use. Since the data cover the performance of nine varieties of cutback coatings furnished by some of the leading manufacturers of this type of material, the conclusion seems justified that it is improbable that any coating of this type will prove satisfactory for the permanent protection of metal placed underground. Cutbacks reduce temporarily the total amount of corrosion and make the pipe easier to clean. They may be used to advantage on temporary lines or lines which are to receive a heavier coating if the soil proves to be corrosive.

3. SHIELDED CUTBACKS

The effect of protecting cutbacks from direct contact with the soil is shown in table 8. In considering this table it should be kept in mind that each coating consisted of a primer and two coats of the cutback in addition to the wrapper.

Coatings *Y* and *x* are quite similar in composition and differ chiefly in thickness. Coating *Y* was applied to working oil lines, while coating *x* was applied to a 2-foot length of 3-inch outside-diameter pipe. Both coatings were covered with aluminum foil. It will be noted from table 8 that although coating *Y* is 50 percent thicker than coating *x*, its record is not nearly so good. This is partly because the successful application of a coating in the field is more difficult than in a shop and partly because the area examined for pits beneath coating *Y* was considerably greater. In addition, the pipe line may have been affected by long-line currents, difference of potential between top and bottom of the pipe, and soil pressure attributable to the weight of the pipe.

TABLE 8.—*Performance of shielded asphalt-base cutbacks*

Exposure	Number of soils	Identification	Thickness (3 coats without shields)	Pipes corroded	Pipes with pits deeper than 9 mils	Pipes with pits deeper than on bare pipe
yr			in.	%	%	%
0.96	10	*Y*	0.029	65	10	10
1.84	10	*Y*	.029	85	40	15
1.82	14	*x*	.018	57	7	0
1.82	14	*l*	.081	85	7	0
3.78	10	*Y*	.029	95	55	10
3.78	14	*x*	.018	86	21	7
3.78	14	*l*	.081	100	43	0

Table 8 shows that under coating *l*, which was four times as thick as coating *x*, the pipe was pitted in a larger percentage of cases. While this result might be attributed to some difference in the coating material, this explanation does not seem adequate since table 7 indicates that the variety of cutback is not very important. A better explanation is that coating *x* was shielded by aluminum foil, which is stiffer and more nearly permanent than the kraft paper which shielded coating *l*. The aluminum may have afforded some cathodic protection also. Comparison of tables 7 and 8 indicates that the application of a shield reduced the pitting of the specimens. It cannot be said, however, that table 8 indicates that a shielded cutback coating gives satisfactory protection against corrosive soils.

4. EMULSIONS

For a proper application of the cutbacks, which have been discussed above, the surface of the metal to be coated must be clean and dry. This is a condition difficult to obtain under field conditions, and it is especially difficult when the pipe has been reconditioned. A satisfactory coating which could be applied to a moist pipe would have an advantage over one that could not, other things being equal. Since asphalt emulsions can be applied to moist pipe, their value as pipe coatings is of particular interest.

Table 9 is a summary of the data on emulsion coatings. These data are derived from two sources, the AGA and the API field exposures, as indicated in the table. Data from the two sources are not comparable because of differences in test sites and periods of exposure. The data in table 9 have been arranged according to

the period of exposure of the specimens and secondarily according to the thickness of the coating. The data on the simple and reinforced or shielded specimens have been separated. Those on the same horizontal line are not necessarily for specimens having the same base material.

TABLE 9.—*Performance of emulsion coatings*

Exposure	Sponsor	Number of soils	Emulsions					Shielded and reinforced emulsions					
			Identification	Thickness	Pipes corroded	Pipes with pits deeper than 9 mils	Pipes with pits deeper than on bare pipe	Identification	Thickness	Shield	Pipes corroded	Pipes with pits deeper than 9 mils	Pipes with pits deeper than on bare pipe
yr				in.	%	%	%		in.		%	%	%
0.78	AGA	11	*G*	0.016	100	25	25						
.78	AGA	11	*E*	.047	91	0	0	*EE*	0.061	Neat cement	100	0	0
.78	AGA	11	*F*[1]	.082	100	0	0	*FF*[1]	.029	Cement added	100	18	9
.96	API	9	*A*[1]	.065	100	50	39						
1.82	API	14	*j*	.015	100	64	21						
1.82	API	14	*ppp*[2]	.015	100	29	7						
1.82	API	14	*fff*[1]	.037	100	64	0	*ff*[1]	.190	Cement mortar	43	0	0
1.82	API	9	*A*[1]	.065	100	67	33	*f*[1]	.149	Asbestos felt	43	0	0
2.44	AGA	14	*G*	.016	100	71	7						
2.44	AGA	14	*E*	.047	33	43	7	*EE*	.061	Neat cement	100	7	0
2.44	AGA	14	*F*[1]	.082	64	14	0	*FF*	.029	Cement added	100	70	0
3.78	API	14	*j*	.015	100	79	21						
3.78	API	14	*ppp*[2]	.015	100	50	7						
3.78	API	14	*fff*[1]	.037	100	93	29	*ff*[1]	.190	Cement mortar	57	0	0
3.78	API	9	*A*[1]	.065	100	89	40	*f*[1]	.149	Asbestos felt	64	0	0
5.47	AGA	14	*G*	.016	100	93	21						
5.47	AGA	14	*E*	.047	100	86	14	*EE*	.061	Neat cement	100	36	7
5.47	AGA	14	*F*[1]	.082	100	50	0	*FF*[1]	.029	Cement added	100	72	7

[1] Contains a chromate inhibitor.
[2] Applied over a priming coat of red-lead paint baked on.

Asphalt emulsions are made from several kinds of asphalt and by the use of many emulsifying agents and methods. Several types of emulsions are represented in table 9; but because of other variables mentioned above, it is not possible to determine the effect of the kind of asphalt or the method of emulsification. However, the table gives a general idea as to what may be expected from emulsions as pipe coatings.

Table 9 indicates, as do tables 7 and 8, that very thin coatings are unsatisfactory. The common characteristic of all of the emulsion coatings is the development of corrosion beneath them within a short time after they have been exposed to soil. This is evidence that this type of coating is not impervious to moisture since, in many cases, the corrosion is too severe to be accounted for by the water originally in the coating. This statement is also supported by the fact that for all types of emulsions corrosion is progressive, i. e., the percentage of specimens with measurable pits increases with the period of exposure.

Coating *ppp* differs from coatings *G* and *j* in that a primer of red-lead paint was used beneath the emulsion. This apparently increased the effectiveness of the coating, but none in this group could be considered satisfactory.

Several of the emulsions contained a chromate intended to inhibit corrosion. It is evident from the table that the inhibiting agent was not completely effective.

Although corrosion was observed under most of the coatings, probably because they did not exclude moisture, the specimens protected by the thickest coatings showed less pitting. This is probably because the thickest coatings prevented direct contact between soil particles and the pipe. The improvement in performance because of the use of a shield is quite evident. Although rust was found under the concrete shielded coating, *ff*, no pits developed within approximately 4 years. When the relative thicknesses of the concrete and the emulsion are considered, it is doubtful whether coating *ff* should be classified as an emulsion or as a cement-mortar coating.

The results of the tests of asphalt emulsion coatings may be summarized in the statement that this type of coating is inadequate as a protection against corrosive soils.

5. DIP COATINGS

(a) FOR WROUGHT PIPE

Bituminous coatings are frequently applied to pipe by dipping the latter in a tank of molten coal-tar pitch or asphalt. The process may be repeated after the pipe has cooled in order to reduce the number of pinholes and to produce a thicker coating. The thickness of the coating will depend somewhat on the temperature at which the bitumen is maintained in the dipping vat, but in most cases, the coating is not much thicker than a paint.

In 1924 the National Bureau of Standards buried specimens of coal-tar pitch and asphalt coatings in 47 soils. In seven of these soils nine varieties of coatings were placed. However, as all of the coatings behaved similarly and all proved inadequate, it seems sufficient to present only the data on the coatings which were exposed to all soils. The data for 10-year-old specimens given in table 10 have not been previously published. For this reason more detailed data are presented. The table shows also the condition of bare pipe having approximately the same area exposed to the soil.

While several of the soils listed in table 10 are very corrosive, as indicated by the last column of the table, others are only moderately so. The rates of corrosion in a number of the latter are so low that unprotected pipe would last a long time. The data in table 10 are therefore more favorable to the coatings than they would have been if the tests had been confined to corrosive soils. This is also indicated by the data for the 8-year-old specimens in table 11, which summarizes the data on the dip coatings for all periods of exposure. Eight-year-old specimens were not removed from the less corrosive soils. It will be noted that for this period the average condition of the specimens is much worse than for the 6-year period and almost as bad as for the 10-year period of exposure.

TABLE 10.—*Pit depths on pipes protected by asphalt and coal-tar-pitch dip coatings*

[Exposures of approximately 10 years]

(Pit depth in mils)

Soil type	Asphalt coating	Coal-tar pitch coating	Bare steel
Allis silt loam	99	53	92
Bell clay	32	28	79
Cecil clay loam	14	11	85
Chester loam	63	46	72
Dublin clay loam	37	145+[a]	45
Everett gravelly sandy loam	M[b]	22	20
Fairmount silt loam		22	39
Fargo clay loam	101	42	62
Genessee silt loam	25	31	54
Gloucester sandy loam	56	22	42
Hagerstown loam	50	29	73
Hanford fine sandy loam	14	M[b]	43
Hempstead silt loam		M[b]	145
Houston black clay	60	36	61
Kalmia fine sandy loam	53	45	74
Keyport loam	29	24	38
Knox silt loam	13	20	61
Lindley silt loam	M[b]	14	58
Mahoning silt loam	35	28	36
Memphis silt loam	37	28	64
Merced silt loam	25	35	145+[a]
Merrimac gravelly sandy loam		14	25
Miami clay loam	13	12	42
Miami silt loam	23	22	46
Montezuma clay adobe	54	75	103
Muck	79	52	93
Muscatine silt loam	27	90	53
Norfolk sand	32	13	36
Ontario loam	1[illegible]	17	50
Peat	46		93
Penn silt loam	48	53	131
Ramona loam	M[b]	12	27
Ruston sandy loam	M[b]	18	47
St. Johns fine sand	18	17	87
Sassafras gravelly sandy loam	19	M[b]	32
Sharkey clay	66	47	92
Summit silt loam	40	33	84
Susquehanna clay	U[c]	42	116
Tidal marsh	M[b]	145+[a]	82
Alkali soil	70	42	150
Unidentified sandy loam	32	39	98
Unidentified silt loam	M[b]	37	28

[a] Pipe wall punctured.
[b] Metal attack.
[c] Unaffected.

TABLE 11.—*Summary of data on dip coatings*

Average approximate exposure	Number of soils	Identification number	Thickness	Pipes corroded	Pipes with pits deeper than 9 mils	Pipes with pits deeper than those on bare pipes
yr			*Mils*	%	%	%
2.4	44	4	0.011	77	34	9
2.4	44	7	.007	82	43	9
6.4	43	4	.011	98	42	16
6.4	43	7	.007	100	42	7
8.4	21	4	.011	100	76	9.5
8.4	22	7	.007	100	86	4.5
10.3	40	4	.011	98	80	7.5
10.3	41	7	.007	100	90	12.2

There seems to be a slight difference between the asphalt (no. 4) and the coal-tar-pitch (no. 7) coatings in favor of the former. This is probably due to the greater thickness of this coating.

Table 10 and 11 show again that thin bituminous coatings do not afford adequate protection against soils. Three-fourths of the specimens were found to be corroded when they were first removed and a third of them were pitted.

(b) FOR CAST-IRON PIPE

For many years the specifications of the American Water Works Association have included a requirement that the pipe shall be coated inside and out with coal-tar-pitch varnish to be applied by dipping the heated pipe in the heated varnish. In order to obtain some idea of the effectiveness of this coating, sections of 4-inch cast-iron pipe, coated according to these specifications in the ordinary course of pipe manufacture, were cut into 17-inch lengths. Since the coating was injured in places in the course of cutting the pipe, the injured spots were repaired with a solution of the same material applied by a brush. Specimens of this pipe were buried in several corrosive soils in 1926, the pipes being filled with soil from the trench.

When the pipes were returned to the Bureau they were split and both the inside and outside surfaces were examined. Table 12 shows the results of the examination of the specimens removed in 1934. To make the data comparable with data on 6-inch lengths of bare pipes, each 17-inch section was divided into three equal parts. The deepest pit on each part was measured and the average of these pit depths was recorded as the maximum pit. Measurements were made on the outside of the pipe, on the inside, and on the ends which were unprotected. The last-named measurement, together with the maximum pits on the bare specimens of 6-inch cast-iron pipe 6 inches long, indicates the corrosiveness of the soil. The differences between the pit depths on the coated and uncoated sections indicate the effectiveness of the coating.

TABLE 12.—*Pit depths on coated and uncoated cast-iron pipe*

[Approximately 8-years old; pit depth in mils]

Soil	Pit depth			
	Coated pipe		Bare pipe	
	Inside	Outside	End	6-in. cast-iron pipe 6 in. long
3	13	39	75	202
23	19	21	77	230
29	37	60	100	206
40	34	77	50	182
42	11	79	230	117
43	17	42	375	83
45	33	57	95	99
47	9	45	34	23

It is impossible to determine positively why the pit depths on the inside of the pipe were so much shallower than those on the outside of the same pipes. Conditions inside the pipe may have been less

corrosive because of different packing of the soil or the coating may have been thicker. It is improbable that the coating on the outside of the pipe was injured before the pipes were buried since they were packed in sawdust for transportation.

It is evident from table 12 that in most cases the coating materially reduced the depths of the maximum pits. It is also evident that, as in the case of other thin coatings, the protection was imperfect. Pattern tests indicated that the coating contained many fine holes, and conductance tests showed that the electrical resistance of the coating was negligible.

6. THICK UNFILLED COATINGS

When the National Bureau of Standards soil-corrosion investigation was started in 1922, specimens of four types of bituminous coatings were included. Two of these were asphalt-base coatings and two coal tar-pitch-base materials. One coating of each material was reinforced by loosely woven cotton fabric somewhat heavier than cheese-cloth.

Specimens of these coatings were removed after 4 and after 12 years of exposure. The pit depths on the pipes to which the coatings were applied are shown in table 13. The unreinforced pitch had so low a softening point, 96° F, that it flowed from the top of the pipe in many soils. For this reason the effect of thickness cannot be determined from the performance of this coating.

TABLE 13.—*Behavior of unfilled thick coatings*

[Pit depth in mils.]

Soil type	4 years' exposure					12 years' exposure				
	Pitch		Asphalt		Steel	Pitch		Asphalt		Steel
	Unreinforced	Reinforced	Unreinforced	Reinforced	Bare	Unreinforced	Reinforced	Unreinforced	Reinforced	Bare
Allis silt loam	62	[a] *U*	*U*	[b] *R*	41	65	20	[c] *M*	55	100
Cecil clay loam	20	*U*	*R*	*R*	63	25	*R*	21	12	78
Chester loam	10	*U*	*U*	*R*	36	67	29	38	23	115
Fairmount silt loam						54	*U*	29	18	59
Fargo clay loam	20	*U*	*R*	*R*	64	70	*M*	72	16	104
Genessee silt loam	23	*U*	*R*	*U*	60	91	*U*	*M*	30	49
Gloucester sandy loam	20	*U*	*R*	*R*	10	42	10	33	16	70
Hagerstown loam	38	*U*	*R*	*R*	70					73
Hemford fine sandy loam						23	*U*	19	*M*	60
Hanford very fine sandy loam	38	*U*	*R*	*R*	73					
Hempstead silt loam	*R*	*U*	*R*	*R*	63	53	*U*	*R*	*R*	88
Kalmia fine sandy loam	24	*U*	*R*	*R*	56	101	*U*	21	25	100
Keyport loam	22	*U*	*U*	*R*	30	68	*U*	*M*	12	48
Knox silt loam	32	*U*	*U*	*R*	57	33	*U*	17	39	76
Lindley silt loam	30	*U*	*R*	*R*	54	23	*R*	*R*	25	93
Mahoning silt loam	30	*U*	*R*	*U*	10	101	17	*M*	*M*	81
Marshall silt loam	16	*U*	*R*	*R*	41					
Memphis silt loam	*M*	*U*	*R*	*U*		38	26			59
Merced silt loam	84	*U*	*U*	*R*	132	96	*U*	43	30	171
Merrimac gravelly sandy loam	*R*	*U*	*R*	*R*	10	21	*U*	13	34	35
Miami clay loam	12	*U*	*R*		32	19	*U*	*R*		53
Miami silt loam	13	*U*	*R*	*R*	51	23	*M*	*M*	*M*	50
Muck	36	*U*	*R*	*M*	88	[d] 135	21	54	[d] 135+	216

[a] Unaffected. [b] Rusted. [c] Metal attack. [d] Pipe punctured.

TABLE 13.—*Behavior of unfilled thick coatings*—Continued

[Pit depth in mils.]

Soil type	4 years' exposure					12 years' exposure				
	Pitch		Asphalt		Steel	Pitch		Asphalt		Steel
	Unreinforced	Reinforced	Unreinforced	Reinforced	Bare	Unreinforced	Reinforced	Unreinforced	Reinforced	Bare
Muscatine silt loam	40	*U*	*R*	*U*	10	118	*U*	*M*	*M*	57
Ontario loam						52	*R*	*M*	69	96
Peat	23	*U*	*U*	*U*	33					135
Penn silt loam	31	*U*	*R*	*R*	27	42	*U*	*M*	49	42
Ramona loam	20	*U*	*U*	*U*	24	29	*U*	*M*	25	48
Sassafras gravelly sandy loam			*U*	*R*						38
Sassafras silt loam	69	*U*	*R*	*R*	31	84	*M*	*M*	74	75
Summit silt loam			*R*	*R*		40	*U*	23	25	74
Tidal marsh	135+	*U*	*M*	*U*	100	[d] 135+	20	*M*	114	100
Alkali soil				*U*		68		42		117
Sandy loam	18		*R*	*U*	75	25	*U*	*M*	15	91
Silt loam	26		*U*	*U*		13	*R*	10	*M*	30
Percentage corroded	100	0	74	65		100	48	100	100	
Percentage pitted (9 mils)	90	0	0	0		100	24	48	78	
Percentage with pits on bare pipe	26	0	0	0		27	0	0	0	

[d] Pipe punctured.

Within 4 years the unreinforced asphalt coating permitted rust to form beneath the coating in 74 percent of the soils to which it was exposed. At the close of the 12-year period of exposure all of the specimens had developed rust beneath the coating and 48 percent of them had developed measurable pits.

The effect of the fabric reinforcement may be seen by comparing the reinforced with the unreinforced asphalt coating. At the close of the shorter test period 65 percent of the specimens of the reinforced, as compared with 74 percent of the unreinforced, coating were rusty. At the close of the longer period of exposure, all pipes beneath the asphalt coatings had rusted. On many specimens the fabric had rotted so badly that only traces of it could be found; and 78 percent of the reinforced asphalt-coated specimens showed measurable pits, as compared with 48 percent of the unreinforced asphalt-coated specimens. In several soils the pits beneath the reinforced asphalt coating were almost as deep as those on a corresponding area of unprotected pipe. Thus in this experiment, in which the coatings had approximately the same thickness, the cotton fabric was a detriment to the asphalt coating. It is probable that the fabric acted as a wick which carried moisture into the material. Nevertheless the table indicates that, on the average, both asphalt coatings reduced corrosion considerably.

Table 13 shows that the reinforced pitch coating was better than the reinforced asphalt, probably because the asphalt absorbed water more readily. More than 50 percent of the reinforced pitch coatings showed no rust and in most cases the fabric was still strong.

The data discussed in the earlier sections of this report show so obviously that the thin coatings are unsatisfactory for severe soil condi-

tions, that no attempt has been made to estimate their performance when applied to pipe lines. Some of the coatings in table 13, although imperfect, are sufficiently good to justify an attempt to interpret the data in terms of the performance to be expected of coatings applied to working lines.

The effectiveness of the coatings in a group of seven soils, which produced pit depth on bare pipes, more than 99 mils in 12 years was estimated by calculating the length of pipe, of a specified material and wall thickness, which is associated with a leak in 12 years. The extension of the length of the pipe from that of the specimens to the length associated with a pit depth equal to the wall thickness was made by means of Scott's pit-depth-area relation. Scott[21] has shown that, as the area from which the deepest pit is selected is increased, the average value of the pit depth increases according to the formula $P_2=P_1(A_2/A_1)^a$, in which A_2 and A_1 are the areas from which the pit depths P_2 and P_1, respectively, are selected, and "a" is a function of soil characteristics. He found that for the data which he examined the value of "a" ranged from 0.376 to 0.150, the average being 0.261. This empirical formula roughly represents the pit-depth–area relation for data upon which it has been tried over a small range, but the extent of its usefulness is uncertain.

The data presented in table 14 are intended only to give a rough idea of the effectiveness of the coatings under discussion. Obviously, if data from other soils were used, or if some other value were taken for "a," the results might have been different.

TABLE 14.—*Effectiveness of the bituminous protective coatings in table 13, as indicated by Scott's pit-depth–area relation*

Coating	Pit depths on specimens			Estimated feet per leak at 12 years					Effectiveness of coatings	
				1½-in. service pipe		8-in. distribution main				
						Steel				
	Average maximum pit depth [1]	Standard deviation	Standard error of the average	Steel [2] $A=71.6$ $t=0.145$	Cast iron $A=79.9$ $t=0.22$ in.	Light $A=325$ $t=0.109$ in.	Heavy $A=325$ $t=0.322$ in.	Class B cast iron $A=341$ $t=0.51$ in.	Ratio of protected to bare length per leak	Percentage increase in thickness of bare pipe wall for equal length per leak
	Mils	*Mils*	*Mils*							
						$a=0.261$				
None	138	42	17	3	12	0.2	13	72		
Unreinforced asphalt	33	24	10	630	2,800	47	2,950	16,300	226	312
Reinforced asphalt	57	45	18	78	347	6	367	2,030	28	139
Unreinforced pitch	96	29	12	11	47	0.8	50	276	4	42
Reinforced pitch	13	11	5	23,000	100,000	1,700	106,000	586,000	8,100	950
						$a=0.150$				
None						0.1	144	2,940		
Unreinforced asphalt						1,400	1,860,000	37,900,000	12,900	314
Reinforced asphalt						38	49,700	1,010,000	345	140
						$a=0.376$				
None						0.3	5	16		
Unreinforced asphalt						11	200	691	42	308
Reinforced asphalt						3	48	164	10	137

[1] Average of data for soils 1, 4, 8, 16, 23, 29, and 43.
[2] A=square inches per foot of length.
[3] t=thickness of pipe wall.

[21] G. N. Scott. *Adjustment of soil-corrosion pit-depth measurements for size of sample.* Proc. Am. Petroleum Inst. 14, pt. IV, 204 (1934).

Columns 2, 3, and 4 illustrate the nature of data on underground corrosion. Taking the data on the pit depths on the unprotected pipe as an example, and assuming that the individual observations from which the average pit depths were obtained are distributed normally, it is to be expected that if other measurements of the maximum pit on a unit area were made, the values would not differ from the average of 138 mils by more than 2.5 times σ_x or 42 mils oftener than 5 times in 100. In other words, the probability is 0.95 that a single value lies between $138+2.5\times42$ and $138-2.5\times42$ or between 243 and 33, or, in one case out of 20 the pit depth might be greater than 243 mils or less than 33 mils. Actually, among the seven values used to obtain the average, the maximum was 216 and the minimum 100. Usually, as in the case cited, the difference between the maximum and the average is greater than that between the minimum and the average, i. e., the data do not follow a normal distribution curve.

The values of σ_m indicate the reproducibility of the average in the same way that σ_x shows the reproducibility of a single observation. The values for σ_m indicate that the data for the coated specimens are more erratic than those for the bare pipe. In columns 5 to 9 are shown the lengths of pipe per leak predicted by Scott's formula for pipes having different diameters and wall thicknesses. When the predicted length is not greatly different from the length of the specimen from which the original data were obtained, it is probable that the formula gives reasonably accurate results. When the differences are large, the computed results may be smaller than would actually be found under the assumed soil conditions.

The purpose of the table is not only to compare the effectiveness of four coatings but also to show the effect of different wall thicknesses on the length of pipe per leak. The pipe diameters and thicknesses chosen to illustrate these points are those of pipes in common use. While the thickest pipe of each diameter has been designated as cast iron because, for the diameters assumed, the wall thickness commonly used is greater for this material, the same results would be obtained if any ferrous material of the same wall thickness were used, i. e., the table shows the effect of the thickness of the pipe wall regardless of the ferrous material used to secure that thickness.

The data in columns 5 to 9 for bare pipe indicate that the soils under consideration are very corrosive. In practice, pipes would be replaced before they developed leak frequencies as great as those corresponding to the data shown for any of the unprotected pipes, i. e., none of the pipes would last 12 years.

Following the data for specimens are data on the leak frequencies for pipes protected in four ways, based on Scott's formula, and the assumption of the values for a found by him. If the average value for a is assumed, the reinforced asphalt coating increased the length of pipe per leak to about 28 times that for unprotected pipe, which is more than sufficient to pay for the application of the coatings but not enough to be considered satisfactory protection. If the length of a house service is assumed to be 50 feet and the length of a city block 500 feet, the use of the reinforced asphalt coating on 1½-inch steel service pipe would result in two services out of three leaking within 12 years, while a heavy 8-inch steel main similarly protected would average in the same time one leak per city block.

The reinforced pitch coating was the most effective. It would reduce the leaking steel services to 1 in 460 and the leaks on the thick steel main to about one leak in 21 miles of main.

In considering this coating, it should be remembered that the estimates of effectiveness are based on the performance of the coatings in corrosive soils rather than in those which were destructive to coatings. If the coating had been exposed to soils having large shrinkages the results might have been less favorable.

When pipes are laid in very uniform soils the corrosion is more nearly uniform and the value of the exponent a in Scott's formula is smaller. Conversely, this exponent is larger for soils which are not uniform or for sections of pipe line which traverse more than one soil.

The data in the last column of table 14 indicate that the addition of a protective coating is equivalent to increasing the thickness of the pipe wall by a certain percentage. For example, when $a=0.261$ the application of the reinforced asphalt coating has the same effect on the number of leaks as increasing the thickness of the pipe wall by 139 percent. Under the assumed conditions the light-weight steel pipe protected by reinforced asphalt would not be as effective as the bare heavy steel pipe because the latter is 195 percent thicker. The ratio of the length per leak of protected to unprotected pipe increases with the effectiveness of the coating. The light-weight steel pipe protected by the reinforced pitch coating is shown in the table to be much more effective over the 12-year period of test than any of the bare pipe, because the addition of this coating is equivalent to making the pipe wall 10 times as thick.

It is impossible to determine, from the data presented, how the coatings would be affected by longer periods of exposure, and consequently the relative effectiveness of light-weight coated pipe and heavier uncoated pipe cannot be estimated at this time. However, since many coatings deteriorate within a few years, and since in most soils the rate of corrosion of ferrous materials decreases, it seems probable that the apparent advantage of coated light-weight pipe over unprotected thick-walled pipe will decrease as the period of exposure is increased.

It will be evident from a study of table 14 that a light-weight pipe protected by a very good coating is superior to an unprotected thick-walled pipe during the first 12 years of exposure, and that the thick-walled pipe is superior if the coating does not reduce the leaks to a very small percentage of those on bare pipe. The amount of reduction in leaks equivalent to a given increase in the thickness of the pipe wall can be calculated from Scott's formula by taking P_2 and P_1 equal to the two thicknesses and calculating the reciprocal of the ratio of the corresponding areas per leak. Thus, by means of the formula it can be shown that when a is 0.261, a coating must reduce the leaks on a coated light-weight 8-inch steel pipe to 0.27 percent of those on the bare pipe in order to equal the service of an 8-inch class B cast-iron pipe. If the pipe is in a uniform soil, for which the value of a is 0.15, it is necessary to reduce the leaks to 0.004 percent of those on the bare thin pipe, i. e., the coating must prevent practically all leaks.

In concluding this discussion of the effectiveness of protective coatings it should be pointed out that the deductions are only as reliable as the data and the assumptions upon which the calculations are based. The pit depths in the table 14 have large standard errors

and the calculations of effectiveness of coatings are based on an empirical formula which has been tested only to a limited extent.

The measure of effectiveness given in table 14 must therefore be regarded as somewhat questionable. Nevertheless, the bases for the table are sufficiently reliable to give the reader a rough idea of the usefulness of certain types of protective coatings. The usefulness of other coatings may be roughly estimated by comparing the conditions of the protected pipes for equal periods of exposure.

7. BITUMINOUS ENAMELS

One of the characteristics of bitumens as protective coatings is their tendency to flow under low pressures. This tendency can be reduced by using a material of higher softening point, but this usually makes a more brittle coating. A reduction in the tendency to flow can also be accomplished by the addition of finely divided inert material commonly known as a filler. A bitumen to which a filler has been added is frequently called an enamel, although the term is also used to designate a bituminous varnish to which a pigment has been added. In this paper the term "enamel" is used to designate a bitumen yielding between 15 and 50 percent of residue on ignition. Ewing and Scott have reported all the data on the performance of enamels tested with the cooperation of the National Bureau of Standards, and the present discussion of the enamels will be limited to a summary of the data of these investigations together with some new data on the properties of these materials.

Because of the limited amount of pipe line available for his tests, Scott was unable to apply all of his coatings to the line at all test sites. Although there are 15 test sites, there are only 6 sites at which all of the 4 unreinforced enamels can be compared. Two or three of these coatings can be compared at two other sites. Data for these latter sites are also presented because the soils at these sites are corrosive and the behavior of coatings in them is therefore of especial interest.

Since the effectiveness of a coating depends to some extent on its thickness, Scott determined the thickness of each coating at each site by four measurements taken 90° apart, 1 foot from each end of each coated section. Table 15 shows the maximum, minimum, and average thicknesses of the four enamel coatings at each site. The maximum and minimum values are averages of 4 measurements, while the average value is the average of 16 measurements.

TABLE 15.—*Thickness of coal-tar-enamel coatings in the API tests*

[Thickness in mils]

Site	Coating *K*			Coating *L*			Coating *M*			Coating *N*		
	Maximum	Minimum	Average	Maximum	Minimum	Average	Maximum	Minimum	Average	Maximum	Minimum	Average
II	55	46	52	142	80	100	50	44	47	52	46	49
III	73	59	66	107	63	84	42	39	41	54	44	48
VI	161	48	81	92	66	76	73	58	64	81	58	68
VII	78	62	71	------	------	112	73	64	69	75	69	71
VIII	------	------	------	65	51	56	------	------	------	62	44	53
X	164	67	107	91	86	89	90	68	79	104	64	83
XI	85	48	64	84	64	73	46	39	43	84	53	74
XVI	------	------	------	65	49	55	69	37	56	70	49	60

Obviously, the extreme values would cover a wider range of coating thicknesses. All of the coatings varied considerably in thickness and the average value for the thickness of a given coating was not the same at all of the sites. It seems probable that the variation in the pit depths found on the protected sections is in part the result of variations in the thickness of the coating.

The more important indication of the values for coating thickness is the fact that it is not practicable to apply a coating of uniform thickness by the methods employed in this test. So far as the protective value of the coating is concerned, the value for minimum thickness is the most important since breakdowns of the coating are more likely to recur at this spot.

At each site all of the coatings were inspected on two sections of line on three occasions. Table 15 gives the pit-depth measurements for these examinations. The table also includes data for two sites where not all of the enamels were represented.

Each coated section had adjacent to it an uncoated section for comparison. In table 16 the pit depth on the uncoated section is given as well as the pit depth on the coated section. It will be noted that the corrosiveness of the soil at the test sites, as indicated by the pit depths on the bare sections, varied considerably. It is possible, therefore, that abnormally low or abnormally high rates for pit depths on coated sections are partly the result of variations in the corrosiveness of the soils.

TABLE 16.—*Pit depth on pipe in American Petroleum Institute tests of coal-tar enamels* *

[Pit depth in mils]

Site	Section	Coating *K*						Coating *M*					
		1 year		2 years		4 years		1 year		2 years		4 years	
		Bare	Coated	Bare	Coated	Bare	Coated	Bare	Coated	Bare	Coated	Bare	Coated
II	*a*	20	0	43	5	31	5	18	5	44	13	51	16
	b	5	0	39	1	51	17	5	21	27	34	47	18
III	*a*	61	53	77	57	157	94	43	25	113	52	189	117
	b	41	79	114	113	94	40	67	44	114	66	94	119
VI	*a*	5	0	30	0	39	5	23	0	25	22	34	22
	b	29	0	52	36	68	5	29	1	52	73	68	43
VII	*a*	13	5	22	5	50	33	26	17	57	16	63	22
	b	23	1	32	5	50	5	19	33	46	52	45	45
VIII	*a*	------	------	------	------	------	------	------	------	------	------	------	------
	b	------	------	------	------	------	------	------	------	------	------	------	------
X	*a*	52	0	59	0	49	0	54	5	57	28	77	32
	b	40	0	37	0	28	5	25	5	42	5	48	12
XI	*a*	14	43	33	0	46	5	17	32	45	58	45	48
	b	15	0	30	77	33	0	11	19	27	23	47	44
XVI	*a*	------	------	------	------	------	------	5	17	5	33	103	130
	b	------	------	------	------	------	------	1	1	5	5	63	70

* Coating *K* is a blend of coal-tar pitch and asphalt.

TABLE 16.—*Pit depth on pipe in American Petroleum Institute tests of coal-tar enamels*—Continued

[Pit depth in mils]

Site	Section	Coating *L*						Coating *N*					
		1 year		2 years		4 years		1 year		2 years		4 years	
		Bare	Coated	Bare	Coated	Bare	Coated	Bare	Coated	Bare	Coated	Bare	Coated
II	*a*	18	0	44	0	51	0	20	5	43	1	31	5
	b	5	0	27	1	47	1	5	0	39	0	51	0
III	*a*	61	82	77	78	157	165	61	74	87	5	128	110
	b	41	56	114	134	94	177	53	68	78	5	133	229
VI	*a*	5	1	30	24	39	42	45	36	40	5	44	38
	b	1	53	26	13	43	39	28	0	54	5	29	19
VII	*a*	13	0	22	0	50	0	26	22	57	20	63	1
	b	23	0	32	0	50	0	19	1	46	5	45	5
VIII	*a*	13	5	47	27	54	39	19	15	37	31	63	91
	b	18	34	56	80	101	54	19	5	46	70	85	42
X	*a*	42	0	47	0	54	1	54	0	57	1	77	5
	b	27	0	41	5	47	16	25	0	42	1	48	1
XI	*a*	17	0	45	30	45	35	5	13	48	44	54	13
	b	11	5	27	5	47	0	21	5	32	5	37	27
XVI	*a*	5	5	5	5	66	5	14	27	42	71	90	122
	b	1	1	5	5	63	5	1	1	30	63	17	63

Table 16 shows that, when two sections of the same coating at the same site are compared, the maximum pit depth on one pipe may be more than twice that on the other. This is true for each of the coatings. Out of the 174 cases in which the pit depths on the coated and adjacent uncoated sections can be compared, there are 37 cases or 21.3 percent in which the pit depths were deeper on the coated sections. In eight additional cases the pit depths on the coated and uncoated sections were equal. When it is considered that the data apply to areas of from approximately 5 to 8 square feet and for periods of exposure of 4 years or less, it is evident that the protection afforded by these coatings was far from complete.

There can be no doubt, however, that each coating has materially reduced the number of pits as well as the loss of metal, and consequetly, for the period under consideration, each coating has reduced the cost of reconditioning the pipe, although in some cases the time for the first leak may have been shortened.

The agreement under which the API line tests were conducted prevents the disclosure of the names of the coatings or their makers. It may be said, however, that the coatings represent four of the enamels most commonly used at the time of their application and that they were applied by manufacturers' representatives. It is possible that as a result of the tests, the manufacturers have modified their products or methods of application. While it is hoped that any such changes resulted in improvements of the coatings it must be remembered that this remains to be demonstrated.

Because the differences between the coatings were not sufficient to result in outstanding differences in the data, and because of the erratic nature of the data, the best idea of the effectiveness of enamels as a

type of coating can be obtained by combining the data for all four coatings. This has been done in table 17. Columns 3 to 6 show the corrosiveness of the soils as indicated by the pit depths on the bare pipe. The significance of the standard deviation and the standard error of the mean, as well as the method used in determining the length of pipe for a leak, are the same as described in the discussion of table 14, except that because of the smaller number of observations, the accuracy of the results is somewhat less than in table 14. The extrapolation involved in computing the length for a leak in the less corrosive soils is so great that the results are of little value except for showing the general relationship between coated and uncoated pipe in these soils. Since the trend of the errors would be similar for both bare and coated pipe, the indication of their relative performances is probably sufficiently accurate for this purpose.

The table indicates that in the three most corrosive soils, III, VIII, and XVI, the coatings were not very effective. In the less corrosive soils the effectiveness of the enamels was much greater.

The table indicates only the effectiveness of the coatings for an exposure of approximately 4 years. This of course is much too short a period for anything but the elimination of the poorer coatings.

TABLE 17.—*Average effectiveness of coal-tar enamels in API line tests for exposures of approximately 4 years*

[Pit depth in mils.]

Site		Uncoated sections				Enamel-coated sections			
Designation	Rank as to corrosiveness	Pit depth	Standard deviation	Standard error	Estimated feet per leak on 8-in. pipe, 0.322-in. wall	Pit depth	Standard deviation	Standard error	Estimated feet per leak on 8-in. pipe, 0.322-in. wall
II	9	46	7	2	5,186	8	7	3	5,629,000
III	1	135	32	10	84	131	54	20	125
VI	8	46	12	4	6,471	27	15	6	66,480
VII	5	53	19	6	3,016	14	16	6	659,500
VIII[a]	2	79	21	6	653	57	21	12	3,043
X	7	47	13	4	4,779	9	10	4	3,586,000
XI	10	45	10	3	4,333	22	18	7	89,730
XVI[b]	3	70	33	9	1,039	66	50	22	1,734

[a] Two coatings only.
[b] Three coatings only.

The available data are insufficient for an accurate prediction of the trend of the deterioration. It is evident, however, from table 16, that the condition of the coated sections was somewhat worse at the third examination than at the first. An attempt to show the trend in the performance of the four coatings as a whole has been made in figures 3, 4, and 5. The broken lines show the progress in the pit depths on the unprotected sections while the continuous lines show that for the coated specimens. The curves for the bare sections are based on all pit measurements for those sections rather than for only those sections adjacent to the enameled sections. The values are therefore slightly different from those in table 16, but they are probably more characteristic of the test sites. While in some cases the positions of the curves are defined quite well by the observations, in other cases the locations of the curves are doubtful.

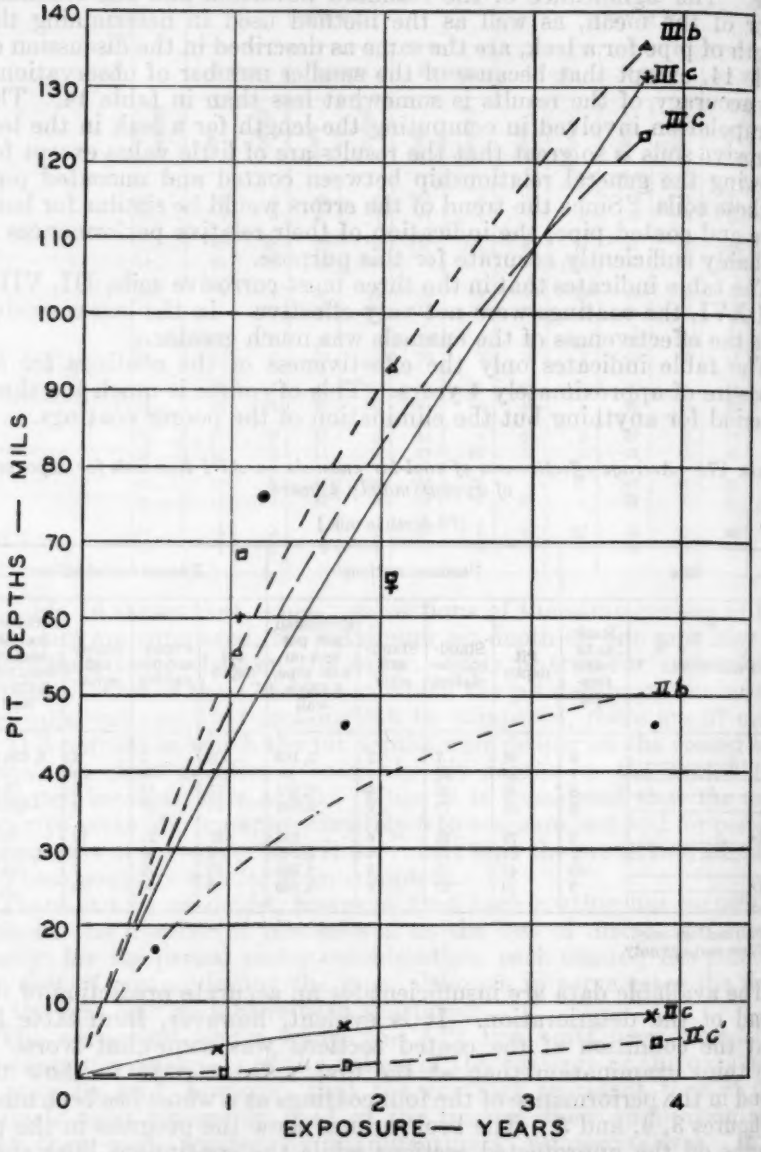

FIGURE 3.—*Effect of time on pit depths on bare and enamel-coated pipe at sites II and III.*

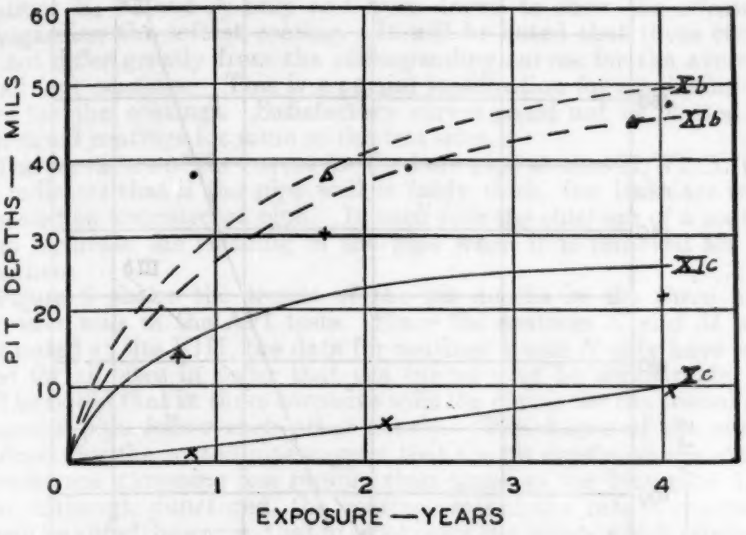

FIGURE 4.—*Effect of time on pit depths on bare and enamel-coated pipe at sites X and XI.*

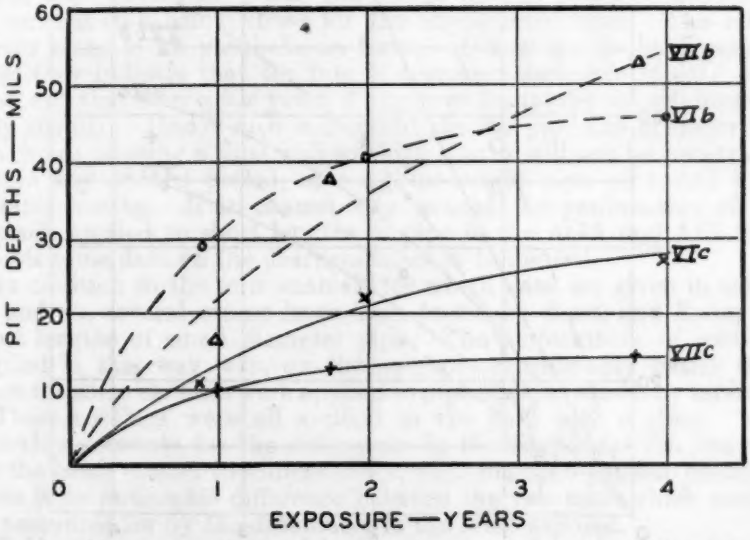

FIGURE 5.—*Effect of time on pit depths on bare and enamel-coated lines at sites VI and VII.*

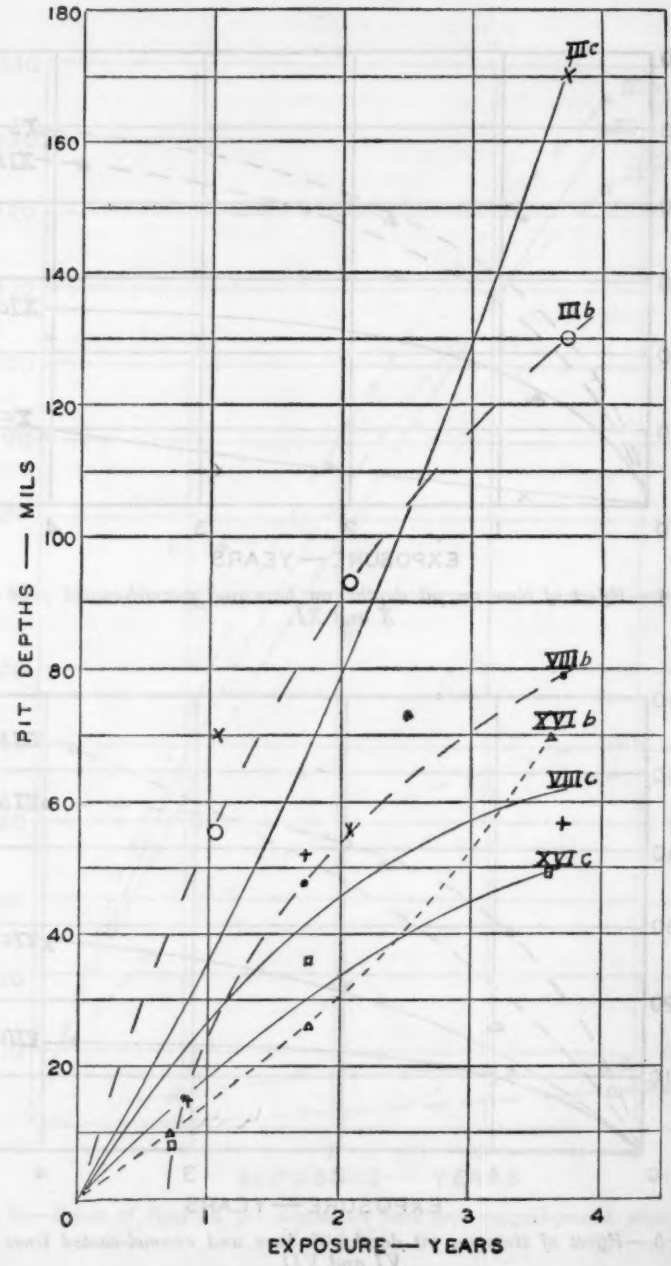

FIGURE 6.—*Effect of time on pit depths on bare and enamel-coated pipes in the three most corrosive soils in the API tests.*

The curves for the coated and uncoated sections in the same site are in most cases similar, with those for the coated pipe lying below the others. In figure 3, curves *IIc'* and *IIIc'* are for the average of coatings *K*, *L*, and *N* only and were drawn to show the effects of disregarding the softest coating. It will be noted that these curves do not differ greatly from the corresponding curves for the averages of all four coatings. This is a partial justification for combining the data for the coatings. Satisfactory curves could not be plotted for individual coatings for some of the test sites.

The curvature of the curves for the bare pipe at sites II, VI, X, and XI indicates that if the pipe wall is fairly thick, few leaks are to be expected on unprotected pipe. In such soils the chief use of a coating is to facilitate the cleaning of the pipe when it is removed for use elsewhere.

Figure 6 shows the trends of the pit depths in the three most corrosive soils in the API tests. Since the coatings *K* and *M* were not tested at site VIII, the data for coatings *L* and *N* only have been used for all sites in order that the curves may be comparable. It will be noted that in these corrosive soils the curves for the coated and uncoated pipe follow each other closely. The shapes of the curves as drawn for the coated pipe suggest that the pit depths on the coated sections are increasing less rapidly than those on the bare pipe, i. e., that, although punctured, the coatings retard the rate of corrosion. It will be noted, however, that in most cases the points which represent the data from which the curves are plotted do not lie close to the curves and there is therefore considerable uncertainty as to the actual trend of the data.

For the less-corrosive soils the curves for the enamel-coated lines lie considerably below those for the unprotected lines. The latter curves seem to be parabolic in form. If they are to be depended upon they indicate that the rate of corrosion decreases rapidly with time, and that after a few years of exposure the pit depths will increase only slightly. Under such soil conditions the pipe-line operator has the choice of using a pipe wall so thick that it will not be penetrated within any desired period, or a lighter-weight pipe protected by a suitable coating. If an enamel is to be used, the performance of the enamels applied to short lengths of pipe in the AGA and API tests affords some data on the characteristics to be desired.

In addition to the four enamels for which data are given in tables 15 and 16, several others have been tested by Scott and Ewing on short lengths of small diameter pipe. The performance of coatings applied in this way was, on the average, considerably better than when the same enamels were applied to pipe lines, as shown by table 18. These coatings were all applied in the field with a sling. This probably accounts for the differences in the results for the line and for the small coated specimens since, with machine-applied coatings, there is no noticeable difference between the two tests which cannot be accounted for by the differences in the areas exposed.

Table 18 indicates that, with the exception of coating 3 in sites II, III, and X, the pit depths were much less on the coated nipples than on the similarly coated line. Either the application of the coatings to the nipples was much better or the nipple test is not as severe as the line test.

TABLE 18.—*Relation between maximum pit depths on enamel-coated line pipe and on similarly coated nipples (API tests)*

[Pit depth in mils]

Site	Bare pipe		Coating 1		Coating 2		Coating 3		Coating 4	
	Line	Nipple	Line	Nipple	Line	Nipple	Line	Nipple	Line	Nipple
II	46	35	11	0	1	26	17	19	3	0
III	135	129	67	0	171	24	118	148	170	16
VI	46	49	5	0	41	13	33	16	29	5
VII	53	37	19	0	0	0	34	15	3	0
X	47	43	3	0	9	0	22	19	3	0
XI	45	46	3	0	18	0	46	19	21	0
Average	62	57	18	0	40	11	45	39	38	4

Table 19 shows the variation in some of the properties of the enamel which is probably the most uniform in the API tests. With the exception of the value of 11.7 for ductility at site VIII, the data appear to be reasonably consistent. The differences in the properties of the coating at different sites must therefore be attributed to real differences in the several lots of the material from which the samples were taken.

Table 19 indicates that the product sold under a single name is not always the same and shows, therefore, the need for specifying such properties as are known to be essential. Unfortunately, there are at this time few data to justify a rigid specification.

Figure 7 shows the conditions of the four coatings applied to 3-inch pipe after 0.83 year exposure at site VIII (Acadia clay). The soil is a heavy clay containing crystals of gypsum. It will be noted that the distortion was greatest for coating *M* and least for coating *N*, as might be expected on account of their softening points.

TABLE 19.—*Physical properties of the same enamel at different test sites*

[Determinations by H. S. Christopher]

Site	Ring and ball softening point	Ductility (Dow) at 115 °F	Consistometer hardness (Abraham) at 115° F	Insoluble in CS_2	Ash
	°F	cm.		%	%
VIII	185	11.7		53.6	36.3
XIII	198	2.8	42.7	51.2	33.2
XI	201	3.4	51.9	56.9	37.4
III	205	5.2	46.4	57.2	40.3
IV	207	4.7	54.3	56.0	38.2
VII	207	4.3	49.3	57.4	37.7
XIV	210	2.2	62.1	56.0	38.3
XII	212	1.5	63.0	53.1	39.1
XVI	212	1.8	61.3	55.2	38.9
1929	208	5.0	51.9	55.7	38.7
1930	205	3.8	61.3	55.6	35.3

The behavior of enamels in heavy clay soils is further illustrated in figure 8, which shows coatings furnished under the same trade designations for the AGA tests after an exposure of 0.77 year to Miller

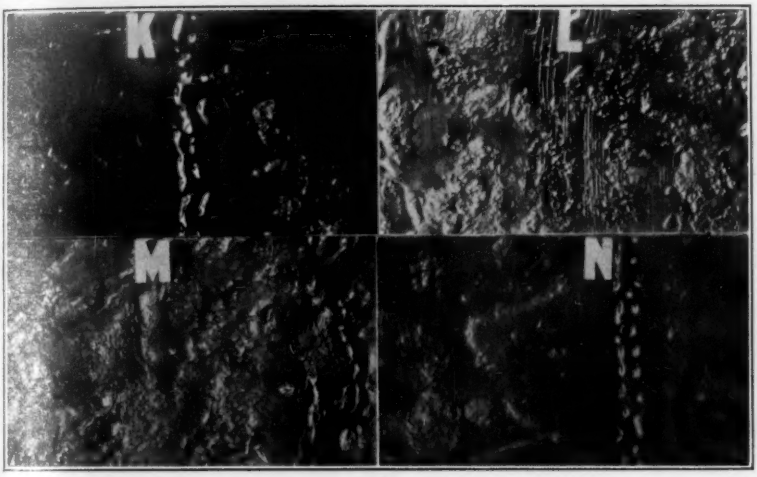

FIGURE 7.—*Condition of four coal-tar-enamel coatings after 0.83 year of exposure to Acadia clay.*

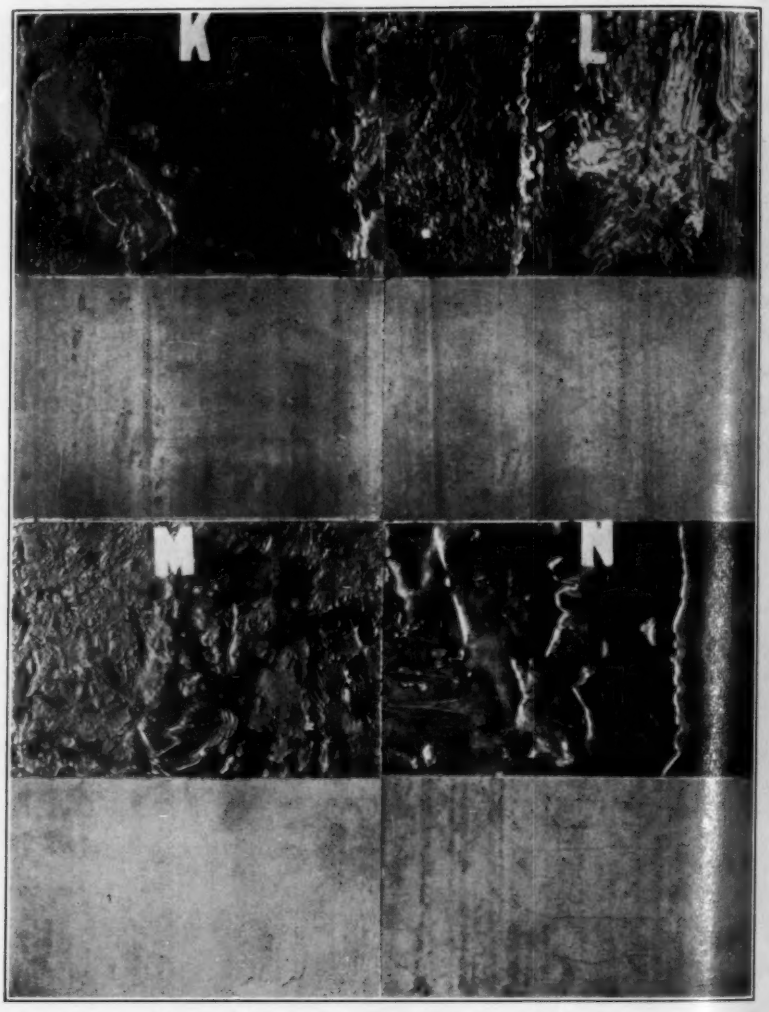

FIGURE 8.—*Condition of four coal-tar-enamel coatings after 0.77 year of exposure to Miller clay.*

[Note rust streaks on pipe of coating *N* corresponding to cracks in the coating (same coatings as in fig. 6).]

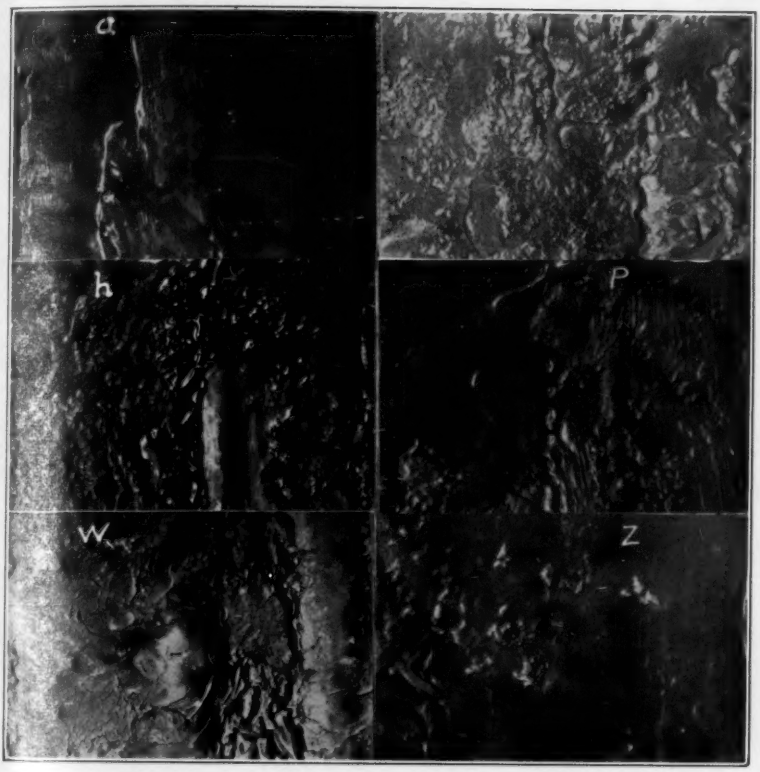

FIGURE 9.—*Condition of six enamel coatings after 0.83 year of exposure to Acadia clay.*

UNIV. OF MICH.

clay at Bryan, Tex. This soil is somewhat heavier than that at API site VIII but the former contains little corrosive material. This is indicated by the lower half of each illustration, which shows the condition of the pipe from which the coating has been removed. Indeed, this soil is one of the least corrosive of the AGA sites.

Figure 8 illustrates several things which may happen to coal-tar enamels under adverse soil conditions. The left side of the illustration for coating *K* shows a spot where the soil has pulled the coating from the pipe. To the right of the bare spot the coating has been distorted by clod pressure, while near the upper right corner the coating has been spalled off, probably because of a blow.

At the left of the illustration of coating *L* distortion is shown together with shallow grooves which may have been made by roots. The white near the center of the picture is whitewash with which the coating was originally covered. Coating *M* shows more serious distortion. The picture of coating *N* shows another type of coating failure—cracking, which was observed at several test sites. That the cracks extended through the coating and remained in this condition for some time is indicated by the rust lines on the section of pipe from which the coating has been removed.

The API tests of enamels applied to short lengths of small-diameter pipe include six enamels in addition to those applied to pipe lines. The appearance of these enamels when removed after 0.83 year exposure to Acadia clay is shown in figure 9, which is comparable with figure 7. The data for the pit depths on all of the enamels after 4 years of exposure in the API tests are shown in table 20. The table also shows the thickness and the ring and ball softening points of those enamels. The first four of these coatings are duplicates of coatings in table 16, which is a better indicator of the performance of the coatings under working conditions. Coating *k* is a blend of coal tar and asphalt. Coatings *h* and *w* are asphalt enamels; the others are coal-tar-pitch enamels. Since there was only a single specimen of each coating it is possible that the apparent relative merits of the coatings are in part accidental, and conclusions as to the relative merits are subject to revision when more data become available.

The table indicates that the thickness and softening points are important factors in the performance of the enamels.

Coatings *p* and *zzz* were identical except that coating *p* was applied over a priming coat of red lead. The asphalt enamels were apparently slightly inferior to the others, possibly because of a greater tendency to absorb water, since at most sites their conductance was relatively high.

The enamels in table 20 are all proprietary materials and are identified in Scott's report [22] on the installations of his specimens. However, since most coating manufacturers modify their products from time to time it seems best to treat each material on the basis of its properties rather than as a product having a certain name. It is quite possible that the product sold later under the same name has been modified to overcome the defects described by Scott. Only tests or experience will tell whether the modifications are effective.

[22] G. N. Scott. *API coating tests.* Proc. Am. Petroleum Inst. 12, pt. IV, 55 (1931).

TABLE 20.—*Pit depths on 4-year-old enamel coated small-diameter pipe in the API tests*

(Pit depth in mils)

Site	Coatings—										Bare
	t	*s*	*zzz*	*k*	*dd*	*a*	*h*	*p*[1]	*z*	*w*	
II	19	0	26	0	18	5	5	0	0	21	35
III	15	16	24	0	136	19	85	0	52	110	129
VI	16	5	13	0	19	1	14	15	22	30	49
VII	15	0	0	0	5	0	17	0	0	17	37
X	19	0	0	0	0	5	5	0	0	5	43
XI	19	0	0	0	20	0	5	0	0	1	46
Thickness (mils)	52	41	77	75	50	54	69	71	72	92	None
Softening point (°F)	158	195	205	192	190	241	189	205	222	163	

[1] Applied over a red-lead paint, baked on.

In Ewing's [23] tests there are four soils which are corrosive but in which little soil stress would be expected because they are wet much of the time. Soils 3 and 4 are tidal marshes. Soils 5 and 6 are mucks. All of these soils are corrosive, as indicated in the last column of table 21. This column shows that for these soils the maximum pit depth is roughly proportional to the period of exposure. With the exceptions of coatings *WL* and *WR*, which differ only in the primer used, the enamels listed in table 21 are nominally the same as those buried by Scott a year later. In most cases, however, Scott's coatings were considerably thicker.

It will be noted that the deterioration of the coatings was progressive not only as to pit depths, but also as to the number of failures. None of these enamels has a perfect record in all four soils throughout the test. No soil is outstanding in its corrosiveness with respect to the enameled specimens. The data are insufficient and too erratic to justify the plotting of curves to show the progress of the corrosion. It can be seen that the thinner coatings had the most failures and that the coatings with the lower softening points were in general thinner than those having higher softening points. The latter contained larger amounts of inert material. The points of difference between the coatings are, however, too many to permit the determination of the characteristics which control their performance. It seems advisable, therefore, that any specification for an enamel should be based on its reaction to forces representing the soil characteristics and operating conditions which tend to destroy coatings rather than on the composition and physical characteristics of the coating as conventionally determined.

Among the important influences on coating behavior to be considered in the writing of specifications are soil pressure, adhesion of the coating to the soil and to the pipe, temperature changes, shocks, and moisture.

In view of the performance of the enamels in the wet soils it seems doubtful whether they should be recommended for such conditions in cases where superior coatings can be secured at but slightly greater costs. There can be no doubt, however, that the better enamels

[23] S. Ewing. *AGA studies of pipe-line coatings.* Proc. Am. Gas Assn., p. 774 (1931), p. 741 (1933), p. 637 (1936).

will materially reduce corrosion in wet soils for at least five years and probably for a considerably longer period.

TABLE 21.—*Performance of AGA enamels in poorly drained organic soils*

(Pit depth in mils)

Exposure	Soil	Coatings									Bare
		C	*S*	*H*	*B*	*WR*	*WL*[1]	*W*	*R*	*A*	
yr											
0.86	3	0	0	0	0	0	0	0	0	0	0
.86	4	0	0	0	0	0	0	0	0	0	0
.75	5	0	0	0	0	0	0	0	0	0	26
.74	6	0	0	0	0	0	0	0	0	0	0
2.49	3	0	44	0	0	0	0	0	0	0	15
2.49	4	38	0	27	0	0	0	0	0	0	24
2.52	5	0	12	0	30	0	0	0	0	0	45
2.51	6	0	0	0	40	20	0	0	0	0	51
5.80	3	70	38	0	135+	0	13	16	5	0	43
5.75	4	5	122	135+	5	0	0	0	0	0	42
5.46	5	20	23	5	30	33	37	35	0	5	63
5.46	6	47	37	5	50	42	0	25	0	0	115
Thickness (mils)	------	14	34	34	38	50	52	58	61	70	0
Softening point (°F)	------	156	162	187	167	184	184	208	201	232	------

[1] Coating applied over red-lead paint.

8. REINFORCED BITUMINOUS COATINGS

It has been shown that asphalts and coal-tar pitches may have in varying degree four faults which detract from their value as protective-coating materials: absorption of water, low resistance to shock, susceptibility to changes in temperature, and cold flow under stress. The addition of finely divided inert materials improves the bitumens as coating materials but does not result in products which are entirely satisfactory for use under severe soil conditions. Further improvements have been attempted through the use of reinforcing fabrics, either imbedded in the coating or placed over the coating as a shield. At first, various organic fabrics such as burlap and coarse cotton cloth were used as reinforcements. Later, bitumen-impregnated organic and asbestos felts similar to roofing felts were used extensively. The use of these materials not only results in coatings which are more resistant to shock and to soil stress but usually involves the application of more bitumen. It is generally agreed that the protection of the pipe against moisture depends upon the kind and amount of bitumen present. Most fabrics, even though impregnated with bitumen, absorb some moisture. In this respect their incorporation in a coating may be a source of weakness, although the net result may be favorable because of the improvement in the mechanical properties of the coating.

Because the incorporation of the fabric in the body of the coating may introduce moisture, some coating manufacturers and users have thought it better to place the fabric on the outside of the coating as a shield. The chief objection to this method is that frequently less bitumen is applied to the pipe. The idea of shielding the bituminous coating resulted in the development of new types of shields, such as thin sheet metal.

The general effect of using a fabric reinforcement with unfilled bitumen has been shown in tables 13 and 14. The effect of the fabric on enamels and on some other coatings is shown in table 22, which is a rearrangement of data reported by Scott.[24]

In the third and fifth columns of table 22 the standard deviations of the data in the second and fourth columns have been given in order that the reader may realize more clearly the uncertainties of the data. Since there were but two specimens of most of the materials at each site, the reproducibility of the data is less definitely known than is the reproducibility of the data for bare pipe or for the enamels. Because not all materials could be tested at each site on account of lack of space, it is not possible to compare the performances of all of the coatings in all soils. However, the table furnishes a sufficient number of comparisons to indicate in a general way the relative merits of several coatings. In making comparisons one should keep in mind the fact that the thickness of the asbestos felt was about 25 mils and that of the rag felt about 50 mils. The thickness of the concrete was about 350 mils, but it varied considerably at different sites. The thickness of the cotton fabrics was about 15 mils, but the weave was so open that a considerable amount of bitumen was included with the fabric.

A comparison of the data for the unreinforced enamels with those for the shielded enamel *G* indicates that the shield materially reduced the pit depths at all sites, although the shielded enamel was not as thick as the average of the unshielded enamels. All of the other coatings, with the exception of the unreinforced emulsion, were so much thicker than the enamels that it is impossible to determine from the data whether the superiority of the reinforced coatings was the result of the reinforcement or of the added bitumen. Likewise, it is difficult to determine whether the asbestos felt was more serviceable than the rag felt.

Coating *T*, which contained two layers of rag felt with intervening layers of enamel, appeared to be slightly superior to coating *U*, which is less than half as thick, and contained a single layer of asbestos felt. The unfilled asphalt reinforced with rag felt, *S*, appears to be slightly superior to the asphalt enamel reinforced with asbestos felt, *R*, possibly because the latter coating was not as thick, although this difference may be accounted for by the difference in thickness of the felts. In most soils, where comparisons can be made, the coatings reinforced with cotton fabric appear to have been slightly inferior to the coatings reinforced with felt, although the former were thicker and contained more mopped asphalt per unit area.

The investigation conducted by Ewing [25] throws additional light on the relative merits of reinforcing materials. This investigator has found that the organic materials, even when impregnated with grease or bitumen, absorb moisture, and decay. The absorption of moisture increases the conductivity of the coating and decreases its value if used in connection with cathodic protection.

The use of burlap is extensive in some countries but has largely been discontinued in the United States because of the tendency of the fibers to protrude through the coating and to act as small capillaries which conduct water into the coating.

[24] G. N. Scott. *API coating tests, IV.* Proc. Am. Petroleum Inst., 15, pt. IV 18 (1934).
[25] S. Ewing. *AGA field tests of pipe coatings.* Proc. Am. Gas Assn. p. 627 (1936).

In a laboratory test of materials available for the reinforcement of bituminous coatings, Scott and Ewing [26] tested 26 materials by exposing them to moist soil. All of the fabrics decreased in strength within 1 year. The decrease was much greater for the organic fabrics. Rot inhibitors delayed but did not prevent rotting.

Table 22 indicates that for the period of the test, the emulsion protected by the heavy layer of sand and cement mortar appears to have been somewhat more effective than the other coatings in table 22 with which it can be compared.

Three facts regarding the data in table 22 are outstanding. One is that although the exposures of the coatings are only 4 years, measurable pits developed beneath all of these coatings in most of the soils to which they were exposed. Another is the relatively great thickness and the large number of parts of the more effective coatings. A third fact of importance is that the same degree of effectiveness can be secured in several ways. None of the coatings in table 22 is outstanding in its performance though, in general, the effectiveness of the coating appears to be roughly proportional to its thickness and nearly independent of its structure. More data will be needed to define the engineering principles upon which a coating should be designed. To obtain such data was the purpose of the API coating tests.

TABLE 22.—*Effect of reinforcement on bituminous coatings on working lines*

[Average depth of maximum pits, in mils, after 4 years]

Site	Bare pipe		Coal-tar-enamel coatings					Reinforced-asphalt coatings [1]					
			Not reinforced [2]		Reinforced or shielded			Unfilled				Emulsions	
	Average of 12 specimens	Standard deviation	*K, L, N*	Standard deviation	*G*, asbestos-felt shield	*U*, asbestos felt, reinforced	*T*, double rag felt, reinforced	*R*, enamel and asbestos felt	*S*, rag felt, reinforced	*E*, single cotton fabric, reinforced	*Z*, double cotton fabric, reinforced	*A*, inhibitor only	*F*, inhibitor and sand, and cement shield
II	46	7	5	6	1	3	------	24	8	8	9	63	------
III	135	32	136	61	3	1	------	12	------	------	10	140	------
VI	46	12	25	16	17	------	1	------	------	26	------	41	5
VII	53	19	7	12	28	5	16	14	5	------	33	------	------
VIII	79	21	[3] 57	21	40	31	5	40	46	------	20	------	28
IX	65	27	3	2	11	0	1	3	------	------	19	------	1
X	47	13	5	5	0	------	3	------	------	1	------	33	1
XI	45	10	14	13	------	3	1	9	------	27	19	------	------
XIII	50	16	[1] 54	4	1	9	------	------	72	58	36	67	6
XIV	18	8	[1] 8	3	------	3	------	5	3	3	------	10	3
XVI	70	33	49	48	23	8	7	------	------	25	37	------	61
Thickness (mils)	------	------	70	------	63	171	351	143	150	151	206	65	419

[1] Average of 2 specimens.
[2] Average of 6 specimens.
[3] Average of 4 specimens.

[26] G. N. Scott and S. Ewing. *Deterioration of pipe-line fabrics.* Oil and Gas J. 34, 112 (Oct. 24, 1933).

9. GREASE COATINGS

Several manufacturers and pipe-line operators have suggested greases as a means of retarding the corrosion of pipe lines. The API line tests of protective coatings included one grease coating reinforced by cotton fabric. The grease contained a material intended to inhibit corrosion and the fabric was treated to retard decay. The outer layer was a heavy grease. The average thickness of the coating was 107 mils. No section of the line protected by grease was free from corrosion at the close of the 2-year test period and only 4 of the 20 sections were free from rust at the end of the 1-year period.

Evidently the rust inhibitor contained in the grease was only partially effective even for a period of less than 1 year. Nevertheless, at the close of the 4-year period the fabric-reinforced grease appeared to be as effective in reducing pit depths as any coating of its thickness and more effective than several thicker coatings. The coating was not exposed to the three most corrosive soils. The effectiveness of the coating after 4 years is indicated by table 23.

TABLE 23.—*Maximum pit depths on pipe protected by reinforced grease and other coatings (API tests)*

[Average depth of maximum pit after 4 years]

[Pit depth in mils]

Site	Bare pipe	*B*, cotton fabric-reinforced grease	*E*, cotton fabric-reinforced asphalt	*K*, coal-tar enamel, unreinforced	*U*, coal-tar enamel, reinforced with asbestos felt
I	20	5	3	----------	1
II	46	11	8	11	3
IV	38	1	3	----------	0
V	38	3	3	23	----------
VI	46	19	26	5	----------
VII	53	5	----------	19	4
IX	65	5	----------	----------	0
X	47	3	1	3	----------
XI	45	14	27	3	3
XIV	18	9	3	8	3

Unreinforced grease coatings have been used to a considerable extent but few definite data are available on their performance. They seem to render the best service when applied in soils which are continuously wet and to fail soonest in soils that frequently become very dry.

One pipe line company has tried grease shielded by a wrapper of copper foil. The writer has seen no data on the performance of this coating but there appears to be a possibility of galvanic action between the copper shield and the steel pipe if pressure forces the shield into metallic contact with the pipe at any point. Possibly a copper foil backed by organic or inorganic fabric would prove more satisfactory.

10. MASTIC COATINGS

Of all the coatings in the API tests the mastic coating was the best for the first 4 years of the test. This coating was made of a mixture of asphalt and graded mineral matter applied by machine to

a thickness of 0.519 inch. Even this coating showed rust spots on two sections at the 4-year inspection. Whether this rusting was the result of imperfections in the coating or of deterioration cannot be determined until additional inspections have been made.

VI. APPLICATION OF DATA TO PIPE LINES

Since readers may wish to apply the data in this report to the solution of the problem of protecting a pipe line or service pipe, the relation of the data to pipe-line protection will be considered briefly.

Those who wish to estimate the pit depth on any chosen area of protected pipe from the performance of a similarly coated specimen may do so by the application of Scott's pit-depth-area relation which has been discussed on page 719. If this formula is used it should be remembered that the results become less reliable as the extrapolation is extended and that the values for the exponent a in Scott's equation differ for different soil conditions.

Few if any experiments completely duplicate the service conditions upon which they are supposed to throw light. This is especially true of experiments with protective coatings even when the coatings are applied to working lines. In the first place, the serviceability of a pipe line or service pipe is governed largely by its worst condition, since a single leak may involve a temporary shut-down of the line and possibly large expenses because of damages to pavements or because of the escape of the transported fluid. On this account the worst performance of a coating is of more importance than its average performance. On the other hand, an imperfect coating may be greatly preferable to none at all. The danger lies in expecting greater protection from a coating than is justified by the character of the coating.

In this connection a phenomenon common to all problems involving maxima must be kept in mind. The larger the sample from which the maximum is chosen, the larger will be that maximum. In other words, the first leak will probably occur on a long line before it appears on a short one exposed to the same conditions. It is to be expected then that even if the average performance of a coating on the short length of pipe is representative of the average performance of the coating on a working pipe line, the first failure of the coating on the line will occur in a shorter time than it occurred in the experiment. How serious this is in a particular case depends upon the amount of trouble caused by a single leak. On lines which are easily accessible the average condition of the line is much more important than the worst condition. On lines under pavement and on lines on which a single leak may result in an explosion the worst condition is the controlling factor.

It may be assumed that the coatings used in the experiments were applied to the pipes with greater care than they would have been applied under average pipe line conditions. However, the results of the tests have shown the necessity for care and have probably caused improvements in materials and in operating practice.

Most bituminous coatings cannot be successfully applied to damp or dirty pipe. It is very difficult to avoid these conditions when coatings are applied in the field.

The resistance of most bituminous coatings to shock and abrasion is much less than that of the pipe to which the coating is applied. It follows that if a coating is to start its service uninjured the coated line must be handled with greater care than would be required for an uncoated pipe.

While it is customary to test a pipe line to determine whether it is free from flaws and imperfections, there is no satisfactory way of making similar tests of a protective coating after it has been placed in the trench. The best that can be done is to test the coating by means of an electrical fault finder [27] at the latest practicable point in the laying of the line. Obviously, because of the ease with which a coating may be injured as the coated pipe is handled and as the trench is backfilled, and because of the difficulty in making satisfactory field joints for the coating, the probability that the line will be completely protected is small. With respect to pipe lines this difficulty may be overcome by the application of cathodic protection.[28]

If cathodic protection is to be applied to a coated line the current required will depend on the electrical resistance of the coating and upon its freedom from flaws and pinholes. The resistance of the coating is largely affected by the amount of moisture which it will absorb. From this standpoint coal-tar-pitch coatings appear to be superior to asphalt-base materials, but either material if of sufficient thickness will have a sufficiently high specific resistance.

It is not possible to say that one material should be generally used in preference to any other. The selection of the coating material should be governed by such data as have been presented, supplemented by equally important data as to availability, ease of application, suitability of the material for local field and labor conditions, and the estimated cost of the coating throughout the life of the line. It follows that whenever possible the choice of the protective coating should be made by some one thoroughly familiar with the characteristics and uses of pipe coatings.

VII. SUMMARY

Although protective coatings have been applied to pipe lines for half a century or more and many tests of protective coatings have been made, few data are available upon which an engineer can base a reliable estimate of the saving which can be expected through the use of a protective coating.

There are several methods by which certain characteristics of coatings can be indicated, but there is no recognized way of expressing the serviceability of a coating. Because of this, ideas as to the protective value of coatings are vague and lead to uncertain results when applied to the design of a pipe line.

The experiments upon which this report is based were started between 1922 and 1930 and represent pipe-coating practice at that period. They have resulted in the modification of pipe-coating practice and in the development of better coatings. Unfortunately, the testing of

[27] C. W. Clarvoe. *The detection of flaws in pipe-line coatings before burial.* Pipe Line News 5, 13 (July 1933).

[28] S. P. Ewing. *Cathodic protection of pipe lines from soil corrosion.* Natural Gas 16 (March and April 1935).

new coatings in the field by national organizations has been discontinued. The effectiveness of the newer coatings must be determined largely by the experiences of users of the coatings. Data obtained in this way are accumulated but slowly. They are usually lacking in essential details of the conditions which determine the success or failure of the coating and are sometimes influenced by the interests of those who report the data. The reader of this report should neither assume that the results presented are the best that can be obtained with protective coatings nor that the causes of failures of coatings have been overcome completely.

The results of the tests under the general supervision of the National Bureau of Standards seem to warrant the following generalizations.

The performance of a protective coating is controlled by the soil conditions to which it is subjected. The shrinkage and the relative density of the soils are important factors in the distortion of coatings. Distortion is especially severe in dense soils which undergo marked changes in volume with change in moisture content. Because of the effect of soil characteristics on coating behavior, when practicable, coatings should be selected with reference to the soil conditions to which they are to be exposed.

Although no coating tested completely prevented corrosion under all soil conditions for as long as 4 years, almost all of them materially reduced the loss of metal during the period of test.

Coatings which are somewhat porous, such as cut-backs and asphalt emulsions, are effective in preventing pitting in well aerated soils.

The thickness of the bitumen is an important factor in the effectiveness of a coating. Very thin bituminous coatings are unsuitable for severe soil conditions.

Thickness for thickness, coal-tar-base coatings absorb less water and have better insulating qualities than coatings having asphalt as a base.

The coal-tar-base coatings are, in general, more severely affected by soil stresses, sudden changes in temperature, and shocks.

The application of coatings by means of a sling as used in the API tests results in imperfect coatings.

Shields and reinforcements reduce the depth of the deepest pit to a great extent during the first few years of exposure, probably because of their resistance to soil stress, although the relatively great thickness of reinforced and shielded coatings may be a factor.

Asbestos felt offers more permanent reinforcement to bituminous materials than rag felt.

No bituminous coating or coating material is inherently greatly superior to all others. It is possible to secure similar results by several methods.

Although protective coatings have been in use many years there are few detailed records of the performance of coatings covering periods of more than 5 years. The life of protective coatings is therefore somewhat uncertain.

Bituminous coating materials suitable for the service required of them materially reduce corrosion losses. However, because of the nature of the materials used and the conditions under which pipe

lines are usually laid, a pipe coating free from imperfections and injuries is scarcely to be expected.

The conclusions drawn above are based on the performance of types of coatings. The best coating in each type was somewhat more effective than the average upon which the conclusions are based. It is probable that the tests have resulted in the production of coatings that are better than any in the tests which form the basis for these conclusions.

WASHINGTON, August 21, 1937.

INDEX TO VOLUME 19

A

Page

Accelerated-aging tests of traffic paints, RP1007.. 21
Acree, S. F., Baker Wingfield and, Temperatures and hysteresis errors in calomel half-cells, RP1018.. 163
Afterglow of cesium discharge, recombination of ions in, RP1036.. 447
Afterglow of mercury-arc discharge, recombination, RP1045.. 559
Aging of photographic film and paper, RP1051.. 613
Aircraft, radio guidance, RP1006.. 1
Aircraft, transparent plastics for use on, RP1031.. 367
Airport, locating in fog, RP1006.. 1
Airport radio transmitter, location of, RP1006.. 1
Airship fabrics, permeability, RP1020.. 181
Airstream inclination, effect on performance of anemometers, RP1056.. 685
Amino nitrogen, estimation in insoluble proteins, RP1038.. 467
Anemometer errors, RP1056.. 685
Anemometers, performance, RP1056.. 685
Antenna, radio, location of, in pit for blind landing of aircraft, RP1006.. 1
Antiknock value of hydrocarbons isolated from crude synthetic isooctane (2,2,4-trimethylpentane), RP1027.. 319
Arc, mercury, discharge, recombination in afterglow, RP1045.. 559
Arc spectrum of lutecium, RP1008.. 31
Arc spectrum of ytterbium, RP1053.. 651
Arsenious oxide, use of in standardizing solutions of potassium permanganate, RP1057.. 691
Asphalt floor covering, tests, RP1046.. 567
Automotive ignition systems, electrical character of spark discharge, RP1032.. 401
Azilrod, Benjamin M., and Gordon M. Kline, Study of transparent plastics for use on aircraft, RP1031.. 367

B

Ballif, Paul S., Roy H. Heald and, Effect of yaw on vane anemometers, RP1056.. 685
Balloon fabrics, permeability, RP1020.. 181
Ball packings for rectifying columns, RP1049.. 593
Barium guloheptonates, preparation and properties, RP1052.. 639
Battery, diffusion, experimental, extraction of artichoke juices, RP1025.. 263
Bearings, journal, design, RP1037.. 457
Bekkedahl, Norman, and Lawrence A. Wood, Entropy of isoprene from heat-capacity measurements, RP1044.. 551
Benzene, boiling and freezing points, density, and refractive index, RP1029.. 347
Bituminous coatings for underground pipe lines, RP1058.. 695
Blackburn, George F., Paul T. Hannen, Melville F. Peters and, Electrical character of the spark discharge of automotive ignition systems, RP1032.. 401
Blind landing of aircraft, antenna location for use in, RP1006.. 1
Bodies, whiteware, formulation of, RP1011.. 65
Bogan, John A., Richard F. Jackson, Max J. Proffitt and, Extraction of jerusalem-artichoke juices in an experimental diffusion battery, RP1025.. 263
Boiling point of benzene, RP1029.. 347
Brick, fire-clay, deformation, RP1030.. 353
Brick, moisture penetration, RP1015.. 105
Brickwedde, Ferdinand G., Russell B. Scott and, Molecular volumes and expansivities of liquid normal hydrogen and parahydrogen, RP1023.. 237
Brick, wick test, RP1015.. 105

Page

Bright, Harry A., Use of arsenious oxide in the standardization of potassium permanganate, RP1057.. 691
Brooks, Herbert B., and Arthur B. Lewis, Improved continuously variable self and mutual inductor, RP1040.. 493
Brooks, Donald B., Robetta B. Cleaton, and Frank R. Carter, Paraffin hydrocarbons isolated from crude synthetic isooctane (2,2,4-trimethylpentane), RP1027.. 319

C

Calibration of testing machines, RP1009.. 41
Calomel half-cells, effect of temperature on, RP1018.. 163
Carbonizing process for wool, RP1012.. 81
Carter, Frank R., Robetta B. Cleaton, Donald B. Brooks and, Paraffin hydrocarbons isolated from crude synthetic isooctane (2,2,4-trimethylpentane), RP1027.. 319
Cement, dental silicate, optical specification, RP1026.. 287
Cement-water ratio, influence on properties of vibrated concrete, RP1048.. 575
Cesium discharge, recombination of ions in afterglow, RP1036.. 447
Charts for stresses from strain data, RP1034.. 437
Chlorination of wool, RP1012.. 81
Clark, George L., Enno Wolthuis, and W. Harold Smith, X-ray diffraction patterns of sol, gel, and total rubber when stretched and when crystallized by freezing and from solutions, RP1039.. 479
Clays, domestic, substitution of, for imported clays in whiteware, RP1011.. 65
Cleaton, Robetta B., Frank R. Carter, Donald B. Brooks, and, Paraffin hydrocarbons isolated from crude synthetic isooctane (2,2,4-trimethylpentane), RP1027.. 319
Cleveland, Richard S., An improved apparatus for measuring the thermal transmission of textiles, RP1055.. 675
Coatings, bituminous, for underground pipe lines, RP1058.. 695
Columns, rectifying, efficiency, RP1049.. 593
Combustion of ethylene and propylene, heats of, RP1024.. 249
Combustion of the normal olefin (alkene-1) hydrocarbons, heat of, RP1028.. 339
Compressometer method of evaluating crush resistance of fabrics, RP1047.. 571
Concrete, effect of vibrational placement on properties, RP1048.. 575
Concrete floor covering, test, RP1046.. 567
Concrete, vibrated, properties, RP1048.. 575
Corrosion of underground pipe lines, RP1058.. 695
Coverings, floor, test, RP1046.. 567
Crush-resistant finishes, evaluation of, RP1047.. 571
Current transformers, effect of wave form on performance, RP1041.. 517

D

Davis, Raymond, and Emery J. Stovall, Jr., Dimensional changes in aerial photographic films and papers, RP1051.. 613
Deamination of wool {RP1012.. 81 / RP1043.. 535}
Deformation of fire-clay brick, RP1030.. 353
Dellinger, John Howard, Sudden disturbances of the ionosphere, RP1016.. 111
Density of benzene, RP1029.. 347
Density of forms of hydrogen, RP1023.. 237

Page

Dental silicate cement, optical specification, RP1026 287
Determination of degree of hydration of magnesia in dolomitic limes, RP1022 215
Deuterium, conversion of deuterium oxide into, RP1050 605
Deuterium oxide, conversion into deuterium, RP1050 605
Diamond, Harry, and Francis W. Dunmore, Experiments with underground ultra-high-frequency antenna for airplane landing beam, RP1006 1
Diffraction (X-ray) patterns of sol, gel, and total rubber, RP1039 479
Diffusion battery, experimental, extraction of artichoke juices in, RP1025 263
Dilution pipettes, testing of, RP1019 177
Distillation, packed columns for, RP1049 593
Dolomitic limes, hydration of magnesia in, RP1022 215
Dunmore, Francis W., Harry Diamond and, Experiments with underground ultra-high-frequency antenna for airplane landing beam, RP1006 1
Dyeing of wool with acid dyes, RP1012 81
Dynamic loading, calibration of testing machines under, RP1009 41

E

Efflorescence of building brick, RP1015 105
Elastic properties of wool, RP1043 535
Electrical character of spark discharge of automotive ignition systems, RP1032 401
Electrovalent linkages in wool, RP1043 535
Emley, Warren E., and Carl E. Hofer, Tests of floor coverings for post-office workrooms, RP1046 567
Entropy of isoprene, RP1044 551
Ethylene, heat of combustion, RP1024 249
Expansion of liquid normal hydrogen and parahydrogen, RP1023 237
Expansivity of forms of hydrogen, RP1023 237
Expansivity of paper, RP1054 665
Extraction of juices from jerusalem artichokes, RP1025 263

F

Fabrics, airship, permeability, RP1020 181
Fabrics, evaluation of crush resistance of, RP1047 571
Fadeouts, radio, RP1016 111
Feldspar in whiteware bodies, RP1011 65
Film, photographic, dimensional changes, RP1051 613
Finishes, evaluation of crush-resistant, RP1047 571
Finn, Alfred N., George Q. Voigt, Clarence Hahner and, Gases in some optical and other glasses, RP1014 95
Fire-clay brick, deformation, RP1030 353
Floor coverings, test, RP1046 567
Fog, radio guidance of aircraft in, RP1006 1
Formation of the normal olefin (alkene-1) hydrocarbons, heat of, RP1028 339
Fractionation of methyloctanes in petroleum, RP1033 423
Fractionation of petroleum {RP1017 143; RP1033 423}
Freezing point of benzene, RP1029 347

G

Galactal, preparation and oxidation reactions of, RP1021 189
Gases in glass, RP1014 95
Gases, permeability of organic polysulphide resins to, RP1020 181
Gel, sol, and total rubber, X-ray diffraction patterns, RP1039 479
Geib, Martin N. V., Charles G. Weber and, New test for dimensional changes in offset papers, RP1054 665
Glasgow, Jr., Augustus R., Joseph D. White and, Separation of the three methyloctanes from midcontinent petroleum, RP1033 423
——, *and Sylvester T. Schicktanz*, Study of ball packings for laboratory rectifying columns, RP1049 593
Glass, gases in, RP1014 95

Page

Graphical computation of stresses, RP1034 437
Greenspan, Martin, Ambrose E. Stang and, Graphical computation of stresses from strain data, RP1034 437
Guloheptonic γ-lactone and phenylhydrazide, preparation and properties, RP1052 639
Guloheptose, α-*d*-α preparation and mutarotation, RP1052 639

H

Haemacytometer testing, micrometer device for, RP1019 177
Hahner, Clarence, George Q. Voigt, and Alfred N. Finn, Gases in some optical and other glasses, RP1014 95
Half-cells, calomel, temperature and hysteresis errors in, RP1018 163
Hannen, Paul T., George F. Blackburn, Melville F. Peters and, Electrical character of the spark discharge of automotive ignition systems, RP1032 401
Harmonics, effect on performance of current transformers, RP1041 517
Harris, Milton, Arnold M. Sookne and, Stress-strain characteristics of wool as related to its chemical constitution, RP1043 535
——, *Arthur L. Smith and*, Nature of the acid-dyeing process, RP1012 81
——, ——, *Henry A. Rutherford and*, Estimation of amino nitrogen in insoluble proteins, RP1038 467
Heald, Roy H., and Paul S. Ballif, Effect of yaw on vane anemometers, RP1056 685
Heat capacity of isoprene, RP1044 551
Heat of fusion of isoprene, RP1044 551
Heat of solution of dolomitic limes, RP1022 215
Heats of combustion and formation of the normal olefin (alkene-1) hydrocarbons, RP1028 339
Heats of combustion of ethylene and propylene, RP1024 249
Heat transmission of textiles, RP1055 675
Heindl, Raymond A., and William L. Pendergast, Deformation and Young's modulus of fire-clay brick in flexure at 1,220° C, RP1030 353
Helium, permeability, RP1020 181
Heptoses, nomenclature of, RP1052 639
Hickson, Eugene F., Some properties and tests of traffic or zone paints, RP1007 21
Hofer, Carl E., Warren E. Emley and, Tests of floor coverings for post-office workrooms, RP1046 567
Hoffman, James I., and G. E. F. Lundell, Determination of phosphoric anhydride in phosphate rock, superphosphate, and "metaphosphate", RP1010 59
Humidity, effect on dimensions of offset papers, RP1054 665
Humidity, effect on dimensions of photographic film and paper, RP1051 613
Hydration of magnesia in dolomitic limes, RP1022 215
Hydrocarbons, heats of combustion and formation of the normal olefin (alkene-1), RP1028 339
Hydrocarbons in petroleum {RP1017 143; RP1033 423}
Hydrocarbons, paraffin, isolation from crude synthetic isooctane (2,2,4-trimethylpentane), RP1027 319
Hydrocarbons, structure of, by near infrared absorption spectra, RP1017 143
Hydrogen, molecular volumes and expansivities, RP1023 237
Hydrogen, permeability, RP1020 181
Hysteresis in calomel half-cells, RP1018 163

I

Ignition systems, automotive, electrical character of spark discharge, RP1032 401
Inductance, variable, RP1040 493
Inductor, variable self and mutual, RP1040 493
Infrared absorption spectra of hydrocarbons, RP1017 143
Ionosphere measurements, RP1016 111
Ionosphere measurements applied to radio transmissions, RP1013 89
Ions, recombination in afterglow of cesium discharge, RP1036 447

Page

Isbell, Horace S., Guloheptonic acid and α-d-α-guloheptose, RP1052 639
—, *William Ward Pigman and*, Mutarotation of *l*-sorbose, RP1035 443
—, —, β-*d*-talose and *d*-talose acetates and orthoesters, RP1021 189
Isooctane, crude synthetic, isolation of paraffin hydrocarbons from, RP1027 319
Isoprene, heat-capacity and entropy, RP1044 551

J

Jackson, Richard F., John A. Bogan, Max J. Proffitt and, Extraction of jerusalem-artichoke juices in an experimental diffusion battery, RP1025 263
Jerusalem-artichoke juices, extraction, RP1025 263
Johnson, Carl, Bruce Wilson and, Calibration of testing machines under dynamic loading, RP1009 41
Journal bearings, design, RP1037 457
Judd, Deane B., Optical specification of light-scattering materials, RP1026 287

K

Kennelly-Heaviside layer (see ionosphere), RP1013 89
Ketoses, mutarotation of *l*-sorbose, RP1035 443
Klinefelter, Theron A., William A. Meyer and, Substitution of domestic for imported clays in whiteware bodies, RP1011 65
Kline, Gordon M., Benjamin M. Arilrod and, Study of transparent plastics for use on aircraft, RP1031 367
Knowlton, John W., Frederick D. Rossini and, Calorimetric determination of the heats of combustion of ethylene and propylene, RP1024 249
—, —, Heats of combustion and of formation of the normal olefin (alkene-1) hydrocarbons in the gaseous state, RP1028 339
—, —, Method and apparatus for the rapid conversion of deuterium oxide into deuterium, RP1050 605

L

Lead guloheptonates, preparation and properties, RP1052 639
Levulose-containing juices, extraction in diffusion battery, RP1025 263
Lewis, Arthur B., Herbert B. Brooks and, Improved continuously variable self and mutual inductor, RP1040 493
Light-scattering materials, optical specification, RP1026 287
Limes, hydration of magnesia in, RP1022 215
Linkages, salt, in wool, RP1043 535
Linoleum floor covering, test, RP1046 567
Liquid hydrogen, molecular volumes and expansivities, RP1023 237
Logan, Kirk H., Soil-corrosion studies, 1934. Bituminous coatings for underground service, RP1058 695
Lubrication of journal bearings, RP1037 457
Lundell, G. E. F., James I. Hoffman and, Determination of phosphoric anhydride in phosphate rock, superphosphate, and "metaphosphate," RP1010 59
Lutecium, arc and spark spectra, RP1008 31

M

McBurney, John W., and Douglas E. Parsons, Wick test for efflorescence of building brick, RP1015 105
McKee, Samuel A., Journal-bearing design as related to maximum loads, speeds, and operating temperatures, RP1037 457
Machines, testing, calibration of, RP1009 41
Magnesia, hydration of, RP1022 215
Magnesite floor covering, test, RP1046 567
Meggers, William F., and Bourdon F. Scribner, Arc and spark spectra of lutecium, RP1008 31
—, —, Arc and spark spectra of ytterbium, RP1053 651
Mercury-arc discharge, recombination in afterglow, RP1045 559

Page

Metaphosphate, determination of phosphorus in, RP1010 59
Methyloctanes, separation of, from petroleum, RP1033 423
Meyer, William W., and Theron A. Klinefelter, Substitution of domestic for imported clays in whiteware bodies, RP1011 65
Micrometer device for testing pipettes, RP1019 177
Midcolumn dosage in jerusalem artichoke extraction, RP1025 263
Mohler, Fred L., Recombination of ions in the afterglow of a cesium discharge, RP1036 447
—, Recombination in the afterglow of a mercury discharge, RP1045 559
Molecular volumes of liquid normal hydrogen and parahydrogen, RP1023 237
Monobenzoyl-d-talose, preparation from galactal, RP1021 189
Mutarotation of α-*d*-α-guloheptose, RP1052 639
Mutarotation of β-*d*-talose, RP1021 189
Mutarotation of *l*-sorbose, RP1035 443

N

Navigation of aircraft in fog, RP1006 1
Nitrogen, amino, estimation in proteins, RP1038 467
Nomographs for stresses from strain data, RP1034 437
Normal hydrogen and parahydrogen, molecular volumes and expansivities, RP1023 237

O

Offset paper, expansivity, RP1054 665
Olefin hydrocarbons, heats of combustion and formation, RP1028 339
Opacity of paper, paint, vitreous enamel, and dental silicate cement, RP1026 287
Optical glass, gases in, RP1014 95
Optical rotation of α-*d*-α-guloheptose, RP1052 639
Optical rotation of *l*-sorbose, RP1035 443
Optical specification of light-scattering materials, RP1026 287
Organic plastics for use on aircraft, RP1031 367
Organic plastics, permeability, RP1020 181
Organic polysulphide resins, RP1020 181
Orthoacid derivatives of sugars, RP1021 189
Orthohydrogen, liquid, molecular volumes and expansivities, RP1023 237
Oxidation of β-*d*-talose, RP1021 189
Oxidation of wool, RP1012 81
Oxide content of whiteware bodies, effect of, on vitrification, RP1011 65

P

Packings for rectifying columns, RP1049 593
Paint, cold-water, optical specifications, RP1026 287
Paints, traffic or zone, properties, RP1007 21
Paper, expansivity, RP1054 665
Paper, optical specification, RP1026 287
Paper, photographic, dimensional changes, RP1051 613
Paraffin hydrocarbons, isolation from crude synthetic isooctane (2,2,4-trimethylpentane), RP1027 319
Parahydrogen, liquid, molecular volumes and expansivities, RP1023 237
Park, John H., Effect of wave form upon the performance of current transformers, RP1041 517
Parsons, Douglas E., John W. McBurney and, Wick test for efflorescence of building brick, RP1015 105
Peffer, Elmer L., Device for testing haemacytometer and other pipettes of small capacity, RP1019 177
Pendergast, William L., Raymond A. Heindland, Deformation and Young's modulus of fire-clay brick in flexure at 1,220° C., RP1030 353
Permanganate, standardizing with arsenious oxide, RP1057 691
Permeability of organic polysulphide resins, RP1020 181
Peters, Melville F., George A. Blackburn and Paul T. Hannen, Electrical character of the spark discharge of automotive iginition systems, RP1032 401
Petroleum hydrocarbons {RP1017 ..... 143 / RP1033 ..... 423}

Page

Petroleum, near infrared absorption of hydrocarbons in, RP1017 ... 143
Petroleum, separation of methyloctanes from, RP1033 ... 423
Phosphate rock, determination of phosphorus in, RP1010 ... 59
Phosphorus, determination of, in phosphate rock, superphosphate, and "metaphosphate", RP1010 ... 59
Photographic film, dimensional changes, RP1051 ... 613
Photographic papers, dimensional changes, RP1051 ... 613
Pigman, G. L., E. A. Pisapia, J. S. Rogers, John Tucker, Jr., and, Study of vibrated concrete, RP1048 ... 575
Pigman, William Ward, and Horace S. Isbell, β-d-Talose and d-talose acetates and orthoesters, RP1021 ... 189
——, ——, Mutarotation of l-sorbose, RP1035 ... 443
Pile fabrics, evaluation of crush resistance of, RP1047 ... 571
Pipe lines, underground corrosion, RP1058 ... 695
Pipette testing, micrometer device for, RP1019 ... 177
Pisapia, E. A., G. L. Pigman, J. S. Rogers, John Tucker, Jr., and, Study of vibrated concrete, RP1048 ... 575
Pit, location of antenna in, for blind landing, RP1006 ... 1
Plastics, organic, permeability, RP1020 ... 181
Plastics, transparent, for aircraft, RP1031 ... 367
Polysaccharide extraction in experimental diffusion battery, RP1025 ... 263
Post-office workrooms, floor coverings, test, RP1046 ... 567
Potassium permanganate, standardizing solutions of, with arsenious oxide, RP1057 ... 691
Printing paper, expansivity, RP1054 ... 665
Proffitt, Max J., John A. Bogan, and Richard F. Jackson, Extraction of jerusalem-artichoke juices in an experimental diffusion battery, RP1025 ... 263
Propylene, heat of combustion, RP1024 ... 249
Proteins, estimation of amino nitrogen in, RP1038 ... 467
Pulp from jerusalem artichokes, RP1025 ... 263

Q

Quick, G. Willard, Service-test results of titanium-treated and silicon-treated steel rails, RP1042 ... 531
Quinone-tanning of wool, RP1043 ... 535

R

Radio, blind landing of aircraft by, RP1006 ... 1
Radio fadeouts, RP1016 ... 111
Radio guidance of aircraft, RP1006 ... 1
Radio navigation of aircraft, RP1006 ... 1
Radio, skip distance and ionosphere measurements, RP1013 ... 89
Radio transmission and normal incidence ionosphere measurements, RP1013 ... 89
Radio wave, behavior of, when emerging from pit, RP1006 ... 1
Rails, service tests, RP1042 ... 531
Reagent dosage in diffusion battery, RP1025 ... 263
Recombination of ions in afterglow of a cesium discharge, RP1036 ... 447
Recombination in afterglow of a mercury-arc discharge, RP1045 ... 559
Rectifying columns, packings, RP1049 ... 593
Refractive index of benzene, RP1029 ... 347
Reflectance of paper, paint, vitreous enamel, and dental silicate cement, RP1026 ... 287
Resins, permeability of organic polysulphide, RP1020 ... 181
Rogers, J. S., G. L. Pigman, E. A. Pisapia, John Tucker, Jr., and, Study of vibrated concrete, RP1048 ... 575
Rose, Jr., Frank W., Infrared absorption of nineteen hydrocarbons, including ten of high molecular weight, RP1017 ... 143
Rossini, Frederick D., and John W. Knowlton, Calorimetric determination of the heats of combustion of ethylene and propylene, RP1024 ... 249
——, ——, Heats of combustion and of formation of the normal olefin (alkene-1) hydrocarbons in the gaseous state, RP1028 ... 339

Page

Rossini, Frederick D., and John W. Knowlton, Method and apparatus for the rapid conversion of deuterium oxide into deuterium, RP1050 ... 605
Rubber crystallized from solution, X-ray patterns, RP1039 ... 479
Rubber floor covering, test, RP1046 ... 567
Rubber substitutes, RP1020 ... 181
Rutherford, Henry A., Milton Harris, and Arthur L. Smith, Estimation of amino nitrogen in insoluble proteins, RP1038 ... 467

S

Sager, Theron P., Permeability of organic polysulphide resins to hydrogen, RP1020 ... 181
Salt linkages in wool, RP1043 ... 535
Schicktanz, Sylvester T., Augustus R. Glasgow, Jr., and, Study of ball packings for laboratory rectifying columns, RP1049 ... 593
Schiefer, Herbert F., Evaluation of crush-resistant finishing treatments for fabrics, RP1047 ... 571
Scott, Russell B., and Ferdinand G. Brickwedde, Molecular volumes and expansivities of liquid normal hydrogen and parahydrogen, RP1023 ... 227
Scribner, Bourdon F., William F. Meggers and, Arc and spark spectra of lutecium, RP1008 ... 31
——, ——, Arc and spark spectra of ytterbium, RP1053 ... 651
Shrinkage of photographic film and paper, RP1051 ... 613
Silicate cement, dental, optical specification, RP1026 ... 287
Silicon-treated rails, service tests, RP1042 ... 531
Smith, Arthur L., Milton Harris, Henry A. Rutherford and, Estimation of amino nitrogen in insoluble proteins, RP1038 ... 467
——, ——, Nature of the acid-dyeing process, RP1012 ... 81
Smith, W. Harold, Enno Wolthuis, George L. Clark and, X-ray diffraction patterns of sol, gel, and total rubber when stretched and when crystallized by freezing and from solutions, RP1039 ... 479
Smith, Newbern, Extension of normal-incidence ionosphere measurements to oblique-incidence radio transmission, RP1013 ... 89
Soil-corrosion studies of bituminous materials, RP1058 ... 695
Solar phenomena affecting radio, RP1016 ... 111
Sol, gel, and total rubber, X-ray diffraction patterns, RP1039 ... 479
Sookne, Arnold M., and Milton Harris, Stress-strain characteristics of wool as related to its chemical constitution, RP1043 ... 535
Sorbose, mutarotation of, RP1035 ... 443
Spark discharge of automotive ignition systems, electrical character, RP1032 ... 401
Spark spectrum of lutecium, RP1008 ... 31
Spark spectrum of ytterbium, RP1053 ... 651
Specifications for traffic paints, RP1007 ... 21
Specific heat of isoprene, RP1044 ... 551
Spectra of lutecium, RP1008 ... 31
Spectra of ytterbium, RP1053 ... 651
Stang, Ambrose H., and Martin Greenspan, Graphical computation of stresses from strain data, RP1034 ... 437
Steel rails, service tests, RP1042 ... 531
Stills for fractionation, RP1049 ... 593
Stovall, Jr., Emory J., Raymond Davis and, Dimensional changes in aerial photographic films and papers, RP1051 ... 613
Strain, stresses from RP1034 ... 437
Stress, graphical computation, RP1034 ... 437
Stress-strain measurements on wool fibers, RP1043 ... 535
Structure of fire-clay brick, RP1030 ... 353
Sugars, orthoacid derivatives, RP1021 ... 189
Sulfuric acid, action on wool, RP1012 ... 81
Sun, phenomena on, affecting radio, RP1016 ... 111
Superphosphate, determination of phosphorus in, RP1010 ... 59
Synthetic resins for use on aircraft, RP1031 ... 367

T

Talose, preparation, properties, and derivatives, RP1021 ... 189
Tanning of wool, RP1043 ... 535

Page

Taylor, Kenneth, Lansing S. Wells and, Hydration of magnesia in dolomitic hydrated limes and putties, RP1022 ... 215
Temperature, effect on calomel half-cells, RP1018 ... 163
Testing machines, calibration of, RP1009 ... 41
Testing of dilution pipettes, RP1019 ... 177
Textiles, estimation of amino nitrogen in some, RP1038 ... 467
Textiles, stress-strain characteristics of wool, RP1043 ... 535
Textiles, thermal transmission, RP1055 ... 675
Thermal properties and entropy of isoprene, RP1044 ... 551
Thermal transmission of textiles, RP1055 ... 675
Titanium-treated rails, service tests, RP1042 ... 531
Traffic paints, properties, RP1007 ... 21
Transformers, current, effect of wave form on performance, RP1041 ... 517
Translucency of dental silicate cements, RP1026 ... 287
Transmitter, location of, at airports, RP1006 ... 1
Transparent velvets, evaluation of crush resistance of, RP1047 ... 571
Tucker, Jr., John, G. L. Pigman, E. A. Pisapia, and J. S. Rogers, Study of vibrated concrete, RP1048 ... 575

U

Underground, behavior of ultra-high-radio frequencies emanating from, RP1006 ... 1
Underground corrosion of pipe lines, RP1058 ... 695

V

Vane anemometers, effect of airstream inclination on performance, RP1056 ... 685
Variometer, see Inductor, variable, RP1040 ... 493
Velvets, evaluation of crush resistance of transparent, RP1047 ... 571
Vibrated concrete, properties, RP1048 ... 575
Vitreous enamel, optical specification, RP1026 ... 287
Vitrification, effect of RO content of whiteware bodies on, RP1011 ... 65
Voigt, George Q., Alfred N. Finn, Clarence Hahner and, Gases in some optical and other glasses, RP1014 ... 95
Volumetric standards, use of arsenious oxide in permanganimetry, RP1057 ... 691
Volumetric testing of dilution pipettes, RP1019 ... 177

W

Wave form, effect on performance of current transformers, RP1041 ... 517
Wave, radio, theory and propagation of from a pit, RP1006 ... 1
Wearing tests of traffic paints, RP1007 ... 21
Weber, Charles G., and Martin N. V. Geib, New test for dimensional changes in offset papers, RP1054 ... 665
Wells, Lansing S., and Kenneth Taylor, Hydration of magnesia in dolomitic hydrated limes and putties, RP1022 ... 215
White, Joseph D., and Augustus R. Glasgow, Jr., Separation of the three methyloctanes from midcontinent petroleum, RP1033 ... 423
Whiteware bodies, physical properties, RP1011 ... 65
Whiteware, substitution of domestic for imported clays in, RP1011 ... 65
Wick test for efflorescence of building brick, RP1015 ... 105
Wilson, Bruce, and Carl Johnson, Calibration of testing machines under dynamic loading RP1009 ... 41
Windshields of aircraft, plastics for, RP1031 ... 367
Wingfield, Baker, and S. F. Acree, Temperatures and hysteresis errors in calomel half-cells, RP1018 ... 163
Wojciechowski, Mieczyslaw, Measurements of certain physicochemical constants of benzene, RP1029 ... 347
Wolthuis, Enno, W. Harold Smith, George L. Clark, and, X-ray diffraction patterns of sol, gel, and total rubber when stretched and when crystallized by freezing and from solutions, RP1039 ... 479
Wood floor coverings, test, RP1046 ... 567
Wood, Lawrence A., Norman Bakkedahl and, Entropy of isoprene from heat-capacity measurements, RP1044 ... 551
Wool, acid-dyeing process, RP1012 ... 81
Wool, chemical constitution, RP1043 ... 535
Wool, stress-strain properties, RP1043 ... 535

X

X-ray diffraction patterns of sol, gel, and total rubber, RP1039 ... 479

Y

Yaw, effect of, on vane anemometers, RP1056 ... 685
Ytterbium, arc and spark spectra, RP1053 ... 651

Z

Zone paints, traffic, properties of, RP1007 ... 21